Carbon Dioxide Exchange of Sahelian Vegetation

Peter E. Levy B.Sc. (Hons)

Doctor of Philosophy

University of Edinburgh

1995

Declaration

I declare that this thesis has been composed by myself from the results of my own work, except where stated otherwise, and has not been submitted in any previous application for a degree.

Peter Levy

July 1995

Abstract

Measurements of leaf and ecosystem scale CO_2 flux were made at the millet, fallow and tiger bush sites at the HAPEX-Sahel Southern supersite. These were analysed in relation to biological and environmental variables. In the five species studied, leaf scale photosynthesis was strongly influenced by photosynthetic photon flux density (Q) and stomatal conductance, and was well described by the non-rectangular hyperbola model of Jarvis, Miranda and Muetzelfeldt (1985). Stem respiration was measured in two species, and increased exponentially with temperature. Stem respiration rates were higher in the wet seaon than in the dry season and this difference was used to separate growth and maintenance respiration. Effects of Q and sap flow on stem CO_2 efflux were observed. A small number of soil respiration measurements were also made. Direct measurements of leaf area index, biomass and canopy structure were made at the millet and fallow sites. Two indirect methods of estimating leaf area index, from hemispherical photographs and measurements of transmitted Q, were used at all three sites.

Together with measurements of canopy structure at each site, the measurements of leaf photosynthesis, stomatal conductance and stem and soil respiration were used to parameterise two models which predict ecosystem net CO_2 flux: a simple one-dimensional "big leaf" model and a complex three-dimensional model "MAESTRO". Model predictions were compared with independent ecosystem flux measurements made by eddy covariance. Generally, both models agreed well with measurements. Differences between measurements and predictions were very small in millet and largest in tiger bush, and were attributed to the effect of canopy heterogeneity on eddy covariance measurements and the accuracy with which canopy structure parameters could be estimated. Differences between predictions from the two models were also very small in millet and largest in tiger bush, and were attributed to the uncertainties in canopy structure parameters and the validity of the assumptions in the big leaf model, again related to canopy heterogeneity.

MAESTRO was used to extrapolate measurements in time, and, using weather data for the whole of the 1992 wet season, predicted a value for carbon sequestration at the millet site close to harvest measurements. A simple procedure was used for scaling leaf fluxes to the regional scale, using the MAESTRO predictions of ecosystem scale CO_2 flux for each site, weighted by the proportion of the region covered by the different vegetation types. An attempt was made to validate this by comparison with regional fluxes calculated from the mass budget of the convective boundary layer (CBL). Values of regional scale CO_2 flux from the CBL budget method were considerably higher than MAESTRO predictions.

Models are necessary as a means of scaling up measurements, which usually cover small spatial and temporal scales, to the larger scales more relevant to the problems of global environmental change, so it is essential that they be validated. Comparison of simple and complex models with independent ecosystem flux measurements at different sites gives an indication of the range of canopy types where the models work satisfactorily, and where simplifying assumptions may be invalid. Also, comparison of model predictions with measurements is informative, as the models represent an integration of our knowledge of the system, and so differences highlight weak points in our understanding.

Acknowledgements

Firstly, I would like to thank Prof. Paul Jarvis for his supervision of the project, and for his extremely thorough editing of this thesis. I would also like to thank Dr John Moncrieff for his guidance on matters micrometeorological and for his inspirational undergraduate teaching.

Particular thanks are due to Mark Smith, who dealt with more than his share of the problems which faced us Niger, and who was an education to live and work with. I am eternally grateful to Mark, Shona Wynd, Jon Massheder, Steve Scott and Martina Mayus, who coped so brilliantly with my accident, and gave me constant care and attention while I was bed-ridden in Gamkallé.

Thanks are due to all the staff of ICRISAT Sahelian Centre, but particularly to Dr Joost Brouwer, who was an invaluable source of help and encouragement, Dr Bill Payne, and the Agroforestry Section staff, particularly Djabté Traoré, Soulayeman Adamou, Boubacar Moussa, and also Abel.

Many thanks are also due to: Jon Massheder, for help with MAESTRO and a myriad of computer problems; Craig Barton for his technical wisdom on all matters; Colin MacGillivray, Lindsay MacKinlay and everyone at Radio Guiera FM, for the stem diameter survey; Jake Sudlow and Tony Barker for innumerable lifts, *conjunctures* and copies of *Viz*; Patrick Meir for collaboration on the sap CO_2 concentration measurements and for useful discussion on respiration and pop trivia; Bart Kruijt and Prof. John Monteith, for help with the boundary layer budget method; Simon Allen for collaboration on the sap flow measurements; Cathy Howill for the diagrams in Chapter 2; Niall Hanan for sharing a lot of his data with me; all the staff at Edinburgh Royal Infirmary and Princess Margaret Rose Orthapaedic Hospital, who could not have been better, particularly Mr James Christie and wee Angie; Ken "drinking heavily again" Barrett, Andrew Anthony, Stuart Campbell, Stewart Mattress and Louis O'Donnell; my parents, for their constant support, financial and otherwise; Sophie Hale, for patiently proof-reading the chapters, and more besides.

Symbols

Roman alphabet

A_e	ecosystem net photosynthetic assimilation rate of CO_2 (μmol m^{-2} s^{-1})
A_{eo}	observed A_e, measured by eddy covariance (μmol m^{-2} s^{-1})
A_l	leaf net photosynthetic assimilation rate of CO_2 (μmol m^{-2} s^{-1})
A_{lmax}	asymptotic value of A_l with respect to Q (μmol m^{-2} s^{-1})
A_{lo}	observed A_l (μmol m^{-2} s^{-1})
A_{lp}	predicted A_l (μmol m^{-2} s^{-1})
A_r	regional net photosynthetic assimilation rate of CO_2 (mol m^{-2} d^{-1})
C_+	mole fraction of CO_2 in free atmosphere above CBL (μmol mol^{-1})
C_a	mole fraction of CO_2 in ambient air (μmol mol^{-1})
C_i	mole fraction of CO_2 in leaf intercellular space (μmol mol^{-1})
C_{min}	daily minimum value of mole fraction of CO_2 in ambient air (μmol mol^{-1})
D	saturation vapour pressure deficit (kPa)
D_o	parameter defining decrease in g_s with D (arbitrary)
d	stem diameter (mm)
E	transpiration rate (mmol m^{-2} s^{-1})
e	vapour pressure of air (kPa)
e_s	saturation vapour pressure of air (kPa)
g_m	mesophyll conductance (mol m^{-2} s^{-1})
g_s	stomatal conductance (mmol m^{-2} s^{-1})
g_{sdark}	stomatal conductance in darkness (mmol m^{-2} s^{-1})
g_{slope}	initial slope of g_s-Q curve (mmol H_2O per mol quanta)
g_{smax}	maximum stomatal conductance (mmol m^{-2} s^{-1})
g_{so}	observed stomatal conductance (mmol m^{-2} s^{-1})
g_{sp}	predicted stomatal conductance (mmol m^{-2} s^{-1})
H	relative humidity (%)
h	height (m)
h_t	tiller height (cm)
K	dissociation constant (dimensionless)
K	extinction coefficient for Q
k	coefficient for increase in respiration with temperature ($°C^{-1}$)
L_d	directly measured total plant surface area index (dimensionless)
L_i	indirectly measured total plant surface area index (dimensionless)
L_l	leaf area index (dimensionless)

L_s	surface area index of woody stems (dimensionless)
L_t	total plant surface area index (dimensionless)
l	length of stem section (mm)
n	number in sample
P	leaf gross photosynthetic rate ($=A_l + R_d$)(μmol m^{-2} s^{-1})
P_{max}	asymptotic value of P with respect to Q (μmol m^{-2} s^{-1})
pCO_2	partial pressure of CO_2 (μbar bar^{-1}, equivalent to mole fraction)
Q	photosynthetic photon flux density (μmol m^{-2} s^{-1})
Q_{10}	increase factor for a 10 °C rise in temperature
Q_{abs}	absorbed photosynthetic photon flux density (μmol m^{-2} s^{-1})
Q_{in}	incident photosynthetic photon flux density (μmol m^{-2} s^{-1})
Q_{ref}	reflected photosynthetic photon flux density (μmol m^{-2} s^{-1})
Q_{trans}	transmitted photosynthetic photon flux density (μmol m^{-2} s^{-1})
R	respiration rate (μmol m^{-2} s^{-1})
R_d	leaf dark respiration rate (μmol m^{-2} s^{-1})
R_g	growth respiration rate (μmol m^{-2} s^{-1})
R_o	respiration rate at 0 °C (μmol m^{-2} s^{-1})
R_{og}	growth respiration rate at 0 °C (μmol m^{-2} s^{-1})
R_{om}	maintenance respiration rate at 0 °C (μmol m^{-2} s^{-1})
r	stem radius (mm)
r_a	aerodynamic resistance (s m^{-1})
S	surface area (mm^2 or cm^2)
T_a	air temperature (°C)
T_l	leaf temperature (°C)
t	time (s or h)
V	volume (mm^3)

Greek alphabet

α	quantum efficiency (mol CO_2 per mol quanta)
Γ	CO_2 compensation concentration (μmol mol^{-1})
θ	convexity parameter in A_l-Q response; zenith angle (radians)
κ	contact number (Equation 6.6)
ρ	reflection coefficient in the photosynthetic waveband
ρ_a	density of air (mol m^{-3})
τ	canopy transmittance (Q_{trans} / Q_{in}) (dimensionless)

Chapter 1

Introduction

1.1 Rising atmospheric CO_2 and terrestrial vegetation

Anthropogenic releases of CO_2 from fossil fuel burning and deforestation have brought about an increase in the atmospheric concentration of CO_2 from 280 μmol mol^{-1} in pre-industrial times to around 350 μmol mol^{-1} in 1990 (Neftel *et al.*, 1985; Friedli *et al.*, 1986). This represents a serious perturbation of the global carbon cycle and is currently a matter of great concern (IPCC, 1990, 1992, 1994). Atmospheric CO_2 concentration, vegetation and climate are interlinked and may influence each other in complex ways (Smith and Shugart, 1993). Atmospheric CO_2 may affect vegetation directly through its effects on photosynthesis and stomatal conductance (Eamus and Jarvis, 1989) and indirectly via its effects on climate, particularly elevated temperatures resulting from the "greenhouse effect" and possible ensuing changes in precipitation patterns (IPCC, 1990; Adams *et al.*, 1990). In turn, vegetation may influence atmospheric CO_2 concentration (and thus climate) through photosynthesis and respiration by absorbing or evolving CO_2. There are thus feedbacks in the global carbon cycle which make its behaviour difficult to predict (Kellog, 1983; Mooney, Drake and Luxmoore, 1991).

Any even-aged stand of vegetation is likely to be "CO_2 neutral" (ie. it does not act as a source or sink for CO_2) when considered over its rotation period. This may range from one year for arable crops up to 40 to 100 years for plantation forests. However, on a landscape scale or in uneven aged vegetation, biomass is always present, representing a pool of carbon which may shrink or grow, thereby acting as a source or sink. Although the anthropogenic input to the atmosphere from fossil fuel burning and land use change is estimated to be around 8.5 Gt CO_2 yr^{-1}, the measured increase in the atmosphere is only 3.4 Gt CO_2 yr^{-1}, leaving a large amount of CO_2 which is difficult to account for with current understanding of the oceans and terrestrial vegetation - an apparent "missing sink" (Jarvis and Dewar, 1993). In the global carbon budget presented by Jarvis and Dewar (1993), it is tentatively postulated that vegetation represents a sink of 4.3 Gt CO_2 yr^{-1} in order that sources and sinks balance, although there is a large degree of uncertainty associated with the values (around 100 %). It is thus important to understand the flux of CO_2 between the vegetation and the atmosphere in order to be able to predict (i) how atmospheric CO_2 concentration will change in the future with further additions from fossil fuels and deforestation and (ii) how vegetation will change with elevated CO_2 and climate change.

There are several possible ways of studying this atmosphere-vegetation exchange of CO_2. Direct measurements of carbon stored in vegetation are not practicable on a large scale, but can be used

where good forest inventories are kept. Remote sensing from satellites offers some promise as an indirect means of measuring this but there are difficulties with the saturation of radiative indices in dense vegetation, cloudy environments, and compromises between spatial and temporal resolution. The seasonal variation in observations of atmospheric CO_2 concentration from the flask network around the globe may be used to infer latitudinal variations in CO_2 source or sink strength (Enting and Mansbridge, 1989, 1991; Tans, Fung and Takahashi, 1990). However, the resolution achieved is currently very poor and the potential errors very large. Alternatively, CO_2 fluxes can be directly measured at leaf and ecosystem scales by established techniques. Although these measurements can be made accurately, they cover small spatial and temporal scales, relative to the long term, global scale which is of interest.

1.2 Measurement and modelling of CO_2 flux in HAPEX-Sahel

The objective of this study was to make direct measurements of CO_2 flux at leaf and ecosystem scales, and to extrapolate these measurements to larger scales using modelling. Measurements were made in Niger, in the Sahelian zone of West Africa (Figure 1.1) as part of the international experiment HAPEX-Sahel (Hydrological Atmospheric Pilot EXperiment in the Sahel). Full details of HAPEX-Sahel are contained in Goutorbe *et al.* (1992, 1993). The University of Edinburgh group was responsible for the ground-based measurements of CO_2 flux at the southern supersite, 45 km to the south of Niamey.

Aims

(1) The main objective of this project was to determine the magnitude of the leaf and ecosystem-scale fluxes and their dependence on pertinent controlling variables.

(2) The experiment provides a test of scaling up procedures. It is desirable to be able to predict the effects of elevated CO_2 and climate change on vegetation at a large scale. However, the experiments in which these are investigated can only be carried out on relatively small scales. It is therefore essential that the scaling up process be demonstrably correct and can provide adequate estimates of ecosystem CO_2 flux in the current climate.

(3) In order to understand the global carbon cycle, it is necessary to know which areas of vegetation represent sinks and sources for CO_2 and how they will respond to further environmental change. If scaling up procedures can be successfully validated, they can be used to extrapolate observations to the larger scales more relevant to this problem.

(4) A further objective is to provide "ground truth" measurements of CO_2 flux and canopy properties for comparison with aircraft and satellite remote sensing measurements. Various techniques may potentially be used for remote sensing of surface fluxes and vegetation properties, such as biomass, leaf area index (L_l) and height. However, these techniques remain largely untested in tropical regions.

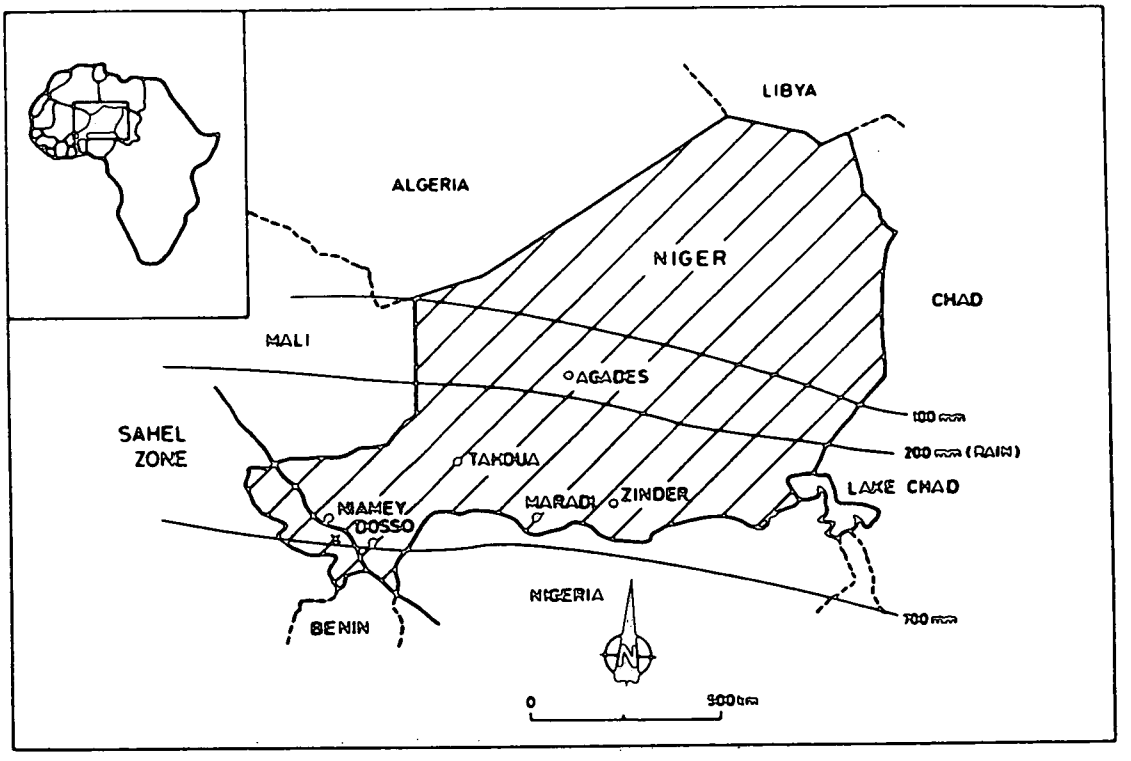

Figure 1.1 Location of the southern supersite (x) within Niger, showing major towns and isohyets. Inset: Location of Niger within Africa.

Simultaneous ground based and satellite/aircraft measurements are needed in order to validate and develop these techniques. These data will be analysed and interpreted by the remote sensing scientists involved (Prince *et al.*, in press), and will not be discussed in detail here.

Information on the functioning of vegetation can be gained from measurements of growth and leaf-scale gas exchange ("leaf scale" is used here as a general term and may include stem and soil chamber measurements). However, growth measurements give little information on the control of processes, and leaf-scale gas exchange measurements cannot be directly extrapolated to give information concerning the vegetation as a whole. Hence micrometeorological techniques such as eddy covariance are important as they permit measurements to be made on large spatial scales (over an area of several hundred square metres) and on short-time scales (fluxes were averaged over half hour periods). In this way, the short-term dependence of the ecosystem-scale CO_2 flux on environmental and biological variables can be studied (Mooney, Vitousek and Matson, 1987; Baldocchi, Hicks and Meyers, 1988).

The approach of this project was to measure photosynthetic and respiratory properties at the leaf scale, together with canopy properties (L_1, leaf area density distribution in three dimensions), in order to predict ecosystem-scale CO_2 fluxes using a scaling-up model known as MAESTRO (Wang and Jarvis, 1990) and a very simple "big leaf" model. The fluxes of the components (leaves, stems and soil) were investigated by enclosing sections in chambers and measuring the CO_2 and water vapour content of air flowing in and out. These flux measurements can be related to biological and environmental variables such as temperature, radiation and humidity, and parameters for the response functions derived. In the scaling-up models, these functions are combined with a model describing the distribution of environmental variables within the canopy, particularly radiation, producing a prediction of the net CO_2 flux to the ecosystem as a whole.

The models were parameterised for each of the three subsites at the southern supersite using leaf physiology and canopy structure data and tested against direct measurements of CO_2 flux made at these sites during the Intensive Observation Period (IOP, 15 August - 10 October 1992) using the eddy covariance technique. Extrapolation to the regional scale was attempted using the parameterised ecosystem models and the distribution of vegetation types. This approach was compared with a technique (McNaughton, 1989; Raupach *et al.*, 1992, 1994) that attempts to infer the regional flux from diurnal changes in atmospheric CO_2 concentration. Extrapolations to the whole of the wet season were made by incorporating leaf phenology in the model from measurements of the seasonal changes in leaf area. These simulations could be tested to some extent against measurements of biomass made over the whole growing season. It may also be possible to make predictions about vegetation functioning under conditions of projected climatic change, such as elevated CO_2, higher temperature and drought.

1.3 HAPEX-SAHEL: Hydrological Atmospheric Pilot Experiment in the Sahel

The aim of the HAPEX experiment was to gain a better understanding of the interactions between the land surface and the atmosphere so as to improve General Circulation Models (GCMs) of the climate system (Hoepffner and Goutorbe, 1989; IGBP, 1990; Goutorbe *et al.*, 1992, 1994). The land surface acts as the main energy input for the climate system. Characteristics of the land surface, particularly soil properties, vegetation type and cover affect the radiation balance and determine the partitioning of energy between the sensible heat flux (directly heating air) and the latent heat flux (evaporation of water) (Henderson-Sellers, 1987). These fluxes act as the driving force behind the climate system. This energy partitioning is controlled by such processes as interception of precipitation by plant canopies, infiltration, runoff, soil evaporation, water uptake by plant roots and transpiration. Such effects of the land surface are very important in models of the climate system. Several experiments using General Circulation Models (GCMs) have shown that the results are very sensitive to the way in which the land surface is parameterised (Potter *et al.*, 1975; Yeh, Wetherald and Manabe, 1984; Cunnington and Rowntree, 1986; Xue, Liou and Kasahara, 1990; Xue and Shukla, 1993). However, until recently the land surface has been represented very simplistically in these models. For example, runoff has often been simulated using Budyko's "bucket" model whereby any excess to a threshold soil moisture value forms runoff, oversimplifying a complicated and important process (Sellers, 1987). Similarly, the role of vegetation in controlling evapotranspiration has also been largely ignored, plants being represented simply as passive evaporating surfaces.

Recently, climate modellers have come to acknowledge the importance of representing surface processes accurately, including taking vegetation into account (Dickinson, 1984; Wood, 1991). New models have been developed to simulate the transfer processes in more detail, such as the Simple Biosphere Model (SiB) (Sellers *et al.*, 1986; Sud *et al.*, 1990) and the Biosphere-Atmosphere Transfer Scheme (BATS) of Dickinson (1984). However, if these models are to be successful, it is essential that they are correctly parameterised. A database is needed to describe the different types of land surface found on the earth in terms of the variables relevant to the model. HAPEX-Sahel is one in a series of experiments designed to establish this database. Others include the earlier HAPEX-MOBILHY (Modelisation du Bilan Hydrique) in temperate agriculture/forest in France (Andre *et al.*, 1988), the First ISLSCP Field Experiment (FIFE) in temperate grassland in the USA (Sellers *et al.*, 1988, 1992), the ECHIVAL Field Experiment in Desertification-threatened Area (EFEDA) in Spain (Bolle *et al.*, 1993) and the Boreal Ecosystem-Atmosphere Study (BOREAS) in Canadian boreal forest. Future experiments are planned in Brazilian rain forest (LAMBADA-BATERISTA-AMBIACE) and arctic tundra. The Sahel was chosen for several reasons: it provides a sharp contrast with conditions in the temperate zone experiments; vegetation-atmosphere interactions are important in desertification processes; it forms a large zone of 3 million km^2 and is suitably representative of the large area of semi-arid land across the globe; the infrastructure to run such an

experiment exists in Niger (Goutorbe *et al.*, 1992). The Sahel may also be particularly sensitive to environmental change, occurring as it does on a steep climatic gradient on the edge of the Sahara desert, where a small change in this gradient could shift the borders between different ecoclimatic zones and affect large areas of land (Cloudsley-Thompson, 1974). It is generally accepted that rainfall over the Sahel has been declining over the past two or three decades (Nicholson, 1989). Various ideas have been suggested to explain this phenomenon (Hare, 1977), such as a positive feedback between vegetation cover and rainfall mediated through the surface albedo (Charney, 1975; Charney, Stone and Quirk, 1975; Ripley, 1976), and an influence of Atlantic sea surface temperature (Folland *et al.*, 1986). GCMs are the main tool available for investigating these ideas (eg. Laval and Picon, 1986) and their representation and parameterisation of the land surface needs to be realistic if they are to be successful.

The main objectives of HAPEX can be summarised as:
(1) Measurement of fluxes of radiation, sensible heat, water and CO_2 over a wide range of spatial scales at sites representative of the different surface conditions in the Sahelian zone.
(2) Relation of these fluxes to properties of the vegetation, soil and atmosphere in order to elucidate the controlling processes and allow development of predictive models.
(3) Testing and validation of techniques for remotely sensing the surface properties associated with these fluxes.

The main HAPEX experiment was carried out during an intensive observation period (IOP) from 15th August to 10th October 1992, which encompasses the transition from wet to dry season. The area that was studied is centred to the north east of Niamey, Niger and forms a 100 x 100 km square, a scale large enough for the results to be useful to GCM modellers. Within the square are three supersites: East Central, West Central and Southern. At each supersite are three or more subsites representing the major land surface types (millet, fallow and tiger bush), each of the order of 1 km^2. At all the subsites, ground based measurements were made of fluxes of radiation, heat, water, CO_2 and momentum, together with vegetation and soil properties and meteorological and hydrological variables. At the supersite scale, aircraft remote sensing and flux measurements were made. Satellites were used to make radiometric measurements on the scale of the entire HAPEX grid square.

1.4 The scaling problem

Much of the work in HAPEX is focussed on the so-called scaling problem, the extrapolation of small scale measurements and models to larger scales. "Scale" here may refer to both spatial and temporal scales. In the context of CO_2 exchange, we wish to infer values for ecosystem-scale fluxes over months and years from leaf-scale measurements made over periods of seconds. In addition, we also wish to extrapolate ecosystem-scale fluxes to regional scale. In the case of the surface energy balance,

GCMs represent the earth's surface on a very coarse scale, typically using grid squares larger than 10 000 km^2. However, the energy balance is typically measured by micrometeorological techniques over much smaller scales (of the order of 1000 m^2) and so some means of integrating properties and fluxes over a larger area is needed. Such extrapolation is not straightforward for two reasons (Luxmoore, King and Tharp, 1991):

(1) Where the response of a process established at a small scale is non-linear, taking the linear average of an input variable varying over a larger, heterogeneous area gives an incorrect result when used in that model to represent the larger area. For example, the response of leaf photosynthesis to photosynthetic photon flux density (Q) is typically non-linear, being asymptotic. Within canopies, the radiation environment also tends to be very heterogeneous. Therefore, using a simple average value of Q in a photosynthesis model does not yield the correct canopy photosynthetic rate. In mathematical terms,

$$y_i = f(x_i)$$

where this is a nonlinear function.

$$\bar{y} \neq f(\bar{x})$$

$$\bar{y} = \frac{\sum_{i=1}^{n} f(x_i)}{n}$$

When extrapolating from leaf to ecosystem scale, a greater variability in leaves and stems is encountered because of differences in species, age, position, sun/shade acclimation and nutrition etc. Furthermore, many of the natural processes of interest involve non-linear responses.

(2) New phenomena emerge at larger scales which are not considered in the formulation of the system at a small scale. For example, a photosynthetic response to Q established at leaf scale may not apply to the canopy because of the attenuation and scattering of radiation that occurs at the larger scale. Similarly, evaporation can be described as a function of stomatal conductance and saturation vapour pressure deficit (D) at the leaf scale. However at larger spatial scales, water vapour builds up within the leaf, canopy and atmospheric boundary layers, reducing D and providing a negative feedback on evaporation. At still larger scales, evaporation becomes more dependent on net radiation and entrainment into the atmospheric boundary layer (Jarvis and McNaughton, 1986; McNaughton and Jarvis, 1991). Beyond the scale of micrometeorological measurements, mesoscale circulations develop within the atmospheric boundary layer because of surface heterogeneity (Garratt, 1992), giving rise to complex interactions between adjacent surface types. When extrapolating observations in the temporal dimension, seasonal changes in leaf area and physiology have to be considered. These are also important when extrapolating observations to conditions of elevated CO_2 or increased

temperature, as instantaneous reponses may be different from long-term ones because of physiological acclimation and changes in leaf area and its phenology.

The major phenomenon that arises in the transition from leaf to ecosystem scale is the attenuation of radiation as it is absorbed and scattered by leaves and stems. Other feedbacks between vegetation and environmental variables such as D, atmospheric CO_2 concentration (C_a) and air temperature (T_a) may be important, depending on the degree of coupling between the canopy and the atmosphere (Jarvis and McNaughton, 1986), L_l and its three-dimensional distribution. These are summarised in Table 1.1.

Table 1.1 Interactions between vegetation and its atmospheric environment occurring at ecosystem scale.

Environmental variable	Interaction	Effect
Q	absorption	shading
	reflection	scattering
	transmisssion	"
D	transpiration	reduced D
C_a	photosynthesis	reduced C_a
	respiration	increased C_a
T_a	convection	increased T_a

Because of these problems, direct extrapolation from small to large scale is not normally possible and a modelling approach is usually adopted (Huston, 1991; Reynolds *et al.*, 1992; Ehleringer and Field, 1993). These scaling-up models need to be validated against actual measurements and this forms another major component of both this project and the entire HAPEX programme. For this purpose, measurements of surface properties and mass and energy fluxes were made on a range of scales from the single leaf, through individual plants, plant canopies and ecosystems, up to landscape and regional scale, using a variety of ground-based, aircraft and satellite techniques.

The following chapter describes the experimental sites within the context of the Sahelian environment. Chapters 3 and 4 consider the physiology of the system components, and describe the gas exchange measurements made on leaves (Chapter 3) and woody stems and soil (Chapter 4). The direct measurements of leaf area index and biomass are outlined in Chapter 5, and the attempts to measure canopy properties indirectly are described in Chapter 6. All these data are synthesised in Chapter 7, where the use of models to scale up in both space (from leaves to ecosystems and regions) and time (from minutes to the whole growing season) is discussed.

Chapter 2

Experimental Sites

2.1 Climate and Vegetation in West Africa

At the continental scale, a relatively simple broad pattern can be seen in the climate and vegetation of West Africa (Figure 2.1). The annual movement of the inter-tropical convergence zone (ITCZ) produces a rainfall gradient from the Guinea coast in the south to the Sahara desert in the north (Hayward and Oguntoyinbo, 1987). The region is extremely flat and consequently there is very little variation in precipitation related to topography. The intra-annual temporal distribution of rainfall also varies uniformly along the north-south axis. Rainfall is continuous throughout the year on the southern coast, becoming increasingly seasonal to the north until it reaches almost zero in the interior of the Sahara.

The effect of this climatic gradient is to produce a corresponding gradient in the vegetation. This continuum has been classified into discrete units (eg. Huntley and Walker, 1982; White, 1983; Lawson, 1986). Evergreen tropical rain forest predominates along the Guinea coast and up to 100 km inland. To the north is a zone of deciduous woodland which becomes increasingly less dense, eventually forming tree savannah where tree cover is very broken and perennial grasses dominate. Further north and drier still, few grasses can survive the extended dry season and trees become increasingly confined to water courses. The Sahelian zone is characterised by annual grasses, which grow only during the short wet season, and drought-adapted trees and shrubs (Monod, 1986). Where annual rainfall is less than around 100 mm, very little vegetation survives, and is restricted to extremely drought tolerant species and short-lived ruderals which can grow and reproduce in the few days with moist soil after a rain event (Gillet, 1986). There are large areas of the Sahara desert in which no vegetation is present for much of the time.

2.2 The Sahel

Definition

In its broadest sense, the Sahel is defined as the region south of the Sahara desert, between the 100 and 700 mm isohyets. The boundary with the desert to the north is relatively clearcut. The 100 mm isohyet corresponds to the limit between "contracted" vegetation (confined to water courses and depressions) to the north and "scattered" vegetation (more or less continuous, albeit sparse) to the south (Monod, 1954). The southern limit of the Sahel is less clearcut and ranges from the 400 to 700 mm isohyet, depending on the author. However, it is generally taken to be the limit between the

(a) Vegetation

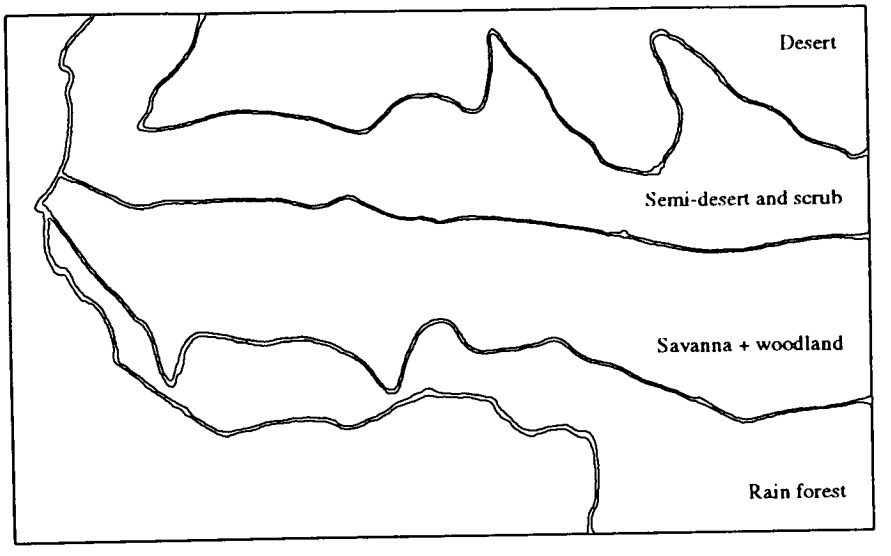

(b) Rainfall

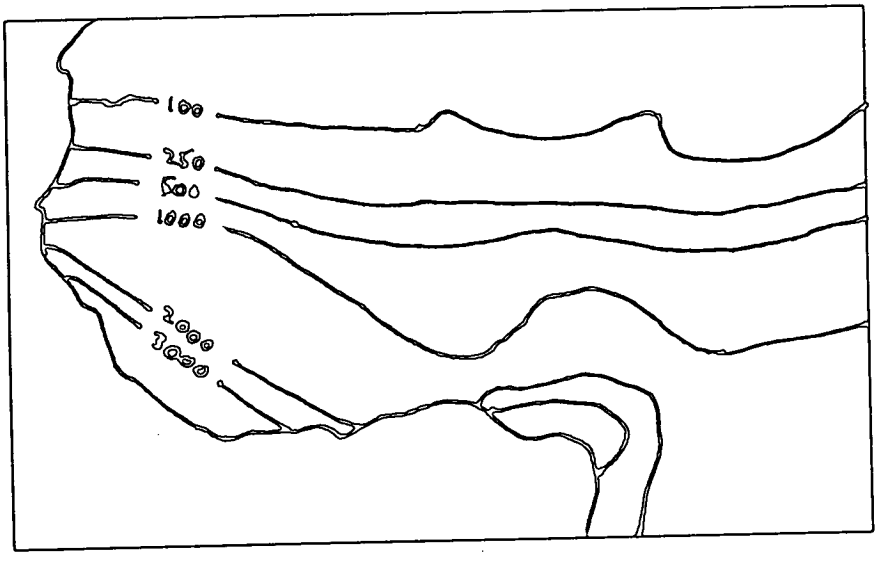

Figure 2.1 Maps showing the distribution of (a) vegetation types and (b) rainfall in West Africa. (b) shows isohyets with annual rainfall values in mm.

annual grasses and widely spaced, drought-hardy trees in the more arid Sahel and the tall perennial grasses and denser tree cover of the Guinea savanna to the south (Le Houerou, 1989).

Similarly, subdivisions within the Sahel vary from author to author, but often three are defined (Le Houerou, 1989). In the north is the Sahara-Sahel transition zone (100 - 200 mm of rainfall), with a sparse vegetation of highly xeromorphic perennial grasses on sandy soil. Trees and shrubs are infrequent except along water courses and in depressions. The true Sahel (200 - 400 mm of rainfall) is characterised by Mimosaceae thorn scrub. Three layers are usually present: a ground layer of annual grasses and forbs, a shrub layer, mostly of Acacia species, and a sparse tree layer also dominated by acacias and a few other species. The trees and shrubs are nearly all thorny with much reduced, narrow (microphyllous) leaves. The Sudano-Sahel zone (400 - 600 mm of rainfall) is similar to the true Sahel except that broad-leaved species, especially of the Combretaceae, are dominant in the tree and shrub layer. The vegetation is more continuous, with higher tree and shrub densities and also with occasional perennial grasses. Vegetation arcs or "tiger bush" (*brousse tigree* in French) may develop on shallow soils with iron hardpans, where strips of vegetation form parallel to the contours, interspersed with areas of bare, indurated soil (White, 1969). Millet may also be cultivated regularly on a rotational system in which land is left fallow for seven to ten years between periods of cultivation. The HAPEX square lies within this last zone.

Climate

The Sahel is hot all year round, with average maximum daily temperatures ranging from 33 °C in January to 41 °C in April. The major annual feature is the wet season (Figure 2.2), approximately from June to September (although the onset of the rains is very variable) during which more than 90 % of the rains fall. This is followed by a warm dry season from October to mid-March and a hot dry season from mid-March to the first rains. Rainfall at Niamey averages 562 mm per year (1905 to 1986 mean). This contrasts with a potential evaporation of 2057 mm per year (1953 to 1962 mean (Sivakumar (1987)). Consequently, the water balance is in deficit for much of the year.

Rainfall in the Sudano-Sahel is largely the result of squall lines (Barry and Chorley, 1992). Between June and October, pressure waves develop in the easterly airflow across West Africa, at the interface with the lower south-westerly airflow. These move towards the west at a speed of 18-35 km h^{-1}, with a periodicity of 3-5 days. In intense waves which extend down to the surface, updraughts are produced, causing thunderstorms and heavy rain. Because of the sporadic nature of squall line formation and the relatively small scale of the storms produced, spatial and temporal heterogeneity in rainfall over the Sudano-Sahel is very large. Rainfall at the three southern subsites in 1992 ranged from 544 to 706 mm although they were only 9 km apart. Together with differences in the northward movement of the ITCZ and other poorly understood factors, such as Atlantic sea surface temperature (Folland *et al.*,

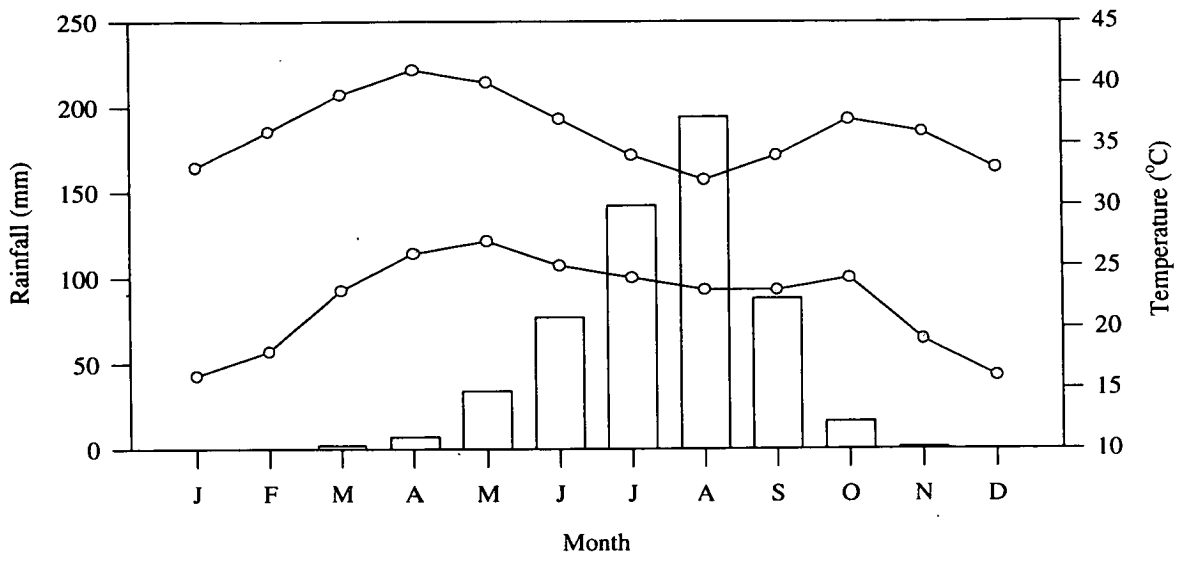

Figure 2.2 Climate diagram for Niamey showing rainfall (bars) and maximum and minimum daily temperatures (lines). Data are means for the period 1905 to 1986.

1986), differences in rainfall between years are also large (Morales, 1977; Sivakumar, 1987).

Land Use

The land is divided into areas where the laterite formation remains intact and those areas where it has been eroded to form a sandy soil. The former constitute slightly elevated plateaux and support the natural tiger bush vegetation, as cultivation is not possible. The latter are almost entirely devoted to millet cultivation, with the natural bush vegetation only present in an early successional stage on fallow land. Three sub-sites were chosen at each supersite to represent these main vegetation types: millet, fallow and tiger bush. The location of the sub-sites at the southern supersite is shown in Figure 2.3.

Compared with landscapes in previous land surface parameterisation experiments in temperate zones (such as FIFE and HAPEX-MOHBILY), the Sahelian vegetation is much more heterogeneous at a small scale, as millet fields, fallow areas and tiger bush all occur in a mosaic within the approximately 100 km^2 supersites. However on a regional scale of 1000-10 000 km^2, the pattern is relatively homogeneous, as few land surface types occur within the landscape other than these three.

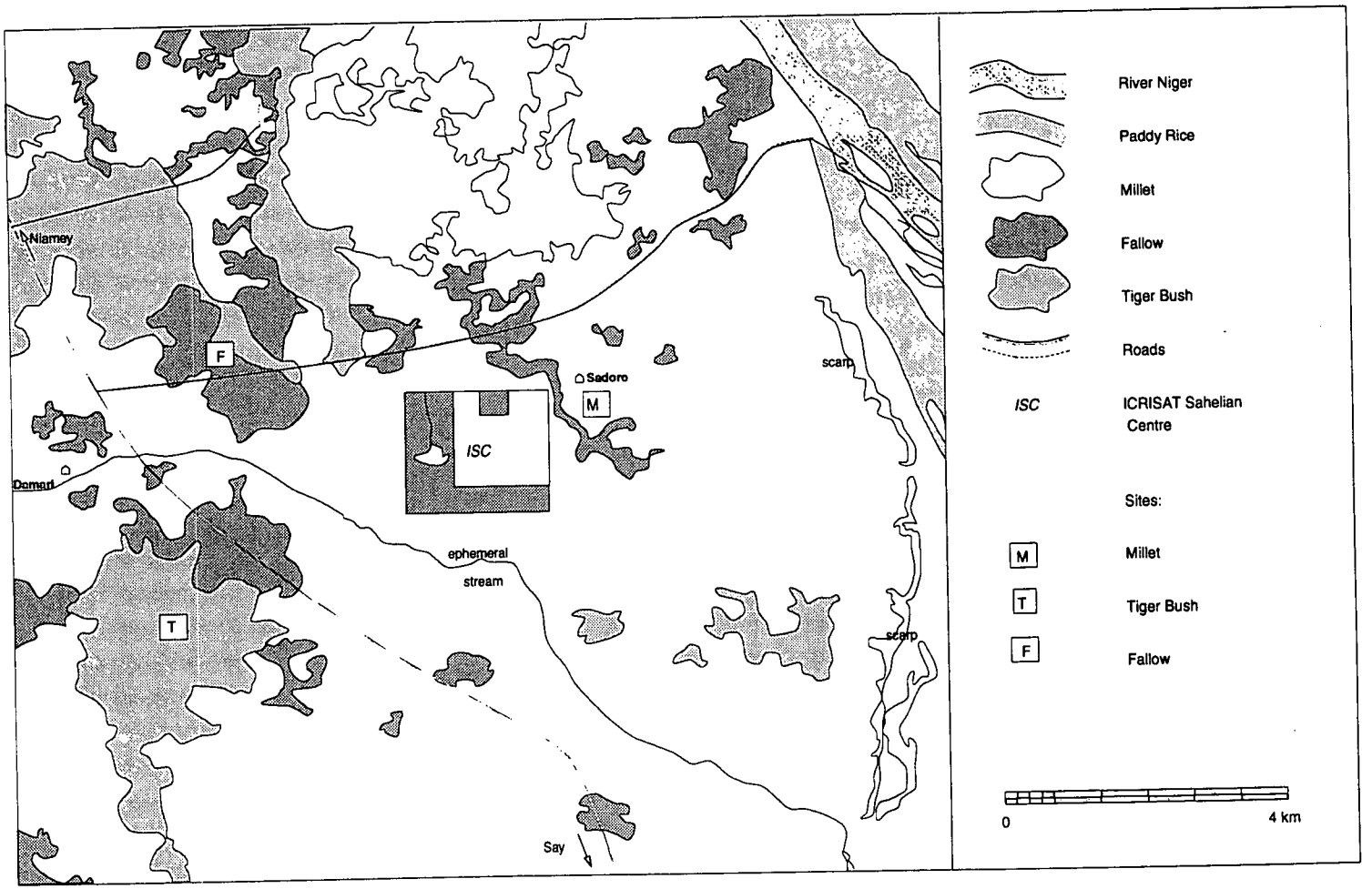

Figure 2.3 Map showing the HAPEX-Sahel southern supersite and the location of the three sub-sites.

2.3 Millet

90 % of the cultivated land is devoted to millet (*Pennisetum* spp.), a C4 cereal grown as a subsistence crop by farmers throughout much of the semi-arid tropics where rainfall is inadequate for other cereals. Millet can produce grain with 200 mm of rainfall although it usually requires 400 to 800 mm. Agricultural work is carried out by hand, using traditional methods. Tree clearing is followed by seeding without soil surface preparation other than addition of cattle manure and weeding. Seed planting is carried out in May or June, depending on when the rains are judged to have started adequately, and harvesting takes place in September.

The millet site was located 1 km to the east of ICRISAT Sahelian Centre (ISC, ICRISAT is an acronym for International Crop Research Institute for the Semi-Arid Tropics) (13° 14.48 N, 2° 17.94 E) (Figures 2.3 and 2.4). Plate 1 shows the view to the south-east from the micrometeorological mast during mid-August 1992. The area was planted with the local millet land race (Sadore local) and cultivated using traditional methods. Measurements were made in the area south and west of the vehicle access route. Several trees were present in the fields, as is typical in the region. These were mainly *Combretum glutinosum* Perrot. ex DC. and *Faidherbia albida* (Del.) A. Chev., with *Annona senegalensis* Pers. also present. The millet was planted between 16 May and early June at an average density of 4600 (s.e. +/- 1260) pockets per hectare (1.4 m spacing), with around three plants per pocket after thinning. With sufficient rainfall, the crop grew well and senescence started in late August. Harvesting began in early September, producing an average yield of 650 kg grain ha^{-1} (s.e. +/- 391, range of 0-2885 in the 400 5x5 m plots in the 1 ha millet growth plot (Figure 2.4) (Brouwer *et al.*, in prep). Cowpea or "niebe" (*Vigna unguiculata* (L.) Walp.) was sown between the millet plants in early July at an average density of 886 (s.e. +/- 463) plants per hectare and harvested in late October. The average yield was 112 kg ha^{-1} (s.e.+/- 88, range of 0-666 in the 400 5x5 m plots). No measurements were made on cowpea or the trees at the site.

Soil at the site was extremely sandy, comprising approximately 90 % sand, 5 % silt and 5 % clay, and classified as Psammentic Paleustalfs (West *et al.*, 1984). One hundred samples taken from the 1 ha millet growth plot (Figure 2.4) gave average values of 0.14 % organic carbon by mass (range of 0.09-0.20 %), 950 meq kg^{-1} effective cation exchange capacity (range of 650-1650) and pH 4.07 (range of 3.85-4.74) (Wallace *et al.*, 1994). The water table was at a depth of around 25 m and there was a layer of very hard laterite at 2.5-3 m.

Plate 1 The millet site, mid-August 1992.

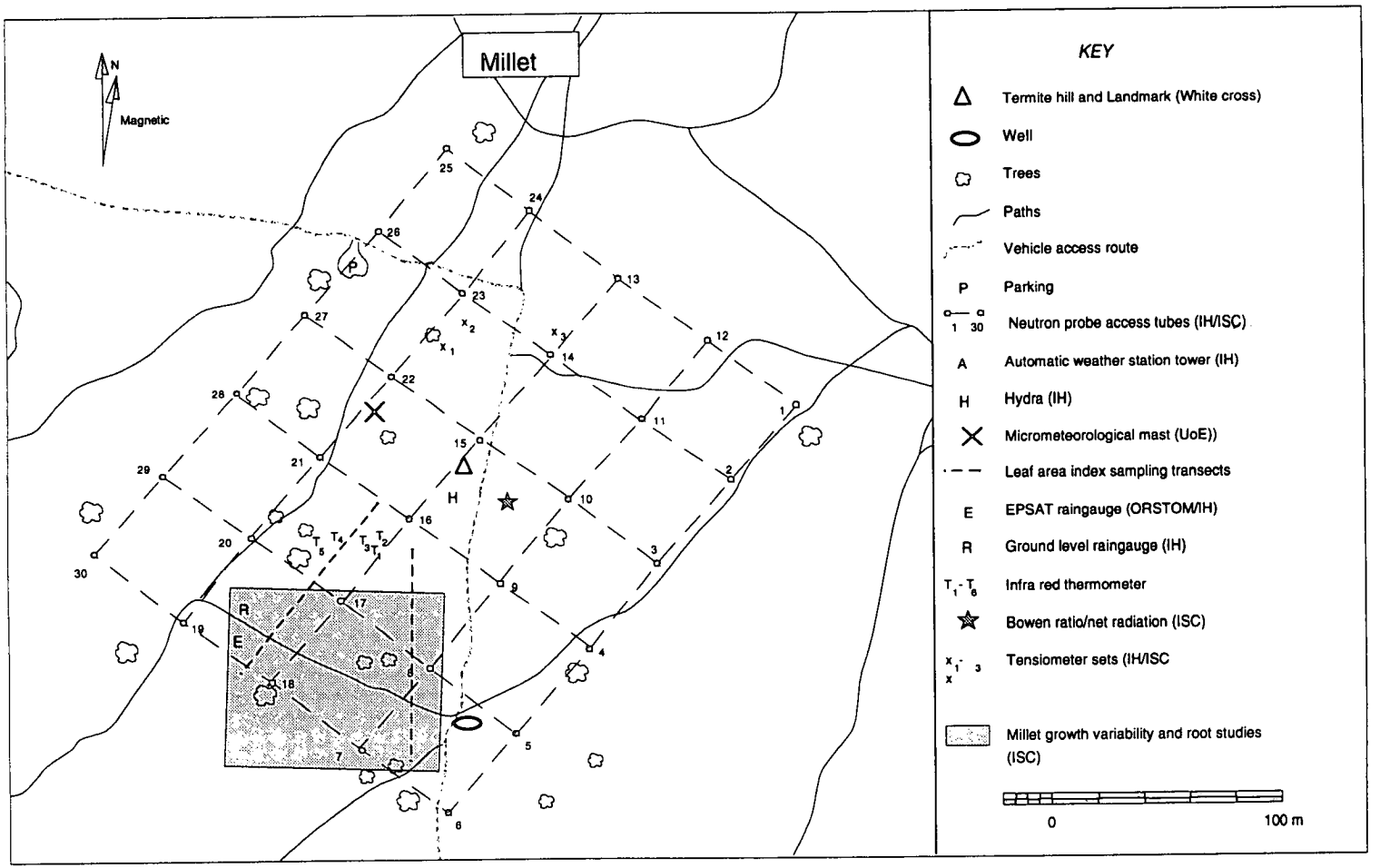

Figure 2.4 Schematic diagram of the millet site, showing positions of the main instrument towers, the neutron probe access tube grid and leaf area measurements.

2.4 Fallow

Fallow land throughout the region is characterised by shrub vegetation dominated by *Guiera senegalensis* L., a bush which grows to 3 m, with a ground layer of annual grasses and legumes. When clearing of shrubs for millet cultivation ceases, *G. senegalensis*, an early succesional species rapidly colonises the ground. If left indefinitely, the natural bush vegetation would presumably develop. The bushes are mostly leafless over much of the dry season, although the remaining leaves are physiologically active. The defoliation is partially the result of grazing by goats when little other fodder is available. Leaf growth in *G. senegalensis* seems to precede the start of the rains, beginning in May. The annual ground layer develops later, after the rains have begun.

The fallow site was located about 4 km west of ISC (13° 14.63 N, 2° 14.65 E) (Figures 2.3 and 2.5), bounded to the north and north-east by tiger bush and by millet fields on other sides. Plate 2 shows the view looking east from the IH micrometeorological tower in mid-August 1992. The area of fallow enclosed had not been planted with millet for about seven years and semi-natural vegetation had regrown. This comprised a shrub component, almost exclusively *G. senegalensis* with an occasional *Combretum micranthum* G. Don., and a herb component dominated by grasses and legumes. Occasional trees, mainly *C. glutinosum*, were also present. The density of *G. senegalensis* bushes measured in a 6750 m^2 sample plot was 327 per hectare. The average height of the bushes was 2.2 m. The ground flora was dominated by *Eragrostis tremula* Hochst. ex Steud, *Mitracarpus villosus* (Sw.) DC., *Cassia mimosoides* L. and *Cenchrus biflorus* Roxb. Grazing by sheep and cattle took place occasionally. The soil was similar to that at the millet site, but the layer of laterite was slightly higher, often starting at 2 m, whilst the water table was slightly deeper at 32 m.

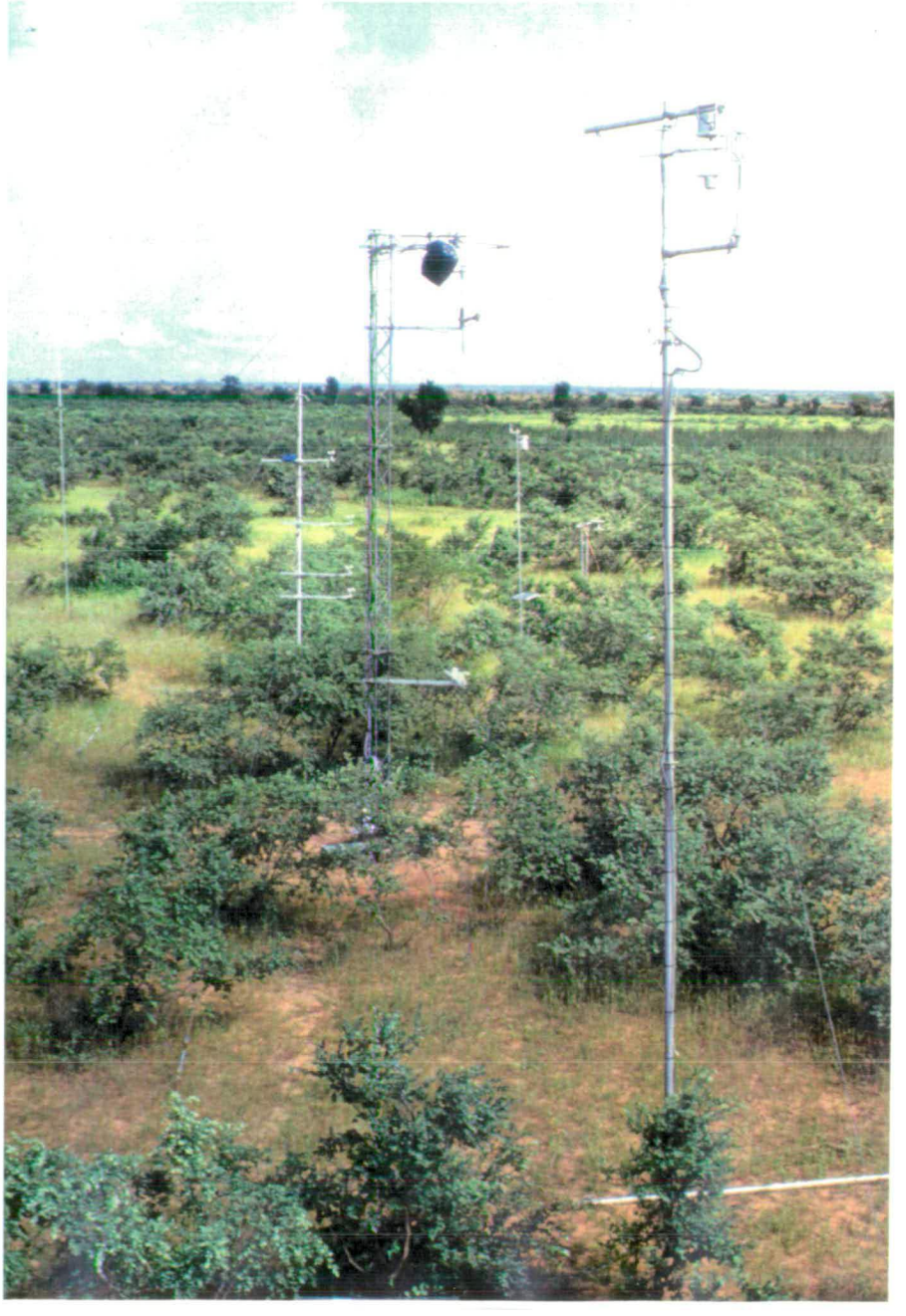

Plate 2 The fallow site, mid-August 1992.

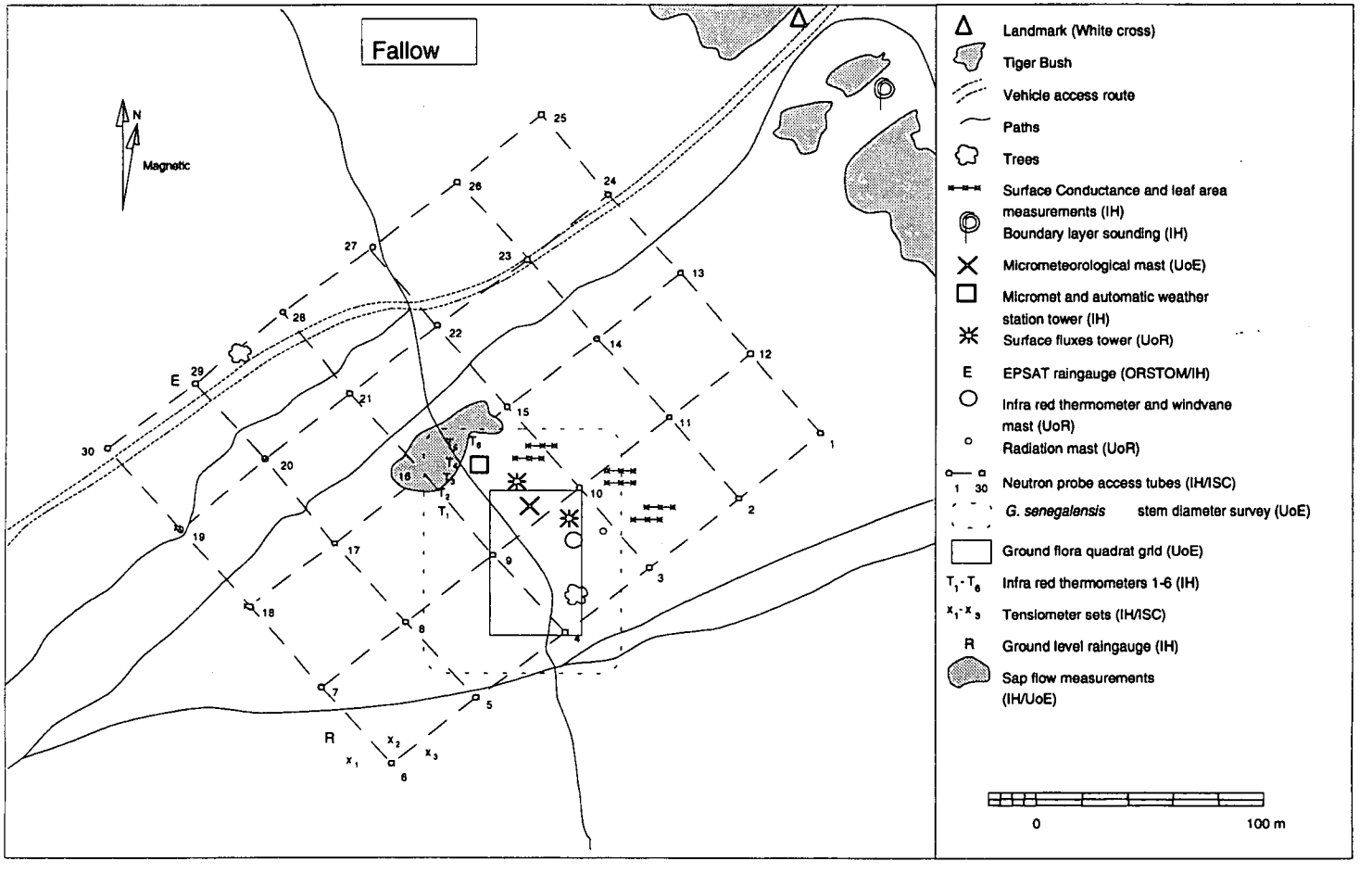

Figure 2.5 Schematic diagram of the fallow site showing the positions of the main instrument towers, the neutron probe access tube grid and leaf area measurements.

2.5 Tiger bush

Tiger bush is characterised by stripes or arcs of vegetation tens of metres in width and up to several hundred metres in length. These are separated by areas of completely bare, indurated soil. The work of Clos Ardec (1956) suggested that the stripes were a static feature related to soil properties, termite activity or wind. However, later work (Worral, 1959, 1960a, 1960b; White, 1969, 1970, 1971; Wickens and Collier, 1971; Ambouta, 1984) suggests that tiger bush and other similar "vegetation arcs" are caused by a positive feedback process between the vegetation and soil moisture in areas where sheet wash is an important source of water for plants. More runoff infiltrates in vegetated areas as plants slow down surface flow and provide avenues of penetration, thus increasing soil moisture and encouraging further growth. Areas downslope of vegetation receive less runoff and vegetation development is consequently inhibited. Within a patch, the plants on the upslope side receive more water than those on the downslope side. The former thus grow and reproduce better and may extend up the slope, further diminishing the input of water to the latter, which slowly die. In this way, stripes may migrate upslope on a time scale of tens of years.

The tiger bush site was located 7 km south-west of ISC (13° 11.89 N, 2° 14.37 E), at the centre of an irregularly-shaped area of tiger bush which was approximately 3 km in diameter (Figure 2.3 and 2.6). Plate 3 shows the University of Edinburgh micrometeorological tower during September 1992. Measurements were concentrated on seven vegetation strips around the micrometeorological towers. The dominant species were *Combretum nigricans* Lepr. ex Guill. et Perrott (a tree up to 10 m) and the shrubs *C. micranthum* and *G. senegalensis*. Other less frequent tree species included *Acacia ataxacantha* DC., *Sclerocarya birrea* (A. Rich) Hochst. and *Boscia angustifolia* A.Rich. A herb layer was present, including all the major species present at the fallow site plus several more. However, the herb layer did not develop to the same extent as on the fallow site and was not measured. The vegetated strips cover approximately 33 % of the surface area, as estimated from aerial photographs of the entire area of tiger bush.

The perennial species are all drought deciduous to some extent, although the tree *C. nigricans* retains approximately half its leaves over the dry season whilst the shrub *C. micranthum* loses all. This may be related to differences in grazing pressure, as many of the leaves of *C. nigricans* are outwith the reach of goats. Leaf growth begins in late May and senescence starts in late September.

The soil at the site was gravelly sandy loam or gravelly loam above weathered laterite, to a depth of 0.1-0.5 m, with solid laterite starting at 0.2-0.9 m. In the open areas, the surface was virtually impermeable because of a hard crust. The soils are classified as Xerothents on the bare areas and Ustorthents under the vegetation (Soil Survey Staff, 1975).

Plate 3 The tiger bush site, September 1992.

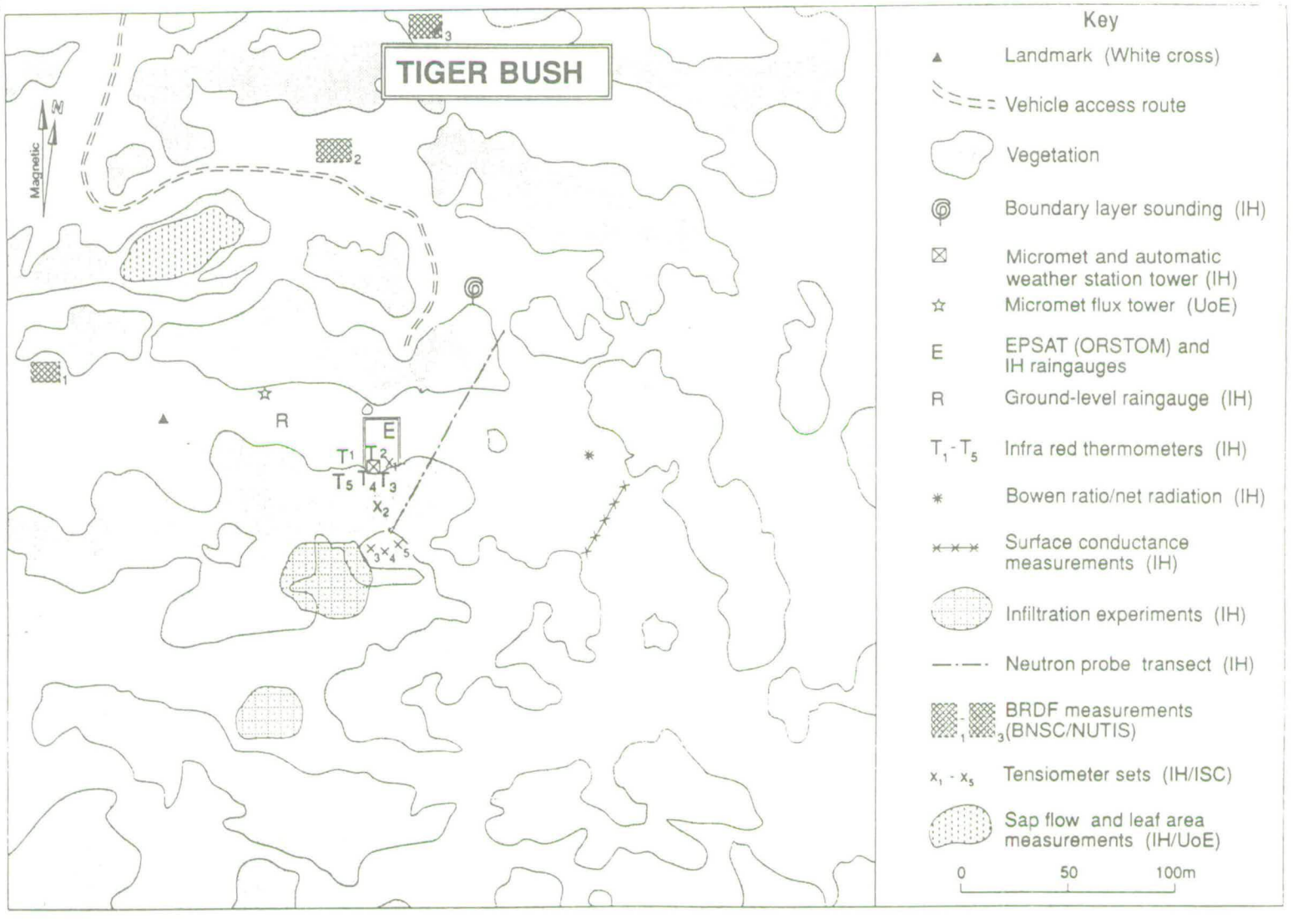

Figure 2.6 A schematic drawing of the central part of tiger-bush sub-site . The positions of the main instruments towers and location of one of the neutron probe access tube transects are shown.

Chapter 3

Leaf Gas Exchange

3.1 Introduction

Photosynthetic assimilation of CO_2 by the leaves, A_l, is the dominant process determining the CO_2 flux to a canopy and is conveniently measured by modern portable gas exchange systems. Such systems also measure stomatal conductance, g_s, which is a key variable determining the diffusion of CO_2 through the stomata. In addition, sensors within the system measure incident photosynthetic photon flux density (Q), air temperature (T_a), and leaf temperature (T_l) simultaneously, which, together with weather station data permit the interpretation of photosynthesis measurements in terms of environmental variables. However, under field conditions, many environmental variables tend to fluctuate together. For example, T_a and the ambient air saturation vapour pressure deficit, D, tend to follow a very similar pattern over the course of a day. Because of these correlations, it is often difficult to attribute an observed change in A_l or g_s to a single environmental variable. Furthermore, because A_l and g_s are affected by several variables, two-dimensional plots of the dependent versus a single independent variable often do not show clear relationships. More commonly, a scatter of points is obtained, where most of the points represent conditions in which the dependent variable is limited by some other variable and only the upper limit of the scatter represents the response to the x-axis variable. This upper limit is often poorly defined as the data are not usually well distributed throughout the n-dimensional variable space. Interpretation of such plots is further complicated as the principle of limiting factors does not apply. Rather than proceeding at the rate set by a single limiting factor, A_l is determined by the overall limitation set by several factors (Woodrow *et al.*, 1990; Jones, 1992). For example, A_l is not simply detemined by whichever variable (such as Q, T_l or g_s) is most limiting, but is a complex function of all of these.

In order to overcome these difficulties of interpretation, photosynthesis data can be fitted to a model accounting for the known responses to environmental variables (Reed *et al.*, 1976; Watson, Landsberg and Thorpe, 1978). The model is fitted to the data using non-linear, least squares regression, which finds the set of model parameters which minimises the residual sum of squares. In principle, if several responses are fitted simultaneously, this is equivalent to defining the upper boundaries on the scatter plots for each of the independent variables. Two photosynthesis models were used. The first was a very simple Q response model, which assumed that photosynthesis can be described by a rectangular hyperbola,

$$A_l = \frac{P_{max}\alpha\ Q}{P_{max} + \alpha\ Q} - R_d \qquad [3.1]$$

where α is the quantum efficiency (moles of CO_2 assimilated per mole of incident quanta), R_d is the dark respiration rate (assumed to be constant) and P_{max} is the asymptotic value of P with respect to Q where

$$P = A_l + R_d. \qquad [3.2]$$

This was only used as a tool for preliminary analysis.

The second model was a modification of Reed *et al.* (1976), described in Jarvis, Miranda and Muetzelfeldt (1985) and illustrated in Figure 3.1(a-d). It assumed that:

(1) photosynthesis is related to Q by a non-rectangular hyperbola

$$\theta\ P^2 - P\ (\alpha\ Q + P_{max}) + \alpha\ Q\ P_{max} = 0 \qquad [3.3]$$

$$P_{max} = A_{lmax} + R_d \qquad [3.4]$$

where θ is a coefficient determining the convexity of the A-Q response;

(2) photosynthesis is linearly related to the mean intercellular space CO_2 concentration, C_i,

$$A_{lmax} = (C_i - \Gamma)\ g_m \qquad [3.5]$$

where Γ is the CO_2 compensation concentration;

(3) C_i depends on the ambient CO_2 concentration, C_a, the rate of photosynthesis and stomatal conductance

$$C_i = C_a - A_l / g_S \qquad [3.6]$$

(4) dark respiration, R_d, is an exponential function of leaf temperature, T_l,

$$R_d = R_o \exp(k\ T_l) \qquad [3.7]$$

where R_o is the respiration rate at 0 °C and k is a temperature coefficient;

(5) mesophyll conductance, g_m, is a bell-shaped function of temperature. The function (Reed *et al.* (1976)) has three parameters which define the maximum, optimum and minimum temperatures for g_m and is illustrated in Figure 3.1(d). In practice, it did not improve the fit of the model.

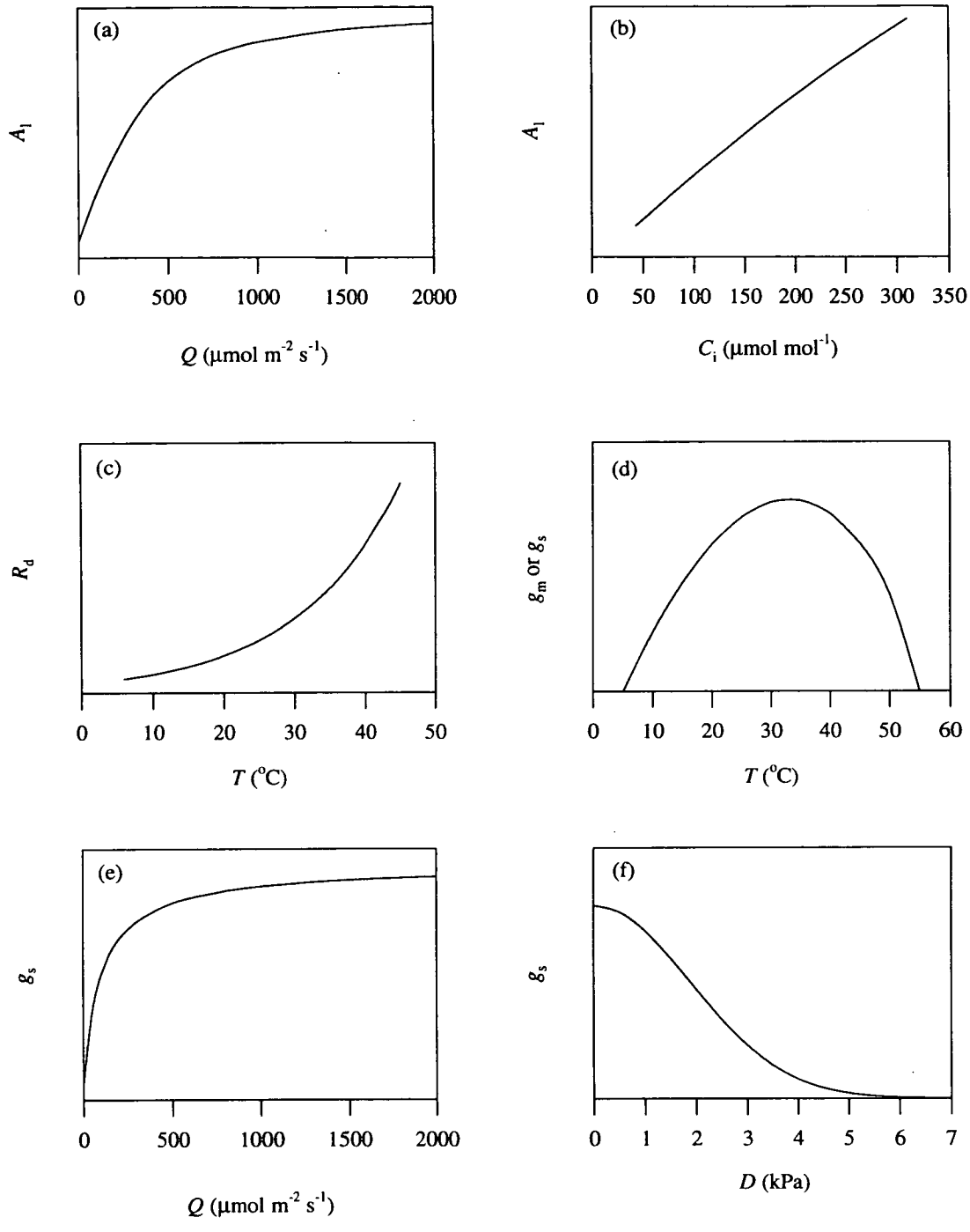

Figure 3.1 Form of the functions used in the Jarvis, Miranda and Muetzelfeldt (1985) photosynthesis model (a-d) and the stomatal conductance model (d-f) based on that of Jarvis (1976).

Combining Equations 3.2-3.6 with the elimination of C_i gives a quadratic equation for A_l in terms of the leaf variables g_s, g_m, α, θ, Γ and R_d, and the environmental variables Q and C_a:

$$A_l = \frac{-b - \sqrt{b^2 - 4ac}}{2a} \qquad [3.8]$$

where

$$a = \theta + \frac{g_m}{g_o} \qquad [3.9]$$

$$b = R_d(2\theta + \frac{g_m}{g_o} - 1) - \alpha\, Q(1 + \frac{g_m}{g_o}) - g_m(C_a - \Gamma) \qquad [3.10]$$

$$c = \alpha\, Q g_m(C_a - \Gamma) + R_d(R_d\theta - R_d - g_m(C_a - \Gamma)) \qquad [3.11]$$

and

$$g_o = \frac{g_s\, g_a}{g_s + g_a}. \qquad [3.12]$$

This phenomenological model was used in preference to the commonly used model of Farqhuar and von Caemmerer (1982), which is more mechanistic as it simulates the carboxylation reactions. However, simulating the more complex sub-leaf scale processes inevitably requires more parameters and additional coefficients pertaining to enzymes kinetics, and is consequently more difficult to fit to field data.

Analagously, g_S data can be fitted to a model accounting for the response of stomata to Q, D, C_a and T_l (Jarvis, 1976), illustrated in Figure 3.1(d-f). This model is inevitably phenomenological as stomatal functioning is still poorly understood at the cellular level, but the general form of the response equations is relatively well known. An exception to this is the reponse of stomata to humidity, which is still controversial (Monteith, 1995). The model is the same as that of Jarvis (1976) except: (1) no response to leaf or soil water potential is included, as the former was not measured and using soil water potential in place of leaf water potential in the Jarvis (1976) model did not improve the fit to the data (2) the response to C_a is ignored, as no effect was observed over the rather small range that was encountered (~50 μmol mol^{-1}), and (3) the form of the humidity response is different. The original model assumed a simple linear decline in g_S with D, but a curvilinear relationship is more usual (eg. Lohammer *et al.*, 1980; Leverenz, 1981; Leuning, 1995; Monteith, 1995) and was found in the present data.

The model assumes that:

(1) g_S is related to Q by a rectangular hyperbola

$$g_s(Q) = \frac{g_{smax}\, g_{slope}(Q + (g_{sdark}/g_{slope}))}{g_{smax} + g_{slope}(Q + (g_{sdark}/g_{slope}))} \qquad [3.13]$$

where g_{smax} is the asymptotic value of stomatal conductance with respect to Q, g_{slope} is the initial slope of the response to Q and g_{sdark} is the stomatal conductance in the dark;

(2) g_S declines exponentially with D

$$g_s(D) = \exp\left(\frac{-D^2}{D_0}\right) \qquad [3.14]$$

where D_0 is a parameter defining the rate of decrease with D;

(3) g_S is a bell-shaped function of temperature; and

(4) there are no interactions between variables, so that

$$g_S = g_S(Q) \cdot g_S(D) \cdot g_S(T). \qquad [3.15]$$

Once the best fit of the model to the data has been found, analysis of the residuals may be informative. If a relationship was found between a particular variable and the residuals, this would suggest that this variable was influencing the dependent variable in a way not accounted for by the model. This may be the result of a causal relationship or systematic error. When a satisfactory fit to the model was obtained and the residuals showed that there was no obvious source of unexplained variation in the data, the model parameters were used in the photosynthesis and conductance sub-models of MAESTRO and the big leaf model.

3.2 Methods

Measurements of leaf CO_2 flux and stomatal conductance were made using the ADC Leaf Chamber Analysis system (LCA3) and ADC Parkinson Leaf Chambers (PLC3(C) and PLC3(N)). The system is fully described in Appendix 1. Measurements were made between July and October 1991, February and March 1992 and June and October 1992 on the species listed in Table 3.1.

Table 3.1 Details of the major species on which leaf gas exchange measurements were made. * N = Narrow leaf chamber PLC3(N), C = conifer chamber PLC3(C).

Species	Authority	Family	Form	Site	Photo -synthetic pathway	Chamber used*
Pennisetum glaucum (Millet)	L. R. Br. cv. Sadore local	Gramineae	Crop	Millet	C4	N
Eragrostis tremula	Hochst. ex Steud.	Gramineae	Grass	Fallow	C4	N
Cenchrus biflorus	Roxb.	Gramineae	Grass	Fallow	C4	N
Mitracarpus villosus	(Sw.) DC.	Rubiaceae	Herb	Fallow	C3/C4	C/N
Cassia mimosoides	L.	Leguminosae	Herb	Fallow	C3	C/N
Guiera senegalensis	J.F. Gmel.	Combretaceae	Bush	Fallow	C3	C
Combretum micranthum	G. Don	Combretaceae	Bush	Tiger bush	C3	N
Combretum nigricans	var. elliotii (Engl. et Diels)	Combretaceae	Tree	Tiger bush	C3	N
Acacia ataxacantha	D.C.	Mimosaceae	Climbing tree	Tiger bush	C3	C

Prior to a measuring session, the system was left to run in the shade for at least ten minutes to allow stabilisation of CO_2 concentration and humidity readings and to ensure that no differential signals were produced by an empty chamber. Reference air was taken from upwind of the recorder at a height of 2.75 m using a fibreglass mast. This was then passed through a 1 dm^3 buffer volume to minimise any fluctuations in reference CO_2 concentration. Before making a measurement, the leaf thermistor was first attached to the underside of the leaf to be measured using a very small amount of "Blue-tac" adhesive. The chamber was then clamped on to the leaf or shoot. When CO_2 concentration and humidity readings stabilised, usually after 0.5 to 1.5 minutes, the values of all variables were stored in the LCA3 memory and the chamber removed. Because of the different response times of photosynthesis and stomatal conductance to a change in their driving variables, rather different approaches were needed in their measurement. Photosynthesis responds almost immediately, so responses can be derived from short term changes to the environment, eg. shading of the chamber. Stomata, on the other hand, respond more slowly but will begin adjusting to new conditions within a minute or two (this is considered fully in Section 3.6). Consequently, measurements were of the following two types:

(1) *Manipulated Q*. These were made over several minutes, during which shading was used to determine the response of A_l to Q. Different cloths were used to cover the chamber, removing a fraction of incident Q. Q could also be changed by altering the orientation of the chamber relative to the sun. In all cases, the first measurement was made quickly to represent ambient Q in the leaf's natural position and the second attempted to achieve a higher Q by altering the chamber orientation. Subsequent measurements were made with progressively lower Q by adding shade cloths and/or changing the chamber orientation.

(2) *Ambient Q*. These were made rapidly so as to be representative of the stomatal conductance of the leaf in ambient conditions. Responses to environmental variables were derived from longer term (diurnal and seasonal) and spatial variation. During measurements, the leaf was held close to its original position and orientated so as to receive a relatively constant Q, close to the original value.

A consistent sampling strategy used to select leaves for measurement. At each site, linear transects were subjectively located so as to pass through areas of vegetation similar to that within the fetch of the micrometeorological instruments. At the millet site, sample points were located at intervals of ten paces along the transect. One tiller from the nearest pocket to each point was chosen at random. Measurements were made on every second leaf on the selected tiller, starting from the bottom working upwards. The midpoint of the leaf was used for measurements. At the fallow site, a similar system was used, except that sample points were twenty paces apart on the transect. When measuring *G. senegalensis*, shoots were selected on the closest bush at heights of 0.5, 1 and 1.5 m. The procedure was the same when measuring the ground flora species, except that leaves were selected from immediately around the sample point. At the tiger bush site, transects perpendicular to the direction of the stripe were used when measuring *C. micranthum*. The distance between sampling points was 10 m but the method was otherwise similar to that used for *G. senegalensis*. Sampling of *C. nigricans* was not systematic because of its scattered distribution and difficulties in reaching upper leaves.

When using the PLC(C), the shoots were removed after measurements and placed in plastic bags inside an insulated cool box in the shade. The area of these shoots was measured in the laboratory using a Li-Cor 3100 area meter. When using the PLC(N), the leaves of millet and *C. nigricans* were usually large enough to cover all of the chamber area (11 cm^2). In the case of *E. tremula* and *C. biflorus*, the leaves were long enough to fit the length of the chamber (5.6 cm) but considerably narrower (typically 3-5 mm). The maximum and minimum leaf width within the chamber was measured and the area calculated assuming a trapezium shape. *M. villosus* and *C. micranthum* would typically cover 60-80 % of the PLC(N) chamber area and this was estimated by eye using a grid overlaid on the chamber window. *C. mimosoides* and *A. ataxacantha* have the finely divided, microphyllous leaves typical of *Acacia* species. The opposite sides of shoots fold together and curl up

within minutes after cutting, making accurate area determination very dificult. Samples were cut up with scissors before being measured with the Li-Cor 3100, but no easy way to prevent or estimate the change in area with curling was found. Few measurements were made on these species, partly for this reason.

Although the calculation of gas exchange parameters can be made by the LCA3 software, all values were recalculated from the measured variables using a spreadsheet, following the equations of Field, Ball and Berry (1989) and ADC (1990). This was done for two reasons: (1) when using the PLC3(C), leaf area was measured after the gas exchange measurement, and (2) software errors sometimes occurred in the measurement of leaf temperature and these cases were recalculated using the leaf temperature derived from the energy balance (Parkinson, 1983). Non-linear regression (SPSS, version 4 for Unix) was used to fit the models describing the expected responses of A_l, R_d and g_S to environmental variables.

3.3 Respiration, R_d

Measurements made using a shade cloth to give complete darkness were used to derive the relationship between leaf temperature and respiration (Figure 3.2). There is a paucity of data and considerable scatter, but an increase in respiration with temperature is detectable in all cases. Non-linear regression was used to fit Equation 3.7 to the data for the four species (Table 3.2). Temperature explains between 18 and 76 % of the variation in the data. Respiration is notably higher in millet than in the other three species shown, with a rate of nearly 4 μmol m^{-2} s^{-1} at 30 °C compared with 1-2 μmol m^{-2} s^{-1} in the other species. This may be a result of higher nutrient status within the fertilised crop plants. Respiration data in the literature are commonly described by a "Q_{10}" temperature coefficient (Q_{10} = exp(10k), which usually takes a value between 1.4 and 2.2 (Larcher, 1980). Values for all the species here fall within this range except *C. micranthum*, where the fit to the data was considered unrealistic.

Table 3.2 Parameters of Equation 3.7 fitted to respiration data from four species. *The fit to the *C. micranthum* data was considered unrealistic.

Species	R_o (μmol m^{-2} s^{-1})	k ($°C^{-1}$)	"Q_{10}" temperature coefficient	r^2	n
Millet	0.885	0.048	1.62	0.32	22
E. tremula	0.188	0.069	1.99	0.76	8
*C. micranthum**	0.0026	0.171	5.53	0.54	12
C. nigricans	0.413	0.054	1.72	0.18	46

All measurements were made during daytime, and the effects of substrate concentration and circadian rythms were not considered, although these may make night-time respiration values different. Also, in

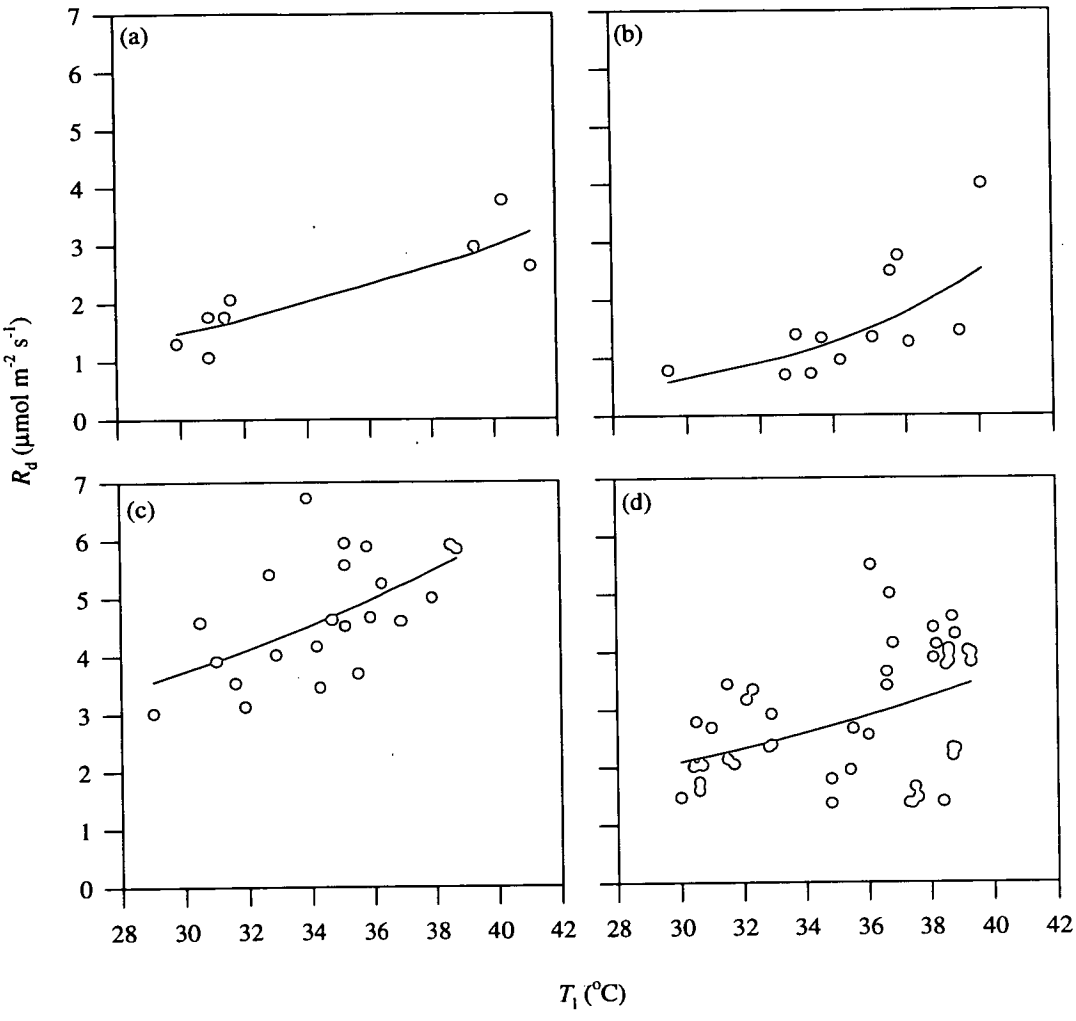

Figure 3.2 Relationship between leaf dark respiration, R_d, and leaf temperature, T_l, in (a) *E. tremula*, (b) *C. micranthum*, (c) millet and (d) *C. nigricans*. Measurements were made by completely shading the cuvette with cloth. The range of temperatures was obtained by making measurements at different times of day. Data are from throughout the growing season in 1992. Lines show the fitted model specified by Equation 3.7.

extrapolating the model to ordinary daytime conditions, it is implicitly assumed that dark respiration does not respond to Q, although this is very difficult to demonstrate because of the confounding effects of photorespiration and photosynthesis (Jackson and Volk, 1970; Cornic and Jarvis, 1972). Measurements would also be expected to be less accurate at low fluxes because of the smaller CO_2 differential obtained. Because of the lack of data and the rather poor fit to the model, the parameters in Table 3.2 are considered as useful initial values for the models in Section 3.4, rather than as definitive descriptions of respiration in these species.

3.4 Photosynthesis

The broad features of the results are summarised in Table 3.3. This shows that maximum A_l and α were around 2-3 times higher in the C4 species (millet and *E. tremula*) than in the C3 species, as is typical (Edwards and Walker, 1983). Differences in maximum A_l and α amongst the C3 species were very small.

Table 3.3 Summary of photosynthesis measurements. Maximum A_l is the maximum measured value from the 1991 and 1992 data sets in μmol m^{-2} s^{-1}. α was derived from linear regression on the A_l -Q response, using all data with Q < 300 μmol m^{-2} s^{-1}, where the response was still linear. The units of α are mol of CO_2 per mol of quanta. *Insufficient data.

Species	Maximum A_l	α	n
Millet	43.9	0.041	176
E. tremula	34.6	0.025	98
M. villosus	15.8	*	19
G. senegalensis	11.6	0.015	383
C. micranthum	13.9	0.019	367
C. nigricans	14.8	0.018	305
A. ataxacantha	14.9	0.013	15

Response to Q

Plots of A_l against Q for the major species are shown in Figures 3.3-3.7. In the C4 species, there are relatively few points where g_s was less than 200 mmol m^{-2} s^{-1} at high Q, and these were mainly measurements from late in the season, when leaves were becoming senescent. Discounting these, the A_l -Q relationship was close to linear over the whole range, with no obvious point of Q saturation (Figures 3.3 and 3.4). This is clearer in the millet data where there is less scatter. The C3 species show an asymptotic response to Q, even at high g_s, with saturation occurring at around Q of 500-700 μ mol m^{-2} s^{-1} (Figures 3.5 - 3.7). These data show the classical difference between C3 and C4 photosynthesis, which is attributable to the different carboxylating enzymes involved, RuBP carboxylase and PEP carboxylase, respectively.

As a preliminary analysis, the data were fitted to the rectangular hyperbola model (Equation 3.1) to examine the extent to which variation in A_l is explained by Q, the primary driving variable. The data in Table 3.3 and estimates of R_d from Figure 3.2 were used as initial values in the model fitting procedure.

Table 3.4 Parameters values fitted to the rectangular hyperbola model (Equation 3.1) by non-linear regression. The units of α are mol of CO_2 per mol of quanta, those of P_{max} and R_d are $\mu mol\ m^{-2}\ s^{-1}$.

Species	Data set	P_{max}	α	R_d	r^2	n
Millet	All data 92	70.3	0.031	3.63	0.74	216
E. tremula	All data 92	32.4	0.032	2.28	0.73	98
G. senegalensis	All data 92	5.8	0.019	1.43	0.61	271
C. micranthum	All data 92	3.3	0.029	1.46	0.21	367
C. nigricans	All data 92	5.6	0.020	2.01	0.54	304
A. ataxacantha	All data 91	17.5	0.041	3.78	0.65	16

Table 3.4 shows that over 70 % of the variation in A_1 in the C4 species was explained solely by Q. Furthermore, when the measurements made in September (when the crop was beginning to senesce) were removed from the millet data set, this percentage increased to 96 %. As would be expected, this percentage was rather less in the C3 species, ranging from 21 to 65 %. Parameter values for *A. ataxacantha* were very high compared to the other C3 species. Although this may be a real physiological difference, the results may be influenced by underestimation of leaf area because of curling (Section 3.2), or sampling error as a result of the small number of observations. Values of P_{max} and α for the C3 species were within the range found by Jarvis and Sandford (1986) for ten temperate tree species (5.0-20.6 and 0.01-0.083, respectively). The R_d values were higher than those found by Jarvis and Sandford (1986) (0.5-0.7 $\mu mol\ m^{-2}\ s^{-1}$), but this is attributable to the higher temperatures.

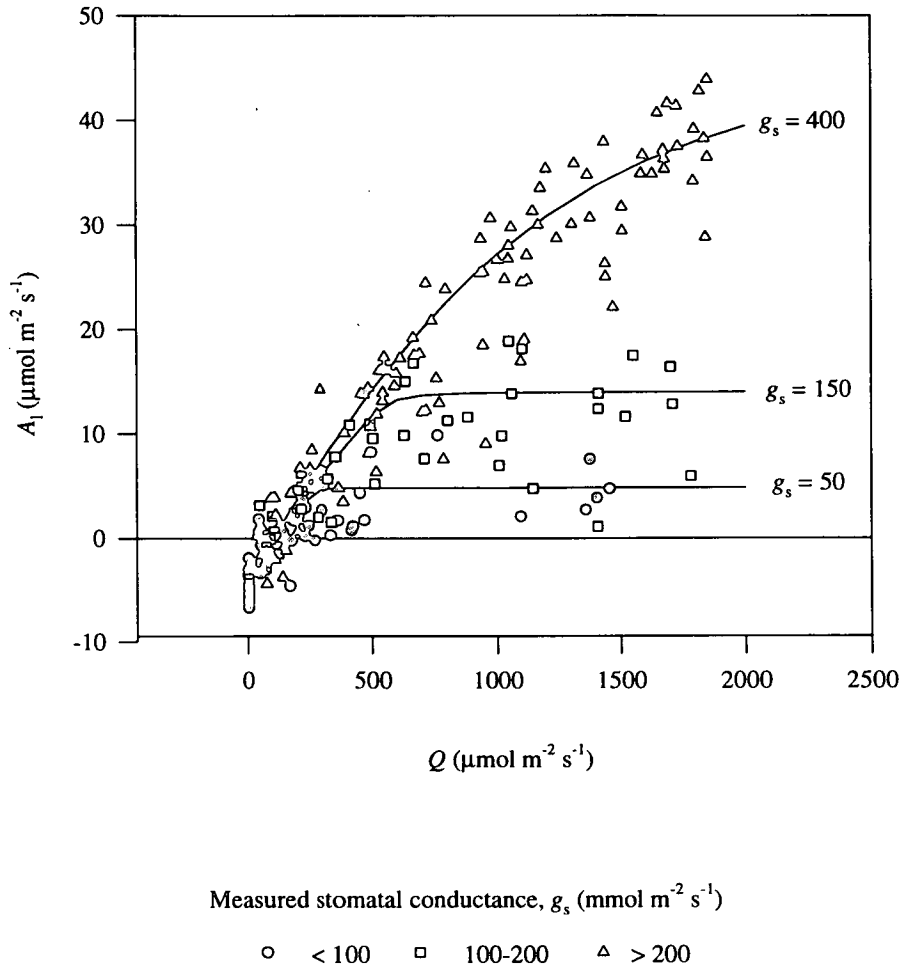

Figure 3.3 The relationship between A_l and Q in millet. Data were collected between July and September 1992, using shading to manipulate Q. Lines show the fitted Jarvis *et al.* (1985) model for three values of g_s.

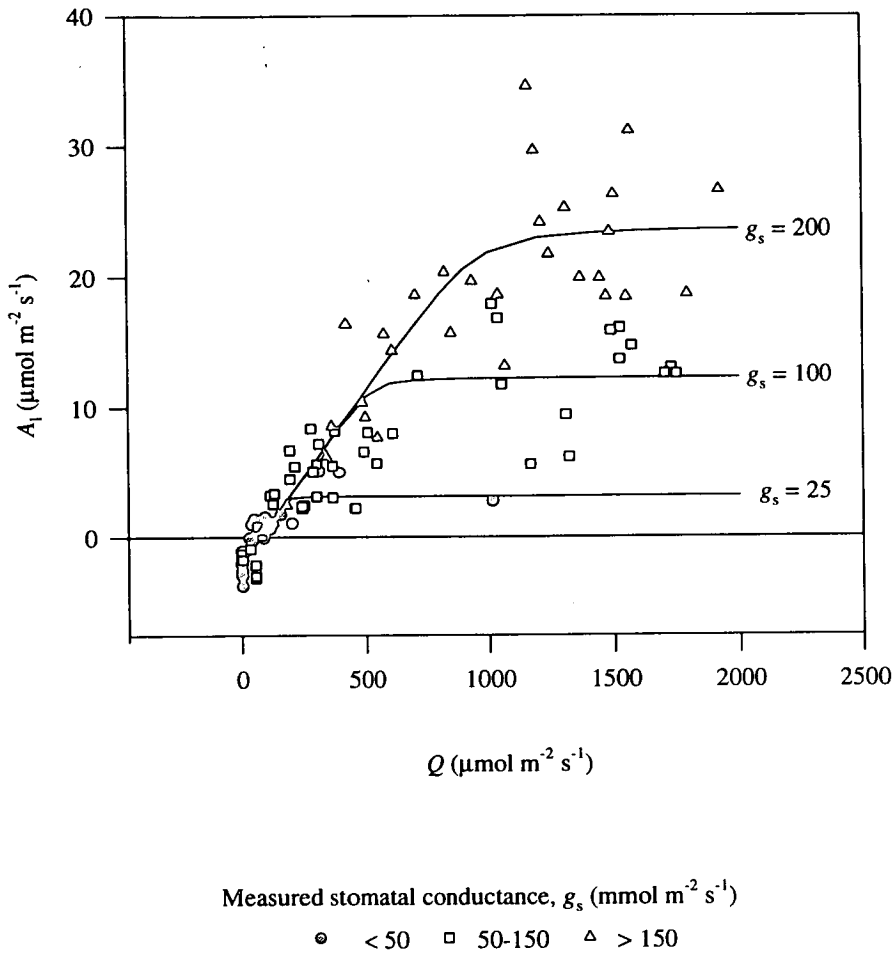

Figure 3.4 The relationship between A_l and Q in *E. tremula*. Data were collected between July and October 1992, using shading to manipulate Q. Lines show the fitted Jarvis *et al.* (1985) model for three values of g_s.

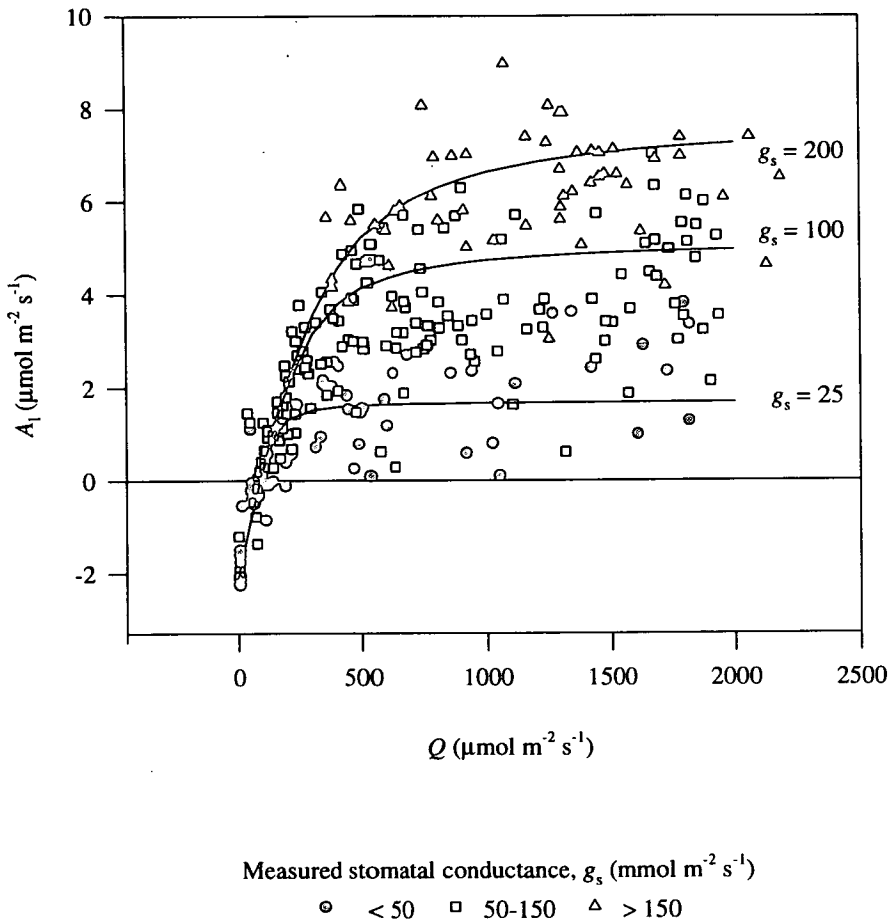

Figure 3.5 The relationship between A_1 and Q in *G. senegalensis*. Data were collected between February and October 1992, using shading to manipulate Q. Lines show the fitted Jarvis *et al.* (1985) model for three values of g_s.

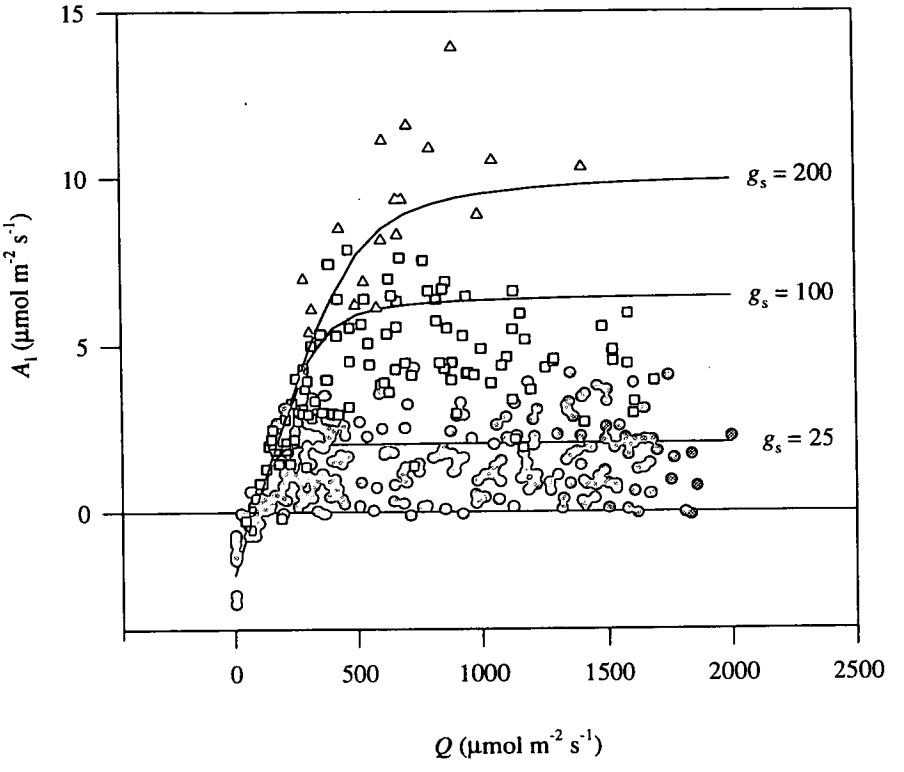

Figure 3.6 The relationship between A_l and Q in *C. micranthum*. Data were collected between June and October 1992, using shading to manipulate Q. Lines show the fitted Jarvis *et al.* (1985) model for three values of g_s.

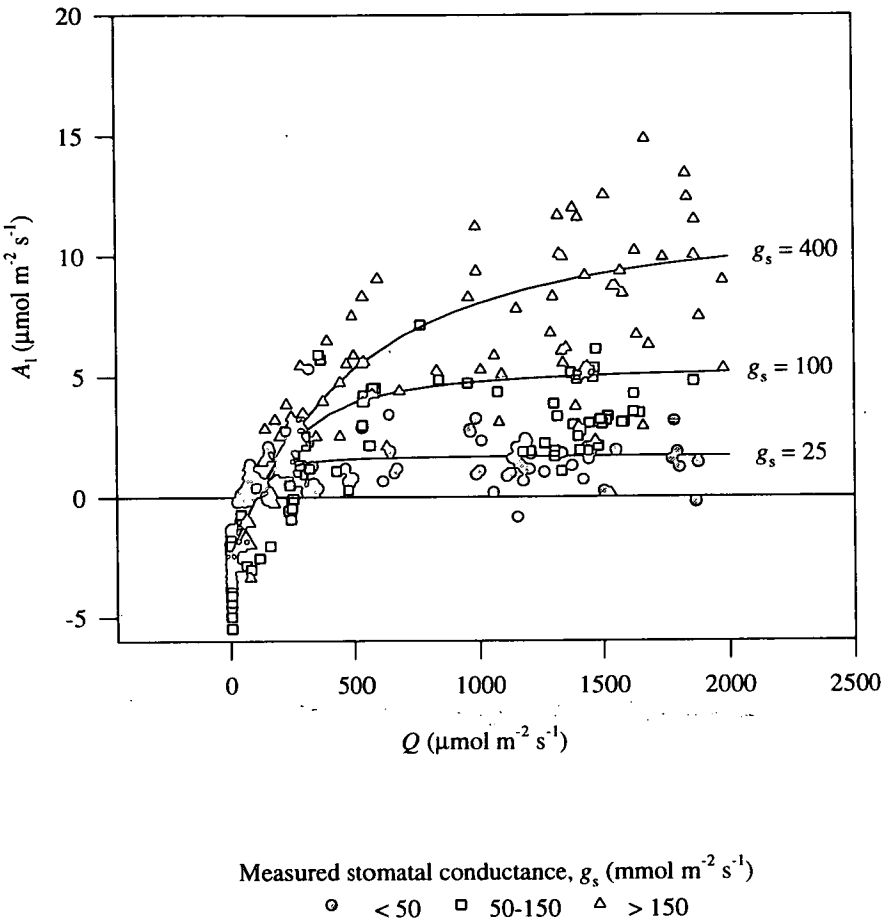

Figure 3.7 The relationship between A_1 and Q in *C. nigricans*. Data were collected between June and October 1992, using shading to manipulate Q. Lines show the fitted Jarvis *et al.* (1985) model for three values of g_s.

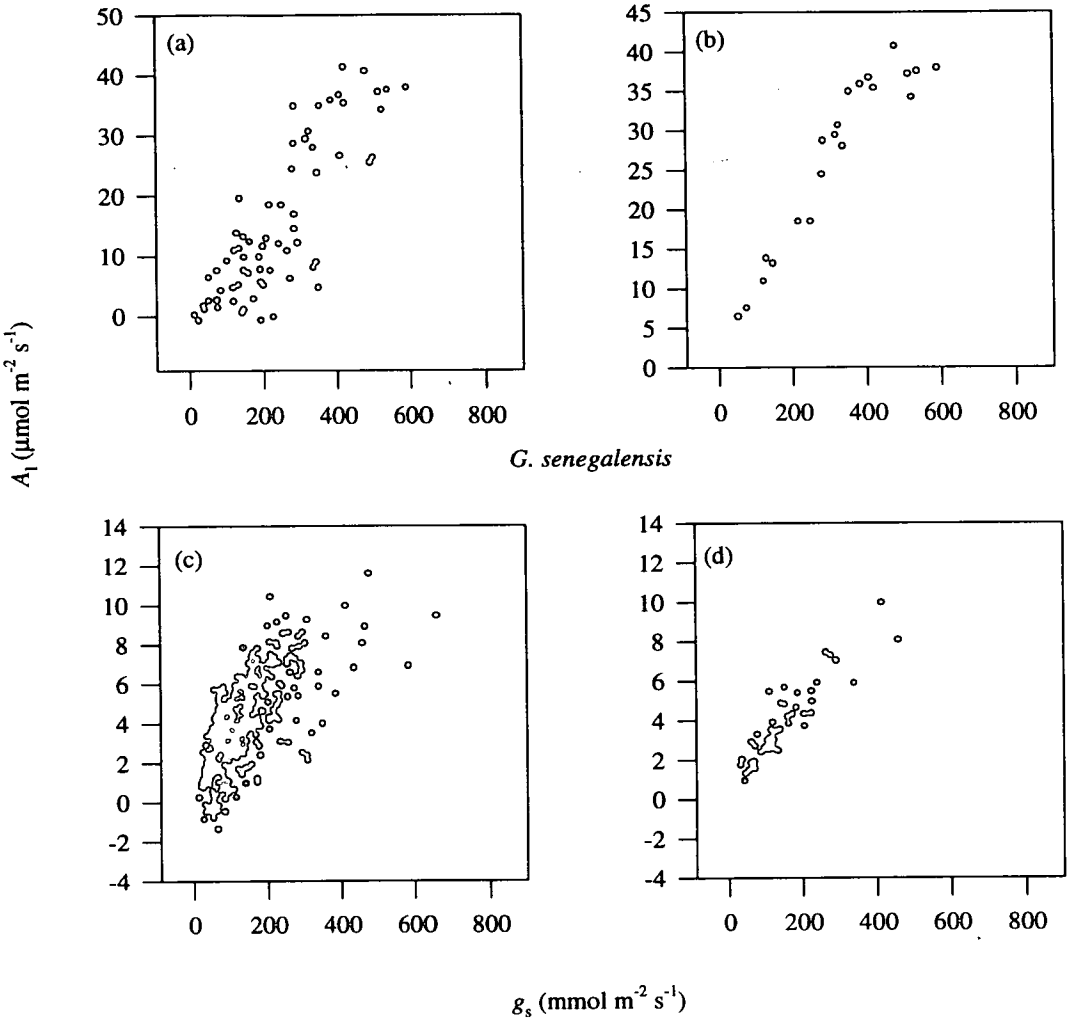

Figure 3.8 The relationship between A_l and g_s in millet (a and b) and *G. senegalensis* (c and d). All data are from measurements made with ambient Q over the 1991 and 1992 growing seasons. In (b) the data are restricted to a C_i range of 50-130 μmol mol^{-1}. In (d) the data are restricted to a C_i range of 230-250 μmol mol^{-1}. Relationships are close to linear in both cases.

Response to g_s and C_i

A correlation between g_s and A_l is apparent in Figure 3.8. To account for this, the second, more complex model described in Section 3.1 was fitted to the data, but without the temperature response function for g_m. The data in Tables 3.2 and 3.4 were used as initial values in the model fitting procedure. Curves showing the fitted Q responses at three g_s values are superimposed on the data in Figures 3.3-3.7, and give good fits to the observations.

Table 3.5 Parameters values fitted to the Jarvis *et al.* (1985) model (Equations 3.2-3.12). The units of α are mol of CO_2 per mol of quanta. * indicates fixed parameters; † indicates parameters which reached their constraint.

Species	α	θ	g_m (mol m^{-2} s^{-1})	Γ (umol mol^{-1})	R_o (μmol m^{-2} s^{-1})	k ($°C^{-1}$)	r^2	n
Millet	0.031	0	0.693	5*	0.697	0.0469	0.87	216
E. tremula	0.024	0.997	0.164	5*	1.179	0.010†	0.89	97
G. senegalensis	0.025	0.442	0.041	50*	1.479	0.010†	0.77	271
C. micranthum	0.024	0.846	0.037	50*	0.868	0.024	0.78	367
C. nigricans	0.025	0	0.048	50*	0.413*	0.054*	0.73	304
A. ataxacantha	0.029	0.694	0.075	50*	1.213	0.004	0.79	16

Table 3.5 shows that the fit of the model to the data is much improved when g_s is incorporated, and that generally around 80 % of the variation in A_l is explicable solely in terms of Q and g_s. The increase in r^2 in Table 3.5 is also attributable to some extent to the more comprehensive non-rectangular Q response model, which allows for greater flexibility in the shape of the response curves.

The g_m values for the C3 species are close to the lower end of the range found by Jarvis and Sandford (1986), for temperate trees (0.028-0.16 mol m^{-2} s^{-1}). The g_m values for the C4 species were much higher than for the C3 species, by a factor of ~4-16. This is attributable to the different carboxylating enzymes involved, RuBP carboxylase and PEP carboxylase. However, the C4 g_m values were not atypical, and were at the lower end of the range quoted by Edwards and Walker (1983) for C4 plants (0.2-1.36 mol m^{-2} s^{-1}). Further parameter sets are listed in Appendix 3 (Tables A.3.1 and A.3.2). It is clear from these parameter sets that a similar fit can be achieved by balancing an increase in one parameter value with a decrease in another and so too much significance should not be attached to individual parameter values. As the parameter are not derived independently, it is the set of parameter values that is significant rather than the individual values.

Physiologically sensible values of Γ were not found when this parameter was unconstrained in the fitting procedure. This was presumably because none of the observations were made in conditions where C_i was varied independently, and so the data are not well suited to deriving A_l-C_i responses. Indeed, as illustrated in Figure 3.9, there is an apparent negative A_l -C_i relationship in the data. This is present because C_i is largely a dependent variable under the LCA3 measurement conditions, and Figure 3.9 does not represent a plot of a dependent variable against an independent variable. In a closed gas exchange system (such as the Li-Cor 6200), A_l reduces C_a, and consequently C_i is reduced, resulting in a decrease in A_l, which continues until A_l reaches zero. In this case, C_i changes independently of the other variables which influence A_l, so a clear positive relationship can be derived. In an open gas exchange system (such as the LCA3), if the CO_2 concentration of the air entering the system is manipulated, thereby changing C_i independently of g_s and A_l, a positive relationship can be

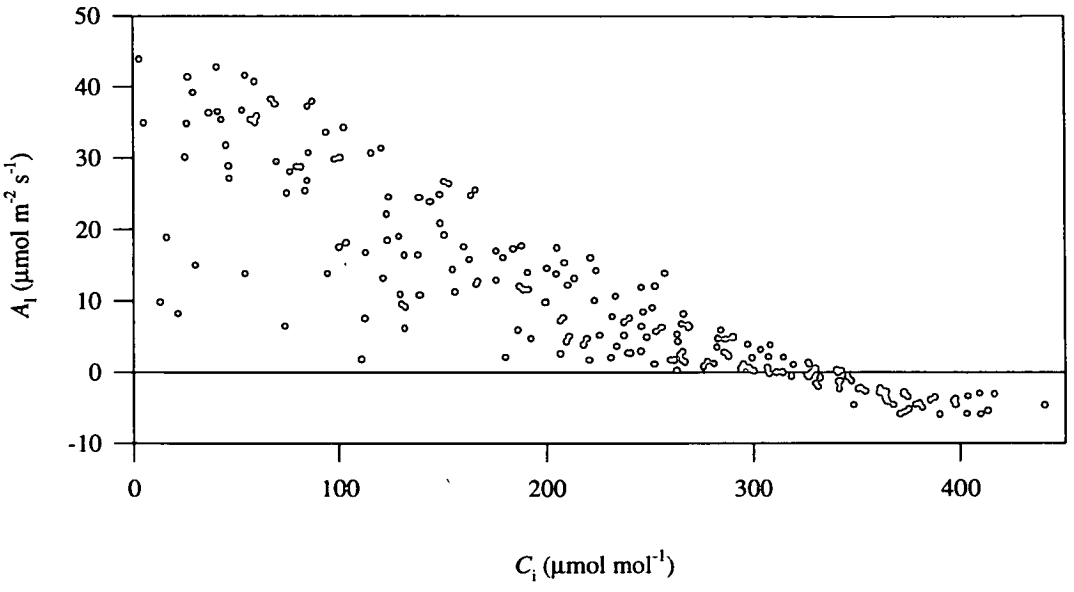

Figure 3.9 (a) The relationship between A_l and C_i in millet. The data are the same as in Fig. 3.3. The apparent negative relationship is found because C_i is largely a dependent variable under the LCA3 measurement conditions. See text for explanation.

derived in the same way. However, when using an open system with ambient air, A_l does not affect C_a much, and C_i varies largely as a result of changes in g_s and A_l. In this case, the A_l -C_i relationship may be positive or negative, depending on which factor is varying. If g_s is altered independently, a positive A_l-C_i relationship is produced. If Q (or any other factor affecting the flux from the sub-stomatal cavity to the mesophyll) is altered independently, an A_l-C_i relationship with a negative slope is produced. The latter case is clearly dominant in these data, because Q was deliberately manipulated by shading.

Closer fits to the data were achieved if Γ was unconstrained in the fitting procedure (r^2 ~0.9 rather than ~0.8). Although the resulting Γ values were unrealistically high, these parameter sets (Appendix 3, Table A.3.1) were used in MAESTRO and big leaf model simulations as they gave the best description of the data. As C_i is eliminated in the model, the implicit A_l-C_i response is not important.

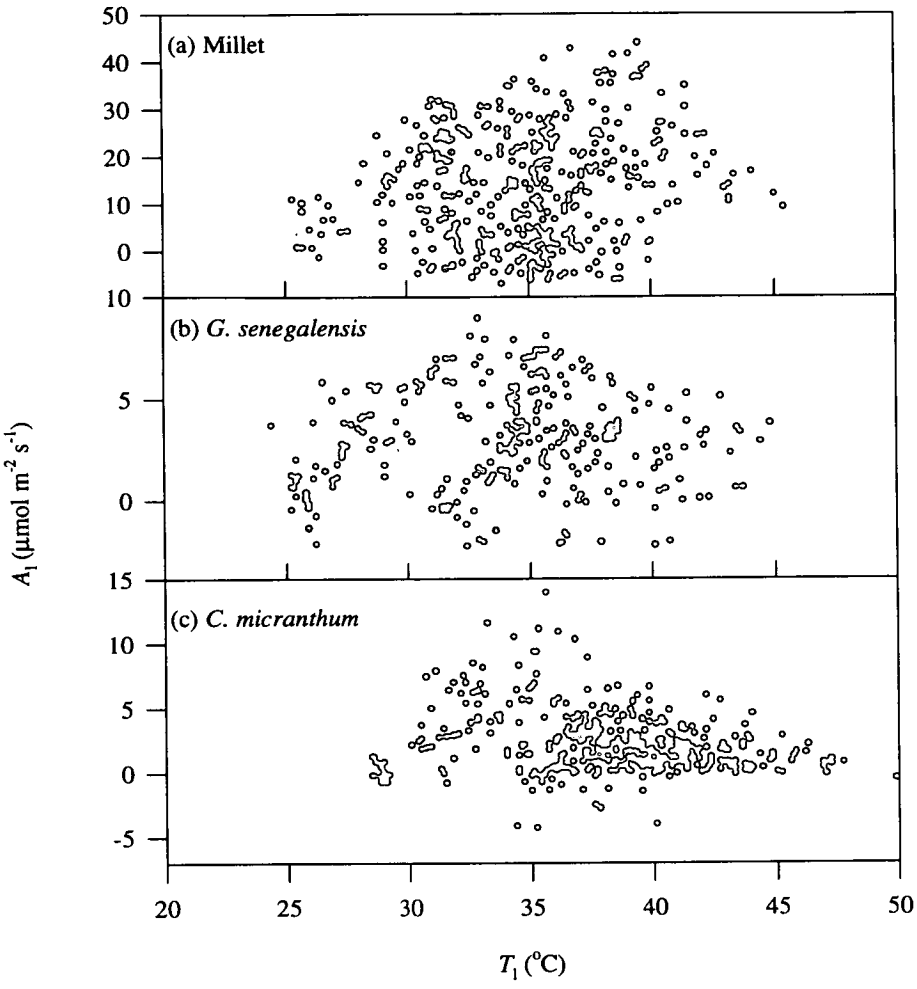

Figure 3.10 The relationship between A_l and T_l in (a) millet, (b) *G. senegalensis* and (c) *C. micranthum*. (a) shows all data from 1991 and 1992. (b) and (c) show all data for 1992.

Response to temperature

Upper boundaries on the scatter diagrams in Figure 3.10 are approximately bell-shaped, similar to the temperature function in Figure 3.1(d). In order to examine whether any of the variation in A_l could be explained by the effect of temperature, the data were fitted to the non-rectangular hyperbola of Jarvis *et al.* (1985) with the temperature function for g_m added. Initial values for the temperature parameters were estimated from Figure 3.10. These parameters had to be constrained within a range so that $T_{max} > T_{opt} > T_{min}$. The data in Table A.3.1 were used as initial values for the other parameters in the model fitting procedure.

Table 3.6 Parameters values fitted to the mesophyll conductance (g_m) temperature function in the Jarvis *et al.* (1985) model. † indicates parameters which reached their constraint.

Species	g_m (mol m^{-2} s^{-1})	T_{max} (°C)	T_{opt} (°C)	T_{min} (°C)	r^2	n
Millet	13.967	46.3	46.2	25.7	0.85	216
E. tremula	13.971	48.0†	47.0†	26.0†	0.90	97
G. senegalensis	0.160	49.5	44.0†	0†	0.77	271
C. micranthum	0.249	50.0†	49.0†	10.6	0.78	367
C. nigricans	0.208	49.0†	39.2	20.0†	0.74	304

Table 3.6 shows that the temperature parameters often reached their constraints, and were often configured with T_{max} and T_{opt} very close to each other beyond the range encountered in the data, so that the function became linear rather than bell-shaped. Also, incorporating the temperature function did not improve the fit of the model, indicating that the function used did not fit the data. Although no effect of T_l is apparent here, it may be that the temperature effect was confounded with Q and g_s. An effect of soil surface temperature on growth has been observed in studies in millet in Niger (Vandenbeldt and Williams, 1992). Correlations amongst the environmental variables might be expected to be a problem in these data, although this should be reduced when shading was used.

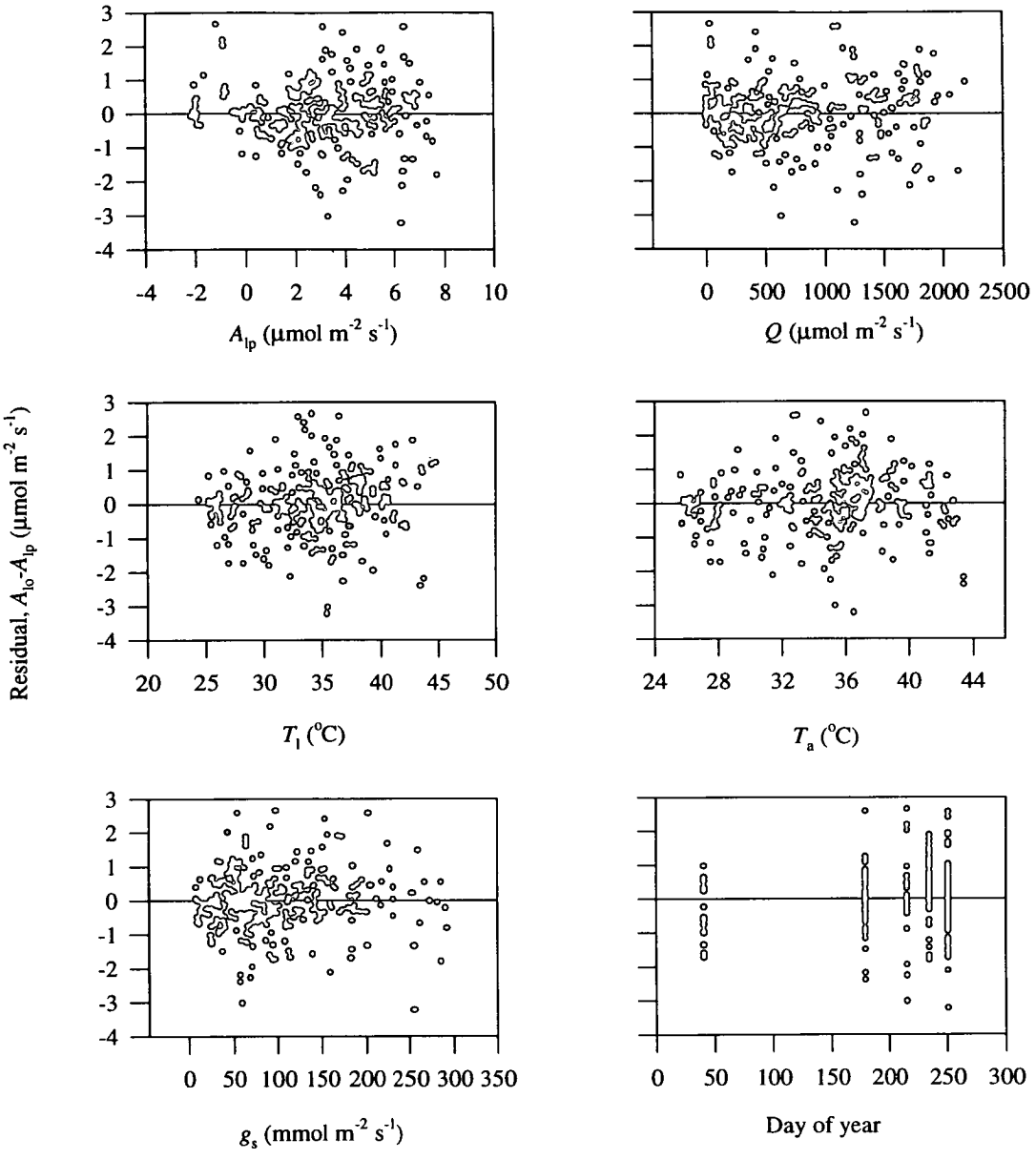

Figure 3.11 The distribution of residuals (the differences between assimilation rate predicted by the fitted Jarvis *et al.* (1985) model, A_{lp}, and observed values, A_{lo}) in relation to A_{lp} and environmental variables. The data shown are for *G. senegalensis*, collected between February and September 1992.

Residual analysis

Figure 3.11 shows plots of the residuals against the predicted dependent variable, A_{lp}, and the major independent variables for the *G. senegalensis* data set. Residual plots for the other species are very similar. No obvious skewing of the residuals is apparent, and it is concluded that the model used is adequate and that there are no obvious relationships with these variables which are unaccounted for.

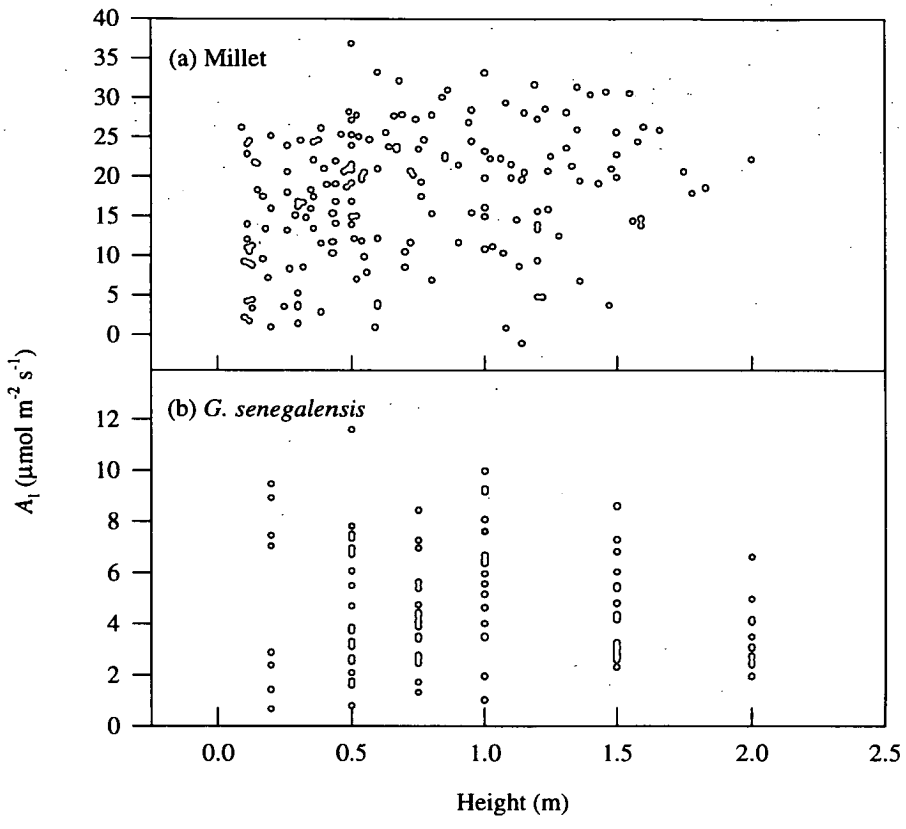

Figure 3.12 Distribution of measured assimilation rate, A_l, with height in the canopy. Data shown are from measurements made in ambient conditions on (a) millet between July and September 1991 and (b) *G. senegalensis* during August and September 1991.

As a simple means of examining whether there was any systematic variation in leaf photosynthetic properties through the canopy, A_l was plotted against height for the millet and *G. senegalensis* data sets. Figure 3.12 shows that no relationship was apparent. This is perhaps not surprising as the millet and fallow canopies were very sparse, and so there was little reduction in Q with depth in the canopy or consequent shade acclimation (cf. Leverenz *et al.*, 1982). Also, there was little variation in leaf age with height in *G. senegalensis*. Seasonal variations in A_l were much more strongly influenced by changes in weather than increasing leaf age.

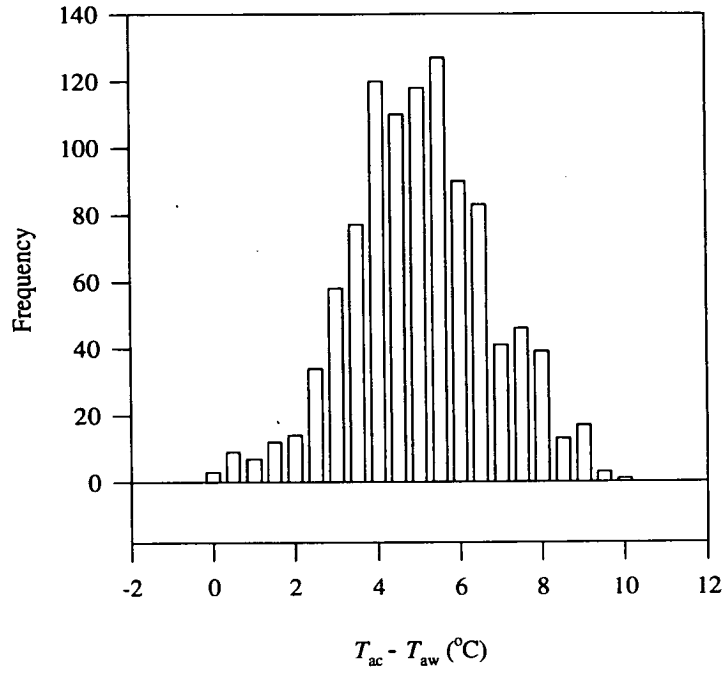

Figure 3.13 Frequency distribution of the difference between air temperature measured within the leaf chamber (T_{ac}) and ambient air temperature measured at the weather station (T_{aw}). Air within the chamber was on average 5 °C warmer than the ambient air, as a result of the chamber and analyser heating up in the sun.

3.5 Stomatal response times

Introduction

When the gas exchange system was used in the field, it inevitably heated up as it was exposed to solar radiation, typically increasing air temperature inside the chamber by about 5 °C above ambient, but by up to 10 °C in one case (Figure 3.13). Consequently, when a leaf was enclosed in the chamber, it was subjected to an environment with higher T_a and higher D. (It would be more pertinent to compare leaf temperature before and after enclosure within the chamber, but displaying the leaf temperature whilst in recording mode caused a software error in the LCA3). Photosynthesis and stomatal conductance would be expected to respond to this change in environment until they reached a fully adjusted state. Photosynthesis is known to respond very quickly to such changes, and will fully adjust to an alteration in an environmental variable within a second. The response time of the gas exchange system is considerably longer and so such changes are outwith the resolution of the instrument. The situation is rather less clear with stomata, however, as they tend to respond over periods of minutes, although this appears to be quite variable amongst species. To clarify this, an experiment was done to determine how quickly the stomata responded to a change in their environment and how quickly they reached full

adjustment. Additional information was also gained from the measurements on millet where shading was used to manipulate incident Q.

Method

Measurements were made on shoots of *G. senegalensis* on 11/6/92, essentially as described in Section 3.2. The shoots were kept in the chamber for up to 40 minutes, during which time Q was alternated between ambient (1000-1600 μmol m^{-2} s^{-1}) and complete darkness by using a black cloth to shade the chamber. In this way the response of the stomata to a step change in one of the driving variables could be examined. However, as leaf and chamber temperatures were affected by shading (and therefore D also), the response cannot be solely attributed to Q. In some cases, the relative humidity (H) of the air entering the chamber was also alternated between ambient (around 40 %) and completely dry, by passing the air through a desiccant column. This had the advantage of not affecting other driving variables. The time of each measurement was recorded by the LCA3, which gives a resolution of only one minute. Manipulated Q measurements were also made on millet, as described in Section 3.2.

Results

The results from three *G. senegalensis* shoots are shown in Figure 3.14. Figure 3.14(a) shows that g_s was reduced by about 50 % within three minutes of shading. Subsequently, g_s continued to decline much more slowly, until the measurements stopped after 12 minutes. Figure 3.14(b) shows a similar pattern, with the stomata starting to respond within one minute of shading or uncovering, but rather more slowly (decreasing by only ~25 % or 63 mmol m^{-2} s^{-1} after eight minutes of shading). Figure 3.14(c) shows a decline of around 40 % within one minute of shading, which continued to decrease at a lower rate over ten minutes. Conductance was returned to the initial value within two minutes of the removal of the shade cloth. A similarly rapid decrease was induced when the chamber humidity was lowered by introducing dry air into the chamber. A similar pattern is seen in data from the other shoots and these results suggest that the stomata began to respond within one to two minutes of a change in their environment and continued to respond over ten minutes.

Figure 3.15 shows similar data for millet, although here the main aim was to study the response of A_l to changes in Q, and information obtained concerning stomatal response times was incidental. In all cases, the first measurement represents ambient Q in the leaf's natural position and the second represents an attempt to achieve a higher Q by altering the chamber orientation. Subsequent measurements were made with progressively lower Q by adding shade cloths and/or changing the chamber orientation. Figure 3.15 shows that there was only a slight decrease in g_s during the first two measurements, when Q remained similar or was increased. Once shading was introduced, g_s declined steadily, by between 16 and 25 mmol m^{-2} s^{-1} each minute. In Figure 3.15(a), this response began within one minute, but this is not clear in (b) and (c) because of the distribution of the measurements.

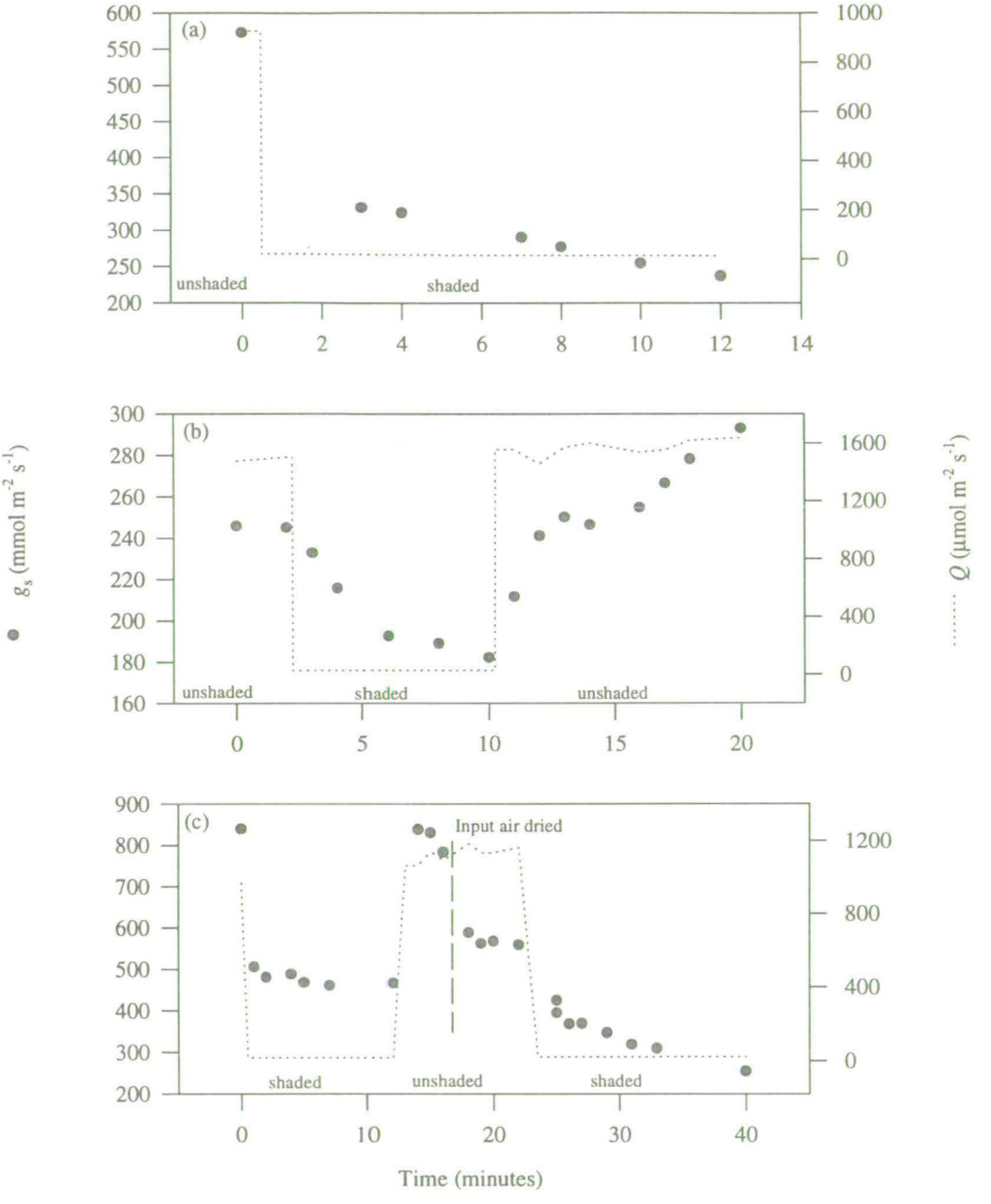

Figure 3.14 Response of stomatal conductance, g_s, to step changes in Q in *G. senegalensis*. Data are shown for three shoots measured on 11/6/92. The shoot within the cuvette was initially exposed to ambient Q and measured after around 30 seconds to find the conductance value before major readjustment. A black cloth was then used to shade the cuvette. Responses are seen within one minute but full adjustment is not reached within 15 minutes. A similar effect was produced in (c) by drying the inlet air by passing it through a desiccant column.

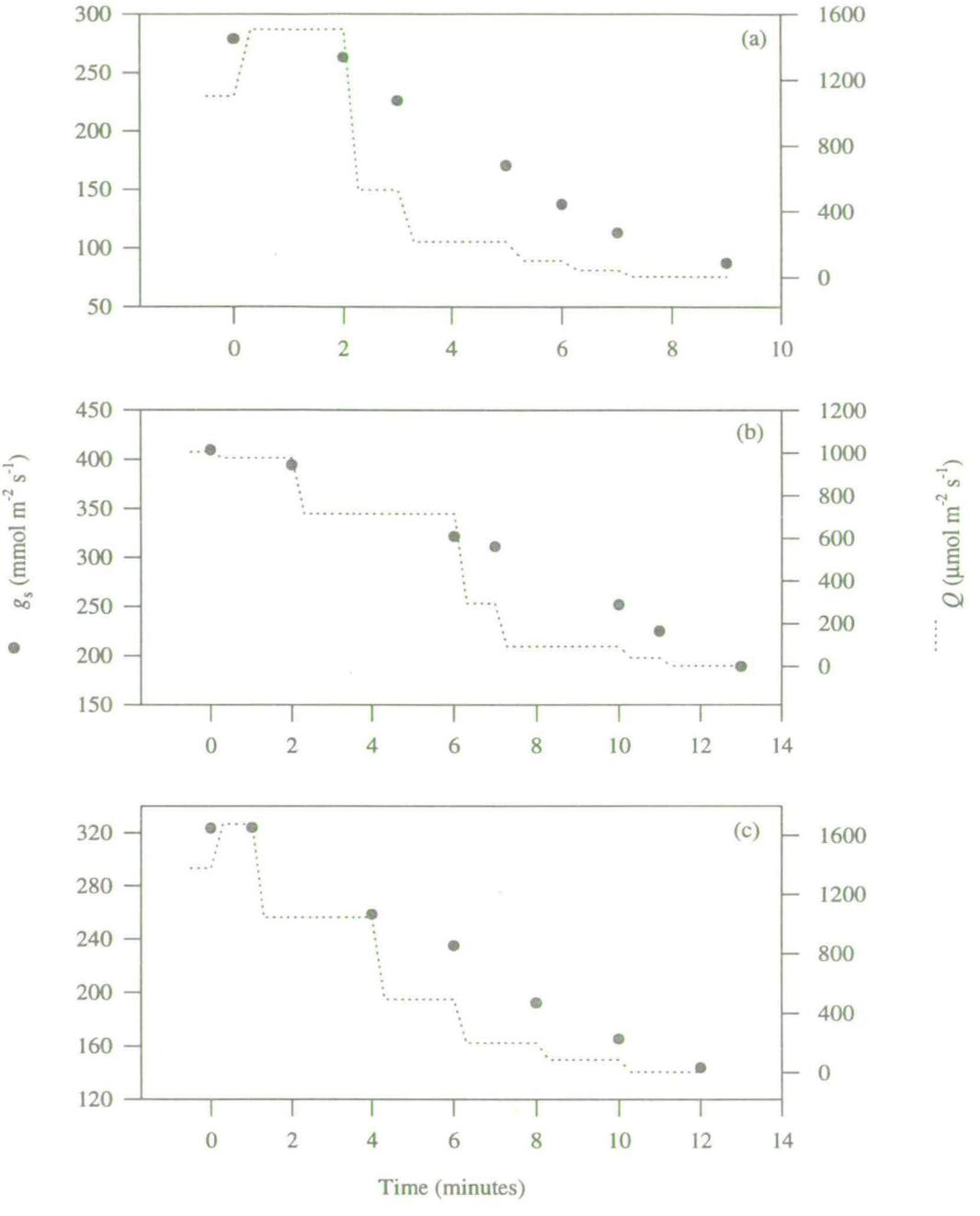

Figure 3.15 Response of stomatal conductance, g_s, to step changes in Q in millet. Data are shown for three leaves measured on 8/7/92. The leaf within the cuvette was initially exposed to ambient Q and measured after around 30 seconds to find the conductance value before major readjustment. For the second measurement, the cuvette was orientated so as to obtain the highest possible Q. In subsequent measurements, a black cloth was used to shade the cuvette. There was little change in g_s over the first two measurements, but it began to decline within 1-3 minutes of shade being introduced.

As shading was altered every few minutes without examining whether g_s had become stable, it is not possible to attribute changes in g_s to individual changes in Q.

Discussion

When a shade cloth was placed over the chamber, so that Q was changed from ambient to complete darkness, the stomata were left far from their equilibrium state. There appeared to be two phases to the response: an initial rapid change within one to two minutes, followed by a much slower readjustment. The initial rapid change coincided with the drop in T_l, and may be a real physiological effect or a measurement artefact. It is not obvious how such an artefact could arise in the measurements, so it is assumed that this is a real physiological effect, although this is questionable. Full adjustment to darkness was not reached within the 12-17 minute periods considered here. When the shade cloth was removed, so that Q was changed from complete darkness back to ambient, the stomata were returned to their equilibrium state by the initial rapid response. This indicates that the time required for the stomata to adjust fully to an environmental change simply depends on the change in aperture that needs to be made.

The results indicate that the stomata begin changing within one to two minutes of a step change in their environment, and that this initial change may be large. This has important implications for the interpretation of the gas exchange data, as this is similar to the length of time required to make a measurement (0.5-1.5 mins, see A.1.4). When making a gas exchange measurement, the stomata will initially be adjusted to the conditions they experienced before enclosure within the chamber. When introduced to the chamber, they will begin to readjust to the warmer, drier environment before the measurement is completed. It is not possible to discern from these data to what extent readjustment will be complete, and so it is not clear whether g_s data should be related to ambient or chamber T_a and D. In either case, if the stomata are not in equilibrium with either set of conditions, this may introduce considerable noise into the data set. In the absence of further information, and as chamber conditions could not be held constant, it was decided to make measurements as rapidly as possible so as to minimise stomatal readjustment and relate these data to ambient conditions. Data obtained during the experiments when Q was manipulated are therefore not included in the following analyses.

3.6 Stomatal conductance, g_s

For the reasons outlined above, only measurements made in ambient Q were used to infer relationships between g_s and environmental variables. Figures 3.16-3.19 show plots of g_s against Q and D for millet, *G. senegalensis*, *C. micranthum* and *C. nigricans*. Relationships are detectable in all of these figures, to a greater or lesser extent, although there is a considerable amount of scatter in the data. g_s did not differ markedly between species, although the highest values were found in millet. The range

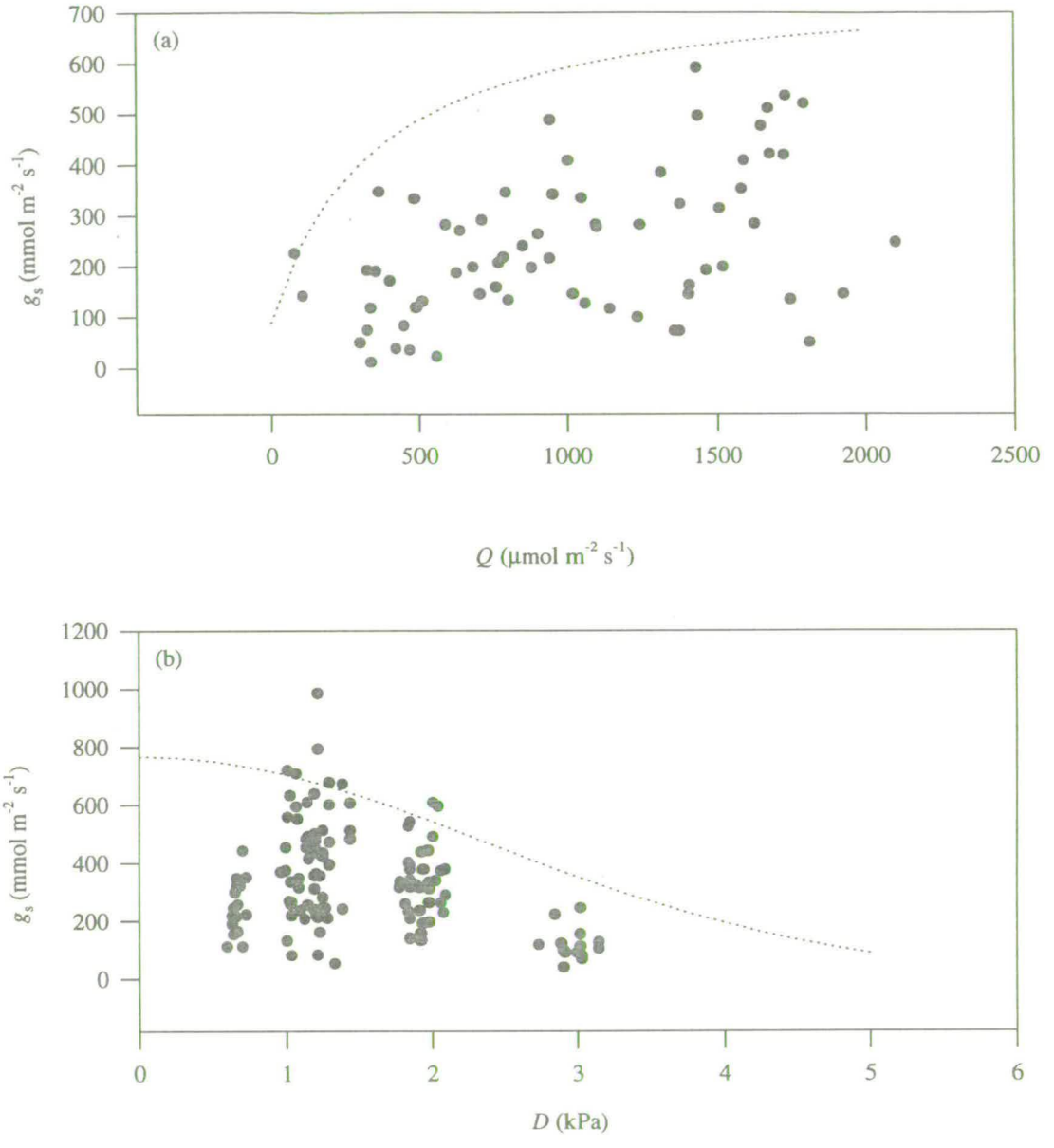

Figure 3.16 (a) Relationship between stomatal conductance, g_s, and Q in millet. Only points where $D < 1.5$ kPa are shown. (b) Relationship between g_s and D in millet. Only points where $Q > 500$ µmol m^{-2} s^{-1} are shown. In both (a) and (b), the data are from ambient measurements made between July 1991 and September 1992. The dotted lines show the fitted functions describing (a) the response to Q when D is 0 and (b) the response to D at infinite Q.

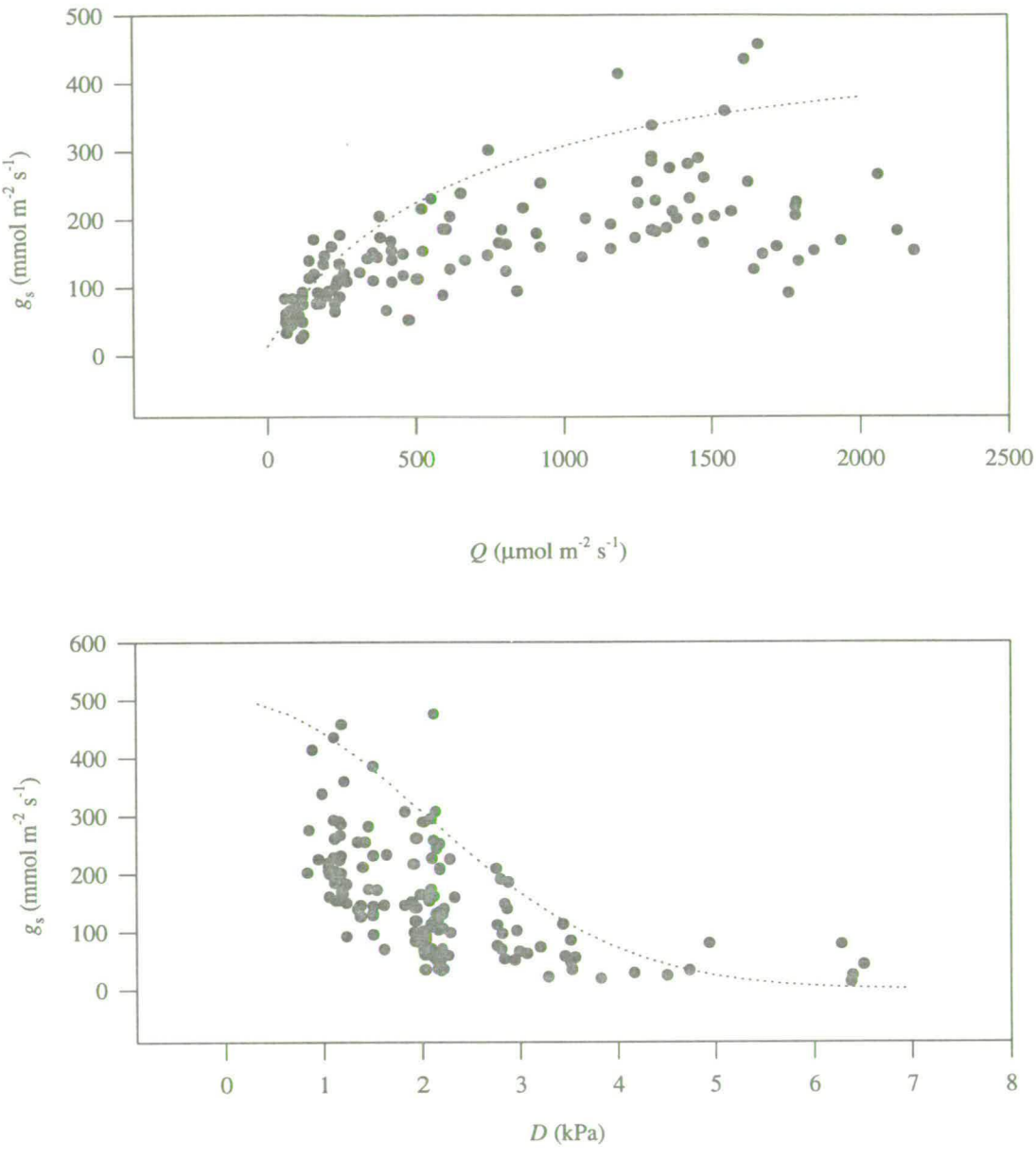

Figure 3.17 (a) Relationship between stomatal conductance, g_s, and Q in *G. senegalensis*. Only points where $D < 2.5$ kPa are shown. (b) Relationship between g_s and D. Only points where $Q > 500$ µmol m^{-2} s^{-1} are shown. In both (a) and (b), the data are from ambient measurements made between July 1991 and September 1992. The dotted lines show the fitted functions describing (a) the response to Q when D is 0 and (b) the response to D at infinite Q.

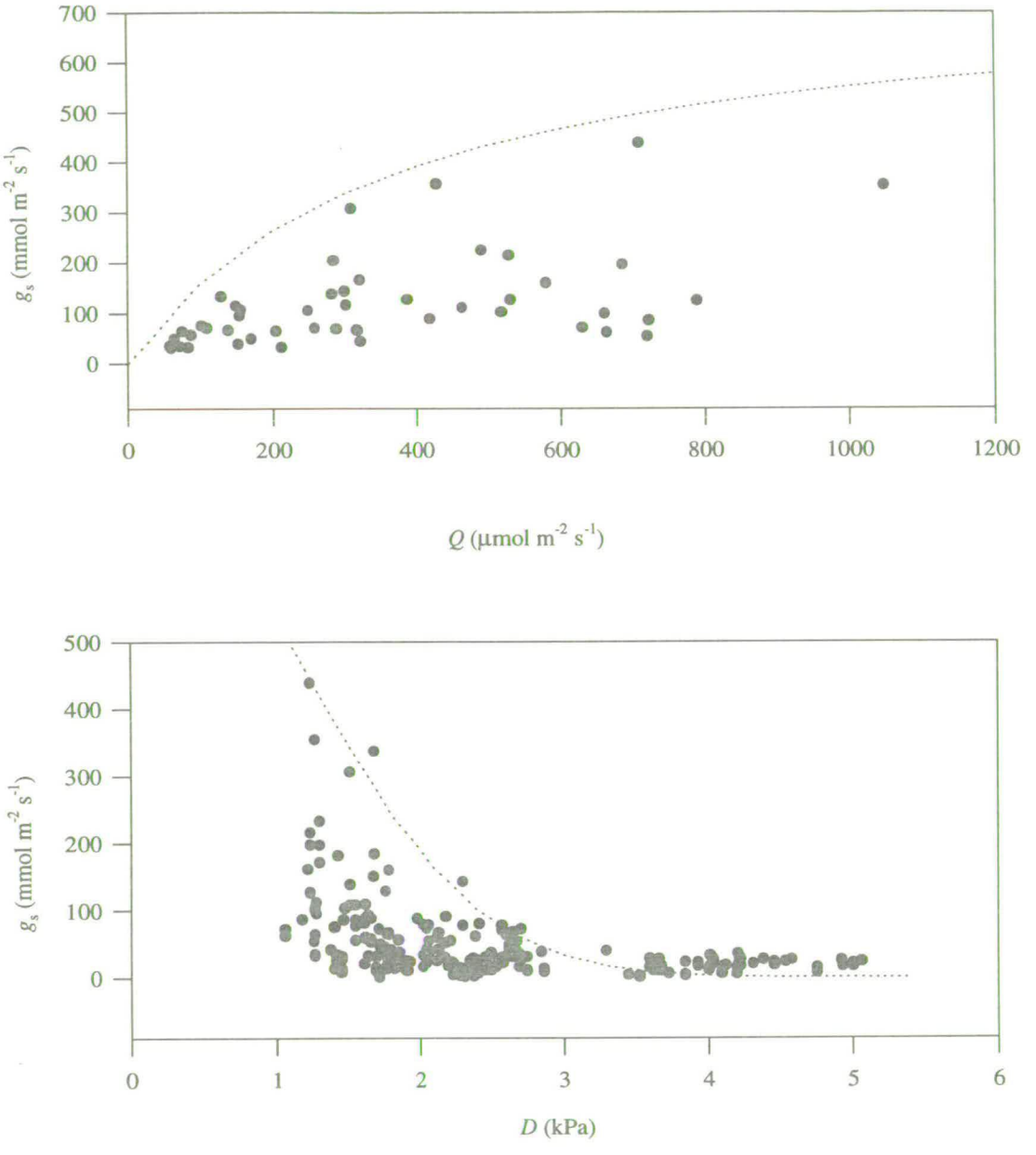

Figure 3.18 (a) Relationship between stomatal conductance, g_s, and Q in *C. micranthum*. Only points where $D < 1.5$ kPa are shown. (b) Relationship between g_s and D. Only points where $Q > 500$ µmol m^{-2} s^{-1} are shown. In both (a) and (b), the data are from ambient measurements made between July 1991 and September 1992. The dotted lines show the fitted functions describing (a) the response to Q when D is 0 and (b) the response to D at infinite Q.

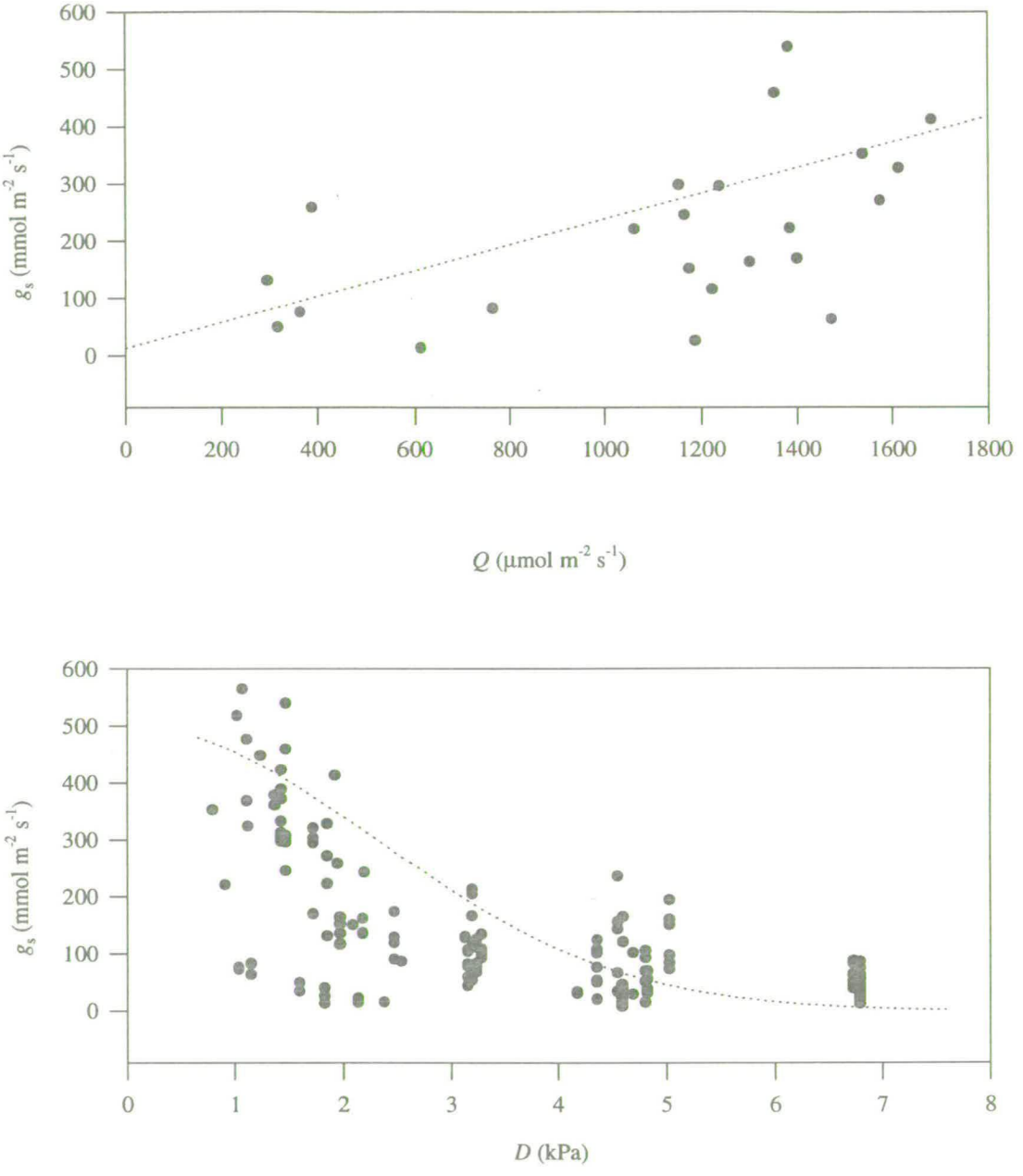

Figure 3.19 (a) Relationship between stomatal conductance, g_s, and Q in *C. nigricans*. Only points where $D < 1.5$ kPa are shown. (b) Relationship between g_s and D. Only points where $Q > 500$ µmol m^{-2} s^{-1} are shown. In both (a) and (b), the data are from ambient measurements made between July 1991 and September 1992. The dotted lines show the fitted functions describing (a) the response to Q when D is 0 and (b) the response to D at infinite Q.

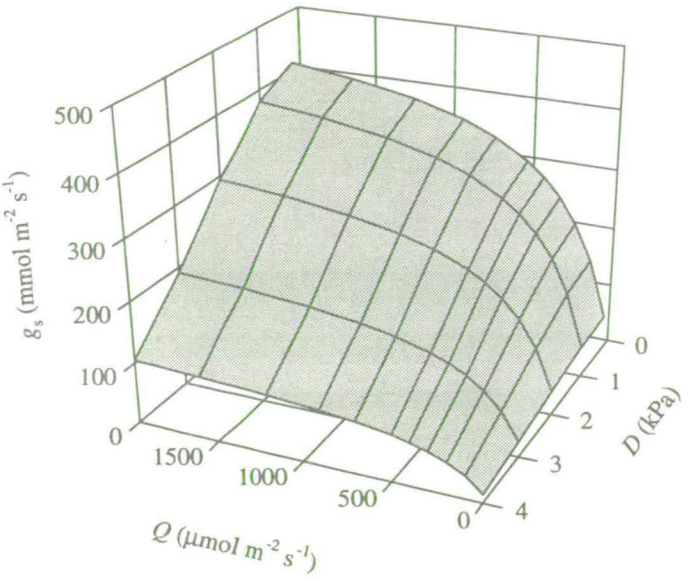

Figure 3.20 Response surface for g_s predicted by the model based on that of Jarvis (1976) fitted to data for millet from 1991.

of values of g_s measured in millet was similar to that found by Wallace, Roberts and Sivakumar (1990). Plots of g_s against leaf or air temperature do not show any clear relationship, although the upper limit is loosely bell-shaped, as in Figure 3.10. The data were fitted simultaneously to the stomatal conductance functions described in Section 3.1 (Equations 3.13-3.15) by non-linear regression, using SPSS statistical software.

Table 3.7 Parameters fitted to the stomatal conductance model (Equations 3.13-3.15) based on that of Jarvis (1976). The units of g_{slope} are mmol of H_2O per mol of quanta. † indicates parameters which reached their constraint.

Species	g_{smax} (mmol m^{-2} s^{-1})	g_{slope}	g_{sdark} (mmol m^{-2} s^{-1})	D_0	r^2	n
Millet	767	0.907	87	11.59	0.23	140
G. senegalensis	490	16.3	0†	8.24	0.28	344
C. micranthum	621	2.63	0†	2.87	0.29	297
C. nigricans	509	0.017	12	10.42	0.46	158

The fitted curves are superimposed on Figures 3.16-3.19 and the fitted response surface for millet is shown in Figure 3.20. Table 3.7 shows that a rather poor fit to the data was achieved, with Q and D accounting for between 23 and 46 % of the variation in g_s. Extensive data analysis was carried out to determine whether any other measured variables could account for the remaining variation. As for the photosynthesis data, the residuals were plotted against the predicted dependent variable, g_{sp}, and the major independent variables. The residual plots for *G. senegalensis* are shown in Figure 3.21, and are

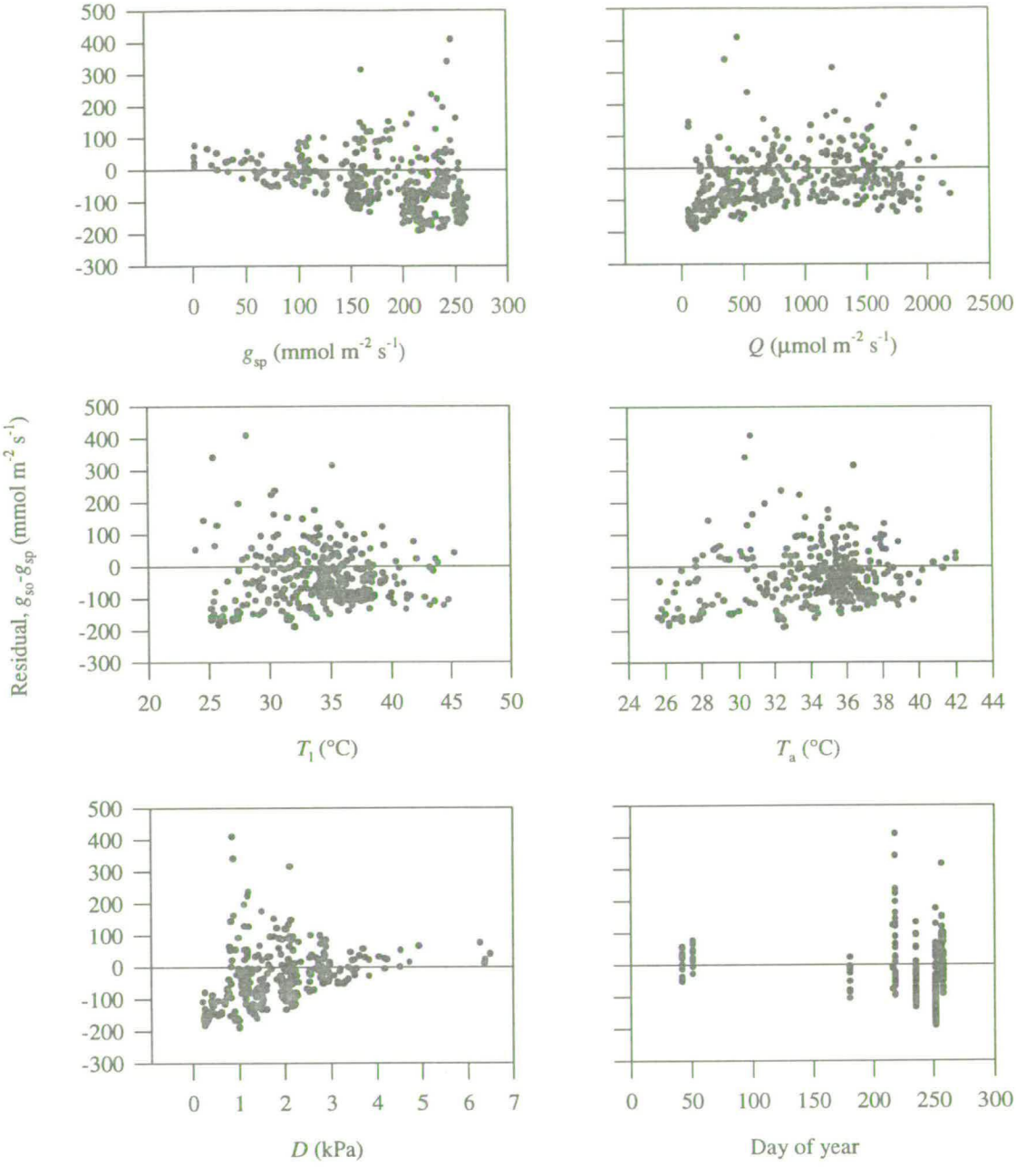

Figure 3.21 The distribution of residuals (the differences between stomatal conductance predicted by the fitted Jarvis (1976) model, g_{sp}, and observed values, g_{so}) in relation to g_{sp} and environmental variables. The data shown are from *G. senegalensis*, collected between February and September 1992.

similar in the other species. No significant skewing of the residuals is apparent. The plots of residuals against temperature show no relationship, and neither adding the temperature function (Section 3.1) nor using the temperature function instead of the humidity function improved the model fit. As in the photosynthesis data, variations in temperature are confounded with D, and so the two are not easily

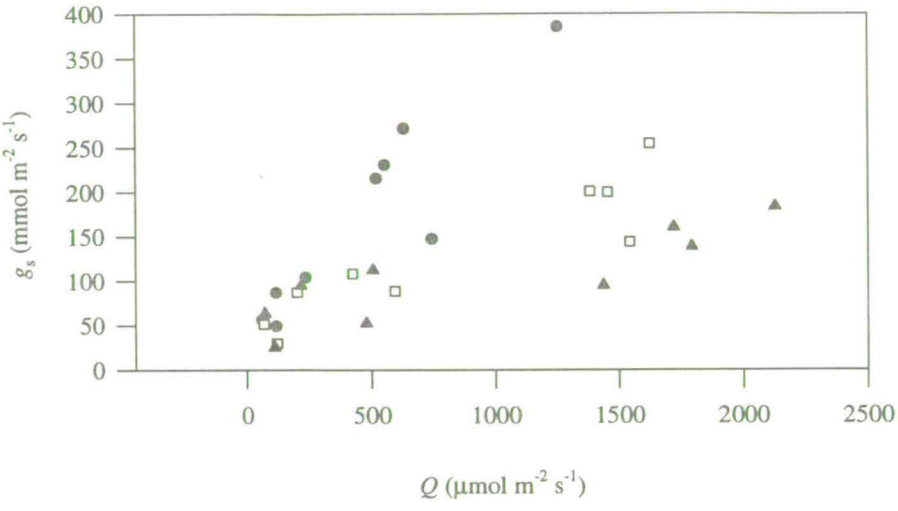

Figure 3.22 Relationships between stomatal conductance, g_s, and Q in three *G. senegalensis* shoots, measured on 12/9/92. The symbols represent data from the different shoots. The three shoots were on the same stem, yet had markedly different conductances, differing by over 200 mmol m^{-2} s^{-1}. Although the Jarvis (1976) model accounted well for the variation in g_s in individual shoots (r^2~0.9), the inter-shoot variabilty could not be accounted for, and so the amount of variation in the pooled data sets accounted for by the model was much lower (r^2 = 0.2-0.6).

separable. Soil moisture might be expected to be important, and this was examined indirectly by looking at differences between days (soil moisture was only measured once every few days). However, the residual variation is as large within days as between days (Figure 3.21).

Leaf water potential might also be an important variable, although this was not measured. However, water potential would be expected to be similar in shoots on the same stem, yet large differences in g_s were found. This is illustrated in Figure 3.22, which shows that the stomatal conductance of different shoots on the same stem, measured at the same time on the same day, could differ by more than 200 mmol m^{-2} s^{-1}, or 100 % of a typical value. Table 3.8 shows that, for the each of these shoots, the model could be fitted extremely closely. When the model was fitted separately to data from each of 14 different shoots from four stems measured on several occasions on the same day, the mean r^2 was 0.87 (Appendix 3, Table A.3.4). However, when data from these shoots were pooled together, the r^2 was reduced to 0.59. Table 3.9 shows the same phenomenon in *C. micranthum*. This indicates that a large proportion of the residual variation is caused by biological differences between samples, rather than environmental variables or measurement error. The nature of these differences is not clear.

Table 3.8 Parameters fitted to the stomatal conductance model (Equations 3.13-3.15) for three *G. senegalensis* shoots from the same stem measured on 12/9/92. The data are shown in Figure 3.22. The units of g_{slope} are mmol of H_2O per mol of quanta.

Data set	g_{smax} (mmol m^{-2} s^{-1})	g_{slope}	g_{sdark} (mmol m^{-2} s^{-1})	D_o	r^2	n
Shoot 1	396 200	0.536	13.1	3.52	0.88	9
Shoot 2	181 400	0.182	38.8	3.76	0.90	9
Shoot 3	1229	0.189	52.8	2.23	0.96	9
All data 12/9/92	304	0.755	17.0	10.51	0.59	122

Table 3.9 Parameters fitted to the stomatal conductance model (Equations 3.13-3.15) for leaves of *C. micranthum* from three stems measured over four days in September 1992. The units of g_{slope} are mmol of H_2O per mol of quanta. † indicates parameters which reached their constraint.

Data set	g_{smax} (mmol m^{-2} s^{-1})	g_{slope}	g_{sdark} (mmol m^{-2} s^{-1})	D_o	r^2	n
Stem 12	436	0.01†	141	2.07	0.60	71
Stem 14	319	0.682	121	3.61	0.57	76
Stem 15	757	2.04	0†	1.81	0.54	106
All data September 1992	229	2.38	0†	2.80	0.30	263

As discussed in Section 3.1, photosynthetic responses were derived from repeated measurements on the same leaf. g_s responses were largely derived from single measurements on different leaves (although some repeated measurements were made on tagged shoots). As a consequence of this, samples in the photosynthesis data are not independent of each other, as several observations come from the same leaf, whereas samples in the stomatal conductance data are largely independent of each other. Hence, the proportion of variation related to between-leaf or between-shoot variability is greater in the g_s data. Some of the residual variation in the g_s data may be related to the response time problem discussed in Section 3.5. If the stomata are readjusting to chamber conditions over the measurement period, yet are analysed with respect to ambient conditions, this will introduce a systematic error into the data. However, the fact that a good fit was obtained to individual shoots suggests that this was not a major problem. Jarvis (1976) fitted the same basic model to data from *Picea sitchensis* and *Pseudotsuga menziesii*, collected over a two month period. Although residuals were evenly distributed, the model only accounted for 51 and 73 %, respectively, of the variation in g_s and so a substantial proportion of the variation was unexplained. Whitehead, Okali and Fasehun (1981) and Grace, Okali and Fasehun (1982) fitted the same model to data from two tropical tree species. The degree of scatter in their plots of g_s against independent variables appears similar to that in Figures 3.16-3.19. Closer fits to the model were found (r^2 of 0.72-0.84), although the sample size was smaller than here (n=16 to 53) and restricted to a few trees over 3-5 days.

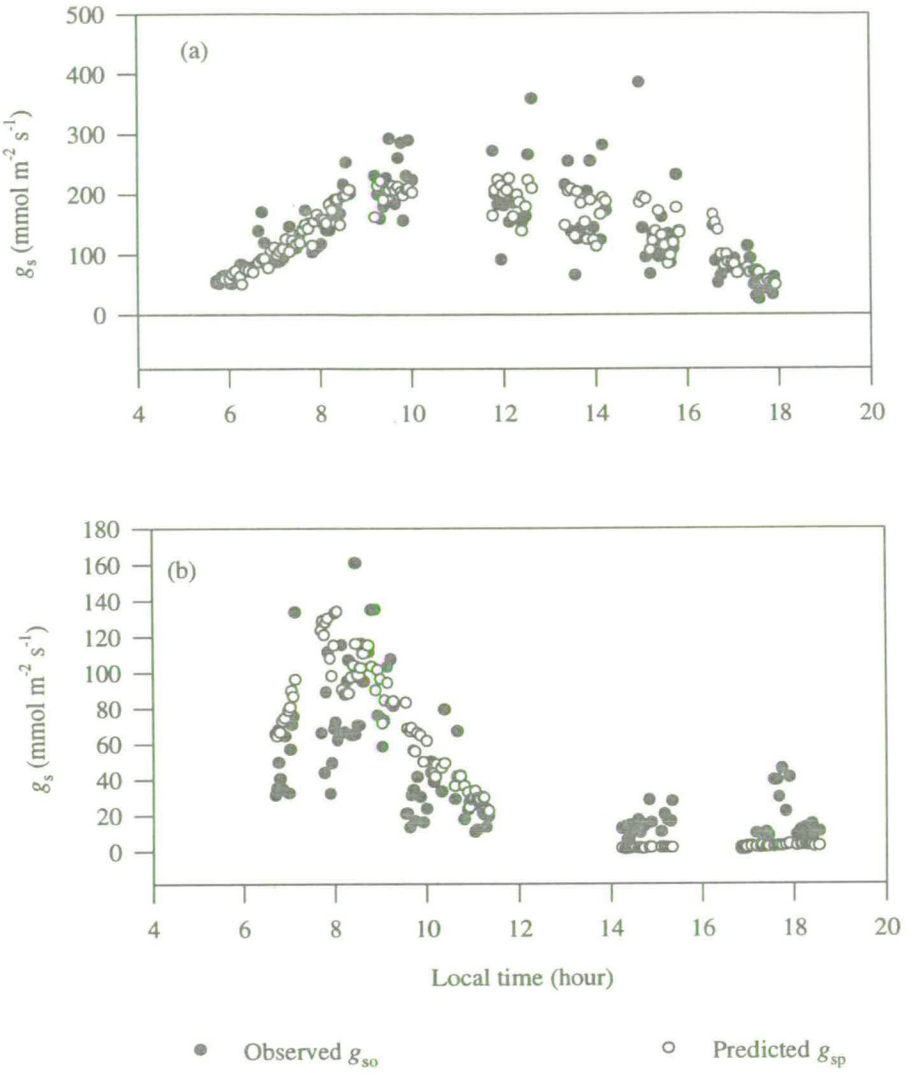

Figure 3.23 Comparison of stomatal conductance predicted by the fitted Jarvis (1976) model, g_{sp}, with observed values, g_{so}, in (a) *G. senegalensis* at the fallow site on 12/9/92 and (b) *C. micranthum* at the tiger bush site on 26/9/92. In both cases, the model predicts the mean diurnal course correctly, although afternoon values are underestimated in (b). Model predictions are conservative, and do not account for the considerable inter-shoot variation in g_{so}.

Although there is a considerable amount of unexplained variation, Figure 3.23 shows that the stomatal conductance model predicts g_S reasonably well, and correctly reproduces the mean diurnal curve, although in *C. micranthum*, it consistently underestimates in the afternoon. The failure to reproduce the variability seen in Figures 3.22-3.23 would be important if g_S was an input to a non-linear function. However, as shown in Figure 3.8, the A_l-g_S response was very close to linear.

3.7 Conclusions

(1) An increase in the respiration rate of leaves with temperature was detectable in the data, although close relationships were not found. Although there was a lack of data, and measurement accuracy may also have been a problem, the analysis gave useful estimates of the parameter values for the dark respiration model. Respiration rates were notably higher in millet than in the other species.

(2) Typical A_l values at high Q were 15-40 μmol m^{-2} s^{-1} in the C4 species and 1-10 μmol m^{-2} s^{-1} in the C3 species. The maximum values of A_l and α were around 2-3 times higher in the C4 species than in the C3 species. Between-species differences in maximum A_l and α were small in the C3 plants. The rate of photosynthesis could be predicted well from Q and g_s only. The empirical non-rectangular hyperbola model of Jarvis *et al.* (1985) accounted for around 90 % of the variation in A_l. The residual variation was not explicable in terms of any of the environmental variables that were measured or factors such as height within the canopy. Seasonal changes in A_l and model parameters were not detected.

(3) The stomata began responding to the leaf chamber environment within one or two minutes of enclosure, but this did not appear to cause a serious problem in acquisition of the data. Stomatal conductance did not differ markedly between species. Relationships between g_s and Q and g_s and D were detectable but not close. The stomatal conductance model only accounted for between 23 and 46 % of the variation in g_s. The residual variation was not clearly related to any of the measured variables, but appeared to be caused by inter-shoot variability, as much better fits were achieved to data from individual shoots. Although the observations showed considerable variability, the model predicted the mean diurnal course reasonably well.

Chapter 4

Stem and Soil CO_2 Flux

4.1 Introduction

In woody stems, CO_2 is produced as a by-product of respiration in the living cells of the xylem parenchyma, cambium and phloem, and is reassimilated to some extent where photosynthetic chlorenchyma is present in the cortex or periderm. Compared with leaves, little work has been done on the gas exchange of woody tissues. As a consequence of this, although respiration is one of the simplest and best understood physiological processes at the biochemical scale (Waygood, 1961), very little well-tested theory exists for the organ scale. There is no equivalent of the von Caemmerer-Farquhar model of photosynthesis giving a generalised description of the organ-scale process in terms of biochemical parameters and organ-scale properties. Even some of the most basic questions remain unanswered (Sprugel and Benecke, 1991). In the present context, the following questions are relevant and provide the aims of this study:

(1) What are the main sources of the respiratory flux within woody tissues? Possibilities include the dividing cambium cells, the live phloem cells, the sapwood (which although it is composed of mostly dead cells, has a large volume) and the live xylem cells in the youngest sapwood (Section 4.3).
(2) What is the magnitude of the stem respiratory flux in the tree and shrub species and how does this change with temperature, the presumed dominant environmental driving variable? (Section 4.4)
(3) What is the importance of corticular photosynthesis, considering that the trees and shrubs are virtually leafless for six months of the year? (Section 4.5)
(4) How does stem respiration change over the year in relation to the periodicity of growth? (Section 4.6)
(5) Is stem CO_2 efflux influenced by xylem sap flux? (Section 4.7)

There are several probable reasons for the apparent lack of sound theory. Firstly, the area has not received attention from crop physiologists, who have developed much of the theory of leaf photosynthesis but are rarely concerned with perennial woody species. Secondly, both the collection and interpretation of respiration data for wood is rather more troublesome than for leaves. Thirdly, respiration does not have the same obvious importance to production as photosynthesis, and so has been largely ignored by tree physiologists (this is illustrated by the lack of any commercially available systems designed to measure wood respiration, despite the plethora of leaf gas exchange systems). However, when considering the carbon balance of an ecosystem over a year or more, it is clearly an important component, as total respiration (including the soil component, considered in Section 4.8)

would be expected to equal photosynthesis in a steady-state system, such as a mature forest or other climax community. Autotrophic respiration is estimated to be 40 to 60 % of gross photosynthesis in cool temperate forest and a similar proportion in tropical forest (Meir *et al.*, in press; Lloyd *et al.*, in press).

There are two main functions of respiration in plants: (1) the production of the high energy compounds ATP and $NADPH_2$, mainly in glycolysis and the Kreb's cycle, and (2) the production of carbon skeletons for the biosynthesis of amino acids, organic acids (such as malate and citrate) and lipids, mainly via the oxidative pentose phosphate pathway (Davies, Goivanelli and Ap Rees, 1964). The primary substrate for respiration is almost exclusively sucrose. Both of these functions are involved in two rather different processes: maintenance and growth. The former (also known as basal or dormant respiration) is that involved in maintaining the cells and provides the energy for protein turnover, repair of membranes and maintaining ion gradients (Penning de Vries, 1975). Maintenance respiration is a strong function of temperature (Larcher, 1980) and is proportional to the mass of active cells, which in turn may be proportional to stem surface area, volume or both. Growth (or construction) respiration results from the metabolic processes involved in producing new tissue. It is therefore a function of the amount of growth and the chemical composition of the tissue formed. Although the distinction is broadly clear, it may be difficult to distinguish between the two in some specific cases and a third "growth-related maintenance respiration" category may exist (Sprugel and Benecke, 1991). However, this distinction still provides a useful conceptual framework for interpreting results, even if the partitioning of respiration between maintenance and growth is only an approximation. Various methods have been used for separating growth and maintenance respiration in agricultural crops (Amthor, 1989). In woody plants, the most common method of distinguishing between the two is to use dormant season measurements to establish the temperature response of maintenance respiration (eg. Ryan *et al.*, in press) and to calculate growth respiration from measurements in the growing season by subtraction. Common problems with this approach include the lack of a fully-dormant season (eg. in humid tropical rain forest) and little overlap in temperature range in dormant and growing seasons (Q_{10} may change at temperature extremes (Larcher, 1980)). Neither of these is a problem in this study, as in Niger the vegetation undergoes a long period of dormancy in the eight-month dry season, during which a larger range of temperatures is experienced than during the wet season.

4.2 Methods

Measurements of CO_2 flux from stems were made on *G. senegalensis* at the fallow site and *C. micranthum* at the tiger bush site in February and March 1992 and between June and October 1992, using the ADC LCA3 and purpose-built chambers. Two techniques were used: (1) measurements on

excised sections of stems in chambers in the laboratory, and (2) *in situ* measurements, in which chambers were sealed on to stems in the field. In both cases, an open system was used with flow rates between 150 and 500 cm^3 min^{-1}. Chambers were also constructed to fit on to the much larger trunk of *Combretum nigricans*, but no measurements were made with them because of time constraints.

4.2.1 Measurements on excised stems

Two cuboidal "Perspex" chambers were constructed with dimensions of 200 x 60 x 60 mm and 150 x 25 x 25 mm. These were fitted with small fans running on 5 V DC. Mixing inside the chambers was examined using cigarette smoke and was clearly adequate. The base section of the cuboid was attached by clips and easily removed to allow stem sections to be placed inside. Rubber foam was glued to the lower surface of the upper part of the cuboid to provide good sealing against the base plate.

Stems were cut at ground level and taken to the laboratory, where they were cut into smaller sections which could be fitted into the chambers. Diameters of the stem sections ranged from 0.1 to 5 cm. The chamber was completely shaded using black cloth except when the response to Q was being investigated. Flow rate was adjusted to give an acceptable compromise between a large differential and slow equilibration, depending on the amount of material in the chamber. Temperature was kept approximately constant by the air-conditioning in the laboratory, ranging from 23 to 27 °C during dark measurements, but always increased when using higher, natural radiation outdoors in Q response experiments. Stem temperature was measured using a copper-constantan (Cu-Con) thermojunction twisted around the stem section and referenced to the panel of a data logger (21X, Campbell Scientific Ltd, UK).

The phenomenon of traumatic or wound respiration is poorly understood and is a potential problem with measurements on excised tissue. Consequently, the ends of the stems were coated with petroleum jelly to minimise any effect of respiration from the cut surface. Measurements were always made within six hours of first excising the stem, and stems were only cut into smaller sections immediately before being measured. Five *G. senegalensis* stem sections were measured both immediately after sectioning and four hours later to check for increases in traumatic respiration over this period. No difference was found. It was intended to carry out a comparison of the *in situ* and excision methods by making in measurements on a stem before and after cutting but this was not done because of lack of time. However, rates measured by both methods were similar at equivalent temperatures.

4.2.2 *In situ* measurements

Cylindrical chambers were constructed out of a "Perspex" tube, split longitudinally with rubber seals fitted to the cut edges (Plate 4). In operation, the two halves of the cylinder were placed together to

Plate 4 Chamber used for *in situ* measurement of stem CO_2 flux.

enclose a section of the stem. A thick layer of neoprene was glued on the inside at either end to provide a seal against the stem. The chambers were 210 mm long and 40 mm in diameter.

The chamber was sealed around the selected stem at a height of 0.2 - 1 m using cable ties and connected to the LCA3 with PVC tubing. Petroleum jelly was put over all seals and the chamber tested for leaks. This was done by lightly spraying with water and checking for bubbles arising from the sealed edges whilst pumping air through the chamber under positive pressure. Reference air was obtained in the same way as described previously (Chapter 3) and flow rates of between 400 and 500 $cm^3\ min^{-1}$ were used. Output voltage signals for reference and differential CO_2 concentration were recorded every five seconds and averaged every five minutes on a data logger. Stem temperatures inside and outside the chamber were measured using Cu-Con thermojunctions placed in cracks in the bark and referenced to the panel temperature in the data logger. During the daytime, the temperature of the stem inside the chamber was typically 2-3 °C higher than the stem temperature measured outside the chamber. Q was measured with a horizontal sensor adjacent to the chamber. Shading could be applied by covering the chamber with a black cloth, effectively reducing incident Q to zero. The system was left to run continuously for one to ten days. The approach was to measure a relatively small number of stems (two to four) each month and to leave the chamber on for several days so as to get complete diurnal curves. This was quite different from the approach used in leaf gas exchange measurements for several reasons. Each individual measurement was more difficult, given the problems of finding suitably smooth, straight stems, sealing and leak testing the chamber, and so it was more efficient to extract the maximum amount of data with a minimum of set-up time. Feedback between the CO_2 efflux and chamber conditions is much less with respiration (eg. there is no stomatal closure as a result of chamber heating) and so the chamber can be left in place with relatively little effect on the process being studied (although there is some evidence that there is a reduction in respiration in elevated CO_2 (Bunce, 1990)). Compared with leaf photosynthesis, it would be expected that variability in stem respiration rate is less at any given time as the distribution of temperature is much more homogeneous than that of Q. Furthermore, stem temperature cannot be manipulated as easily as Q and so the diurnal course of temperature was utilised.

4.3 Source of respiration

An experiment was carried out to identify the sources of the respiratory flux within the woody stems. Sections of several stems of *G. senegalensis* of different diameters were measured as described in Section 4.2.1 in February 1992. The experiment was repeated on *C. micranthum* in July 1992.

Possible sources of respiration include the resting and dividing cambial cells, phloem cells and the protoxylem and xylem parenchyma in the sapwood. If the cambial, phloem or protoxylem cells are the

main source, then the measured flux should be proportional to the *surface area* in the chamber. If sapwood xylem parenchyma cells are more important, the *volume* of wood will be the most important factor. The respiration rate of stem sections of different diameters was measured and the CO_2 efflux was expressed in relation to the diameter of the stem (d), both on a surface area (S) basis and on a volume (V) basis. The sections were assumed to be cylindrical (tapering was insignificant) and the surface area of the cut ends excluded. The surface area to volume ratio (S/V) of the stem sections decreases with stem diameter, as the numerator in Equation 4.1 increases in proportion with the radius, r, but the denominator increases in proportion with the square of the radius.

If the respiration rate, R, is related to the *surface area*, then there should be a positive linear relationship between the reciprocal of stem diameter, d^{-1} and CO_2 flux *per unit volume* (Figure 4.1(a)).

If $R \alpha S$, then $R/V \alpha S/V$

$$S/V = \frac{2\pi rl}{\pi r^2 l} = \frac{2}{r} \qquad [4.1]$$

Thus $R/V \alpha d^{-1}$.

That is, thin stems (high S/V) will have higher rates than thick stems when expressed per unit volume. No relationship with CO_2 flux per unit area would be expected.

Alternatively, if the flux is *volume dependent*, there should be a positive linear relationship between diameter and the *area averaged* flux (Figure 4.1(b)) but no relationship with the volumetrically averaged flux.

If $R \alpha V$, then $R/S \alpha V/S$

$$V/S = \frac{\pi r^2 l}{2\pi rl} = \frac{r}{2} \qquad [4.2]$$

Thus $R/S \alpha d$.

Thin stems would have a smaller amount of respiring volume per unit area than thick stems and thus lower respiration rates on an area basis.

Results and Discussion

The results of both experiments are shown in Figure 4.1. In *C. micranthum*, there is a clear increase in the flux per unit volume with d^{-1} (Figure 4.1(c)) but no relationship with the flux per unit area (Figure 4.1(d)). The data thus indicate that the major respiratory source is area related. The situation is

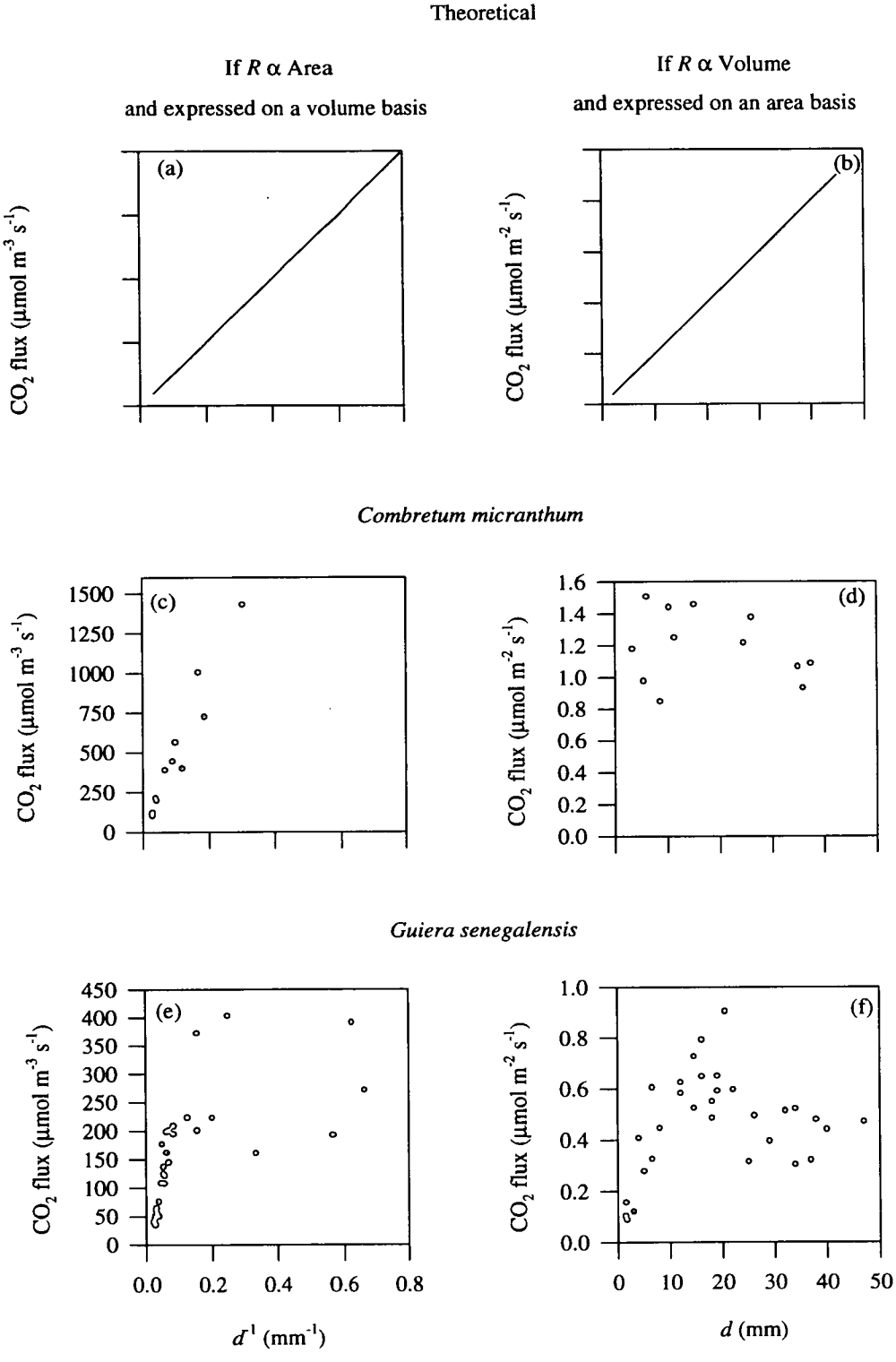

Figure 4.1. Respiration rate of exised stem sections of a range of diameters, *d*, (and *S/V* ratios) expressed on a volume (c and e) and surface area basis (d and f). (a) and (b) show the expected relationship if the respiratory source is proportional to stem surface area or stem volume. With the exception of the four smallest stems of *G. senegalensis*, the data fit the former hypothesis.

slightly less clear in *G. senegalensis*, but results appear very similar if the four smallest stem sections are ignored, ie. there is a linear increase in the flux per unit volume with d^{-1} (Figure 4.1(e)) but no relationship between d and flux per unit area (Figure 4.1(f)). A weak positive relationship between diameter and area averaged flux is found in the smallest stem sections (d <10 mm) of *G. senegalensis* (Figure 4.1(f) $r^2 = 0.693$, n = 9), suggesting that the volume component is more important in these tissues. This may be because a higher proportion of the xylem cells are alive in the young thin stems. However, most of the other points do not fit this relationship, whereas all but four fit with the linear relationship in Figure 4.1(e). Thus, these data also support the idea that the major respiratory source is area related, with the possible exception of very small stems (d < ~5 mm).

These results are in general agreement with the assessment of Landsberg (1986), who concluded that surface area was generally the more important component, attributable to activity of cambial and phloem cells. However, Ryan (1990) found that volume was the major component in large stems of two *Pinus* species, as the volume of living cells in the sapwood surpassed that of the cambium and phloem. Based on this and studies on *Abies amabilis*, Sprugel *et al.* (1993) state that "when construction respiration is absent ... phloem and cambium respiration are insignificant compared with sapwood maintenance respiration" and conclude that area-averaged rates will not be generally useful. While it may be true that no universally applicable relationship exists between respiration rate and either surface area or volume (as these relationships will depend on the distribution and activity of living tissue within in the stem, which will vary with age and species), this study shows that at least in the present cases, respiration can be usefully and simply expressed on an area basis. It may be significant that the relationship with surface area is closer in the measurements made on *C. micranthum* in the growing season than in the measurements made on *G. senegalensis* in the dry season (Figure 4.1), as growth respiration will mostly occur in the cambium, and so is likely to be related to the surface area.

4.4 Response to temperature

Respiration is known to be strongly influenced by temperature, in common with other biochemical processes where enzyme kinetics are important (Larcher, 1980). This classically takes the form of an exponential increase described by the equation

$$R = R_0 \exp(kT) \qquad [4.3]$$

where R_0 is the respiration rate at 0 °C, k is a temperature coefficient and T is temperature. This relationship is also referred to as a "Q_{10}" curve where Q_{10} is equal to $\exp(10k)$ and is the increase factor for a 10 °C rise in temperature. Temperature response was measured in the field using the

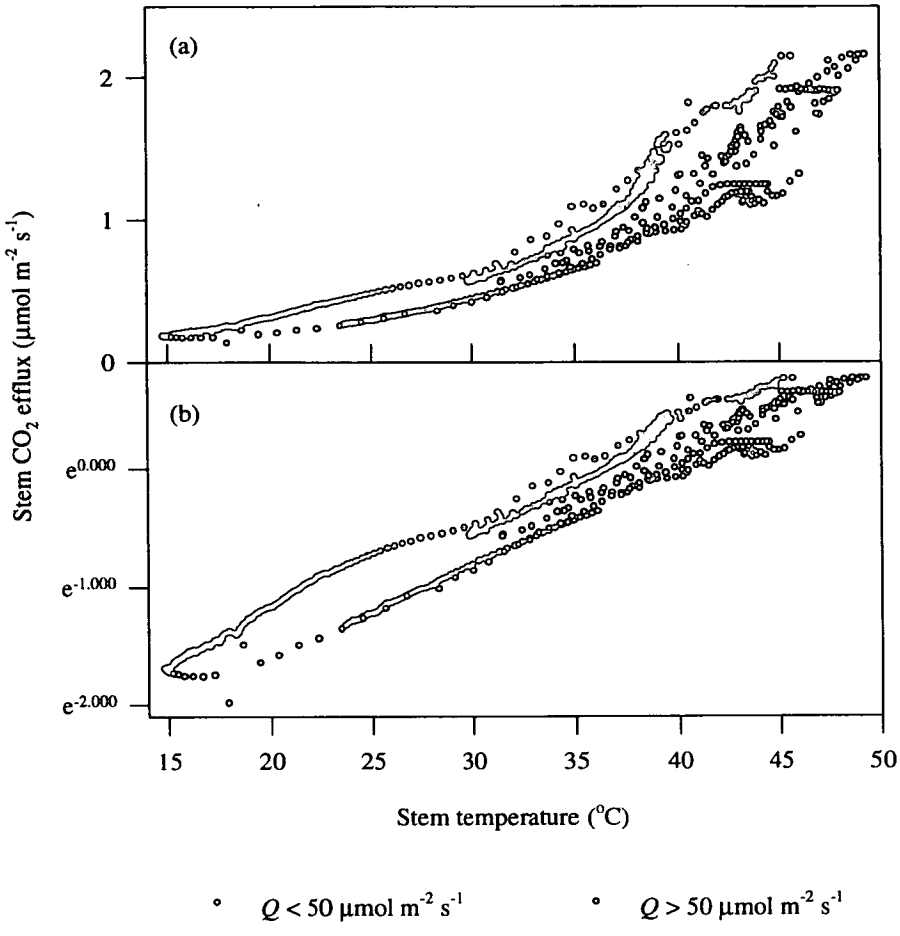

Figure 4.2 Response of stem respiration in *Guiera senegalensis* to temperature during the dry season as (a) a linear plot and (b) on a logarithmic scale. The data are 10 minute averages of *in situ* measurements on two stems. The chamber was shaded for periods with black cloth to investigate the effect of Q. An increase in the efflux was observed when shaded.

methods described in Section 4.2.2. Temperature responses have rarely been derived from *in situ* observations as the diurnal temperature range is often too small. However, in the Sahel, a very large diurnal range is found, particularly in the dry season, providing an excellent situation for this measurement.

Figure 4.2 shows the expected exponential increase in respiration with temperature in data for *G. senegalensis* from the dry season. Field respiration rates were relatively high in *G. senegalensis* because of the high temperatures attained by stem surfaces. This was exaggerated by the increase in stem temperature inside the chamber relative to stem temperature measured adjacent to the chamber,

but this was typically only 2-3 °C and rarely more than 5 °C. The data obtained during the dry season using shading were used to establish the basal maintenance respiration rates as a function of temperature for these two species, as no growth was occurring at this time (discussed in Section 4.6). Values of Q_{10} derived from the dry season data were 2.21 for *G. senegalensis* and 1.89 for *C. micranthum*. The parameters of the fitted exponential equation are given in Table 4.2. Apparent respiration rates were higher in low Q, suggesting that there was significant corticular photosynthesis, discussed in Section 4.5.

4.5 Stem photosynthesis

Photosynthesis has been reported in woody stems of several species (eg. Ludlow and Jarvis, 1971; Perry, 1971; Bossard and Rejmanek, 1992)). The cortex of many *G. senegalensis* stems was clearly green beneath the bark, particularly in fissures where the bark was thin, indicating the presence of chloroplasts and the capacity for photosynthesis. Generally, the cortex in *C. micranthum* stems did not appear green, and the bark was smooth and thicker. An experiment was performed in March 1992 to measure the magnitude of corticular photosynthesis in *G. senegalensis* using excised stem sections as described in Section 4.2.1. Different values of Q were obtained by placing the chamber outdoors in natural light on a clear day and shading with cloth. Q incident on the chamber was measured by a horizontal sensor. Full Q was obtained by orientating the chamber, stem section and Q sensor normal to the solar beam. Temperature inevitably increased over measurement periods (typically by 3.5 to 5.0 °C) which were kept as short as possible for this reason. Measurements were made at four values of Q on five stem sections. *In situ* measurements were also made both in natural light and with black cloth completely shading the chamber, as mentioned in Section 4.4.

The results in Figure 4.3 and Table 4.1 show that a high proportion of respired CO_2 may be refixed. These results are in broad agreement with the data reviewed by Sprugel and Benecke (1991), who

Table 4.1 Refixation in excised *G. senegalensis* stem sections and *in situ*. Refixation is calculated as the difference between the CO_2 efflux in the dark and in full light (Q = 1500 to 1800 μmol m^{-2} s^{-1}). In the dark, temperature ranged between 26.4 and 35.5 °C, and on average, was increased by 4 °C in full light. The *in situ* measurements are the same as those presented in Figure 4.2. Here, temperatures ranged from 15 to 50 °C.

Stem section	CO_2 efflux in dark (μmol m^{-2} s^{-1})	Refixation in full light (μmol m^{-2} s^{-1})	Refixation / dark respiration (%)
1	0.53	0.295	56
2	1.24	0.846	68
3	0.75	0.540	71
4	0.82	0.625	76
In situ	0.2 - 2.1	0 - 0.4	0 - 33

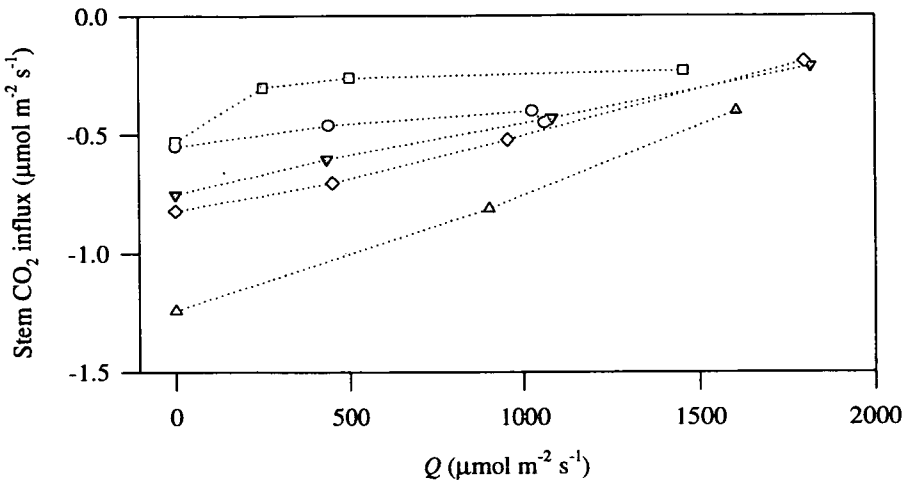

Figure 4.3 The relationship between stem CO_2 influx and Q in five excised stem sections of *G. senegalensis*. Different values of Q were obtained using natural light and shading with cloth. In the dark, stem temperature ranged between 26.4 and 35.5 °C, and on average, was increased by 4 °C in full Q.

found that refixation may reach 80-90 % of respiration. Refixation is expressed on a surface area basis, although only half of this surface received direct radiation, as this permits comparison with respiration rates on an equal basis. Although no net photosynthetic gain occurred even in full Q, the data clearly show a photosynthetic response: the efflux from the stem decreased as Q increased. This response was linear in four out of five cases, suggesting that photosynthesis was Q-limited. This is likely for three reasons: (1) one side of the stem was always in shade, (2) only a small fraction of Q incident on the bark is transmitted to the chloroplasts in the cortex, and (3) the supply of CO_2 to these cells is likely to be plentiful (internal concentration of approximately 30 000 μmol mol^{-1}, see Section 4.7) as CO_2 evolved in respiration of surrounding tissue can be refixed.

The rates of refixation from excised sections are likely to be overestimates of values occurring *in situ*, as the stem was positioned horizontally during the experiment and so would absorb more radiation than a stem that was upright within a bush, shaded by a canopy of leaves. Typical *in situ* rates of refixation are shown in Table 4.1, estimated from the data in Figure 4.2 which shows clear decreases in stem CO_2 efflux when the chamber was unshaded. *In situ* refixation ranged from 0 μmol m^{-2} s^{-1} at 15 °C to around 0.4 μmol m^{-2} s^{-1} at 45 °C, and represents at most 33 % of dark respiration. However, it is harder to relate these data to Q as the irradiance received by the vertical stem may differ considerably from that measured by the sensor in the horizontal plane, depending on solar angle.

It is difficult to measure the amount of Q transmitted through the bark, although Sprugel and Benecke (1991) estimate 15 % as a broad average. Because of the intense shading, it is expected that the highest photosynthetic rates will be found in the exposed chlorenchyma in bark fissures and in young stems where the periderm is still green.

Several reviews of work on leaves tentatively suggest that "dark" respiration *per se* is reduced by Q (eg. Jackson and Volk, 1970), although the effect is difficult to study because of confounding increases in photosynthesis and photorespiration (Cornic and Jarvis, 1972). It is possible that some component of the apparent photosynthetic response in Figure 4.3 is actually photoinhibition of respiration rather than refixation of respired CO_2, but it is not possible to distinguish between the two possibilities with the method used. Photorespiration is likely to be very restricted in the chlorenchyma as CO_2 concentrations are high there (see Section 4.7), together with low O_2 concentrations and Q.

There is probably little or no water loss associated with corticular photosynthesis, as internal CO_2 is refixed and the chlorenchyma is not exposed to the air via stomata or lenticels. Water loss through the periderm was not measured in these experiments, but was probably very low. It seems likely that refixed carbon will be used locally in respiration once again, as corticular photosynthetic rates never exceeded the respiration rate and so an assimilate pool will not accumulate. The effect will, therefore, be a reduction in the maintenance cost of the woody tissue. Corticular photosynthesis will be particularly effective during the six to seven months of the dry season when the plants are leafless and the stems receive a higher Q than in the wet season. Consequently, corticular photosynthesis in *G. senegalensis* can be interpreted as a xerophytic adaptation for carbon economy, and may represent a saving of a significant proportion of the plant's annual carbon budget.

4.6 Seasonal change in respiration

In situ measurements were made in the dry season (in February and March 1992) and in various stages of the wet season (between July and October 1992) to examine how seasonal changes in vegetation activity affect respiration. In the dry season from November to May, both species are more or less leafless and dormant. Leaf growth begins with the onset of the rains in May or June. Leaf area reaches a maximum in late August - early September, before senescence and leaf fall begin in late September - October. The bushes are mostly leafless again by November. The methodology used to measure respiration is described in Section 4.2.2. Only measurements made in the dark are compared so as to remove Q as a complicating variable.

Figures 4.4 and 4.5 show that at 40 °C, respiration rates in *C. micranthum* and *G. senegalensis* were generally less than 1 μmol m^{-2} s^{-1} in the dry season, and between 2 and 6 μmol m^{-2} s^{-1} in the wet

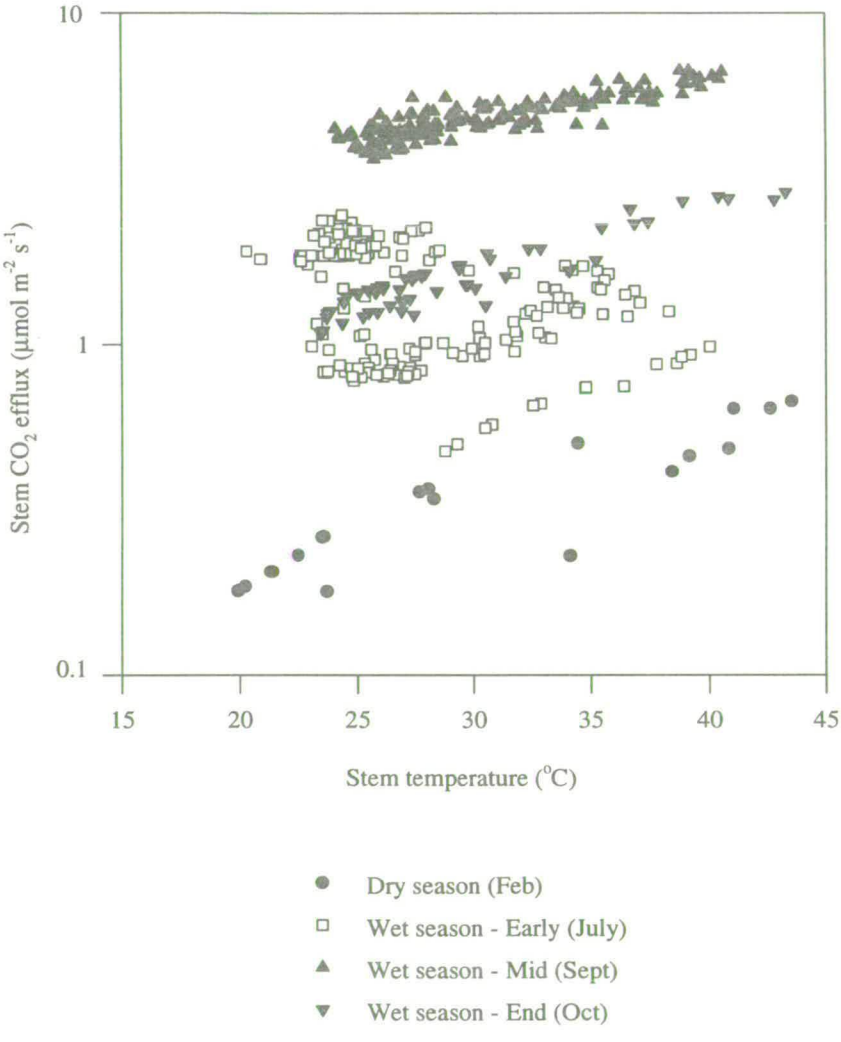

Figure 4.4 Seasonal change in respiration rate in *C. micranthum*. Two to four stems were measured in each sampling period. Data shown are hourly averages. Note the logarithmic scale.

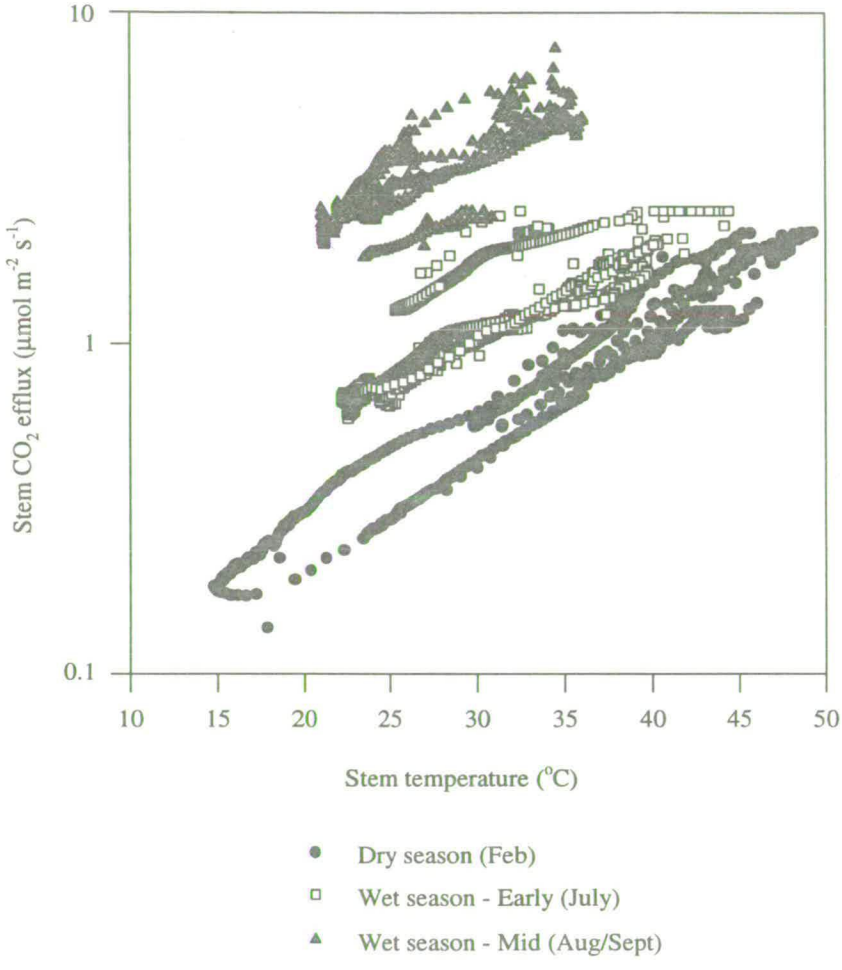

Figure 4.5 Seasonal change in respiration rate in *G. senegalensis*. Data are 10 minute averages. Two to four stems were measured in each sampling period. Note the logarithmic scale.

season. There are also differences within the growing season, as the rates were highest in August and September, the peak of the season, and were lower in July and October. These values fall within the range of 1.3 to 5.3 μmol m^{-2} s^{-1} at 20 °C quoted by Jarvis and Leverenz (1983) for a wide range of species during times of high meristematic activity (a maximum value of 2.8 μmol m^{-2} s^{-1} was obtained for *C. micranthum* by extrapolation to this temperature). The data were fitted to Equation 4.3, describing the exponential response to temperature and the derived parameters are listed in Table 4.2.

Table 4.2 Seasonal change in parameters in the equation $R = R_0 \exp(k\,T)$. Q_{10} is given by $\exp(10k)$. Results for *C. micranthum* in July are not included as too much unexplained variability was present in the data.

Month	R_0	k	Q_{10}	r^2	n
G. senegalensis					
February	0.056	0.0793	2.21	0.95	356
July	0.168	0.0626	1.87	0.85	952
Aug/Sep	0.712	0.0551	1.73	0.74	972
C. micranthum					
February	0.053	0.0638	1.89	0.68	135
July	-	-	-	-	-
September	2.145	0.0269	1.31	0.65	1000
October	0.427	0.0449	1.57	0.85	690

During the growing season, there was a large increase in the R_0 parameter and a small decrease in the k parameter in both species. To try to quantify the change in respiration attributable to growth, the growing season data were fitted to an equation incorporating a growth term, R_{og}

$$R = (R_{om} + R_{og}) \exp(k\,T) \qquad [4.4]$$

where R_{om} and R_{og} are the maintenance and growth respiration rates at 0 °C respectively. The R_{om} and k parameters describing maintenance respiration were assumed to be equivalent to the values derived during the dry season. The assumption that the value of k derived in the dry season was constant throughout the year may be valid, as the temperature response is an intrinsic property of respiration related to enzyme kinetics. Although Table 4.2 shows that k apparently did vary, inspection of Figures 4.4 and 4.5 shows that the major change during the growing season was in the offset ($R_{om} + R_{og}$), not the slope of the temperature response, k. The variation in k was small and may have been caused by sampling error. [The analysis was not used on the *C. micranthum* data from September, where the k value was markedly different, possibly because of interaction with the xylem sap flow (Section 4.7)]. Constancy in the value of k has been observed in apple trees over eight months and in different phenological states (Butler and Landsberg, 1981), in stems and roots of Scots pine throughout the year (Linder and Troeng, 1981) and in a wide range of conifers (Jarvis and Leverenz, 1983). However, some evidence to the contrary was reported by Hagihara and Hozumi (1991), who found a decline in k

in summer and interpreted this as a change in enzyme activation energy. It was also assumed that the rate of maintenance respiration was constant over the year when the effect of temperature was taken into account, ie. the R_{om} parameter was constant. This assumption is less justifiable because R_{om} might be expected to vary in relation to the seasonal changes in the amount, composition and activity of living tissue. However, given these assumptions, Equation 4.4 provides a basis for the quantitative separation of the growth and maintenance components of respiration. The derived R_{og} parameters are shown in Table 4.3.

Table 4.3 Seasonal change in the growth parameter R_{og} and growth respiration, R_g at 25 °C, calculated as $R_g = R_{og} \exp(kT)$. Results are not included for *C. micranthum* in July as too much unexplained variability was present in the data, or for *C. micranthum* in September, when the value of k was markedly different.

Month	R_{og}	R_{om}	k	R_g (at 25 °C)
G. senegalensis				
February	0	0.056	0.0793	0
July	0.029	"	"	0.21
Aug / Sept	0.210	"	"	1.52
C. micranthum				
February	0	0.053	0.0638	0
July				
September				
October	0.150	"	"	0.74

At 25 °C, the growth respiration term in Table 4.3 is approximately 1.5 μmol m^{-2} s^{-1} in *G. senegalensis* and 0.74 μmol m^{-2} s^{-1} in *C. micranthum*. Very few data are available for comparison, especially from tropical species. These estimates are higher than the values of 0.21 and 0.57 μmol m^{-2} s^{-1} for two tropical tree species calculated from growth measurements by Ryan *et al.* (1994), where stem temperatures averaged 24.6 °C. However, Ryan's values were based on several assumptions, including constant growth over the year, and higher rates might be expected in the short growing season of the Sahel.

Changes in the R_0 parameter have been found in other studies and attributed to changes in growth respiration. For example, Linder and Troeng (1981) found similar results to these in Scots pine, with a summer increase in R_0, but a constant value for k. Although an increase in growth respiration is one explanation for these results, there are other possibilities: (1) there is a change in the basal maintenance rate, for example, as a result of an increase in the number and mass of living cells per unit area by augmentation of the cambial layer with partially differentiated xylem cells or changes in phloem activity (Havranek, 1981); (2) there is growth-related maintenance respiration (Sprugel and Benecke, 1991); or (3) there is a change in substrate availability, for which there is some evidence that this is a controlling factor (Hansen, 1977; Azcon-Bieto and Osmond, 1983; Azcon-Bieto, Lambers and

Day, 1983). However, without more sophisticated methodology, these possibilities cannot be distinguished between.

Seasonal differences were confounded to some extent by variation amongst stems, and this appears to be a problem with the July *C. micranthum* data, although the broad seasonal pattern is the same in both species. Seasonal changes may also be confounded by differences in sap flow (see Section 4.7), as the transpiration rate is closely linked to leaf area on the bush, which in turn is related to growth rate.

It was intended to measure wood growth in late October 1992 by re-measuring the diameters previously surveyed in February. This would have allowed comparison of actual growth measurements with predictions based on growth respiration measurements, on the basis that 0.43-0.47 g of CO_2 are evolved for each gramme of biomass produced (Penning de Vries, 1975). Change in basal maintenance rate since February could have been determined by measuring respiration rates after the growing season had ended. Circumstances did not permit these measurements to be made.

4.7 Interaction with sap flow

4.7.1 Introduction

Both respiration and photosynthetic rates are inferred from measurements of the CO_2 concentration in the air enclosed within a chamber. It is assumed that the rate of the process is equivalent to the CO_2 flux between the plant and the chamber air. It is, however, possible that CO_2 produced or consumed by these processes may be transported in the transpiration stream, representing an internal circulation of CO_2 (Hari, Nygren and Korpilahti, 1991). It would be expected, although it has rarely been measured, that CO_2 concentrations in the air spaces within the soil and wood would be high as a result of releases by microbial, root and stem respiration, whilst the intercellular CO_2 concentration in photosynthesisng leaves is typically 80 (C4) to 250 (C3) $\mu mol\ mol^{-1}$ (Chapter 3). If water high in dissolved CO_2 enters a leaf via the transpiration stream, the leaf may assimilate more CO_2 than a chamber measurement would indicate. It is less clear what the effect on stem respiration measurements would be, as little is known about the distribution of CO_2 concentration gradients within stems. This internal circulation has very rarely been considered, although peculiarities in some respiration measurements have occasionally been attributed to it (Negisi, 1981; Ryan, 1990). Indirect evidence for the internal circulation of carbon comes from the studies of Vapaavuori and Pelkonen (1985) and Vuorinen, Vapaavuori and Lapinjoki (1989). In their experiments on willow cuttings growing hydroponically, growth was increased by up to 31 % by adding sodium bicarbonate ($NaHCO_3$) to the water bathing the roots. Experiments using radiocarbon (in the form of $NaH^{14}CO_3$) strongly suggested that either the dissolved CO_2 or HCO_3^- in the transpiration stream was assimilated in photosynthesis.

Chase (1934, cited in Kramer and Kozlowski, 1960) measured CO_2 concentrations between 2 and 25 % (20 000 and 250 000 μmol mol^{-1}) in air within stems of poplar, oak, elm and pine. The concentration appeared to follow the seasonal changes in temperature (and, presumably, respiration) and was higher in the heartwood than in the sapwood. More recently, Raven and Farquhar (1989) measured the CO_2 concentration of air in equilibrium with xylem exudate from decapitated *Phaseolus vulgaris* L. seedlings, and obtained mean values of 2.18 and 3.10 kPa (21 800 and 31 000 μmol mol^{-1}).

Hari, Nygren and Korpilahti (1991) attempted to measure the CO_2 concentration in sap within pine stems by inference from measurements of CO_2 concentration in the air in bore holes drilled in the tree. Samples were taken with a syringe through a rubber septum covering the hole, injected into bottles for dilution and measured with an infra-red gas analyser. Results were variable, ranging from 3000 to 20 000 μmol mol^{-1}. The upper limit was converted to a sap CO_2 concentration using Henry's Law (see Section 4.7.2) and multiplied by a typical transpiration rate in order to estimate the magnitude of internal circulation. The amount of CO_2 carried by the sap flow to the leaves was estimated to be equivalent to 2 to 9 % of the photosynthetic rate.

There are several problems with their methodology which may explain the variability in their data and would lead to underestimates of sap CO_2 concentration. The air samples extracted were larger than the volume of the bore holes (20 cm^3 air from a 15.3 cm^3 hole). This may create a negative pressure in the hole which could induce a leak of atmospheric air into the sample. This appears quite likely given the range of measured concentrations. Wound respiration at the cut surface of the hole may introduce further variability.

Negisi (1979) measured CO_2 flux on detached stems of young *Pinus densiflora* trees through which the flow rate of water was controlled using a vacuum pump. The rate of CO_2 release through the bark of the segments decreased with increasing rate of sap flow (0-60 cm h^{-1}). In the range 15 to 25 cm h^{-1}, typical of the rates of sap flow in these trees on clear summer days, the bark respiration rate was 80 to 40 % of the rate at zero sap flow. However, if the water passed through the stem was initially in equilibrium with laboratory air (this is presumed although not explicit), it will be relatively low in dissolved CO_2 and provide an unnaturally large diffusion gradient within the stem. In natural situations, water coming from the roots would contain a high concentration of dissolved CO_2 and under these circumstances, sap flow may conceivably increase stem CO_2 efflux.

In experiments on potted loblolly pine seedlings, in which the crowns were enclosed in a cuvette in which the saturation vapour pressure deficit could be manipulated, Martin, Teskey and Dougherty (1994) found that stem CO_2 efflux rates were reduced by an average of 0.18 μmol m^{-2} s^{-1} during

periods of high transpiration (1.18 mmol m^{-2} s^{-1}) compared with periods of low transpiration (0.52 mmol m^{-2} s^{-1}). This was attributed to the removal of respired CO_2 by the transpiration stream.

Two experiments were carried out to investigate the influence of sap flow on stem CO_2 efflux:

1) The concentration of CO_2 in sap was measured essentially as by Hari, Nygren and Korpilahti (1991), but with a specially designed chamber so as to remove the pressure and wounding problems. This was carried out in Edinburgh on birch and oak trees as the necessary equipment was not available in Niger and is discussed in Section 4.7.2.

2) The interaction between sap flow and stem CO_2 flux was examined directly by measuring both processes simultaneously on the same stem under natural conditions. This was done on one stem of *C. micranthum* and two stems of *G. senegalensis* in Niger (Section 4.7.3).

4.7.2 Experiment 1 - Concentration of CO_2 in sap

Methods

Measurements were made on one oak tree (*Quercus petraea*) and three silver birch trees (*Betula pendula*) on the King's Buildings campus at the University of Edinburgh in September 1993. Two small chambers were constructed for the collection of samples of gas from the trees. These were sealed on to the tree surface and left until they had equilibrated with the air inside the wood (ie. until the CO_2 concentration inside the chamber had stopped increasing). The drilling of a bore hole was therefore unnecessary and appeared to induce wound respiration on the single occasion when this was done (Figure 4.7). The chambers were fitted with two outlets. To one of these was attached a short piece of butyl rubber, which could be opened and sealed with an adjustable clip, through which samples could be removed by attaching a syringe (without a needle). To the other was fitted a balloon which in effect formed a lung within the chamber, with a mouth open to the atmosphere. This allowed atmospheric pressure to be maintained within the chamber even after removing several gas samples, as the balloon was deflated before attachment of the chamber to the tree and inflated slightly as each sample was withdrawn.

The chambers were sealed on to the tree using "Blue-tac" adhesive and elasticated cords and completely shaded by black cloth to prevent any refixation. They were left in position for up to nine days and samples taken approximately once a day. Sample volume was between 2 and 5 cm^3. The sample was injected into a gas analyser (LI-6200, Li-Cor Inc., Lincoln, Nebraska, USA) operating as a closed system containing ambient air with a volume of 154 cm^3. To avoid increasing pressure within the system, the plunger of the syringe was withdrawn to its original position after injection and allowing 10 seconds for mixing. The concentration of the sample, $[CO_2]_{sample}$, was calculated as:

$$[CO_2]_{sample} = \Delta[CO_2]\frac{V_{system} + V_{sample}}{V_{sample}} + [CO_2]_{initial} \quad [4.5]$$

where $[CO_2]_{initial}$ is the initial CO_2 concentration within the IRGA closed system, V_{system} and V_{sample} are the volumes of the IRGA closed system and the gas sample, respectively, and $\Delta[CO_2]$ is the change from the initial concentration after injecting the sample. The CO_2 concentration of the gas sample was converted to a value for CO_2 dissolved in water ($[CO_2^*]$) using the formulation of Henry's Law below, given by Stumm and Morgan (1981), ie.

$$[CO_2^*] = pCO_2 K_H(T)\left(1 + \frac{K_1(T)}{[H^+]} + \frac{K_1(T)K_2(T)}{[H^+]^2}\right) \quad [4.6]$$

where $[CO_2^*]$ is the concentration of all products of CO_2 dissolved in water, ie.:
$[CO_2^*] = [CO_{2(aq)}] + [H_2CO_3] + [HCO_3^-] + [CO_3^{2-}]$,
pCO_2 is the partial pressure of CO_2 in air,
$K_H(T)$ is Henry's constant for CO_2, and
$K_1(T)$ and $K_2(T)$ are dissociation constants for bicarbonate and carbonate ions.

Results

Figure 4.6 shows that the chamber CO_2 concentration reached equilibrium within a day at around 30 000 µmol mol^{-1}, ie. around 100 times ambient. This equilibrium value can be temporarily increased by wounding and lowered by Q in the unshaded chamber. This value of 30 000 µmol mol^{-1} for pCO_2 was used in Equation 4.6 to calculate the concentration of all products of CO_2 dissolved in water, $[CO_2^*]$. Air temperature was obtained from a nearby weather station, and was *ca* 10 °C over the course of the experiment. The pH of the sap was estimated from other measurements in the literature. A value of 5.6 was found by Carter and Larson (1965) in loblolly pine, similar to the value for water in equilibrium with ambient air. The pH of xylem exudate from *Phaseolus vulgaris*, measured by Raven and Farquhar (1989), ranged between 5.6 and 6.2. Schurr and Schulze (1995) found values of pH between 5.4 and 6.2 in root exudate from castor bean (*Ricinus communis* L.). In a more detailed study, Gollan, Schurr and Schulze (1992) found a diurnal variation in the pH of xylem sap in sunflowers, between 5.6 and 7.2, which appeared to be related to nitrate concentration. Taking the mid-point of this range (pH 6.4) and 30 000 µmol mol^{-1} for pCO_2 Equation 4.6 gives a value of 0.054 µmol CO_2 mmol^{-1} H_2O or 3.02 mmol CO_2 m^{-3} H_2O for $[CO_2^*]$ at 10 °C. This value is very sensitive to pH and, to a lesser extent, temperature (Figure 4.7).

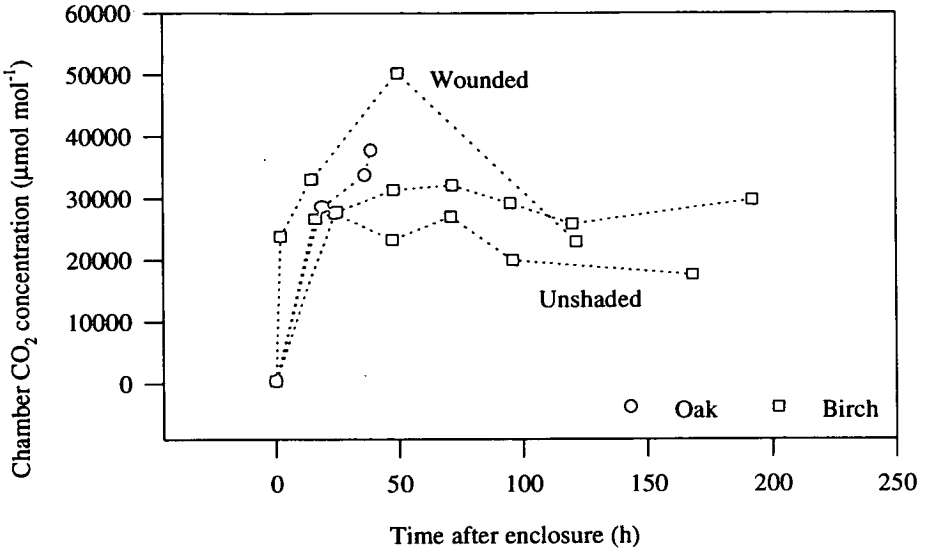

Figure 4.6 Increase in chamber CO_2 concentration with time. An equilibrium value of around 30 000 µmol mol^{-1} was reached after 24 hours. This value was lower in the unshaded chamber and higher where holes were drilled, apparently inducing wound respiration.

Discussion

Figure 4.6 and these calculations show that very high concentrations of CO_2 may be present in the air and water within woody stems. The experiment has since been repeated in Cameroon using one of the same chambers, where values up to 84 000 µmol mol^{-1} were obtained (P. Meir, pers. comm.). Temperature there ranged from 25 to 30 °C, compared to around 10 °C in Edinburgh and so respiration rates might be expected to be rather more than double, assuming a Q_{10} of 2.

Other estimates of xylem sap CO_2 concentration found in the literature arise from studies of parasitic mistletoe growing on tree hosts. The carbon in the sap has a different isotopic signal from the atmosphere and this can be used to calculate how much carbon the mistletoe gains heterotrophically from the sap, and how much is assimilated in the normal way from the atmosphere. The xylem sap CO_2 concentration can then be calculated from this proportional heterotrophy and measured rates of photosynthesis and transpiration (Marshall *et al.*, 1994). Values derived in this way ranged from 3 to 16 mmol CO_2 m^{-3} for eight tree species in Australia (Marshall *et al.*, 1994), and up to 22 mmol CO_2 m^{-3} in *Juniperus osteosperma* (Marshall & Ehleringer, 1990) and 26 mmol CO_2 m^{-3} for *Quercus rubra*

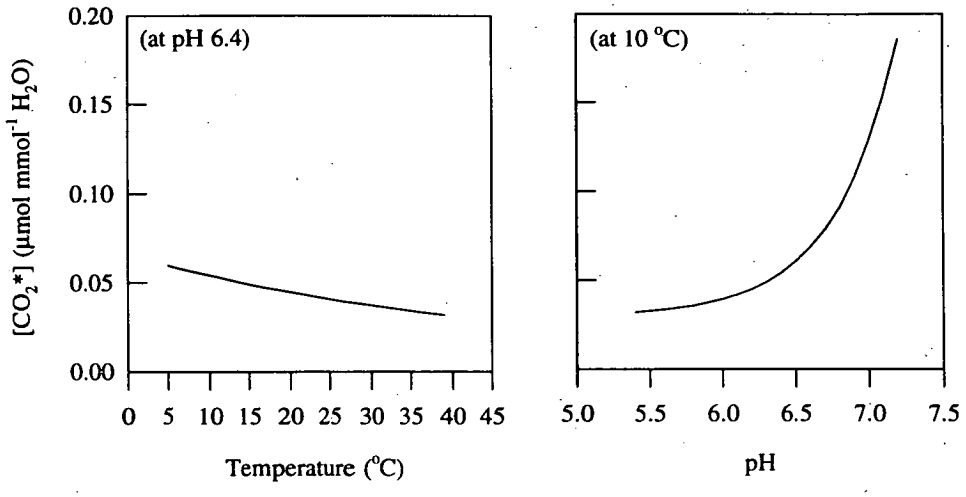

Figure 4.7 Effect of temperature and pH on $[CO_2^*]$, the concentration of all products of CO_2 dissolved in water, ie., $[CO_2^*] = [CO_{2(aq)}] + [H_2CO_3] + [HCO_3^-] + [CO_3^{2-}]$. The curves are given by Henry's Law (Equation 4.6), assuming the water is in equilibrium with air containing 30 000 µmol CO_2 mol^{-1}.

(van Die and Willemse, 1975, cited in Marshall & Ehleringer, 1990). This range corresponds to between 1 and 8.7 times our value measured in birch.

There would seem to be two possible fates for this CO_2 present in the xylem sap: it may be transported to the leaves where it is assimilated or diffuse into the atmosphere through the stem. It is therefore desirable to quantify the effect of this CO_2 on measurements of leaf photosynthesis and stem respiration. The effect on the latter is discussed in Section 4.7.3: the effect on photosynthesis is discussed below.

We can assess the influence of internal circulation of CO_2 on measurement of photosynthesis by multiplying sap CO_2 concentration by the transpiration rate (equal to the rate at which water enters a leaf) and expressing this as a percentage of the photosynthetic rate of the leaf (Table 4.4). For birch in central Scotland, typical rates for transpiration and photosynthesis are 3 mmol H_2O m^{-2} s^{-1} and 10 µmol CO_2 m^{-2} s^{-1}, respectively (A. Rey, pers. comm.). Alternatively, we can apply the estimate of sap CO_2 concentration to the *C. micranthum* stem in Niger, where sap flow and photosynthetic rate were measured. Daytime sap flow rates were on average 3.1 mmol s^{-1}, which, when multiplied by 0.054 µ mol CO_2 $mmol^{-1}$ H_2O, gives a flow of 0.167 µmol CO_2 s^{-1} in the plant transpiration stream and this is distributed over a leaf area of 1.255 m^2, ie. a CO_2 refixation rate of 0.13 µmol CO_2 m^{-2} s^{-1}.

Although the values of refixation in Table 4.4 may seem low, the effect of dissolved CO_2 will be present in virtually all measurements of photosynthesis as it is inextricably linked with transpiration. The effect becomes more significant where pH is high, temperature is low and sap flow is high. If the values obtained in the isotope studies cited earlier are correct, the effect could clearly be much larger and very significant.

Table 4.4 Calculated effect of internal circulation of CO_2 on the measurement of photosynthesis. Internal Refixation of CO_2 is calculated by multiplying the sap CO_2 concentration by the transpiration rate.
(a) Different values of temperature (*T*) and pH are used with typical birch transpiration and photosynthetic rates (3 mmol H_2O m^{-2} s^{-1} and 10 µmol CO_2 m^{-2} s^{-1}, respectively). (b) Actual measurements of transpiration (*E*, mmol m^{-2} s^{-1}) and photosynthesis (A_1, µmol m^{-2} s^{-1}) on *C. micranthum* are used in conjunction with the estimate of sap CO_2 concentration from birch. Values are calculated for the maximum and minimum measured rates of leaf photosynthesis made in September 1992, and for the whole bush, using the sap flow measurement made just after dawn on 24/9/92 with the average leaf photosynthetic rate at that time.

(a) *B. pendula*

T (°C)	Sap pH	Internal Refixation of CO_2 (µmol m^{-2} s^{-1})	Internal Refixation/ Typical Measured Photosynthesis (%)
10	7.2	0.558	5.58
10	6.4	0.163	1.63
10	5.6	0.100	1.00
8	6.4	0.100	1.00

(b) *C. micranthum*

	A_1 (µmol m^{-2} s^{-1})	*T* (°C)	*E* (mmol m^{-2} s^{-1})	Sap pH	Internal Refixation of CO_2 (µmol m^{-2} s^{-1})	Internal Refixation/ Measured Photosynthesis (%)
Whole bush	4.27	34	3.09	5.6	0.056	1.30
Whole bush	4.27	34	3.09	6.4	0.133	3.12
Whole bush	4.27	34	3.09	7.2	0.433	10.14
Max	13.92	35.6	6.02	6.4	0.203	1.46
Min	0.80	40.3	0.96	6.4	0.030	3.76

4.7.3 Experiment 2 - Interaction between sap flow and stem CO_2 flux

Methods

In situ measurements of stem CO_2 flux were made as described in Section 4.2.2 on *C. micranthum* and *G. senegalensis*. Chambers were placed on the stem at about 0.5 m from the base. Below this, on the same stem, a constant power sap flow gauge (Dynamax Inc., Houston, USA) was installed and operated by Dr Simon Allen of the Institue of Hydrology. The sap flow gauge works by the heat balance technique (Baker and van Bavel, 1987) in which heat is applied by an element wrapped around a stem or branch which is well insulated to the outside. The conduction components of the stem heat balance (up and down the stem and through the insulating sheath) are measured by thermocouples. Sap flow is calculated from the remaining component, the convective transfer of heat

in the transpiration stream. The use of sap flow gauges to measure shrub transpiration is discussed further by Allen and Grime (in press). Output was recorded as 10 minute averages on a data logger. The sap flow gauge and respiration chamber were approximately 20 cm apart on the stem and there was no detectable heating of the chamber by the sap flow gauge. The recording of time was not actively synchronised in the stem CO_2 efflux and sap flow measurements, and so there may be a difference of a few minutes between the two.

Results and Discussion

Figure 4.8 shows an apparent influence of sap flow on stem CO_2 efflux. The stem CO_2 efflux largely followed temperature except for a sizeable peak which occurred consistently in the early morning and a much smaller but consistent rise in the late afternoon. On each day, the former coincided with a period of high stomatal conductance and sap flow just after dawn and the latter with an increase in sap flow towards dusk. Other coinciding peaks in stem CO_2 efflux and sap flow can also be seen. Furthermore, although the diurnal stem temperature curve was almost symmetrical, the stem CO_2 efflux mirrored the asymmetry in the diurnal course of sap flow, with lower rates in the afternoon. Plotting the data in three dimensions shows that temperature was the dominant influence, and that the anomalously high values of stem CO_2 efflux consistently occurred in periods of high sap flow (Figure 4.9).

The increase in stem CO_2 efflux with sap flow may have the following explanation. CO_2 concentration will be considerably higher in the roots as CO_2 is not readily removed from the soil matrix by diffusion, in contrast to the stems, which are surrounded by well mixed air. As the transpiration stream moves upwards, the water from the roots, in equilibrium with a high pCO_2, is drawn into the stem, where the pCO_2 is much lower. This results in dissolved CO_2 coming out of solution and being released as a gas inside the stem, as it equilibrates in accordance with Henry's Law, and an efflux of CO_2 from the stem to the air, in addition to the efflux resulting from stem respiration. This may be expected to increase with sap flow rate.

Figure 4.10 shows the data for the mornings of the same days in greater detail. Although stem CO_2 efflux and sap flow began to increase from their night-time values more or less simultaneously, at between 0710 and 0730 h, the peak in stem CO_2 efflux clearly preceded the peak in sap flow by about an hour. This may be the result of the particularly high CO_2 concentration gradient between the roots and stem that may build up overnight. When the transpiration stream becomes very slow in the evening, water in the root xylem will be surrounded by respiring tissue for up to 12 hours and the CO_2

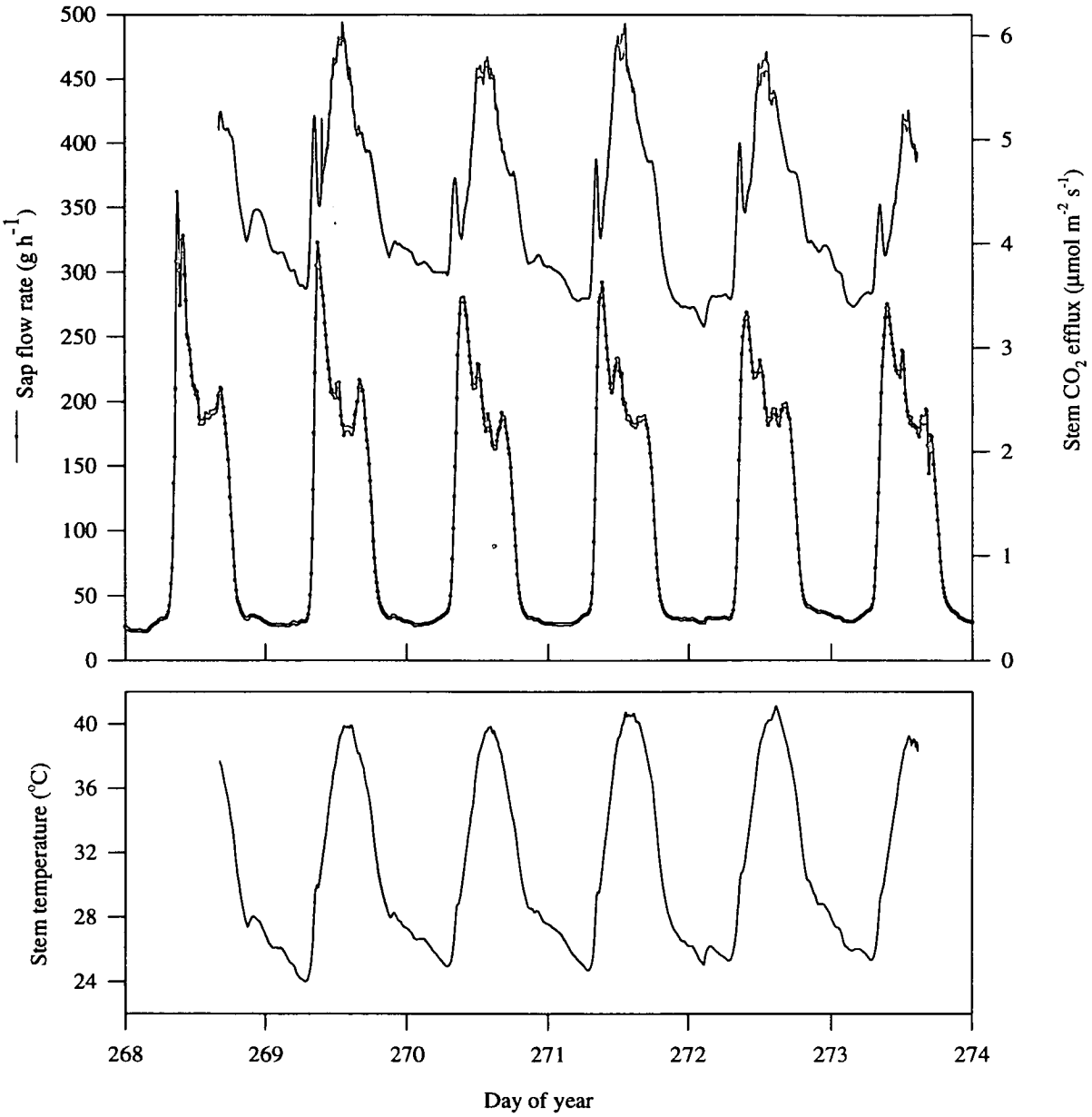

Figure 4.8 Stem CO_2 efflux (upper line), sap flow rate and stem surface temperature measured simultaneously on a *C. micranthum* stem over six days at the tiger bush site, September 1992. The early morning peak in sap flow coincided with high stomatal conductance and produced a sharp increase in stem CO_2 efflux.

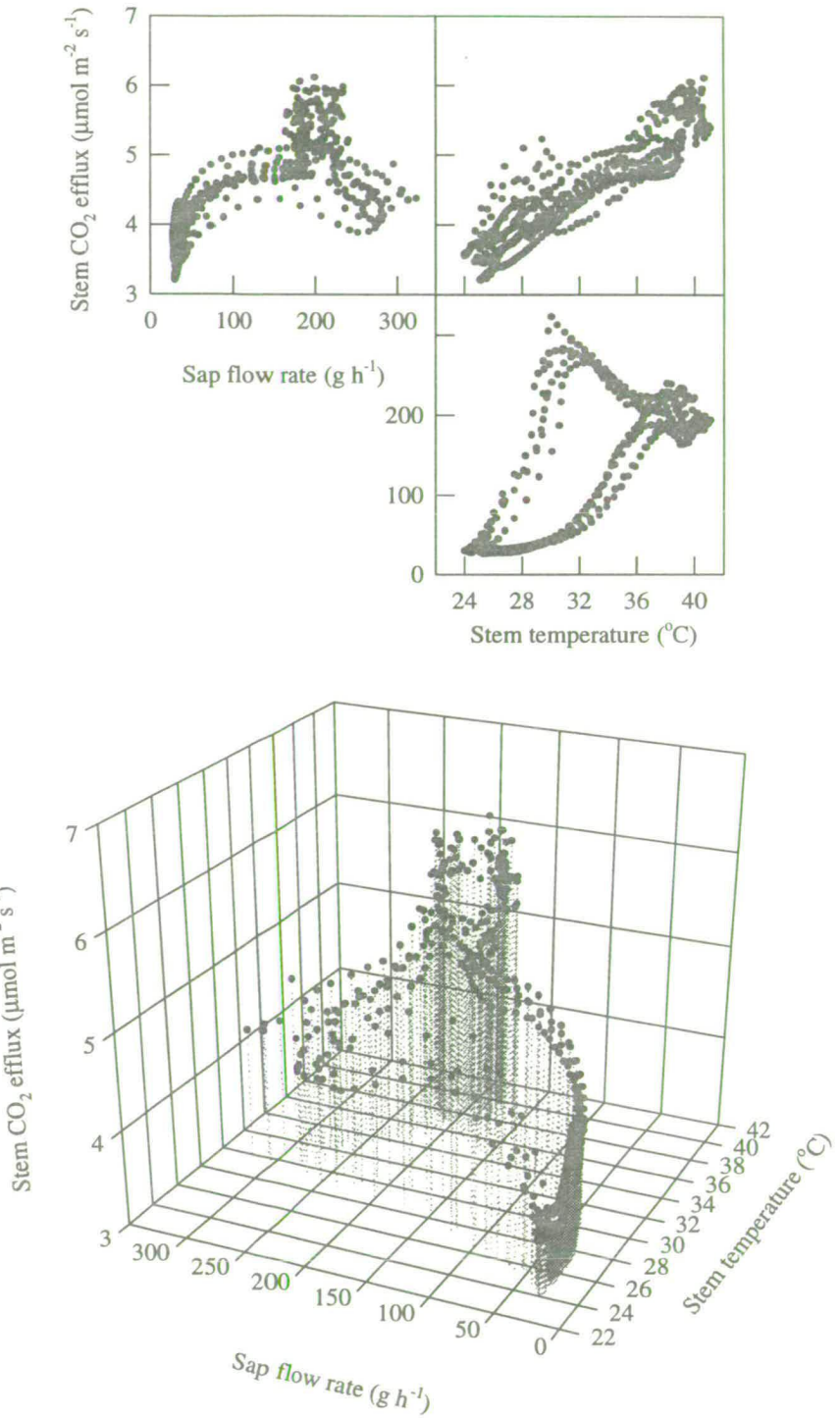

Figure 4.9 Relationships between stem CO_2 efflux, stem temperature and sap flow in *C. micranthum*. Data are the same as in Figure 4.8. Temperature is the dominant influence on stem CO_2 efflux, but the three dimensional plot shows that the anomalously high values of stem CO_2 efflux consistently occurred in periods of high sap flow. Data are ten-minute averages.

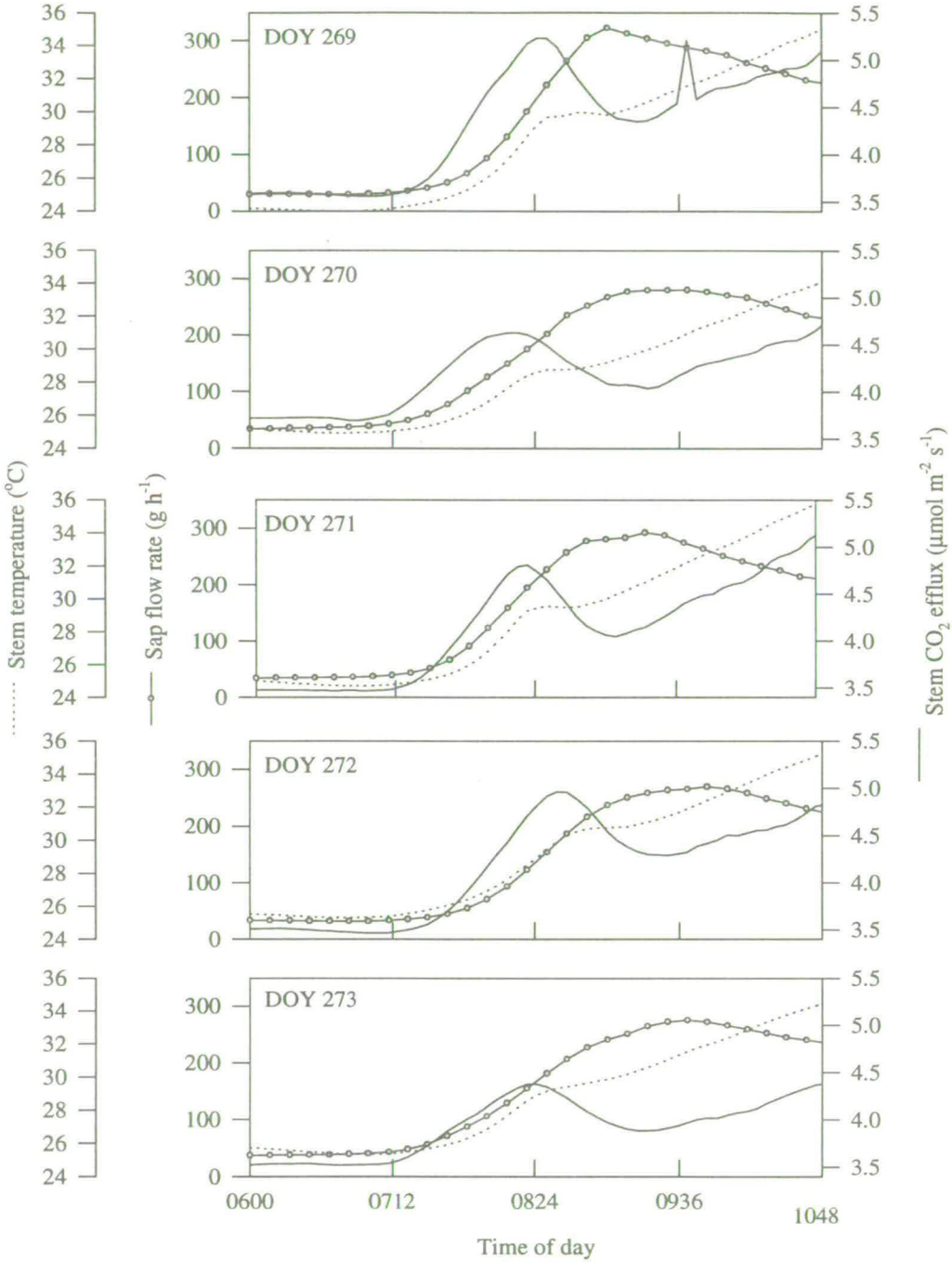

Figure 4.10 Stem CO_2 efflux, sap flow rate and stem temperature measured simultaneously on a *C. micranthum* stem over six days at the tiger bush site, September 1992. Although both began to increase from their night-time values at approximately the same time, the peak in stem CO_2 efflux preceded the peak in sap flow by about an hour.

concentration in the water may become very high. A larger gradient may therefore be present between the roots and stem at dawn than occurs during the rest of the day. If this CO_2 is released through the stem as the water column begins to move after dawn, this gradient will decrease and reach a new equilibrium. Thus, the early morning peak may involve the release of CO_2 built up overnight in the below-ground water column whilst static, and the stem CO_2 efflux may decline after this excess CO_2 has been released with the decline in the gradient in CO_2 concentration between roots and stem. Figure 4.10 also shows a small but anomalous peak in stem temperature, which may also be produced by water which has been stored underground in the roots overnight, as this water will retain more heat and may warm the stem as it rises in the morning.

However, there is a serious problem with the hypothesis discussed above. Measurements of sap flow velocity give values of around 0.1 mm s^{-1} at a sap flow rate of around 200 g h^{-1}. This suggests that it would take around 80 minutes for water from the roots to reach a chamber 0.5 m up the stem. Therefore, if the early morning peak in stem CO_2 efflux is a result of the high CO_2 concentration in water drawn up from the root system, it should occur approximately 80 minutes after the onset of sap flow, which, as Figure 4.10 shows, is clearly not the case.

Although circadian rhythms have been found in the concentrations of compounds such as amino acids and organic acids in xylem fluid (eg. Andersen, Brodbeck and Mizell, 1993), there is no obvious reason why the stem respiration rate should be higher in the morning, and in fact, the reverse might be expected, as the substrate concentration would probably be lower. There is an anomalous peak in stem temperature, which coincides with the early morning peak in stem CO_2 efflux, but the magnitude of this peak is not large enough to account for the peak in stem CO_2 efflux. As no other explanation is readily apparent, and because of the close correspondence between the rise in stem CO_2 efflux and the onset of sap flow, it seems likely that the two are related, but the exact nature of this relationship is not clear. The influence of sap flow could be investigated quite simply by measuring stem CO_2 efflux *in situ* before and after cutting the stem off above the chamber to stop the sap flow.

Whatever the exact cause, it is apparent that the effect of sap flow on stem gas exchange measurements is potentially large (around 1 μmol m^{-2} s^{-1} or ~25 % of the expected rate at 25 °C in Figure 4.10), but may often be difficult to detect. Ambient air temperature and transpiration are usually very highly correlated and follow diurnal changes in radiation. Furthermore, temperature directly influences transpiration via changes in ambient *D*. As changes in temperature and sap flow often occur concomitantly, it is perhaps unsurprising that the effect of sap flow on respiration measurements is generally not obvious. It is only very apparent in these measurements because of the high sap flow in the relatively cool early morning. This is interpreted as a xerophytic adaptation to the low soil

moisture and high D (4-5 kPa) in the afternoon when the measurements were made, during the transition from wet to dry season, two weeks after the last rain had fallen.

These results are in contrast to those from previous experiments (Negisi, 1979; Martin *et al.*, 1994), in which a reduction in stem CO_2 efflux with sap flow was found. The difference may be related to the conditions in which the experiments were done. In Negisi's (1979) experiment, the water that passed through the stem was initially in equilibrium with laboratory air and relatively low in dissolved CO_2, producing a diffusion gradient within the stem opposite to that expected in natural conditions. The contrasting results obtained in the experiment by Martin *et al.* (1994) may be a result of positioning the chamber immediately below the crown (as opposed to lower down on the stem in this experiment). The efflux from the stem of CO_2 produced in the roots is unlikely to be distributed uniformly with height over the stem, and would be expected to decrease with distance above the ground. If the CO_2 dissolved in water flowing up the stem reaches equilibrium with the surrounding tissues, so that there is no net exchange of CO_2 between the transpiration stream and the surrounding tissues, the CO_2 carried in the water would not be expected to have an effect on stem gas exchange measurements. When the water column reaches the leaves, internal circulation may reduce the stem efflux, if CO_2 produced by stem respiration moves along a concentration gradient to the leaves and is assimilated by photosynthesis instead of effluxing to the atmosphere. Thus, the effect of internal circulation on stem gas exchange measurements may depend on the vertical CO_2 concentration gradient in the transpiration stream at the point of measurement, and so may increase, decrease or have no effect on the measured stem CO_2 efflux.

4.7.4 Implications and Conclusions

High CO_2 concentrations of around 30 000 μmol mol^{-1} were measured in the air within woody stems and by inference, in the xylem sap. Similar measurements in Cameroon and isotope studies suggest that concentrations may sometimes reach up to 3 and 8 times this figure, respectively. When carried to leaves by the transpiration stream, this may represent around 1 to 10 % of measured photosynthetic rates (using the 30 000 μmol mol^{-1} value), depending on sap pH and temperature, but could be larger if the higher estimates of sap CO_2 concentration are correct.

An increase in stem CO_2 efflux correlated with sap flow has been demonstrated, but the explanation for this relationship is not certain. The influence of sap flow on stem CO_2 efflux will often be masked by the correlation between temperature and sap flow over the course of a day. If the influence of sap flow is related to internal circulation of CO_2, as seems likely, its effect will depend on the gradients of CO_2 concentration within the plant, and may (1) increase the stem CO_2 efflux, when water entering a stem section has a higher value of $[CO_2^*]$ than the equilibrium value at the local pCO_2, (2) decrease

the stem efflux where respired CO_2 from the stem is assimilated by leaves or (3) have no effect, when there is no gradient in CO_2 concentration within the stem xylem.

Internal circulation of CO_2 may result in chamber measurements underestimating leaf photosynthesis and overestimating stem respiration, and may thereby cause misinterpretation of these measurements, when a mechanistic understanding of photosynthesis or respiration is sought. For example, internal circulation of CO_2 produces a confounding effect when attempting to separate growth and maintenance respiration in stems, as the higher respiration rates in the growing season may partially result from higher flow rates when the bush is in leaf. Similarly in measurements of leaf photosynthesis, the amount of CO_2 assimilated may be underestimated by an amount dependent on the transpiration rate and so would cause error in the values of parameters derived from the data, such as A_{max} and α (Chapter 3).

4.8 Soil CO_2 exchange

Several studies have shown soil respiration to be an appreciable component of ecosystem carbon balance (eg. Redmann, 1970; Kucera and Kirkham, 1971; Kanemasu, Powers and Sij, 1974; Jong, Redmann, and Ripley, 1979; Norman, Garcia and Verma, 1992; Meir *et al.*, in press). An attempt was made to quantify soil CO_2 efflux at the fallow site, using the LCA3 analyser with a cylindrical "Perspex" chamber (20 cm high, 8 cm in diameter), pressed into the soil to a depth of about 4 cm. A fan was fitted inside the chamber to mix the air. A low flow rate of 150 cm^3 min^{-1} was used to minimise the negative pressure exerted on the soil surface, as this negative pressure may cause measurements to overestimate soil respiration (Fang and Moncrieff, 1995). Tests with a manometer showed that the pressure drop within the chamber caused by the suction of the pump was insignificant compared with the pressure fluctuations caused by variations in wind. The system was used to make both spot measurements and extended measurements over several days, in which case the output signals from the LCA3 were recorded on a data logger, as with *in situ* stem respiration measurements (Section 4.2.2). Soil temperature was measured by a Cu-Con thermocouple at about 1 cm depth in the soil within the chamber. Other systems were employed to measure soil CO_2 efflux at the millet and tiger bush sites, but these were not successful, and the quantity of data available is very restricted.

A response to temperature is apparent in Figure 4.11(a). The soil CO_2 efflux lags behind the diurnal course of soil temperature at 1 cm by about four hours. This suggests that the main source of respiration is at some depth below the surface, and so probably associated with the roots of the *G. senegalensis* bushes (the ground flora had not developed when these measurements were made). Figure 4.11(b) shows that there was considerable spatial heterogeneity in soil respiration, apparently

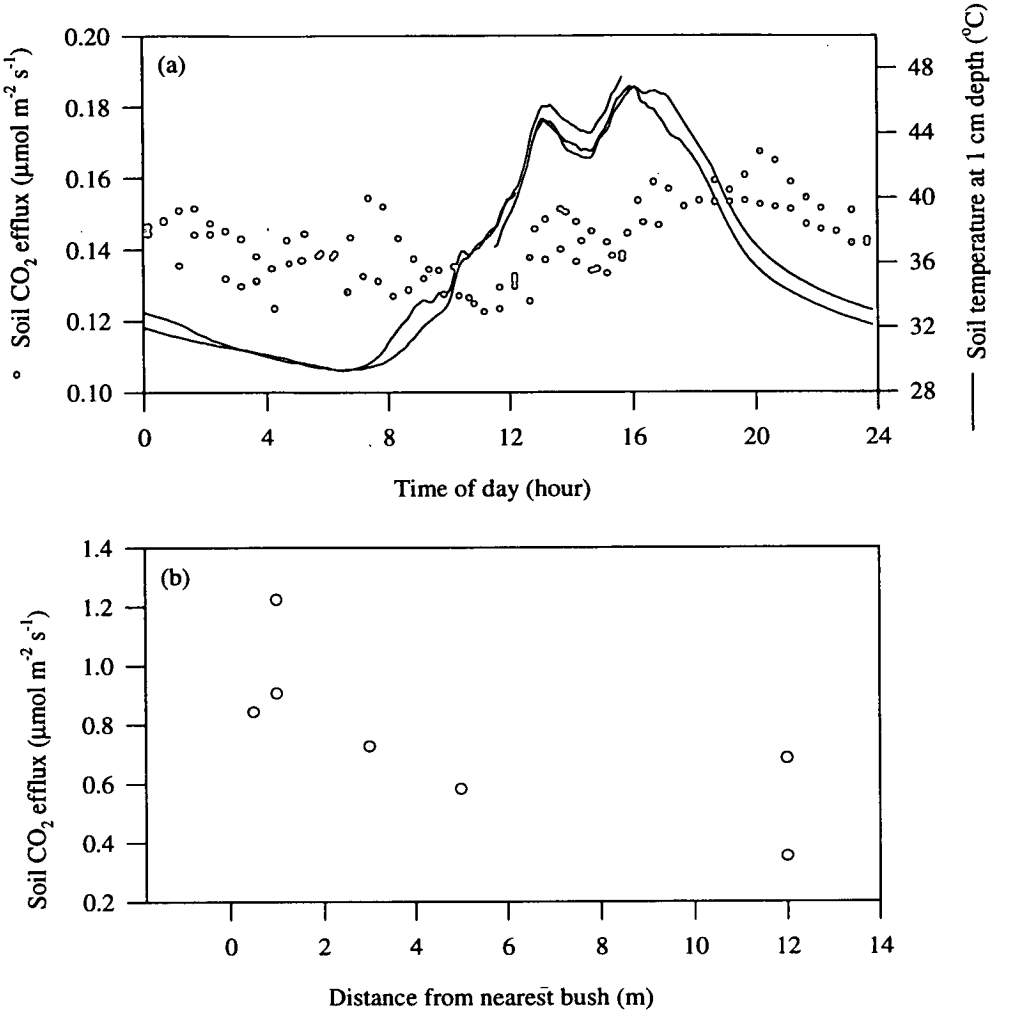

Figure 4.11 (a) Relationship between soil respiration and temperature at the fallow site. Data are half-hourly averages from measurements on 27-29 June 1992. Respiration rates are low and there is a lag of about four hours between the two variables. (b) Relationship between soil respiration and proximity to bushes. Data are spot measurements from two transects at the fallow site on 15 June 1992. There is a notable decrease in soil respiration with distance from the nearest bush, which may be related to both root density and litter content of the soil. Soil temperature was between 28 and 34 °C in these data.

associated with proximity to the *G. senegalensis* bushes. This decrease in soil respiration with distance from the nearest bush may be related to root density and/or litter content of the soil.

With the lag was removed, the data in Figure 4.11(a) were fitted to Equation 4.3, describing the exponential increase with temperature. This gave parameter values of 0.009 and 0.102 for R_0 and k, respectively, which were used to represent soil respiration at the fallow and tiger bush sites in the two models described in Chapter 7. Because of the paucity of data, little confidence can be placed in these

parameter values, and a large degree of uncertainty is associated with estimates of the soil efflux produced in this way. However, the data suggest that soil respiration rates were very low (less than 0.2 μmol m^{-2} s^{-1} in Figure 4.11(a)), and so the error may not be too important, although soil respiration rates would be higher later in the wet season when the vegetation had developed further. At the millet site, root biomass estimates were available from the growth experiment plots (Brouwer *et al.*, in prep.) and these estimates were used to estimate root respiration, by using the parameters derived from measurements of leaf respiration (Section 3.3), and assuming that the respiration rate per unit mass of roots was the same as that of leaves. Although there is no evidence that this assumption is valid, this approach appears more justifiable than basing predictions of soil respiration in millet on the small number of measurements at the fallow site.

4.9 Conclusions

1) In both species studied, stem respiration can be satisfactorily expressed on a per unit surface area basis but not on a volume basis, suggesting that the bulk of the respiring tissue is associated with the cambium and phloem.

2) Stem respiration shows the expected exponential response to temperature. Stem respiration rates were markedly higher in the wet season and this was attributed to the effect of growth. A small decrease in Q_{10} was also observed during the wet season. Growth respiration was separated from maintenance respiration by fitting the data to the exponential equation with an extra growth term (Equation 4.4). Calculated growth respiration at 25 °C (Table 4.3) reached 1.5 and 0.7 μmol m^{-2} s^{-1} in *G. senegalensis* and *C. micranthum*, respectively, representing between three and six times the maintenance respiration rate at this temperature.

3) There was a demonstrable photosynthetic response of stem sections to Q of up to 0.85 μmol m^{-2} s^{-1} when placed horizontally in full Q and 0.4 μmol m^{-2} s^{-1} *in situ*. Refixation did not exceed respiration and represented up to 75 and 33 %, respectively, of stem respiration rates in the dark.

4) Measurements of sap CO_2 concentration show that considerable amounts of CO_2 can be carried in the transpiration stream and this may affect measurements of stem respiration and leaf photosynthesis by up to ~25 % and 10 %, respectively. An increase in stem CO_2 efflux correlated with sap flow was demonstrated and may be present but more difficult to detect in other measurements.

5) A limited number of soil respiration measurements were made at the fallow site. Effects of temperature and proximity to the *G. senegalensis* bushes were detected in the data. Soil respiration rates were rather low, generally less than 1 μmol m^{-2} s^{-1}.

Chapter 5

Leaf Area And Biomass - Direct Measurements

5.1 Introduction

The amount and spatial distribution of above-ground plant material is crucial to interactions between canopy and atmosphere, particularly with respect to the attenuation of solar radiation. In order to extrapolate leaf-scale measurements to canopy scale, it is therefore necessary to have a description of canopy structure. Measurements were made at the sub-sites to provide descriptions of the different canopy structures of the three vegetation types for simulations using MAESTRO. Ideally, it is desirable to have a complete description of the distribution of leaf area and biomass in three dimensions, as well as its variation over time through the seasons. However, this represents an enormous task. For the purposes of MAESTRO, it was assumed that leaf area was distributed homogeneously within discrete units such as millet pockets, individual shrub crowns and the herbaceous ground layer. This chapter describes the measurement of the spatial distribution of these units and the temporal variation of leaf area and biomass within them.

Several approaches to measuring canopy structure are possible, and can be broadly classified as direct or indirect (Norman and Campbell, 1989). In the former, the properties of interest, such as leaf area or biomass, are measured directly on plants by manual methods using a planimeter or balance, or calculated from dimensions and/or regression relationships. Indirect measurements are those in which canopy structure is inferred from observations of another variable, such as transmitted radiation or a spectral reflectance index.

Direct methods are generally more reliable than indirect methods, as they are simple and require fewer assumptions to be made. However, the measurements involved can be very time consuming, making it difficult to get a representative spatial sample. This problem escalates with increasing biomass and heterogeneity of the canopy, and becomes very serious in forest vegetation. A solution may be found where easily measurable properties of the plants correlate well with leaf area or biomass, requiring fewer of the very labour intensive measurements to be made and a larger spatial sample to be obtained. This approach, based on allometric correlation, was employed at the millet and fallow sites and attempted at the tiger bush site. Indirect measurements were also made at all sites and are described in Chapter 6.

In millet, the leaf area index, L_l, and the stem or culm area index, L_s, were considered together as the total plant surface area index, L_t (equal to $L_l + L_s$). The culms were green, morphologically leaf-like

and were assumed to have the same physiological properties as leaves, although no physiological measurements were made on them. In the shrub and tree species, the L_l and L_s terms were considered separately. In the fallow site herbs, all green tissue was considered as leaf area and any non-green tissue was not measured. In the shrubs, no morphological differentiation between stems and branches was apparent and the term "stem area" is used to refer to the surface area of all woody tissue.

5.2 Millet

5.2.1 Methods and Results: 1991

L_t was estimated using a direct method based on allometric correlation. A harvest was carried out and various tiller attributes were measured to examine which correlated well with tiller area and mass. To examine the phenology of leaf area, a method based on repeated estimates of tiller area on marked tillers was used.

Total plant surface area index, L_t

Fifty-five millet tillers were harvested in early September 1991 and the following attributes recorded: leaf area measured using a planimeter (LI-3100, Li-Cor Inc., Lincoln, Nebraska, USA); culm diameter near the base, mid-point and uppermost node; height to the uppermost node and height to the tip of the uppermost leaf when fully extended vertically. Total tiller area was calculated as the sum of leaf area and culm surface area. The latter was calculated on the assumption that the culm approximates three cylinders of equal length with diameters as measured at the base, mid-point and uppermost node. Panicle area was not included.

Table 5.1 Coefficients of regression of tiller area on tiller attributes. n=55.

Tiller Attribute	r^2
Height to uppermost leaf tip	0.90
Height to uppermost node	0.84
Mean of three culm diameters	0.73
Number of leaves	0.58
Height to uppermost leaf tip × mean culm diameter	0.96
Height to uppermost node × mean culm diameter	0.95

It is clear from Figure 5.1 that there are strong relationships between the measured attributes of the tillers and their area. Linear regression was used to derive the relationships between the measured attributes and tiller area. The values of r^2 shown in Table 5.1 show that the closest simple relationship is with tiller height to the uppermost leaf tip.

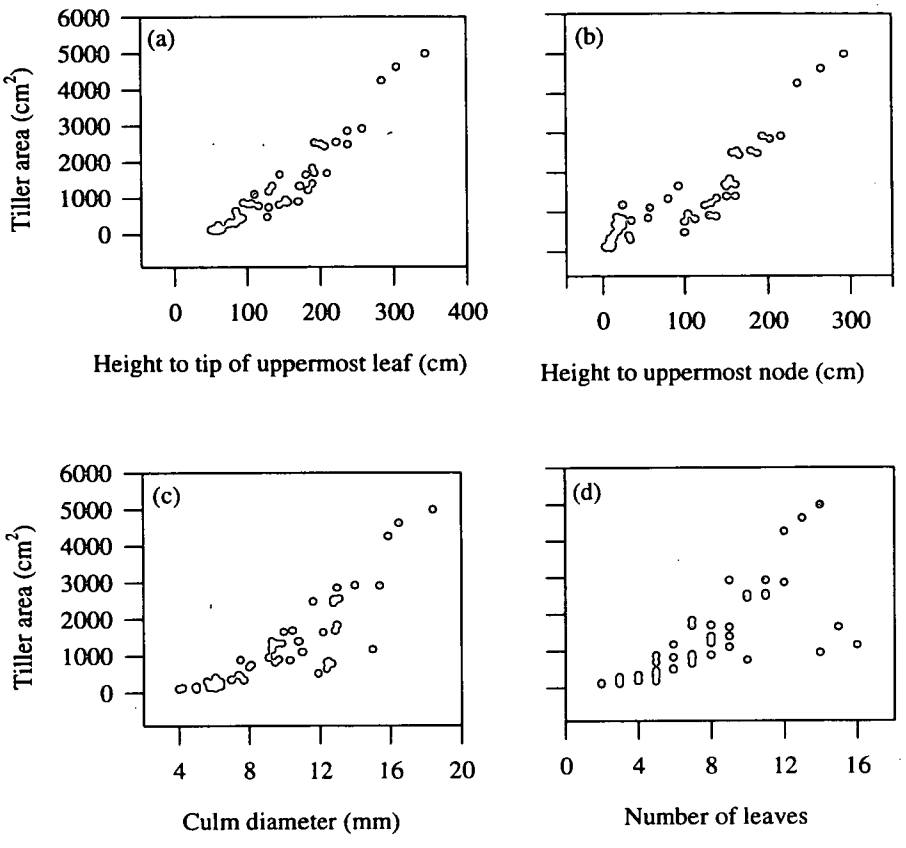

Figure 5.1 Relationships between tiller area and tiller height (a and b), culm diameter (c) and number of leaves (d) measured on millet tillers harvested in early September 1991. The closest relationship is with height measured to the tip of the uppermost leaf when fully extended vertically ($r^2 = 0.90$).

Although slightly easier to measure, height to the uppermost node is less useful because of the different form of flowering and non-flowering tillers. Non-flowering tillers tend to have a short culm with a dense cluster of leaves at the top, whereas leaves (and nodes) are spread more evenly along the length of the taller, flowering tillers. This gives rise to the two slightly different relationships above and below 1 m in Figure 5.1(b). Although a closer fit is obtainable by including culm diameter, the difference is not great and it was not considered worth the extra time required to measure this in the field.

At the same time as the harvest measurements, height to the uppermost leaf tip was measured non-destructively on all tillers in 16 plots located on the neutron probe access tube grid shown in Figure 2.4. As these measurements were begun before the harvest measurements could be analysed, height to

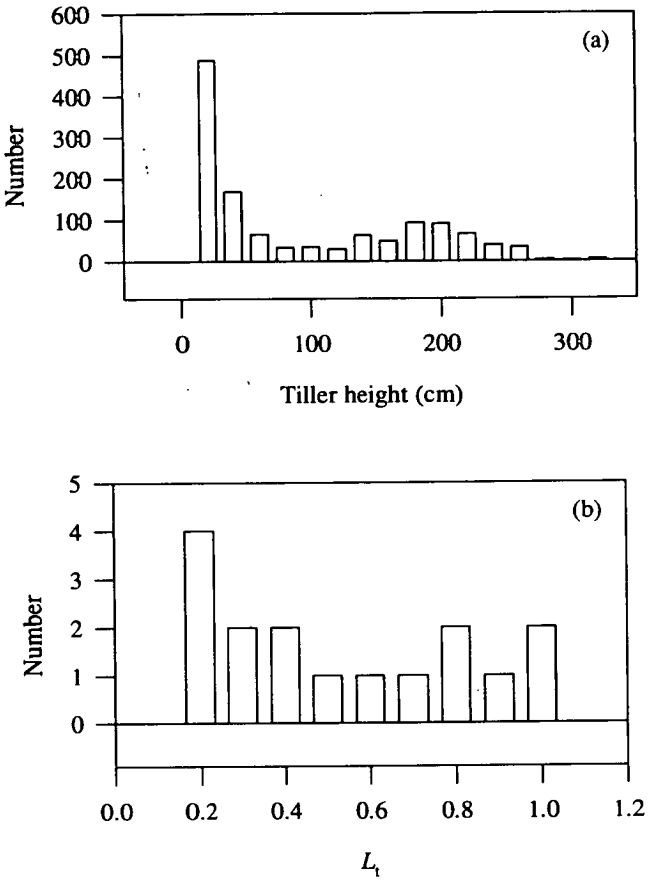

Figure 5.2 (a) Frequency distributions of tiller heights measured in 16 plots at the millet site in early September 1991. (b) Frequency distribution of L_t calculated for these plots using the relationship in Figure 5.1(b) (Equation 5.1).

the uppermost node was chosen as the measurement variable, as this was initially expected to be the most closely correlated with area and mass. The plots were circular, with radii ranging from 2 to 5 m (areas of 12.6 to 78.5 m^2), dependent upon the local heterogeneity of the millet. The frequency distribution of these measurements (Figure 5.2(a)) is bimodal, with peaks at tiller heights of < 20 and 200 cm, reflecting the grouping into short, non-flowering tillers and tall, flowering tillers. L_t was then estimated for each plot by summing the values of tiller area calculated from the following equation:

$$S = 34.5 + 13.338h_t \qquad [5.1]$$

where S is tiller area (cm^2) and h_t is tiller height to uppermost node (cm), and dividing by plot area. This gave a mean L_t of 0.46. The frequency distribution of L_t for these 16 plots is shown in Figure

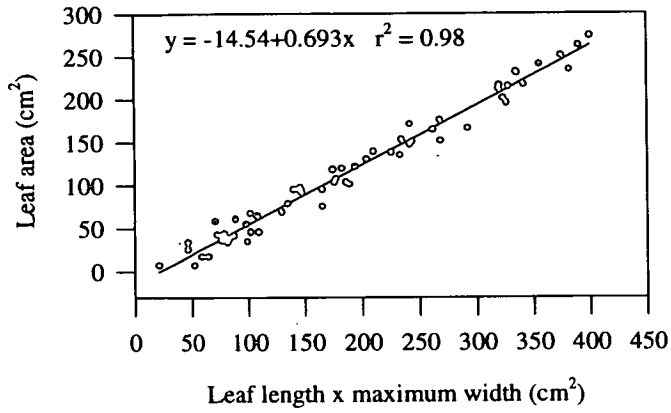

Figure 5.3 Relationship between leaf dimensions and leaf area measured with a leaf area meter, used to estimate leaf area non-destructively on marked tillers in 1991.

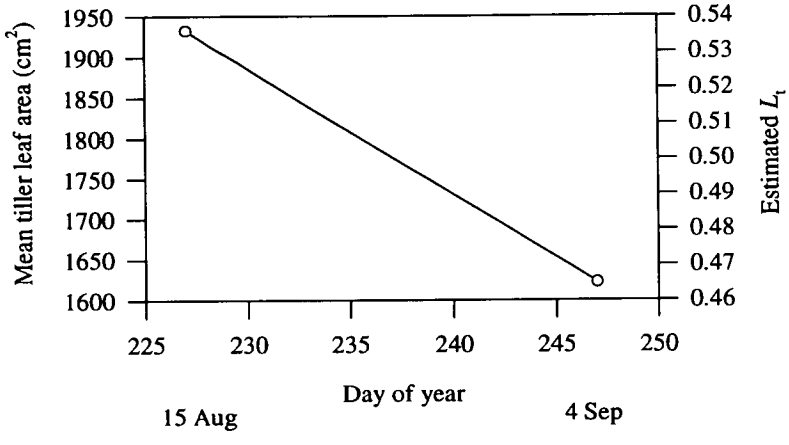

Figure 5.4 Extrapolation of September 1991 L_t estimate to August 1991 using phenology measurements. The change in the mean leaf area of 50 marked tillers was assumed to be proportional to the change in L_t, which was measured as 0.46 in early September.

5.2(b).

Phenology

Leaf length and width were measured on all leaves of 50 marked tillers on three occasions over the season. These were converted to leaf areas using a relationship established by measuring these attributes on a separate set of harvested leaves (Figure 5.3). Two tillers were trampled, so data for only 48 were used. The average of these leaf areas was calculated and used as a relative measure of L_t. In conjunction with the L_t estimate described above, this was used to estimate L_t at other times over the season. The original markers used in July became detached so the data had to be discarded and extrapolation could only be made to the August measurement period (Figure 5.4).

The main problem with this method was the considerable time involved in measuring the leaf lengths and widths. The loss of markers and sample tillers was also a serious problem. It was considered that detailed measurements on 50 tillers would give a poorer L_t estimate than measurements of height on around 500 tillers which could be done in a similar length of time. It was therefore decided to repeat the L_t measurements based on the area-height correlation at intervals over the 1992 season rather than attempt to measure phenology on individual plants. In the L_t measurements, a problem was found where millet pockets occurred on the plot boundary and it was unclear which tillers should be assigned to the plot. Consequently, it was decided to use plots with a fixed number of pockets together with measurements of their spacing rather than plots of a fixed area in 1992.

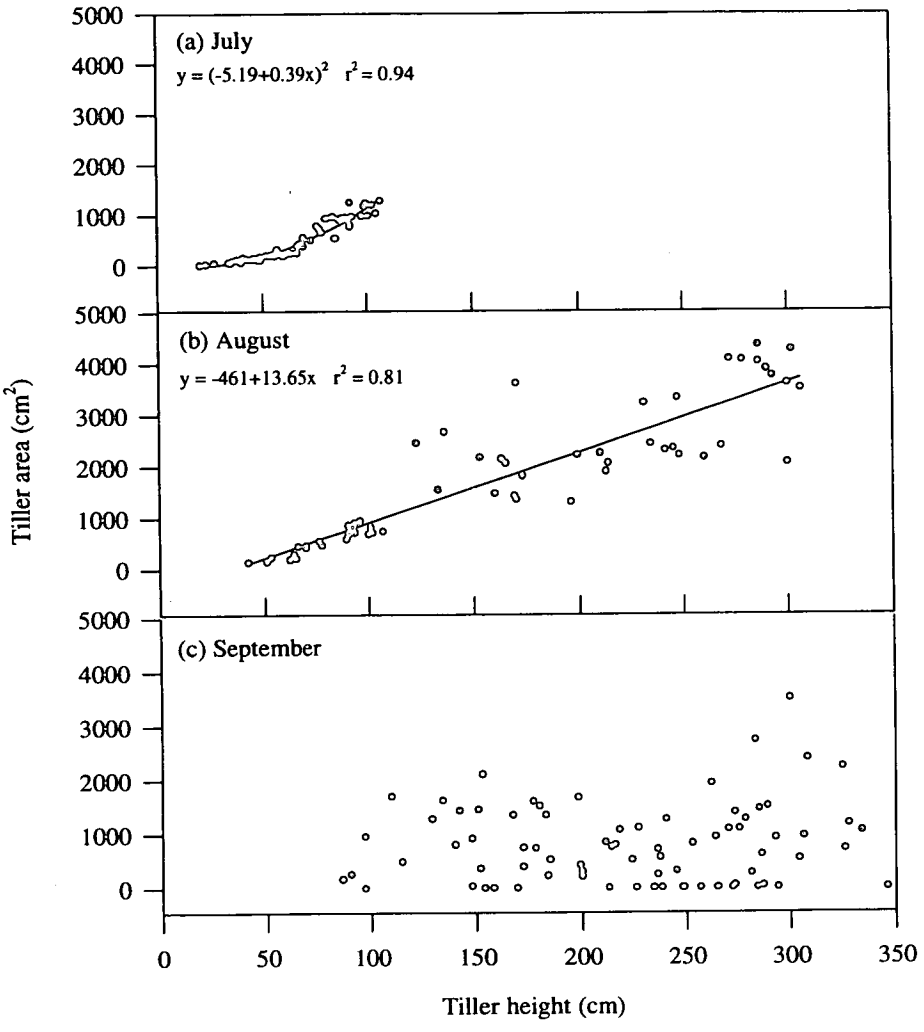

Figure 5.5 Relationships between millet tiller area and height in three harvests in 1992. Good relationships were found in July and August but were not present in September because of senesence.

5.2.2 Methods and Results: 1992

Estimates of L_t were made on three occasions between July and September using the tiller area-height correlation method described above. Around 60 tillers were harvested on each occasion and the following attributes measured: tiller height from the base to the tip of the uppermost leaf when fully extended upwards, green leaf area (using a Li-Cor 3100 area meter) and culm diameter. Dry mass was measured on a sub-sample of tillers in July and August. The data are shown in Figures 5.5 and 5.6. Equations to predict surface area and dry biomass from tiller height were derived by linear regression for each sampling period.

The distribution of tiller heights was measured in the field in July and August. Measurements were

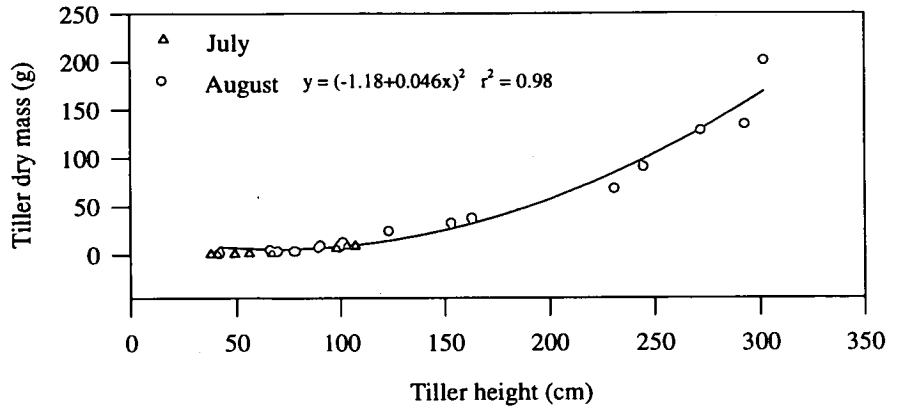

Figure 5.6 Relationship between millet tiller dry mass and height at two harvests in 1992. The regression line for the August measurements is shown.

made at 20 sampling points, located at 10 m intervals on two 100 m transects to the SW of the University of Edinburgh micrometeorological mast (Figure 2.4). At each point, the height of every tiller in the four nearest pockets was measured, along with pocket spacing and pocket diameter. The frequency distribution of these measurements is shown in Figure 5.7. The distribution in July, before anthesis, was unimodal but in August it was very clearly bimodal, peaking at around 90 cm in the shorter, non-flowering tillers and at around 260 cm in the taller, flowering tillers. Tiller areas were calculated from the established relationship with tiller height and summed to give a value of plant surface area for each pocket. L_t was estimated at each point by calculating the mean plant surface area of the four pockets and multiplying by the number of pockets per square metre. Biomass was estimated in an analogous way from the relationship between tiller height and dry mass.

The variation in L_t along the two transects is shown in Figure 5.8. A similar pattern was found along both transects, although they were approximately 30 m apart. This may reflect a large scale trend in growth, possibly influenced by the drainage pattern. The vertical distribution of leaf area within the canopy was calculated from the tiller height distribution, making the assumption that area was distributed evenly along the length of the tiller (Figure 5.9). When averaging over several hundred tillers, this assumption appears reasonable for the tall, flowering group. However, in the short tillers, leaves tended to be held in a cluster at the top of the culm and so the peak leaf area probably occurred between 50 and 100 cm rather than at the bottom of the canopy.

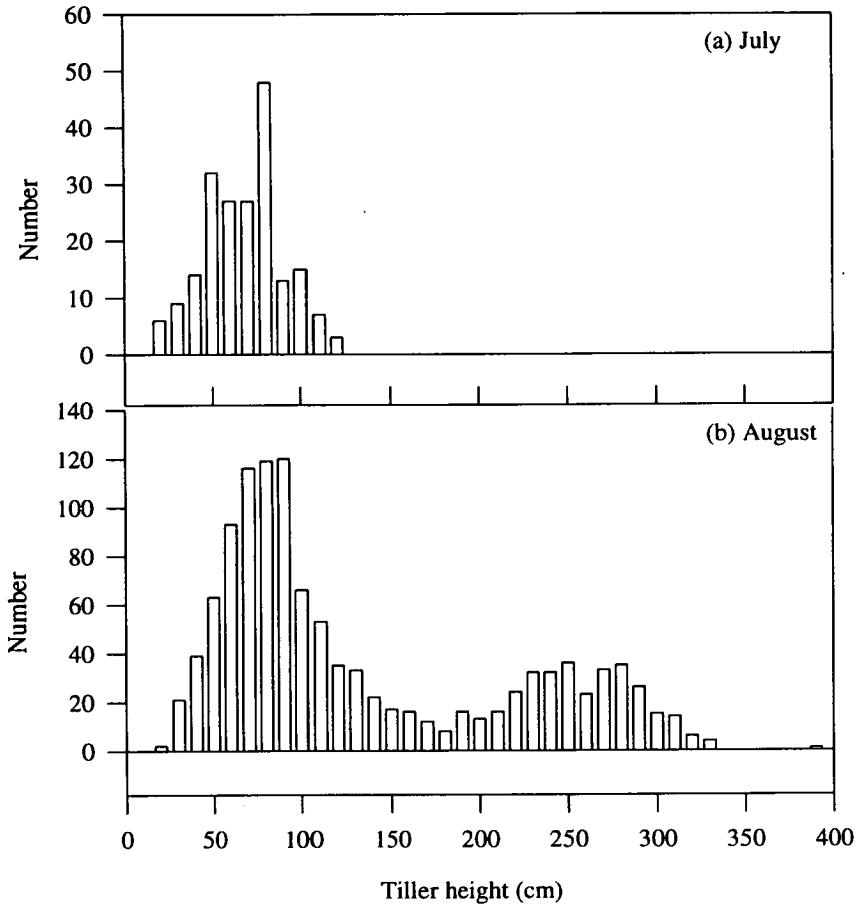

Figure 5.7 Frequency distributions of millet tiller height in (a) July and (b) August 1992 from 20 sampling points on two transects.

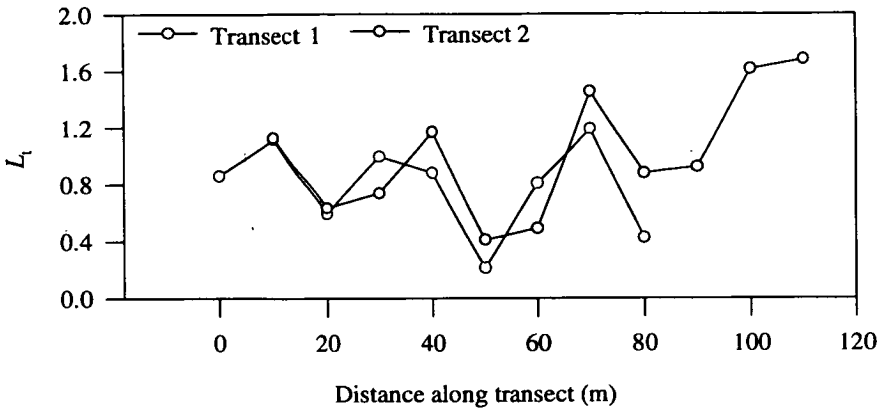

Figure 5.8 Spatial variability in millet L_t along the two transects shown in Figure 2.4. in August 1992. Distance is measured from the NE end. Both show similar trends, indicating a large scale pattern in growth, probably due to microtopographical effects on drainage.

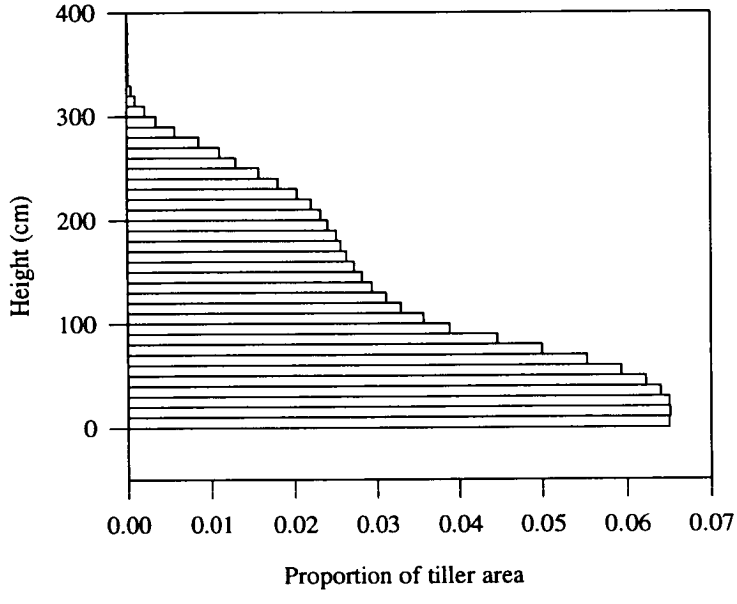

Figure 5.9 Distribution of tiller area with height within the canopy calculated from the distribution of tiller heights measured in August. It is asssumed that area is distributed evenly along the length of tillers.

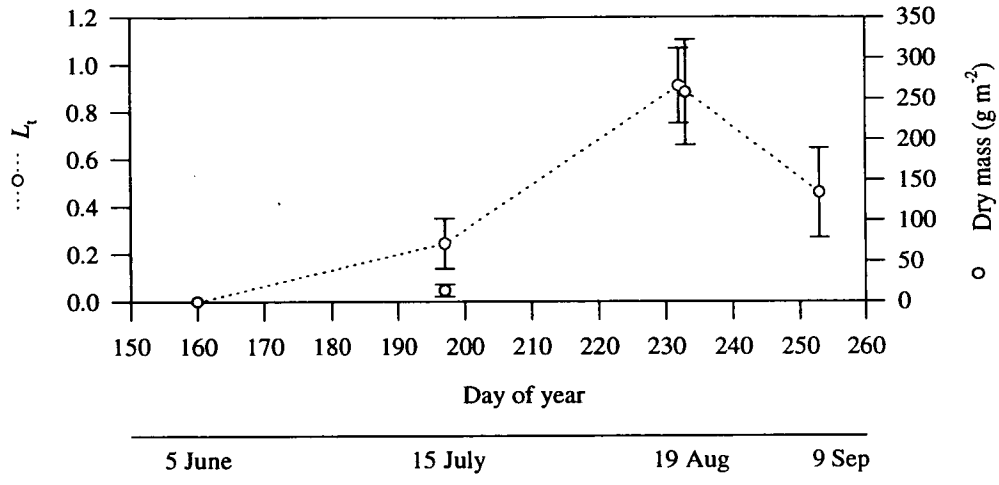

Figure 5.10 Change in millet L_t and dry mass over the 1992 growing season. 95 % confidence intervals are shown.

In early September, little further growth had occurred and large areas of the crop had senesced. A clear relationship between tiller height and area was not present (Figure 5.5(c)). Consequently, estimates of L_t were based on the proportion of leaf area which had become senescent since the August measurement. Tillers were harvested as before and their height and green leaf area measured. For each tiller, senescence was calculated as the measured green leaf area divided by the predicted leaf area given by the equation relating tiller height and leaf area derived in August. No relationship was present between tiller height and percent senescence, so the mean value was taken and applied to the August L_t estimates. The change in L_t and biomass over the growing season is shown in Figure 5.10.

5.2.3 Discussion

The tiller area-height correlation method appeared to work well. Tiller height was easily measurable, so many observations could be made (over 1000 in August), and correlated well with tiller area and biomass. Height measurements on the tall tillers were more difficult, as they had to be pulled over to be within reach and so the culms were curved, but even here, measurements were probably accurate to within a few centimetres. Harvest measurements were also relatively straightforward, and the direct measurements of area and mass could be made quite simply, even on the largest tillers. The sample size required for accurate estimation of canopy properties was smaller than at the other sites because of the relative homogeneity of the millet canopy: there was only a single species, which was even-aged, and planted at a regular spacing. The method had the advantage that information on horizontal and vertical structure was gained.

The mid-August value for dry biomass of 258 g m^{-2} appears reasonable in relation to the mean of 335 g m^{-2} obtained when the millet growth plots (Figure 2.4) were harvested in September (Brouwer *et al.*, in

prep.). The pocket density estimate of 0.48 m^{-2} derived from measurements of pocket spacing agrees closely with the mean of 0.46 m^{-2} measured in the millet growth plots. The values from the September measurements are less reliable, as the variance associated with the mean percentage of senescent leaf area is large (Figure 5.5(c)). There will also be error in these data arising from the subjective judgement of "green" and "brown" leaf area.

5.3 Fallow

5.3.1 Methods and Results

Guiera senegalensis

A direct approach was also used on *G. senegalensis* bushes at the fallow site, based on an allometric correlation between stem diameter and leaf area. A survey of the *G. senegalensis* bushes on the fallow site was carried out in February 1992 in the area shown in Figure 2.5. For each bush, the *x-y* co-ordinates with respect to the University of Edinburgh micrometeorological tower were recorded along with bush height, maximum and minimum radii, height of maximum diameter, number of stems less than 10 mm diameter and diameter of all larger stems. All stem diameters were measured at a point 20 cm above the base. The survey covered 221 bushes in an area of approximately 6750 m^2.

Bush height and the height of maximum diameter were measured with a measuring pole placed vertically in the middle of the bush. A steel tape measure was used to measure the maximum and minimum radii of the bush. The diameter of the stems was measured to the nearest millimetre using callipers. Two measurements were made at right angles to each other and their average recorded. Where individual bushes were not clearly delimited, a group of stems forming a continuous canopy volume was used as the basic unit. The co-ordinates of the bushes were calculated from measurements of angles and bearings to two micrometeorological masts. The pole placed at the centre of the bush was used to sight on each of the two masts whilst standing some distance away. Bearings from magnetic north were measured using a prismatic compass. The elevation angle (from the horizontal) to the top of each tower was also measured using a clinometer whilst standing by the bush. The horizontal distance between the observer and the mast was calculated from the elevation angle by trigonometry using the heights of the mast and the observer. The *x-y* co-ordinates of a bush were calculated by combining the bearing and the distance to one of the masts or by calculating the point of intersection between the bearings on the two masts. A map showing the position of bushes based on bearings and elevation angles on the University of Edinburgh mast is shown in Figure 5.11 and the frequency distribution of the stem diameters of these bushes is shown in Figure 5.12. The other attributes of the bushes are summarised in Table 5.2.

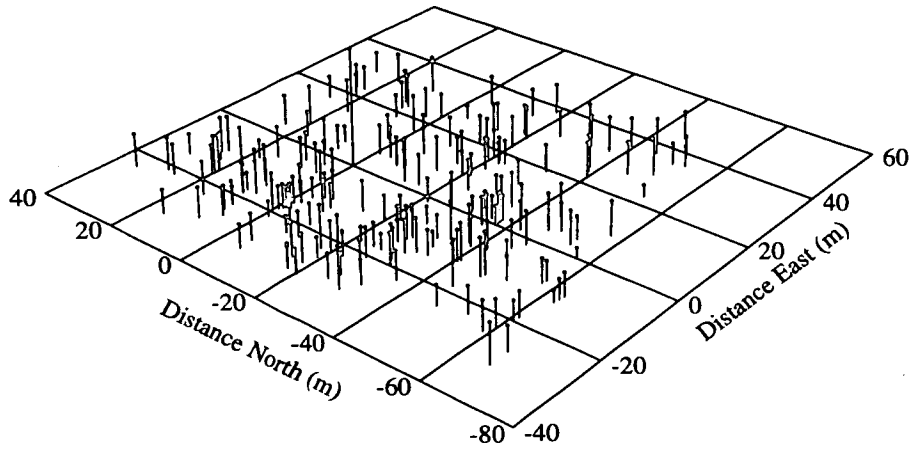

Figure 5.11 Map of *G. senegalensis* bush distribution at the fallow site. The University of Edinburgh micrometeorological mast is at the origin (0,0). Bush height is represented in the z dimension.

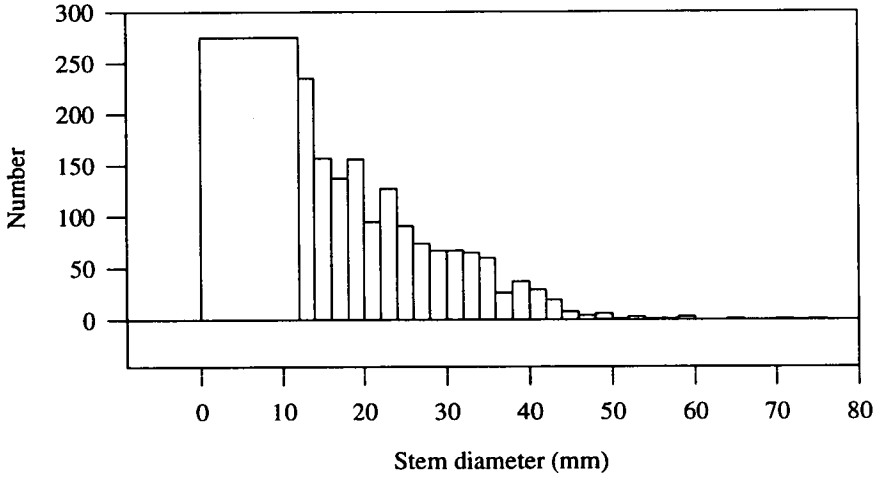

Figure 5.12 Frequency distribution of *G. senegalensis* stem diameters measured at the fallow site in February 1992. Stems smaller than 10 mm diameter were counted but not measured to the nearest millimetre.

Table 5.2 Summary statistics of the variables measured on the 221 *G. senegalensis* bushes in the 6750 m^2 sample plot. *Area of bush projected vertically onto the ground.

	Height (m)	Height of maximum diameter (m)	Maximum radius (m)	Minimum radius (m)	Projected area* (m^2)	No. stems <10 mm diameter	No. stems >10 mm diameter
Mean	2.06	1.49	1.57	0.89	4.88	6.3	6.7
Standard deviation	0.47	0.47	0.58	0.39	3.57	4.5	4.5
Maximum	3.20	2.70	4.14	2.48	23.4	27	21
Minimum	0.80	0.20	0.40	0.15	0.25	0	0

Measurements of leaf area and biomass were made on *G. senegalensis* stems approximately monthly between June and October 1992. Up to 26 stems were harvested on each occasion and the stem diameter, total fresh mass and fresh mass of leaves recorded. The data are shown in Figure 5.13. A sub-sample of leaves was taken from each stem for measurements of fresh mass, dry mass and surface area using a planimeter (LI-3100, Li-Cor Inc., Lincoln, Nebraska, USA). Specific leaf area ($cm^2\ g^{-1}$ dry mass) calculated from these measurements was used to estimate the total leaf area for the stem. The outlier in the October harvest data (Figure 5.13(d)) appears to be very extreme. Although no obvious error could be traced, the value was not included in regression analysis. Linear regression was used to derive relationships between stem cross-sectional area at 20 cm and both leaf area and fresh biomass (Table 5.3). These relationships were then used with the frequency distribution of stem diameters in the surveyed area to estimate L_1 and biomass per square metre of *G. senegalensis*.

Table 5.3 Regression equations relating leaf biomass and leaf area with stem basal area derived in four harvests (B = leaf fresh biomass (g); C = leaf area (cm^2); a = stem basal cross-sectional area (mm^2)).

Month	Equation	n	r^2	Mean specific leaf area ($cm^2\ g^{-1}$)
June	$B = -26.74 + 0.534a$	12	0.94	40.04
	$C = (25.91 + 0.116a)^2$		0.96	
July	$B = -16.62 + 0.602a$	12	0.88	46.58
	$C = (40.74 + 0.130a)^2$		0.94	
September	$B = 17.37 + 0.744a$	24	0.95	40.56
	$C = 1363 + 25.34a$		0.94	
October	$B = -33.83 + 1.020a$	15	0.89	45.56
	$C = (42.11 + 0.191a)^2$		0.92	

For each stem, wood fresh mass was calculated from total stem fresh mass minus leaf fresh mass. No seasonal trend was detected in the relationship between stem diameter and wood fresh biomass (Figure 5.14), so all data were pooled. This relationship was used as above to make a single estimate of wood fresh biomass for the site, and gave a value of 165 g m^{-2} of ground area. The stems harvested in June and September were dried to give wood dry mass. The mean of these values for the dry:fresh mass ratio (0.69) was used to estimate wood dry mass for the site, and gave a value of 114 g m^{-2} of ground area.

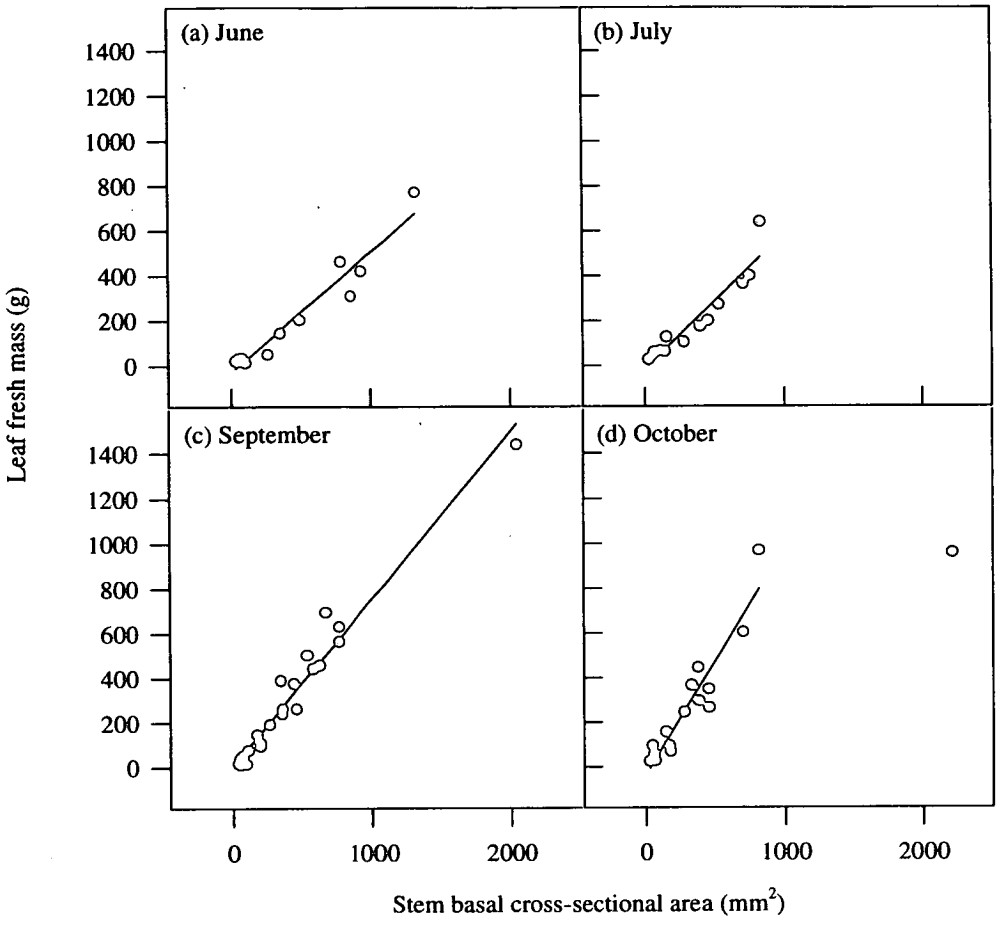

Figure 5.13 Relationship between leaf fresh mass and stem basal area measured in four harvests over the growing season. Specific leaf area was measured on a sub-sample from each stem and used to calculate stem leaf area. Regression lines are shown. The outlier in the October data set was not used in the regression analysis.

Wood surface area was estimated on a small sample of three individual stems. Each stem was cut into small sections which were then sorted into diameter classes incrementing by 5 mm. The volume of wood in each diameter class was calculated from mass and density measurements. These volumes were converted to surface areas by assuming a surface area to volume ratio of a cylinder with diameter equal to the mid-point of the diameter class. The relationship shown in Figure 5.15 was used to predict stem surface area from basal cross-sectional area and hence to estimate L_s for the site in the same way as for L_l. This gave a value of L_s of 0.12.

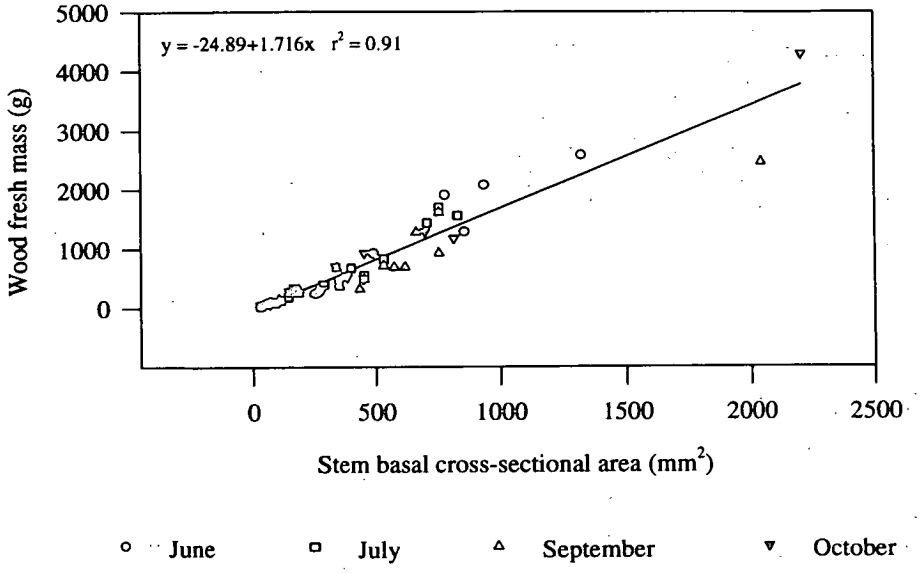

Figure 5.14 Relationship between wood fresh mass and stem basal area. No seasonal difference is apparent and the regression line is shown for the pooled data set.

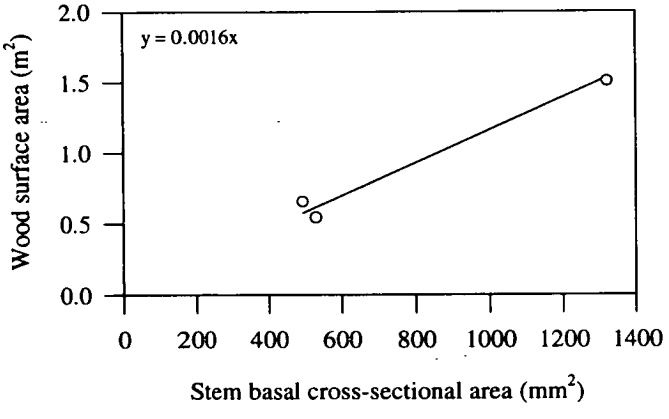

Figure 5.15 Relationship between wood surface area and stem basal area from three stems.

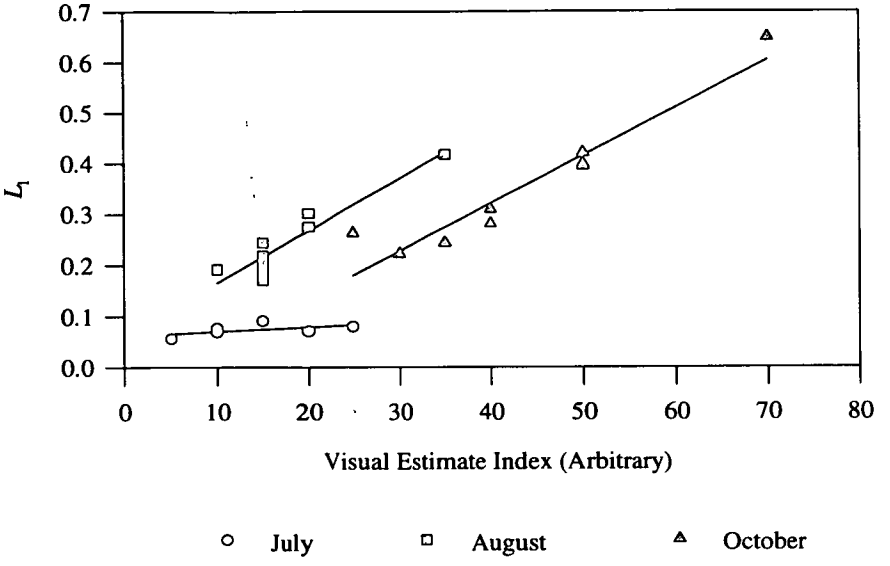

Figure 5.16 Calibration of visual estimation of ground flora L_1 in harvested quadrats.

Ground flora

Estimates of species composition and L_1 of the herbs and grasses in the ground layer were made in 24 permanent quadrats on three occasions over the season. The quadrats were 0.5 x 0.5 m squares arranged on the 70 x 40 m grid shown in Figure 2.5. Each quadrat was visually assessed and assigned a value for an arbitrary index of L_1 between 0 and 100. This index was calibrated on each occasion by making the same assessment in ten other quadrats, which were then measured directly by harvesting and determining the surface area with a planimeter (Li-Cor 3100). Good linear relationships were found between the visual estimates and measured values on each occasion (Figure 5.16) and these were used to estimate the true L_1 for the permanent quadrats. Species composition was assessed at the same time by visually estimating the percentage of the total leaf area that each species represented (Table 5.4). The grass species was predominantly *Eragrostis tremula*, with *Cenchrus biflorus* becoming more prevalent later in the year.

Table 5.4 Species composition of the fallow site ground flora based on 24 permanent quadrats. Values are percentages of L_1, not percent cover.

Date	Day of year	Grasses (%)	*Mitracarpus villosus* (%)	*Cassia mimosoides* (%)	Other (%)
13/7/92	195	66.2	0	18.4	15.4
13/8/92	226	65.6	8.47	10.1	15.7
15/10/92	289	73	12.1	3.5	11.5

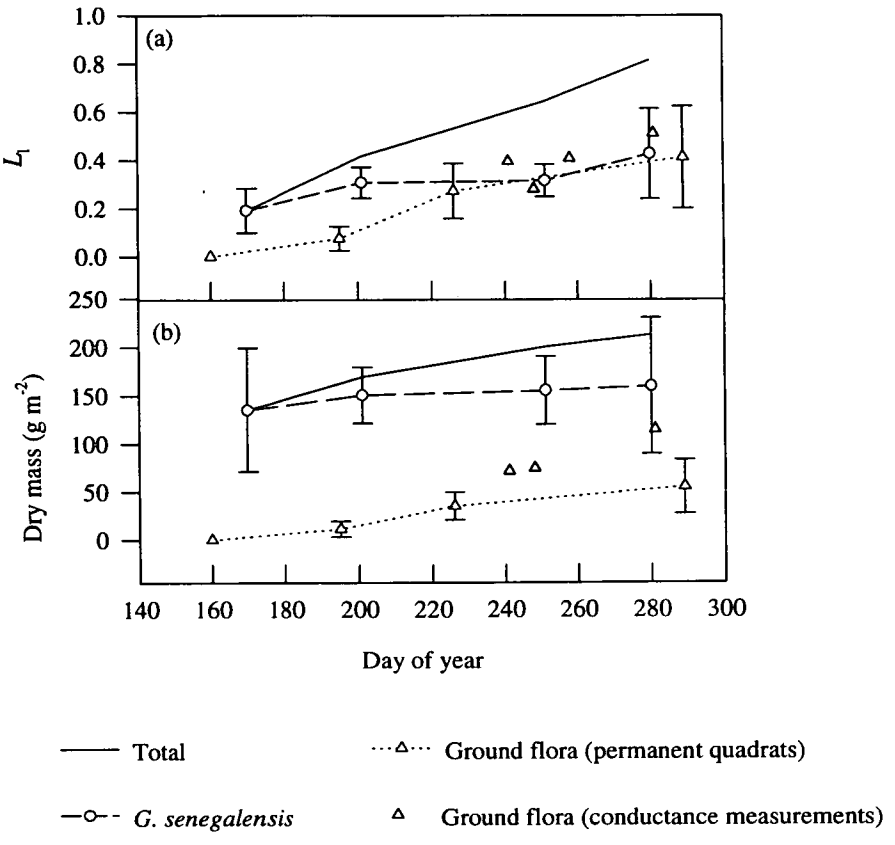

Figure 5.17 Change in fallow site L_1 and dry mass over the 1992 growing season. Error bars show 95 % confidence intervals.

Leaf area and biomass were also measured directly in ten harvested quadrats of approximately 0.25 m^2 on four occasions during the IOP by Cathy Holwill of the Institute of Hydrology (IH). Quadrats were randomly placed within patches of *ca* 2 x 10 m. These data were collected primarily for measurements of surface conductance, and hence did not sample beneath *G. senegalensis* bushes where cover was sparser, and this may explain the higher estimates of L_1 produced by this method (Figure 5.17). Whereas data from the permanent quadrats reflect temporal change in a small spatial sample, temporal change is less apparent in the IH data because each sample was taken from a different location, and so more spatial variability is included in the data. Data from the 24 permanent quadrats were combined with values for *G. senegalensis* to give total L_1 and biomass for the site (Figure 5.17).

5.3.2 Discussion

It is unclear whether the linear relationships between stem basal cross-sectional area and leaf area, which appear close in smaller stems (< 3.5 cm diameter), break down in larger stems, as only three data points were obtained (one each in June, September and October, (Figure 5.13)). The values for the two large stems measured in June and September were still compatible with a linear relationship and so included. The large stem measured in October was clearly not and therefore excluded. Harvests were considerably more difficult than for millet, as leaves had to be picked off the stems which was a time consuming process. Few large stems were harvested because of this, introducing a bias into the regression equations and L_l estimates. If larger stems are more variable, as seems to be the case, the true confidence intervals in Figure 5.17 will be larger than indicated. If the form of the relationship changes, the L_l estimates will be incorrect. However, no other direct measurements are available for comparison. The sample size used for wood surface area measurements was very small because cutting the stems up into size classes was also very laborious. However, the results may be adequately reliable as the relationship obtained was very close (Figure 5.15). The extensive area of the stem diameter survey (6750 m^2) was deemed necessary given the heterogeneity of the canopy but was costly in manpower, requiring two to three people for three weeks.

Figure 5.17 shows little increase in *G. senegalensis* L_l between days 200 and 250. This is unlikely as this was the period of peak rainfall and casual observations showed that leaf growth clearly occurred over this period. If leaf growth proceeded at a roughly constant rate over the season, the true value of the September L_l estimate would be expected to lie close to the upper limit of the confidence interval.

The effect of error in the elevation angle measurement on calculation of the bush co-ordinates increases exponentially with distance from the micrometeorological mast. However, the co-ordinates of a sub-set of bushes were checked using a measuring tape and were found to be accurate to within about 1 m. Senescence was a problem in estimating green L_l in late September and October, as leaves were classified as "green" or "brown" subjectively. Furthermore, some of the *G. senegalensis* bushes had begun to shed leaves at the time of the October harvest, adding a further source of variation to the data. There will also be errors from mass, surface area and diameter measurements. However, these are likely to be very small compared with biological and spatial variability. Sampling error is thus the major source of uncertainty.

The method used for *G. senegalensis* assumed that the stem diameter distribution measured in February remained constant over the year. Clearly, diameters of growing stems will increase, violating this assumption, resulting in an underestimation of L_l and biomass towards the end of the year. However, the error from this is probably negligible compared with the biological variability of *G. senegalensis* stems.

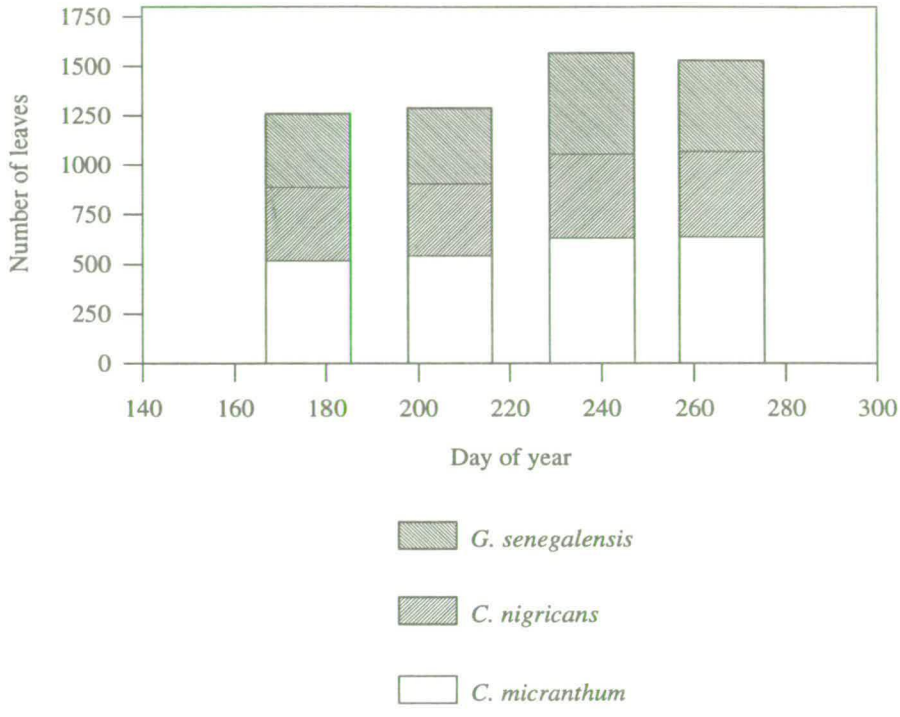

Figure 5.18 Change in number of leaves on tagged shoots at the tiger bush site in 1992.

5.4 Tiger bush

Direct measurements using a similar procedure to that at the fallow were begun at the tiger bush site in February 1992. However, two days after measurements started, a military coup prevented any further work taking place. Measurements of shrub dimensions and stem diameters were only completed in two small areas of 30 x 5 m and 15 x 5 m. Although these were considered much too restricted to estimate site L_1, the shrub co-ordinates and dimensions were used as a basis for the description of canopy structure in MAESTRO. Stems of *C. micranthum* and *G. senegalensis* were harvested during the IOP in order to establish correlations between stem diameter and leaf area and biomass. It was hoped to use these measurements with data from a planned survey of stem diameters in late October 1992. However, circumstances did not permit this and results are not presented.

Phenology

Leaf phenology was examined in *C. nigricans, C. micranthum* and *G. senegalensis* by marking shoots with wire tags and counting the number of leaves present each month. Fifty shoots from each species were marked on individuals on a transect through a single vegetated stripe. An arbitrary minimum size was chosen, approximately 1 cm^2, corresponding to the size of a fingernail. The results are shown in Figure 5.18. Unfortunately, measurements began too late and ended too early to show the major seasonal changes in leaf area.

5.5 Conclusions

Direct methods were successfully used to measure L_l, L_t and biomass at the millet and fallow sites. In millet, tiller height was closely correlated with tiller area, and this was used in conjunction with measurements of the tiller height distribution to estimate L_t. Biomass was estimated in an analogous way. At the fallow site, leaf and stem area were closely correlated with stem basal cross-sectional area in *G. senegalensis*. Measurements were made of all stem diameters within a 6750 m^2 area, and these were used with established correlations at four times during the 1992 growing season to estimate L_l and L_s. Again, biomass was estimated in an analogous way. The fallow site ground flora was measured destructively in harvested quadrats and non-destructively in permanent quadrats. Because of the logistical problems imposed by canopy heterogeneity at the tiger bush site, direct methods were not used to estimate L_l or biomass, and indirect methods had to be relied upon (Chapter 6). The data obtained have been used in several ways: for comparison with indirect methods (Chapter 6), for scaling up leaf-scale flux measurements (Chapter 7) and interpreting ecosystem flux measurements (Moncrieff *et al.*, 1996), in GCM parameterisations (Gedney and Valdes, 1994, 1995; Blyth, 1995) and for comparison with remote sensing data (N.P. Hanan, pers. comm.; J.F. Duncan, pers. comm.).

Chapter 6

Canopy Properties - Indirect Measurements

6.1 Introduction

The work described in this chapter has two aims:

(1) To derive indirect estimates of total plant surface area index (L_t) at the three sites and compare these with direct measurements. Direct measurements are laborious, destructive and time consuming, so methods for determining canopy properties from indirect measurements would be extremely useful, as they are generally quicker, replicable, amenable to automation, and thereby allow a larger spatial sample to be obtained.

(2) To derive empirical values for the extinction coefficient, K, for use in a "big leaf" canopy photosynthesis model.

Indirect measurements are those in which canopy structure is inferred from observations of another variable, such as transmitted radiation (Anderson, 1966). The Beer-Lambert or Monsi-Saeki equation (Monsi-Saeki, 1953 cited in Ross, 1981; Monteith 1965) is a very simple description of radiative transfer through a canopy and is valid if the canopy behaves like a homogeneous medium. The equation describes the exponential attenuation of Q as it passes through the canopy, and the transmitted flux density (Q_{trans}) is given by:

$$Q_{trans} = Q_{in} (1 - \rho) \exp (-K L_t), \qquad [6.1]$$

where Q_{in} is Q incident upon the canopy, ρ is the canopy reflection coefficient in the photosynthetic waveband and K is an extinction coefficient which depends on factors such as the leaf inclination angle distribution, the angular distribution of solar radiation above the canopy, leaf optical properties and the spatial distribution of plant surface area density. Strictly, the equation only applies where the spatial distribution and orientation of canopy elements is random. In real canopies, canopy elements are clumped together within shoots, branches, individual plants, groups of plants such as millet pockets and larger scale entities such as the vegetation arcs in tiger bush. However, the equation has been shown to provide a reasonable approximation in many cases (eg. Thornley, 1976; Pierce and Running, 1988).

This equation is used here in two ways:

(1) *Estimating* L_t

Values of K can be estimated from theory if a simple leaf angle distribution is assumed (Campbell, 1986). For a spherical distribution, the value of K for the direct beam is 0.5. ρ can be ignored as it is typically around 0.03 for leaves (Monteith and Unsworth, 1990). If measurements are made of the transmittance, τ ($\tau = Q_{trans}/Q_{in}$), the equation can be inverted to infer L_t:

$$L_t = -\ln\tau / K. \qquad [6.2]$$

τ may be calculated from radiation measurements above and below the canopy (eg. Bolstad and Gower, 1990; Gazarini *et al.*, 1990). However, these measurements should strictly only include the direct beam component, and there are practical difficulties in separating this from diffuse radiation.

Alternatively, L_t can conveniently be derived by image analysis of hemispherical photographs, as the gap fraction (the ratio of sky to canopy area in a section of the image) can be regarded as equivalent to τ (Wang and Miller, 1987; Norman and Campbell, 1989). This method has several advantages: the whole range of zenith angles is available in each image, a large area is sampled by each photograph, and measurements are fast and easily replicable.

(2) *Estimating canopy Q absorption*

Taking reflection into account, Equation 6.1 can be rearranged to give a "big leaf" model of canopy Q absorption for modelling canopy photosynthesis (Chapter 7):

$$Q_{abs} = Q_{in} - Q_{ref} - Q_{trans} \qquad [6.3]$$

$$= Q_{in} (1 - \rho) (1 - \exp(-K L_t)), \qquad [6.4]$$

where Q_{abs} and Q_{ref} are the Q absorbed and reflected by the canopy, respectively. A value for K, the extinction coefficient is given by rearranging Equation 6.2.

$$K = -\ln\tau / L_t. \qquad [6.5]$$

Values of L_t were obtained from direct measurements at the millet and fallow sites (Chapter 5). The parameters K and ρ in Equation 6.4 can then be derived from measurements of incident, reflected and transmitted Q. These measurements were made at all three sites, although differences in canopy structure and equipment shortages required that different methods were used. In these measurements and Equations 6.4 and 6.5, direct and diffuse radiation are considered together, and K and ρ are treated as empirical constants. Evidence suggests that this reasonable, as direct measurements of radiation in

crops with a wide range of leaf sizes and leaf angle distributions show that the variation in K and ρ over the central 8 hours of the day is usually small enough to neglect (Monteith, 1969; Allen *et al.*, 1994). For the tiger bush site, direct estimates of L_t were not available, but indirect estimates were made from hemispherical photographs. In principle, values of K could also be derived from these photographs. However, the values used were derived from radiation measurements, as these treated direct and diffuse radiation together.

6.2 Methods

6.2.1 Hemispherical photography

Photographs of the vegetation canopy were taken using a Nikon "Fish Eye" hemispherical lens on a standard Nikon 35 mm SLR camera body with Kodak Technical Pan high resolution film. The camera was held on a tripod as close as possible to ground level and pointed vertically upwards. Levelling was done using a spirit level mounted on the lens cap. Exposure was judged using the reading from an ordinary photographic light meter pointed vertically upwards. Photographs were taken at the millet site in 1991 in the 16 plots where L_t was directly measured (Chapter 5). The camera was placed at the centre of the plot, in the middle of the space between pockets. At the fallow site, photographs were taken in June, August and September 1992 on both the 250 x 300 m neutron probe access tube grid and the 40 x 70 m ground flora quadrat grid (Figure 2.5). The latter grid was the same as that used for direct measurements on the ground flora, and was within the area where direct estimates of *G. senegalensis* L_t were made (Chapter 5), enabling comparison with these measurements to be made. Photographs were taken at the tiger bush site at 35 points located on seven transects through vegetated areas around the micrometeorological towers in June, August and September 1992 and at other locations in February 1992.

A uniformly illuminated sky is desirable as a background in the image to provide even contrast. This is best on days with complete cloud cover, or near dawn or dusk. In practice, this was very hard to achieve in Niger, as suitable cloud cover is rare during the growing season, and the logistics of being at the sites at dawn or dusk proved difficult. In all sampling periods, some photographs were not analysed because of poor image quality, usually caused by the solar disc producing uneven contrast.

The negatives were analysed using Optimas image analysis software and a program written by Dr Paul van Gardingen, University of Edinburgh. Negatives were scanned, producing a square image of approximately 1000 x 1000 pixels. A threshold level was set on the computer image differentiating between canopy elements and background sky. The image was then divided into 6 annuli representing different zenith angle classes and further divided into azimuth angle classes to give a total of 84 sectors. Within each sector, the proportion of sky to canopy area (equivalent to τ) was calculated and

transformed to its natural logarithm, before averaging across sectors in each zenith angle class, similar to the method of Lang and Yueqin (1986). This procedure allows for the heterogeneity in τ, which has often caused indirect methods based on light transmission to underestimate L_t (Lang, 1986). This underestimation arises because of the clumped distribution of leaves in natural canopies, resulting in gaps, which allow more light to penetrate than in an idealised canopy with randomly distributed leaves. In sectors where there were no gaps, and so τ was zero and $\ln\tau$ was undefined, the data were discarded. Such sectors were found mainly at the edge of the image, and the maximum zenith angle used in the analysis was occasionally reduced to minimise their occurrence in the data set.

For each image, the data set of $\ln\tau$ and zenith angle (θ) was inverted to give an estimate of L_t. The mathematical inversion procedure used was the linear regression method of Lang (1987). In this method, a quantity referred to as the *contact number* is calculated for each zenith angle class as

$$\kappa = -\cos\theta \ln\tau(\theta) \qquad [6.6]$$

and is linearly regressed against θ. The offset and slope coefficients of this regression (a and b, respectively) are then used to calculate L_t from

$$L_t = 2\,(a + b). \qquad [6.7]$$

The image analysis procedure has a subjective element, in that the threshold level between sky and canopy is set manually. Judgement of this threshold is not always easy, mainly because of variable exposure across the image. The effect of this was tested for by analysing the same film of 36 exposures on two occasions, six months apart. These analyses gave values of L_t of 2.10 and 1.97, suggesting that errors caused by this subjective judgement are not large.

6.2.2 Transmitted Q

Millet - "Ceptometer"

Measurements of incident and transmitted Q were made using a "Ceptometer" (Decagon/Delta-T Devices, Cambridge, UK), a portable radiometer consisting of an 0.8 m long bar with 80 quantum sensors at 1 cm intervals. In 1991, "Ceptometer" measurements were made in 7 of the 16 plots where direct measurements were made (Chapter 5). In each plot, transmitted Q was measured along two perpendicular 6.4 m transects, forming a cross centred on the middle of the plot, giving 1280 individual measurements (2 x 6.4 m x 100 measurements m^{-1}). Measurements of incident Q were made before and afterwards to account for any changes in incoming radiation. In 1992, the same procedure was repeated in the 20 plots on the transects used for direct L_t measurements (Chapter 5). To estimate L_t, a simple inversion method was used, using Equation 6.2. Values of K were calculated

as a function of solar zenith angle and leaf angle distribution (Campbell, 1986). The leaf angle distribution was measured by P. Lewis and M. Barnsley of University College London.

Fallow - Quantum sensor array

An array of quantum sensors was used to measure incident, reflected and transmitted Q continuously for 58 days between mid-August and mid-October (DOY 219 to 277). A data logger (CR10, Campbell Scientific Ltd, UK) was programmed to record the signals from the quantum sensors when incident total solar radiation measured by a solarimeter was greater than 20 Wm^{-2} (as night-time data were of no value). Two sensors were mounted at 9 m on the micrometeorological mast to measure incident and reflected Q. Thirteen sensors were placed at ground level, held in plastic tubes hammered into the soil, to measure transmitted Q. These were initially placed within the projected area of the *G. senegalensis* bushes as growth of the ground flora was not yet significant (period 1). Halfway through the season (DOY 255), these were moved so as to be representative of the whole site (period 2). The sampling was stratified, so that two out of the 13 sensors (15.4 %) sampled within the projected area of the bushes, which occupied 16 % of the site. Absorbed Q was calculated as in Equation 6.3.

Tiger Bush - Quantum sensor transects

As the tiger bush canopy was much more heterogeneous and the number of quantum sensors available was limited, a different approach to measuring Q transmission was used here. A simple instrument was constructed in which a single quantum sensor could be held at ground level whilst walking. This was similar in shape to a hockey stick, with an extended horizontal section so that the sensor could be carried at a suitable distance from the body. A data logger (21X, Campbell Scientific Ltd, UK) was carried in a back pack and programmed to sample at 10 Hz. The instrument was held in front while walking towards the sun, attempting to maintain a steady pace. Prior to making transmission measurements, incident Q was measured in a bare area and the instrument was programmed to record $\ln\tau$. Very high spatial resolution was achieved in these measurements, typically 1-2 cm. Measurements were made in September 1992 on three of the transects used for leaf phenology measurements and hemispherical photographs.

6.3 Results

6.3.1 Estimation of L_t

Millet

Figure 6.1 shows comparisons between indirect estimates of L_t from both hemispherical photographs and "Ceptometer" measurements and direct estimates based on the relationship between tiller height and area at the millet site. Estimates from the "Ceptometer" method show very good agreement (Figure 6.1(a)), and give a mean value within 0.02 or 2 % of direct estimates. The slope and offset in

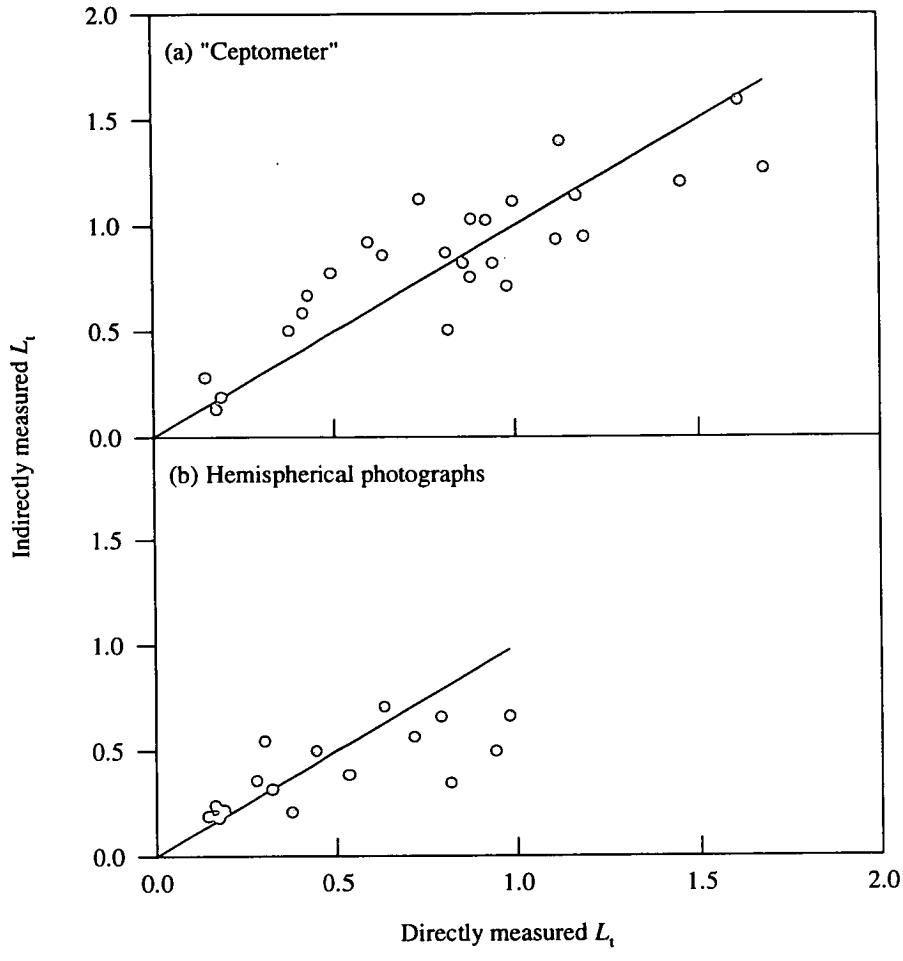

Figure 6.1 Comparison of indirect methods of L_t estimation with direct estimates in millet.
The direct estimates are based on the measured relationship between tiller height and area (Chapter 5
(a) Estimates from "ceptometer" measurements of transmittance made in 26 plots in 1991 and 1992. These were used with theoretical extinction coefficients to calculate L_t from Equation 6.2.
(b) Estimates of L_t from hemispherical photographs taken in 16 plots in 1991. L_t was calculated from these using the inversion method of Lang (1987) (Equation 6.7). 1:1 lines are shown.

the regression relationship (Table 6.1) show a tendency to underestimate at higher values and vice versa. This tendency is more pronounced in estimates from the hemispherical photograph method, which are reasonable at L_t lower than 0.6, but consistently underestimate beyond this point (Figure 6.1(b)). This results in an underestimation of 0.09 or 18 % of the mean of direct estimates of L_t.

Table 6.1 Coefficients of regression relationship between indirect and direct estimates of L_t in millet. Measurements were made in 1991 and 1992 in the plots where direct estimates of L_t were made (Chapter 5). Indirect estimates were related to direct estimates by the regression equation, $L_i = a + bL_d$, where L_i and L_d are the indirect and direct estimates, respectively. *The difference between the mean of indirect L_t estimates and the mean of direct estimates is shown.

Method	Inversion	Offset, a	Slope, b (+/- s.e.)	r^2	n	Mean of direct estimates	Indirect - direct estimate*
Hemispherical photograph	Equation 6.7 [Lang (1987)]	0.122	0.513 (+/- 0.12)	0.567	16	0.49	-0.09
"Ceptometer"	Equation 6.2	0.24	0.728 (+/- 0.09)	0.733	26	0.80	0.02

Fallow

Indirect estimates of L_t from hemispherical photographs at the fallow site do not differ significantly (p=0.05) from the direct estimates (Figure 6.2). The same tendency to underestimate high L_t values and overestimate low ones found in millet is present here, although the significance of this is difficult to judge with only three data points. The error bars are large because of the spatial variability in L_t at the site. Measurements made on the larger neutron probe access tube grid gave lower values than measurements made on the 70 x 40 grid (Table 6.2), but this difference is not significant.

Table 6.2 Mean of indirect estimates of L_t from hemispherical photographs at the fallow site using the inversion method of Lang (1987) (Equation 6.7). *The difference between the mean of indirect L_t estimates and the mean of direct estimates is shown.

Grid	Date	L_t	95 % confidence interval	n	Indirect - direct estimate*
70 x 40	20/6/92	0.42	0.30	18	0.11
70 x 40	11/7/92	0.38	0.22	16	-0.01
70 x 40	15/9/92	0.68	0.24	21	-0.13
250 x 300	13/8/92	0.37	0.16	30	-
250 x 300	15/9/92	0.53	0.21	27	-

Tiger bush

The variation in L_t estimated from hemispherical photographs along the seven transects is shown in Figure 6.3(a). There is considerable point to point variability, ranging from close to zero to 5.5. No direct estimates of L_t were available for comparison at this site. However, a relative index of L_t is given by the leaf phenology measurements (Figure 5.18), and shows little change in leaf number between June and September. This is in agreement with the hemispherical photograph estimates (Figure 6.3(b), Table 6.3), which do not change significantly over this period. The photographs taken in February and August were not analysed because they were generally of poor quality, with uneven contrast.

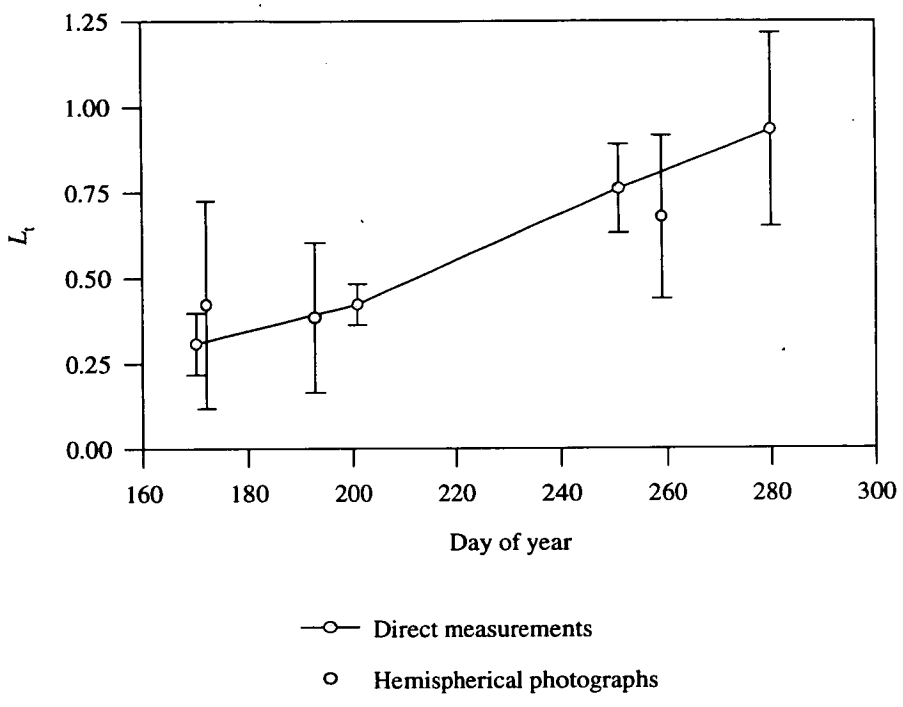

Figure 6.2 Comparison of L_t estimates from direct methods and hemispherical photographs at the fallow site. Photographs were taken on a 70 x 40 m grid within the area where direct measurements were made on the bushes and ground flora. For the purposes of comparison, the direct measurements shown do not include the ground flora in the first two sampling dates, as it had not developed significantly and did not appear on the images. The error bars show 95 % confidence intervals.

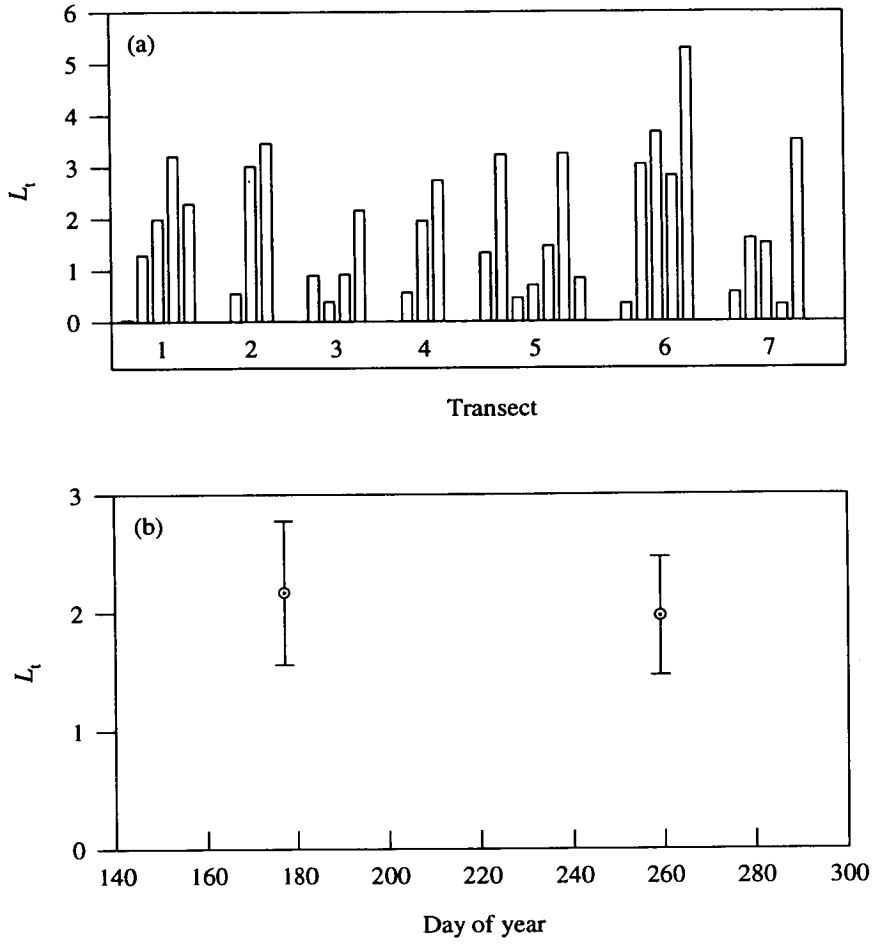

Figure 6.3 (a) Indirect estimates of L_t from hemispherical photographs taken at the tiger bush site in September 1992. Bars show estimates from points 10 m apart on seven transects through vegetated areas. (b) Seasonal change in the mean estimate of L_t from hemispherical photographs between June and September 1992. Error bars show 95 % confidence intervals.

Table 6.3 Mean of indirect estimates of L_t from hemispherical photographs at the tiger bush site using the inversion method of Lang (1987) (Equation 6.7).

Date	L_t	95 % confidence interval	n
25/6/92	2.17	0.61	26
16/9/92	1.97	0.50	32

6.3.2 Estimation of extinction coefficients, K

Millet

The 1992 "Ceptometer" measurements of τ made in the 20 plots where L_t was directly measured (Chapter 5) were used in Equation 6.5 to calculate K (Table 6.4).

Fallow

The decrease in canopy transmittance as L_t increases over the growing season is clearly apparent in Figure 6.4(a). The lower transmittance beneath the bushes is also apparent, as there was a marked increase when the quantum sensor array was moved to include the area covered only by ground flora in the sample. There was considerable point to point variability in transmittance, and the mean value measured by different sensors over period 2 ranged from approximately 0.2 to 0.7. Daily values of K were calculated from Equation 6.5 by using values of L_t corresponding to *G. senegalensis* L_t in the first period, and the total site L_t in the second period. These values of L_t were obtained by linearly interpolating between the direct measurements of L_t in Figure 5.17 and adding the directly measured value of L_s. An average value of K for the site over the whole season was calculated as the mean of these daily K values (Table 6.4). Figure 6.4(b) shows that a relatively small fraction of Q is absorbed (33 %), more than half being transmitted.

Tiger bush

Figure 6.5 shows the considerable small scale variability in τ along one transect at the tiger bush site. A value of K was calculated for each point along the transect from Equation 6.5, using the value of L_t for that transect estimated from hemispherical photographs. A mean value of K for the site was then calculated from the K values for each transect (Table 6.4).

Table 6.4 Values of the extinction coefficient, K, for each site, calculated from measurements of transmitted Q. Values were calculated using measured values of τ and L_t in Equation 6.5. For millet, the 1992 "Ceptometer" measurements of τ made in the 20 plots where L_t was directly measured (Chapter 5) were used. For the fallow site, measurements of τ from the quantum sensor array were used. The value is the average of daily values of K, calculated using values of L_t which were linearly interpolated between the direct measurements in Figure 5.17. For the tiger bush site, values of K were calculated along each transect using values of τ from quantum sensor measurements and the value of L_t for that transect estimated from hemispherical photographs. A mean value of K for the site was then calculated from the K values for each transect.

Site	Millet	Fallow	Tiger bush
Mean	0.67	0.58	0.56
Standard deviation	0.18	0.08	0.12
Maximum	0.92	0.73	0.71
Minimum	0.39	0.36	0.48
n	20	50	3

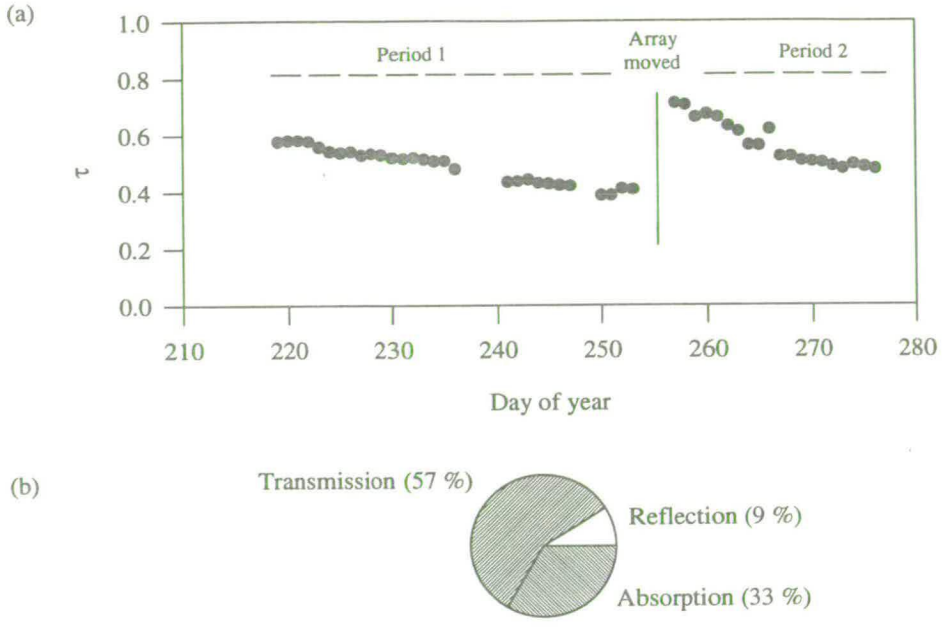

Figure 6.4 (a) Seasonal change in fallow canopy transmittance. Points show the mean transmittance measured by the sensor array whilst positioned beneath bushes (period 1) and whilst sampling the whole site (period 2). (b) Pie chart showing the proportion of Q transmitted, reflected and absorbed by the fallow canopy over period 2.

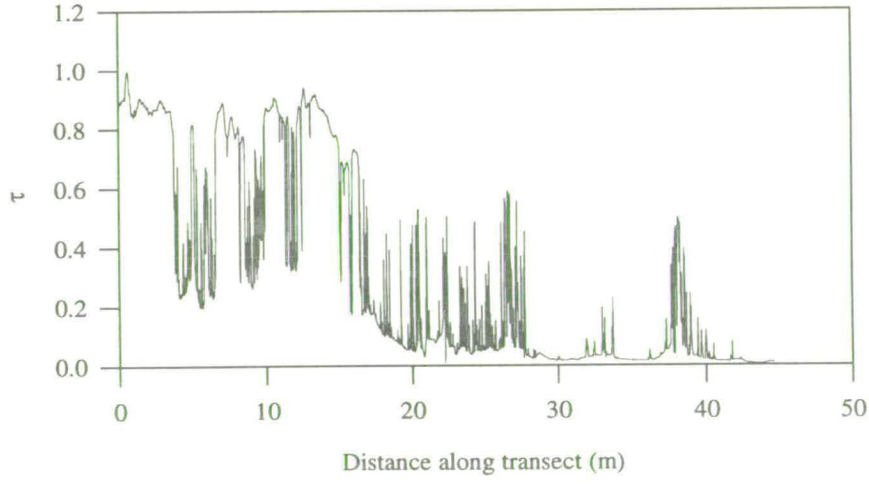

Figure 6.5 Spatial variation in transmittance along a transect through a vegetated area at the tiger bush site. Measurements were made in September 1992 using a quantum sensor held on a specially constructed instrument whilst walking into the sun. The data were used in conjunction with L_t estimates from hemispherical photographs to calculate extinction coefficients.

6.4 Discussion

Whilst L_t estimates from the hemispherical photograph method underestimated direct measurements at higher L_t values by around 20 %, these differences are small in absolute terms (0.09 in millet and 0.13 in fallow). This trend would not be apparent in millet without the three highest points on the x-axis in Figure 6.1(b), so it is not conclusively clear from these results that this trend is generally present. Given that the fallow site has a very heterogeneous canopy and represents an extreme test of the hemispherical photograph method, it performs reasonably well and clearly has potential to be very useful.

In the absence of any direct measurements, it is difficult to say how accurate the hemispherical photograph method was at the tiger bush site on the basis of results at the millet and fallow sites. If the trend seen in Figure 6.1(b) is continued up to a L_t of 2, underestimation of L_t may be very serious (perhaps 30 - 50 %). Alternatively, if the error remained roughly constant, then the estimate of L_t may be acceptable. Ideally, it would be desirable to validate the hemispherical photograph method in a heterogeneous canopy with a higher leaf area, like that at the tiger bush site. However, the time and labour involved made this impossible at the tiger bush site, and these photographs provide the only L_t data for any of the tiger bush sites in HAPEX-Sahel. For the same reasons, validation experiments for similar techniques have mostly been carried out where canopy heterogeneity is much less: in agricultural crops (eg. Lang, Yueqin and Norman, 1985) or in forest, where direct estimates have usually been based on allometric correlations between stem diameter and leaf area collected at other sites (eg. Chen, Black and Adams, 1991).

There are several possible explanations for the observed tendency to underestimate L_t. In millet, the camera was always placed in the middle of the space between pockets, and this may introduce a bias by reducing the plant area seen in the images. This may explain why the "Ceptometer" method gave better agreement than the hemispherical photograph method here, as no such bias was present in the "Ceptometer" measurements. The transects along which the instrument measured could pass directly through the millet pockets and so may have obtained a better spatial average. Images with poor background contrast tend to give underestimates, as the threshold has to be set lower to avoid dark patches of sky being classed as canopy area. In millet, the culms differ from leaves in that they are three dimensional, and their total surface area is included in the direct measurements, whereas only half this area would be projected onto the photographic images. As the culms comprised 29 % of L_t in the September 1991 harvest, the hemispherical photograph method might be expected to underestimate by about 14.5 %, which is ~75 % of the observed underestimation. More generally, the degree of clumping in the images was high, and it is possible that the number of sectors used was inadequate to compensate for this. To investigate this further, the number of sectors could be increased until an asymptotic value of L_t, that may correspond more closely to the true L_t, is reached. A problem with

decreasing the size of sectors is that the probability of obtaining a value of τ of zero increases, and these data have to be discarded or set to some arbitrarily low value.

A potential problem with the hemispherical photograph method is the correct judgement of exposure. Overexposure may lead to lower estimates of L_t, if the setting of the threshold does not compensate fully. However, it is not clear that the exposure set using a standard light meter will necessarily give the correct exposure for L_t determination (Chen *et al.*, 1991). A further problem is that the photographs yield estimates of total plant surface area index rather than leaf area index. This is not a problem at the millet site, where the culms may have photosynthetic properties similar to those of the leaves. However, at the fallow and tiger bush sites the leaves and woody stems have entirely different properties and values of L_t need to be partitioned into leaf and stem areas by some other means.

If the extinction coefficient, K, is treated as an empirical constant, its measurement is relatively straightforward. K has been measured in a large number of experiments in crops, and a very wide range of values has been found, from around 0.3 for erectophile species, such as ryegrass, to close to 1 for planophile species such as clover (Monteith, 1965, 1969). Several studies have been made in maize, which may be comparable with millet, as it has a canopy structure which appears very similar. A value for K of 0.65 was obtained by Allen *et al.* (1964), for example, which is very close to the value of 0.67 obtained here for millet.

The values of K for the fallow and tiger bush sites (0.58 and 0.56, respectively) are slightly higher than the theoretical value of 0.5 for beam radiation in a canopy of randomly distributed foliage with a spherical leaf angle distribution (Campbell, 1986). Rather fewer studies in tree and shrub communities are available for comparison, but a similarily wide range of values occur in the literature: Jarvis and Leverenz (1983) found values of K between 0.29 and 0.65 for broad-leaved species and between 0.28 and 0.62 in coniferous species in their literature review. Bolstad and Gower (1990) measured values between 0.47 and 0.83 for 14 stands of coniferous and broad-leaved species, and a value of 0.84 was reported for eastern white pine (Vose and Swank, 1990). However, values between 0.5 and 0.6 are most common (eg. Landsberg, Jarvis and Slater, 1973; Norman and Jarvis, 1974; Pierce and Running, 1988; Bolstad and Gower, 1990; Gazarini *et al.*, 1990), and the values obtained for the fallow and tiger bush sites are in agreement with these. The tendency for K to be slightly higher than 0.5 may be because leaf angle distributions are generally more planophile than erectophile (at least in broad-leaved species), or be a result of the diffuse component of radiation.

A possible bias may have been introduced into the fallow site data by the act of installing the sensor, as any foliage present at that spot was removed and could not regrow. Although the surrounding herbs continued growing, the foliage did not regrow directly above the sensor. This would lead to an

underestimation of the value of K. The K value calculated for the fallow site is notably lower than at the millet site (0.58 cf. 0.67), although not low in comparison with theoretical values for a spherical leaf angle distribution or other literature values.

6.5 Conclusions

The "Ceptometer" method of estimating L_t worked well in millet. The hemispherical photograph method tended to underestimate millet L_t, and this may be because half of the of culm area was effectively hidden from view, or result from a bias in the positioning of the camera. The hemispherical photograph method agreed well with direct estimates at the fallow site, even though the canopy was more heterogeneous. This tentatively suggests that the hemispherical photograph estimates of L_t at the tiger bush site may be satisfactory. Values of K, the extinction coefficient, were relatively straightforward to obtain, and were close to representative values for comparable vegetation reported in the literature.

Chapter 7

Scaling Up in Space and Time

7.1 Introduction

Since the mid-1980s, eddy covariance has become established as a reliable technique for the measurement of net ecosystem CO_2 flux (A_c) and has been used in many studies (eg. Anderson and Verma, 1986; Verma *et al.*, 1986; Baldocchi, Verma and Anderson, 1987; Verma, Kim and Clement, 1989; Kim and Verma, 1990; McGinn and King, 1990; Moncrieff, Verma and Cook, 1992; Wofsy *et al.*, 1993; Hollinger *et al.*, 1994; others listed by Ruimy *et al.*, 1995). However, eddy covariance measurements are restricted to point locations, and until recently, to only a few days or weeks. As a consequence of this, a relatively restricted range of conditions is encountered, and empirical models based on these may haved limited applicability. If we wish to extrapolate fluxes in space and time over an extended range of biological and environmental variables (eg. sites with different leaf area indices, seasons with different weather conditions), it is necessary to have a mechanistic understanding of the system. This extrapolation or scaling-up procedure is not necessarily straightforward on account of the large scale phenomena and non-linear averaging problems which arise in the transition between scales (Section 1.4). Consequently, there is a need to test these procedures before confidence can be placed in the extrapolations produced.

Here, eddy covariance measurements were used to test different methods of extrapolating the leaf-scale measurements described in Chapters 3 and 4 to ecosystem scale. Two scaling-up methods varying in complexity were compared: a three-dimensional multi-layer model MAESTRO (Section 7.2) and a simple one-dimensional "big leaf" model (Section 7.3). MAESTRO is a sophisticated radiative transfer model, in which individual plants within the canopy are represented with high spatial resolution. This is combined with the stomatal conductance, photosynthesis and respiration models described in Chapters 3 and 4. The same physiological routines are used in the big leaf model but the transfer of radiation is modelled much more simply. The assumption is made that the canopy is homogenous in the horizontal and vertical dimensions and so behaves like a single plane surface or "big leaf". The eddy covariance measurements are described in Section 7.4.1.

7.2 MAESTRO

7.2.1 Model Description

MAESTRO is based on a model of radiative transfer in orchards developed in the 1970s (Norman and Welles, 1983) and further developed for agroforestry and plantation forestry situations (Grace, Jarvis

and Norman, 1987; Wang and Jarvis, 1990). Full details are given in Wang *et al.* (1992). The model can be used to predict ecosystem-scale CO_2 fluxes from the measurements of photosynthetic and respiratory properties of leaves and stems, together with ecosystem-scale properties such as L_l and biomass. The model differs from most others in that it represents canopy structure in three dimensions and can therefore simulate structurally complex plant canopies. It is thus a suitable tool for modelling the non-uniform canopies found at the fallow and tiger bush sites.

MAESTRO simulates the transfer of radiation, transpiration and photosynthesis of a specified stand of plants, given meteorological data as an input (Figure 7.1). All previous applications have involved simulations of trees, and so parameter names often use this term although the plants simulated may take any form. The co-ordinates, dimensions and leaf area of all plants in the stand are specified in a file. Each hour, the radiation regime within the crown of a single "target tree" is calculated in detail, at up to 120 spatial points for Q, near infrared and thermal wavebands, taking into account the effect of all neighbouring trees. At each of these points, which represent a subvolume of the canopy, transmittance to diffuse and direct radiation is calculated. The former changes only with canopy structure and so is only calculated once, or every few days if leaf phenology is simulated. Transmittance of direct radiation changes with solar position and so is calculated on an hourly time-step. The beam fraction is calculated from the ratio of the measured incident radiation above the canopy to a theoretical value for the same solar position with a cloudless sky. The radiation penetrating to each point is calculated as the sum of the transmitted direct and diffuse components. Stomatal conductance is then calculated at each point from the specified response to Q, temperature and D in the multiplicative model described in Chapter 3 (Jarvis, 1976). Transpiration and photosynthesis are then calculated. Transpiration is calculated using the Penman-Monteith equation in the Omega form (Jarvis and McNaughton, 1986; McNaughton and Jarvis, 1991). Leaf photosynthesis is based on the semi-empirical model of response to Q, temperature and CO_2 described in Chapter 3 (Jarvis, Miranda and Muetzelfeldt, 1985); this was used in preference to the model of Farquhar and von Caemmerer (1982), which is more difficult to parameterise with field data. Values are then integrated to the whole plant by summing over the subvolumes.

Where the target "tree" can be assumed to be representative of the stand, this value can be extrapolated to ecosystem scale by dividing by plant leaf area and multiplying by L_l. This procedure was used for the millet, where each millet pocket was represented with the same dimensions and leaf area. Where the canopy was heterogeneous, several plants were simulated in repeated runs of the model and an average value used. For simulations of *G. senegalensis* at the fallow site, the model was run three times using different bushes as the target tree. The three bushes were selected so as to represent a range of bush sizes, with leaf areas of 1.8, 9.6 and 20 m^2 (mean leaf area per bush was 9.6 m^2). For simulations of tiger bush, the model was run once for each of the three dominant species. A weighted

START

Open and read control and parameter files

Calculate 3D co-ordinates of all plants

START DAILY LOOP

Update leaf area in phenology routine

Calculate leaf area in each subvolume

Calculate diffuse transmittances

START HOURLY LOOP

Read meteorological data

Calculate beam fraction and extinction coefficients for direct radiation

Calculate the weighted path lengths for direct radiation to each grid point

Calculate the amount of radiation absorbed in each subvolume

Calculate the boundary layer, stomatal and mesophyll conductances

Calculate transpiration using Penman-Monteith equation

Calculate leaf photosynthesis and respiration

Calculate stem and soil respiration

Calculate rainfall interception and throughfall

Write out hourly values

END HOURLY LOOP

Write out daily values

END DAILY LOOP

END

Figure 7.1 Flow chart showing MAESTRO program structure.

average of these output values was used, on the basis that *C. nigricans* contributed 15 % of the canopy leaf area and the remainder was divided evenly between *G. senegalensis* and *C. micranthum* (42.5 % each). These proportions were visually estimated, not measured quantitatively.

Woody tissue, root and soil respiration were calculated as exponential functions of temperature (Equation 4.3). These were then subtracted from photosynthesis to give the net CO_2 flux to the ecosystem.

7.2.2 Parameterisation

Leaf-scale measurements of photosynthesis, stomatal conductance and respiration (Chapters 3 and 4) and measurements of leaf area and its three-dimensional distribution (Chapters 5 and 6) were used to derive the physiological and canopy structure parameters. MAESTRO uses four main input files: three containing parameters for the site, canopy structure and physiology, and one for the driving meteorological variables. The parameters contained in these files are listed in Appendix 4.

(1) Site file

The site file (referred to as the "structure file" by Wang *et al.* (1992)) contains various parameters describing the site and some crown properties, including site latitude and longitude, slope, leaf area and angle distribution functions, leaf optical properties, crown shape, canopy and soil hydrological parameters. Several of these were obtained from measurements by co-workers in the HAPEX experiment. Millet leaf angle distribution was measured by P. Lewis and M. Barnsley of UCL (Figure 7.2). Measurements of leaf optical properties were made with a portable custom-built instrument by Fedrico Hahn, University of Edinburgh (Figure 7.3). Latitude and longitude of each site was obtained using GPS by Jake Sudlow of IH.

The model has the capability to simulate physiology and canopy structure in more detail than could be parameterised. For example, the maximum mesophyll conductance can be varied with time to represent seasonal or growth-related changes in leaf photosynthetic capacity. However, such changes were not detected in the data. Different age classes of leaves can be represented, but as all species were either annuals or drought-deciduous, this was not used. Leaf area density can be varied throughout the tree crown as a function of height and radial distance, but was assumed to be uniform. The amount of leaf area was held constant in simulations for comparison with eddy covariance measurements made over eight to nine days (Section 7.4) but the leaf phenology routine was used for simulations of the whole wet season (Section 7.5). Parameters for the soil water balance sub-model were not obtained and it was not used.

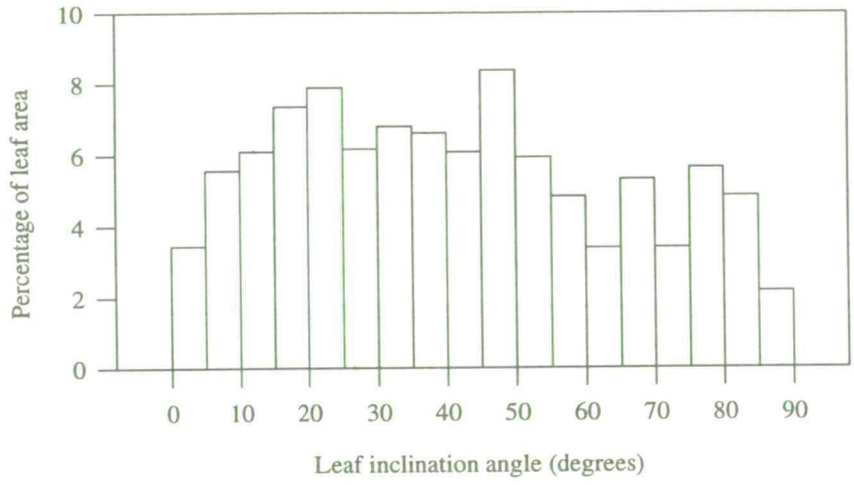

Figure 7.2 Millet leaf angle distribution (courtesy of P. Lewis and M. Barnsley, UCL).

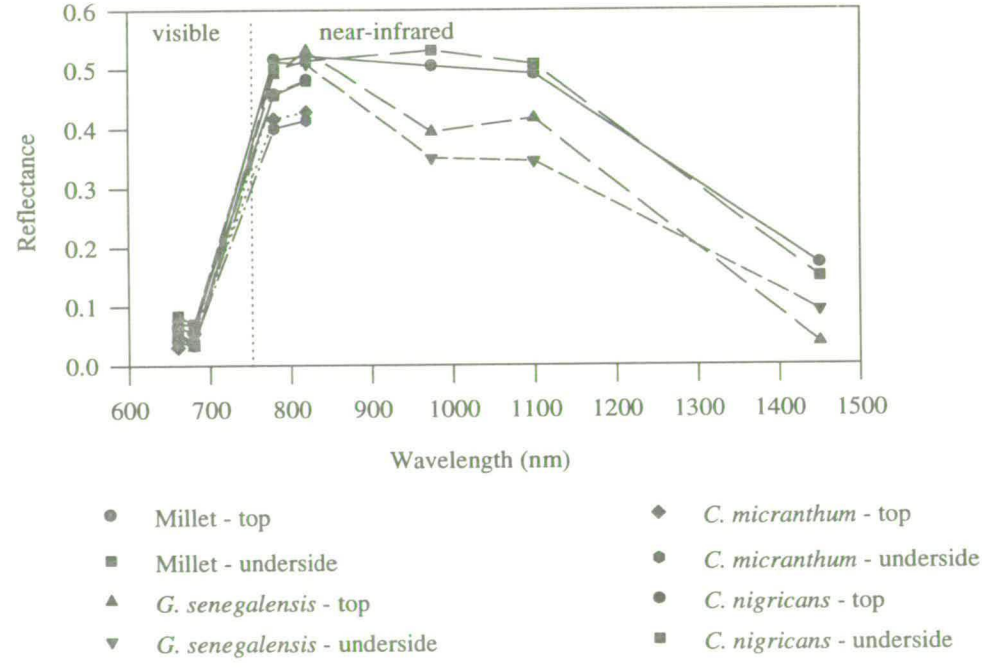

Figure 7.3 Measurements of leaf reflectance (courtesy of F. Hahn).

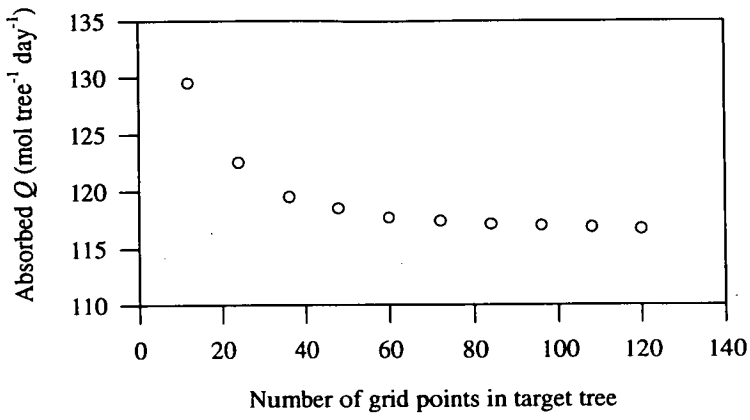

Figure 7.4 Effect of spatial resolution on calculated Q absorption in MAESTRO. 60 grid points were used as a compromise between accuracy and computation time.

Figure 7.4 illustrates the effect of increasing the spatial resolution at which radiative transfer is simulated. Increasing the number of points at which radiation is calculated within the crown decreases the total Q absorbed by the tree asymptotically. This is an artefact of the way in which the points are spread within the crown. Points are grouped into horizontal layers distributed evenly in the vertical dimension, each layer containing 12 points. If only 12 points are specified, a single layer is placed at 0.5 h, where h is canopy height. If 24 points are specified, two layers are placed at 0.66 h and 0.33 h. As the attenuation of radiation is exponential, the amount reaching the lower layer is very much reduced, and the average of the two layers is less than that of a single layer at 0.5 h. This effect becomes negligible when between 60 and 84 points are used. Accordingly, 60 points were used in all simulations as a compromise between accuracy and computation time.

(2) Canopy structure file

The canopy structure file (referred to as "tree file" in Wang *et al.* (1992)) contains co-ordinates, dimensions and leaf area of all plants in the plot. The millet pockets were represented as an array of cones at 1.43 m spacing on a square grid. Each cone was given the same mean dimensions and leaf area, although the measured variability could be represented. In the more heterogeneous canopies of the fallow and tiger bush site, the measurements of shrub dimensions and co-ordinates were used to represent the canopy structure. Each individual was represented as a half-ellipsoid. The canopy structure of the *G. senegalensis* bushes is represented diagramatically in Figure 5.11. The fallow site ground flora was represented as a homogeneous layer beneath the bushes, but was considered to be insignificant at the tiger bush site.

(3) Physiology file

The physiology file contains the parameters for the stomatal conductance, leaf photosynthesis and phenology routines. A number of changes were made to the previously existing physiology routines. A closer fit between the photosynthesis model and the data was obtained if the CO_2 compensation concentration was specified as a fixed parameter instead of as a function of temperature. An exponential decline of stomatal conductance in response to D was found to fit the data better than a linear decrease. Wood respiration was expressed as an exponential function of temperature (using Equation 4.3) on a surface area basis (Chapter 4). Growth respiration was subsumed into the parameters of the temperature function, rather than having an explicit growth term as in Equation 4.4. The parameters were changed according to the growth phase of the vegetation, at approximately monthly intervals. In the absence of any better data, soil respiration at the fallow and tiger bush sites was represented using the results from three days of measurements at the fallow site in late June 1992 (Section 4.8). At the millet site, root biomass estimates were available from the growth experiment plots (Brouwer *et al.*, in prep.). These estimates were used to estimate root respiration using the parameters derived from measurements of leaf respiration (Section 3.3).

(4) Meteorology file

The following meteorological variables are required on an hourly basis: windspeed, soil temperature, air temperature, relative humidity (RH), solar radiation, photosynthetic photon flux density (Q) and precipitation. These data were obtained from the weather station described in Appendix 2, located on or nearby the micrometeorological mast (Figures 2.4-2.6). For some periods, a complete set was not available because of instrument failure (mainly the psychrometer wet bulb drying out) and records from the IH weather station were used (courtesy of C. Lloyd and C. Holwill, IH).

7.3 Big leaf model

So called "big leaf" models simulate the canopy as if it were like a single large leaf (Daudet and Tchamitchian, 1993). That is, it consists of a single plane surface which is uniform in the horizontal and vertical dimensions. In a canopy of randomly distributed elements, radiative transfer is generally assumed to obey Beer's Law, which, by rearranging Equation 6.1, can be written as:

$$Q_{abs} = Q_{in} \ (1 - \exp(-K \times L_l) - \rho) \qquad [7.1]$$

where K is the extinction coefficient and ρ is the reflection coefficient in the photosynthetic waveband. This is clearly a very simple model, with only three parameters describing the canopy and in which direct and diffuse radiation are considered together. As discussed in Section 6.1, K can be considered as a theoretical function of leaf angle distribution and solar zenith angle (Campbell, 1986; Monteith

and Unsworth, 1990), or as an empirically derived constant (France and Thornley, 1984). As the theory relating K to other variables makes several assumptions about leaf area distribution, the latter approach was used. The measurements of transmitted Q described in Chapter 6 were used to estimate values for K at the three sites. Values of ρ were estimated from the data in Figure 7.3. The model uses the same physiology routines as MAESTRO and uses the same hourly Q and T_a data as inputs.

Table 7.1 Parameters used in the big leaf model (Equation 7.1). L_l is the leaf area index, K is the extinction coefficient and ρ is the reflection coefficient in the photosynthetic waveband.

	Millet	Fallow	Tiger bush
L_l	0.46	Bushes: 0.31 Ground flora: 0.36	0.7
K	0.67	0.58	0.56
ρ	0.05	0.03	0.03

7.4 Model Validation

7.4.1 Methods - Ecosystem CO_2 flux measurement by eddy covariance

Eddy covariance measurements were made during the IOP in 1992, and the models were configured to simulate each site over the measurement period. At the tiger bush site, the vegetation was senescing during this period and comparison with the models is only made between 29th September and 7th October (DOY 273-281) to coincide with the L_l estimate made on DOY 275.

Half-hourly fluxes of net ecosystem CO_2 exchange at the three sites were measured using one closed path and two open path eddy covariance systems. At the millet site, an eddy covariance CO_2 system was mounted at a height of 9 m above the ground, with a fetch over millet of ~1500 m in all directions, except for a thin strip of fallow land about 400 m away to the south and west (Figures 2.3 and 2.4). At the fallow site, the eddy covariance CO_2 system was mounted on a mast at a height of 9 m above the ground, with a southerly fetch of ~ 400 m (Plate 2, Figure 2.5). A third eddy covariance CO_2 system at the tiger bush site was mounted on a tall tower at 18 m, with a fetch of at least 1 km in all directions (Plate 3, Figure 2.6). The source area model of Schuepp *et al.*, (1990) showed that fetches were adequate at all the sites. Under normal daytime conditions at the millet and fallow sites, around 90 % of the signal measured at 9 m came from within 400 m of the masts.

Between mid-August and mid-October 1992, the eddy covariance measurement systems were run at two sites simultaneously by a team comprising J.B. Moncrieff, S.L. Scott, J.M. Massheder and P.G. Jarvis, with one of the sites having both a closed and an open path system for comparison of the two methods. Severe problems were encountered with the CO_2 flux measurements from the open path system (drift of calibrations, very noisy signal) and the data have not been used. Only data from the

closed path system are discussed here. Nine days of measurements were obtained at the fallow site between 27th August and 4th September (DOY 241 to 249). *G. senegalensis* L_l was estimated to be 0.314 and the ground flora 0.36 (total site L_l of 0.674) (Chapter 5). A rain storm occurred on DOY 242 and which apparently caused erratic eddy covariance measurements which were discarded. Nine days of measurements were obtained at the millet site between 5th and 12th September (DOY 249 to 257). The crop had begun to sénesce by this time, and the green L_l was estimated to be 0.46 (Chapter 5). Twenty seven days of measurements were obtained at the tiger site between 13th September and 8th October (DOY 257 to 284). L_l estimated from hemispherical photographs during this period was 2.1 within the vegetated areas or 0.7 averaged over the whole site (Chapter 6).

The closed-path system was developed within a consortium of European laboratories and is fully described elsewhere (Moncrieff *et al.*, in press). EddySol software was used to provide real-time and continuous monitoring of CO_2 flux and mean atmospheric concentration of carbon dioxide. Raw fluxes were corrected for density fluctuations (Webb *et al.*, 1980; Leuning and Moncrieff, 1990), separation of the sensors (Moore, 1986) and attenuation of the signal down the tube (Leuning and Moncrieff, 1990). Analysis reported in Moncrieff *et al.* (in press) shows that a fraction of the high-frequency signal is lost in the closed-path system because of "tube smearing". However, the theory of Kaimal *et al.* (1972) predicts the cospectral density function for a perfectly responding eddy covariance system, and by comparison with the Kaimal cospectrum and employing a transfer function, the "true signal" can be reconstructed. The transfer functions depend on variables such as wind speed, thermal stability, height of sensor above the zero-plane etc. In general, the flux losses were less than 15 %. A storage term to account for changes in the CO_2 content of the air within the ecosystem was not used, as the canopies were all well coupled to the atmosphere and such a term would be negligible.

7.4.2 Results

Millet

Figure 7.5 shows very close agreement between the measured fluxes and model predictions. Differences between the two models are hardly discernible, the big leaf model predicting a very slightly higher peak flux. The models predicted a similar pattern for each of the simulated days, as the diurnal course of radiation, temperature and humidity was similar throughout the measurement period. The increase in D between days 251 and 253 was not reflected in the measurements, although the models predicted a sharper decline in the afternoon of day 253 relative to day 252 (the course of radiation is the same on both days). The relatively low fluxes measured on days 252 and 254 cannot be accounted for in terms of the measured environmental variables. Model predictions of night-time respiration were reasonable, although on average, they underestimated by about 1 μmol m^{-2} s^{-1}. Measured night-time fluxes were very variable relative to the model predictions of an almost constant nocturnal flux.

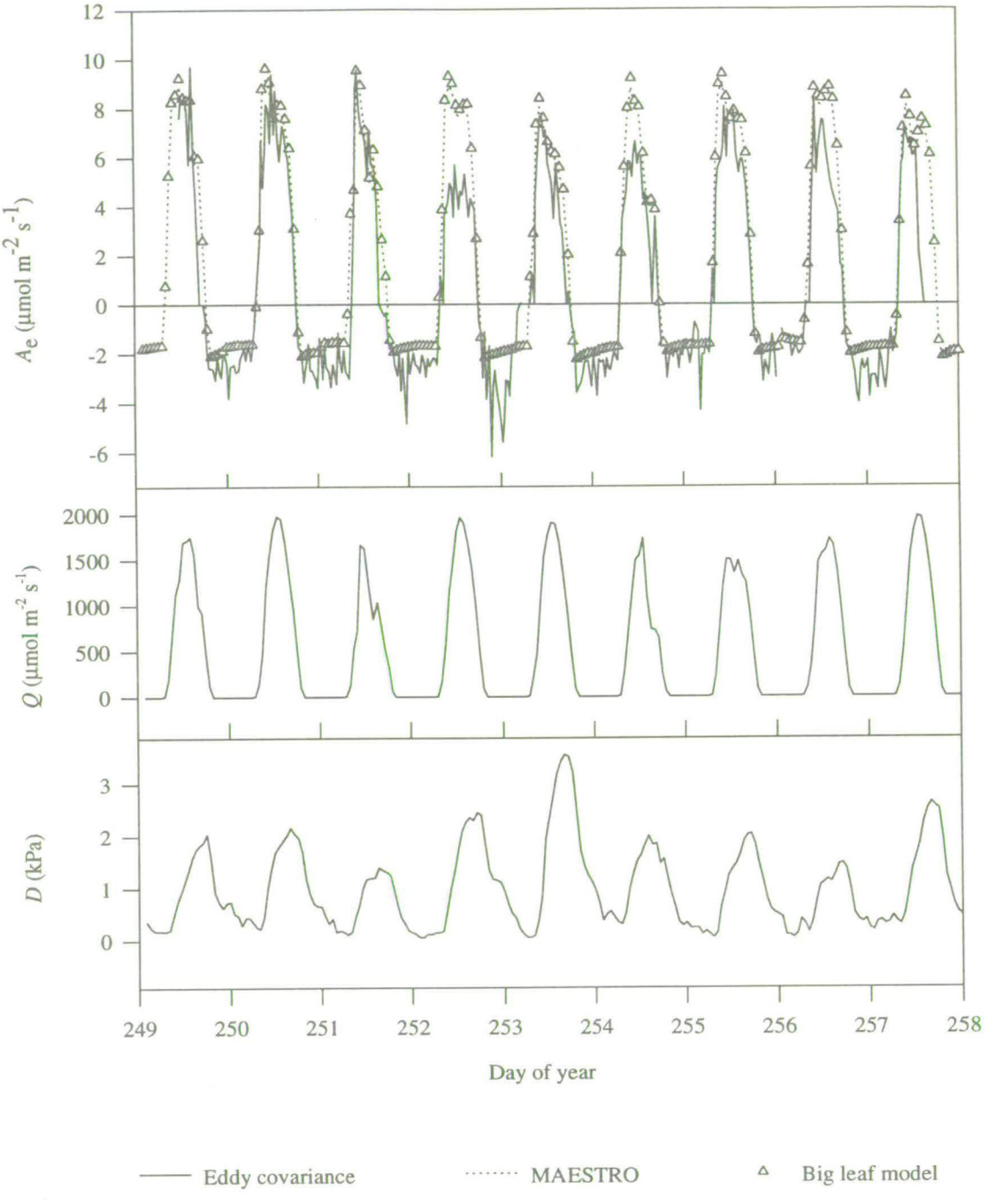

Figure 7.5 Comparison of eddy covariance measurements and model predictions of ecosystem CO_2 flux, A_e, at the millet site for the period 5 to 12 September 1992.

Fallow

Again, there was good agreement between measurements and model predictions at the fallow site (Figure 7.6). Predictions from the big leaf model were close to the measurements, and did not show a clear systematic deviation from the measurements. Predictions from MAESTRO were also close to the measurements, and the predicted peak daytime fluxes were very similar on two days (244 and 245), although they were around 1 to 2 μmol m^{-2} s^{-1} lower than measurements on four days (243 and 246 to 248).

The measurements show a response to the lower radiation on day 243, which appears to be exaggerated by the models. A photosynthetic response of the vegetation to water supply may be seen in the data, as the vegetation became more active after rain on 28 and 30 August (days 241 and 243). This is not simulated well by the model, possibly because the rain has a longer term influence via leaf water status, which was not measured, as well as the effect on *D*. A similar result was found by Kim and Verma (1990, 1991) in temperate grassland, where the measured increase in canopy photosynthesis after rainfall was not simulated well by their model. Night-time fluxes were overestimated by the models by about 1 μmol m^{-2} s^{-1} on six nights and more or less agree with measurements on three nights. Again, measured night-time fluxes were much more variable than the models predicted.

Tiger bush

Figure 7.7 shows that the hour to hour variability in measured fluxes was much greater at the tiger bush site, although the course of radiation, temperature and humidity was very similar on each day. Ignoring the extreme values in the data, the magnitude of daytime fluxes predicted by the big leaf model agreed well with measured values, whilst MAESTRO consistently underestimated by 1 to 2 μ mol m^{-2} s^{-1}. The diurnal course is confused by noise on several days (particularly days 277 and 279) but an asymmetrical pattern similar to that seen in the conductance data (Section 3.4) is detectable, in which the flux peaks at around 0900 h and declines thereafter (eg. on days 274, 275, 278 and 280). This pattern is simulated reasonably well by the models. Night-time fluxes are again very variable and appear to be overestimated by the models, but it is difficult to say where the true mean of the nocturnal flux lies.

A more rigorous comparison is obtained by plotting model predictions of CO_2 flux against eddy covariance measurements (Figure 7.8). The errors in model predictions in millet do not deviate systematically from the measurements (Figure 7.8(a)). MAESTRO tended to slightly overestimate in fallow below about 7 μmol m^{-2} s^{-1}, but underestimated beyond this point, whilst the big leaf model did not deviate systematically from the measurements over the whole range (Figure 7.8(b)). At the tiger bush site, MAESTRO generally underestimated by a roughly constant proportion over the whole

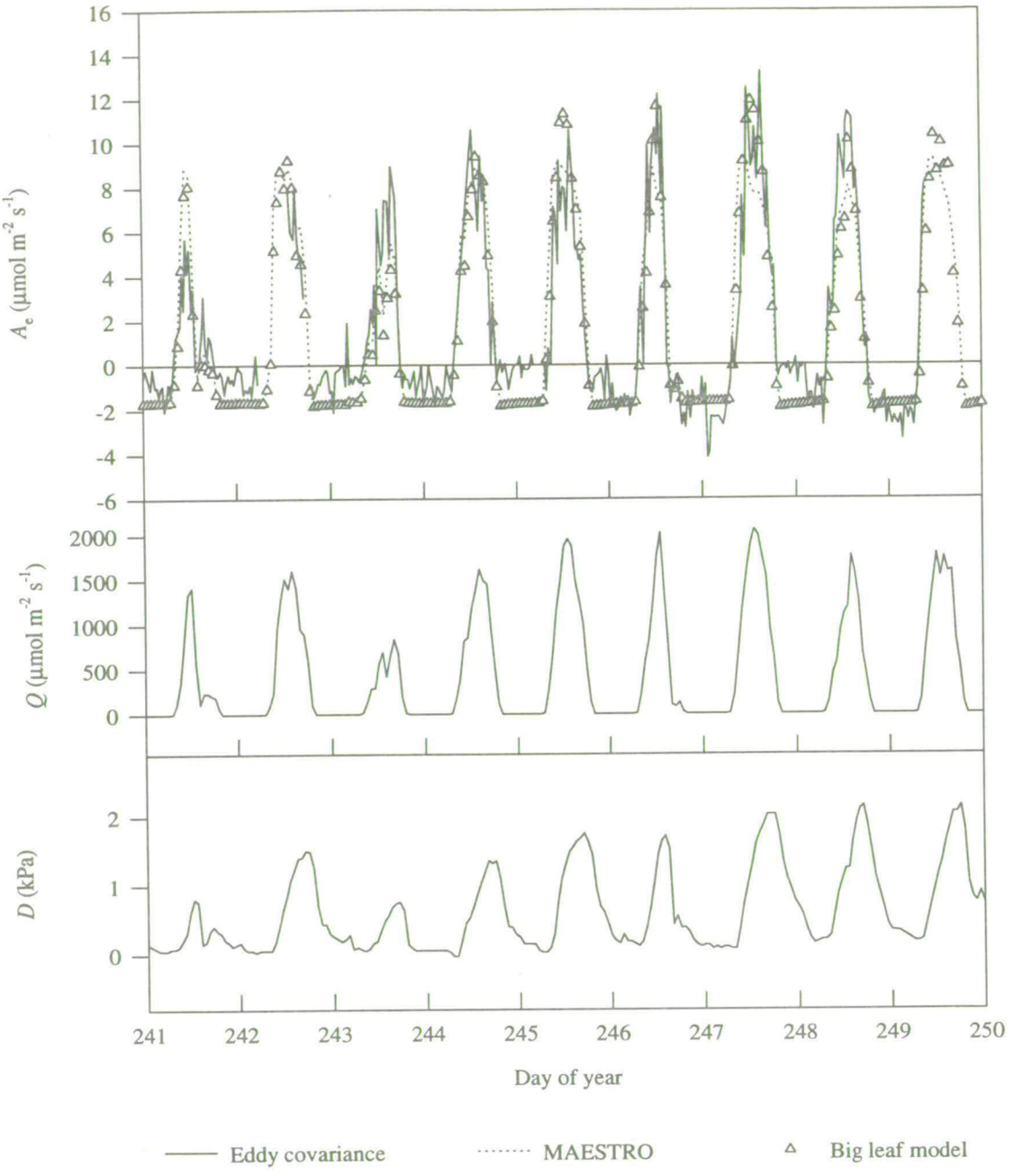

Figure 7.6 Comparison of eddy covariance measurements and model predictions of ecosystem CO_2 flux, A_e, at the fallow site for the period 27 August to 4 September 1992.

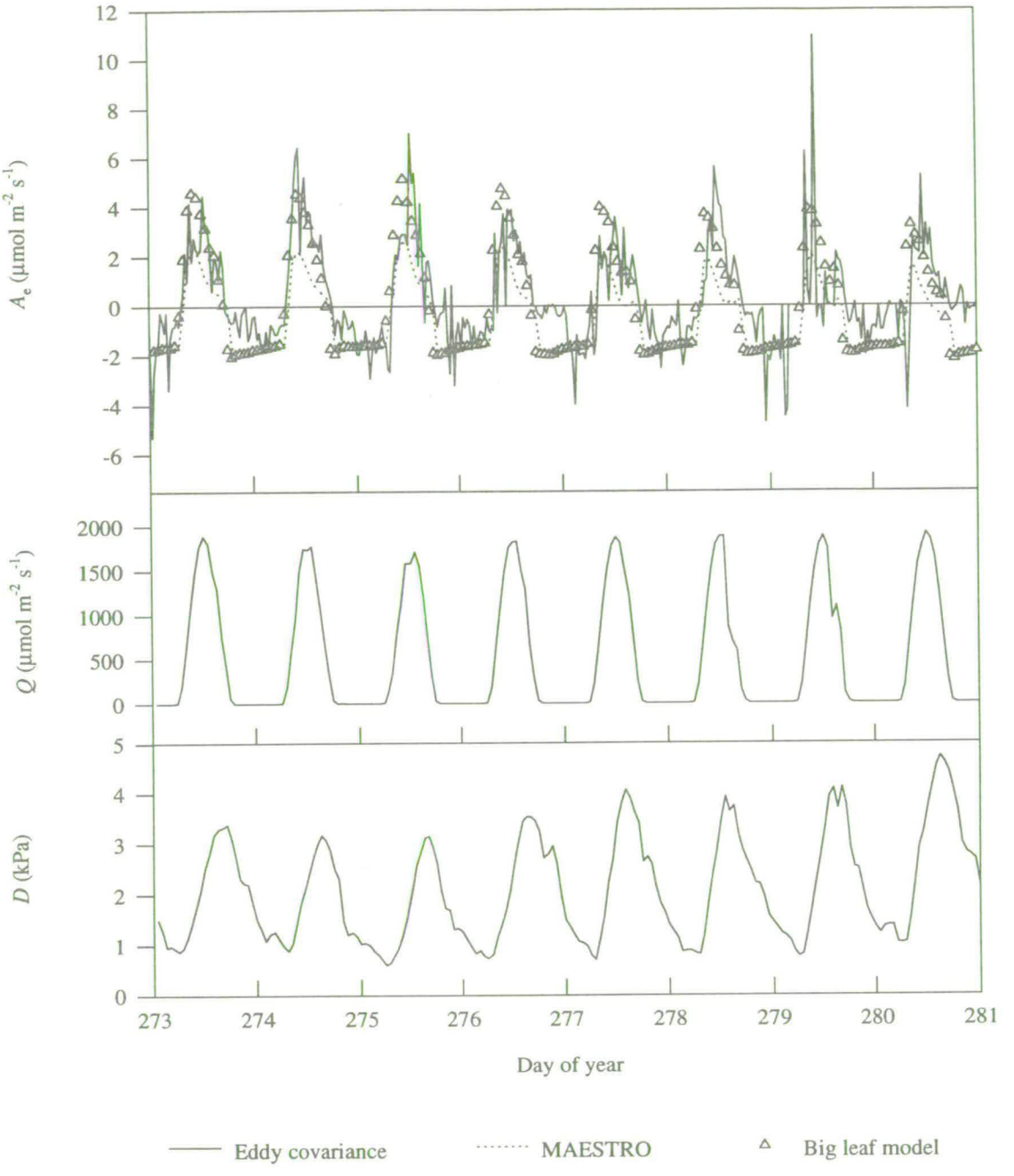

Figure 7.7 Comparison of eddy covariance measurements and model predictions of ecosystem CO_2 flux, A_e, at the tiger bush site for the period 1 to 8 October 1992.

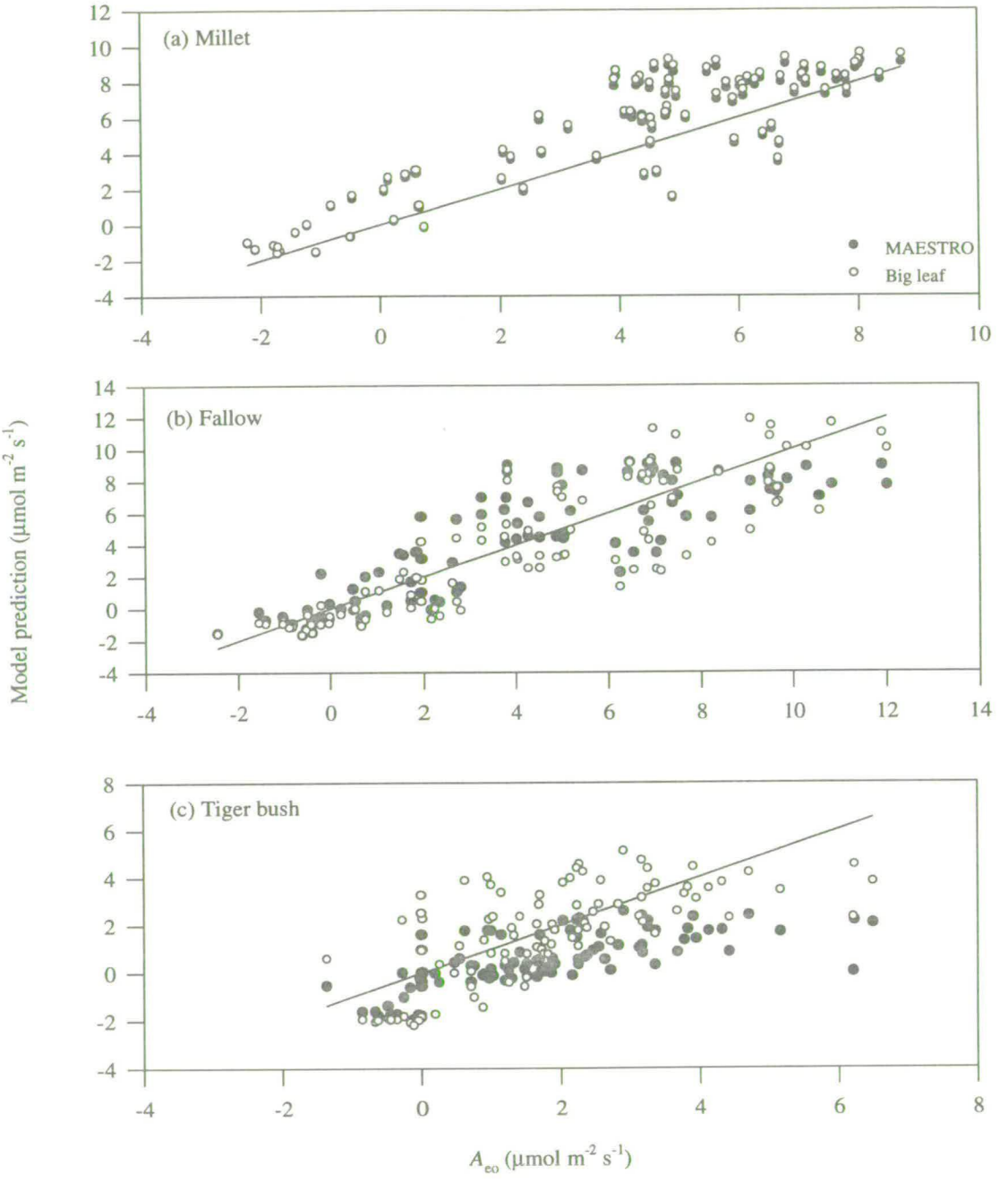

Figure 7.8 Plots of MAESTRO and big leaf model predictions of daytime CO_2 flux against observed values, A_{eo}, measured by eddy covariance for the three sites. Data cover the same periods as in Figures 7.5-7.7. 1:1 lines are shown.

range, whilst the big leaf model overestimated low values and underestimated high values (Figure 7.8(c)). Linear regression between MAESTRO predictions and eddy covariance measurements showed close linear relationships, giving r^2 values of 0.91, 0.84 and 0.71 for the millet, fallow and tiger bush sites, respectively, indicating that the model accounted for most of the variation in the measurement data when systematic error was removed. Linear regression between big leaf model predictions and eddy covariance measurements gave very similar values of r^2 (0.91, 0.85 and 0.68). The decrease in the r^2 values from millet to tiger bush follows the increase in canopy heterogeneity.

Figures 7.9a-c show plots of residuals (the difference between MAESTRO predictions and eddy covariance measurements) against environmental variables. In millet, there is a tendency for MAESTRO to overestimate A_e when D and T_a are high, as the residuals are skewed on these plots (Figure 7.9a). This may be related to the inadequacies of the stomatal conductance model and the limited fit of the data to it (Chapter 3). In the fallow and tiger bush data sets, no strong relationships are present between the residuals and any of the environmental variables. However, particularly in the tiger bush data, a relationship is found with A_{eo}, which could be caused by a systematic error such as an underestimation of L_t. Notably, there is no clear relationship between the residuals and wind direction at any of the sites.

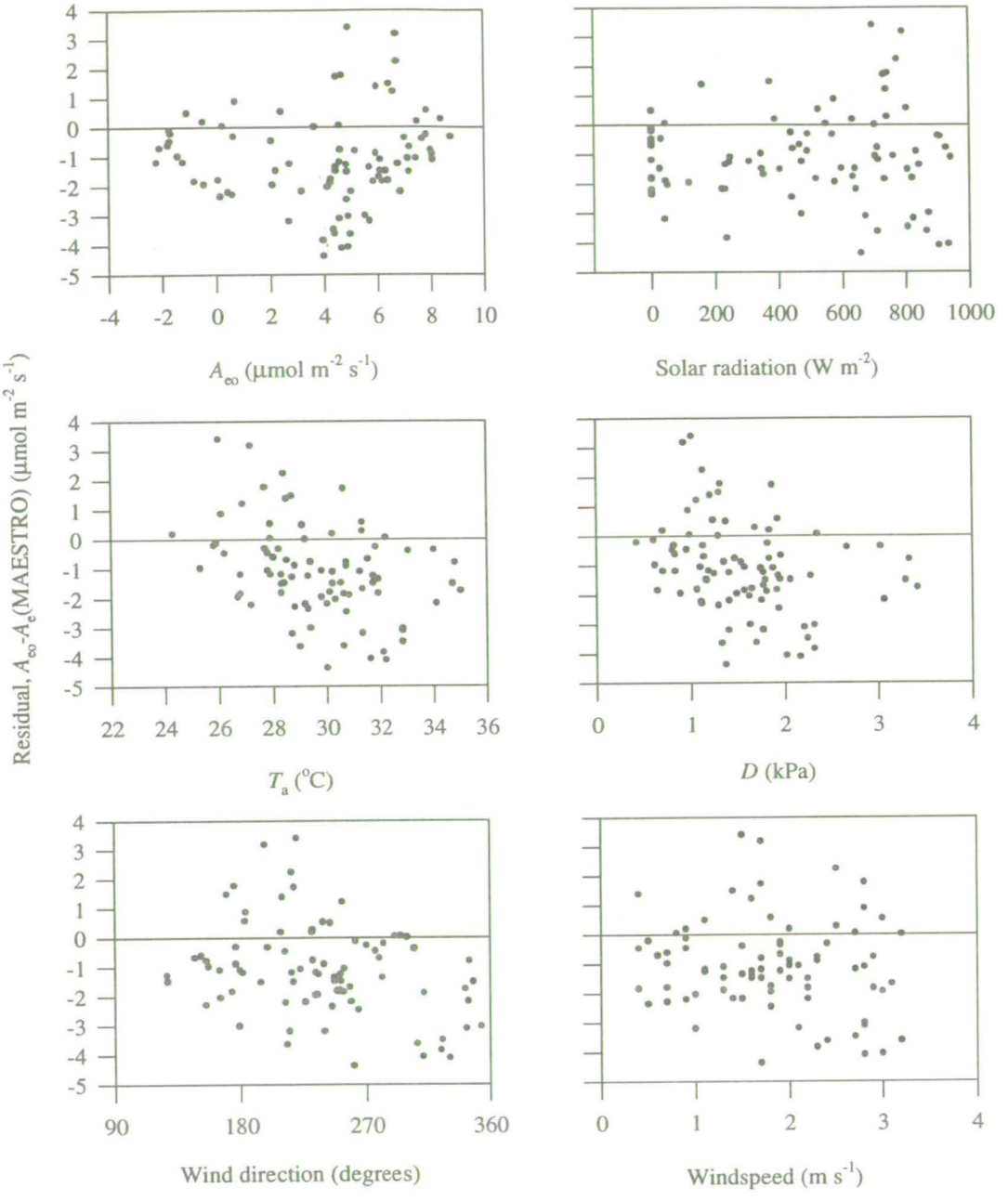

Figure 7.9a The distribution of residuals (the difference between MAESTRO predictions of daytime ecosystem CO_2 flux, A_e(MAESTRO), and values measured by eddy covariance, A_{eo}) in relation to A_{eo} and environmental variables for the millet data set.

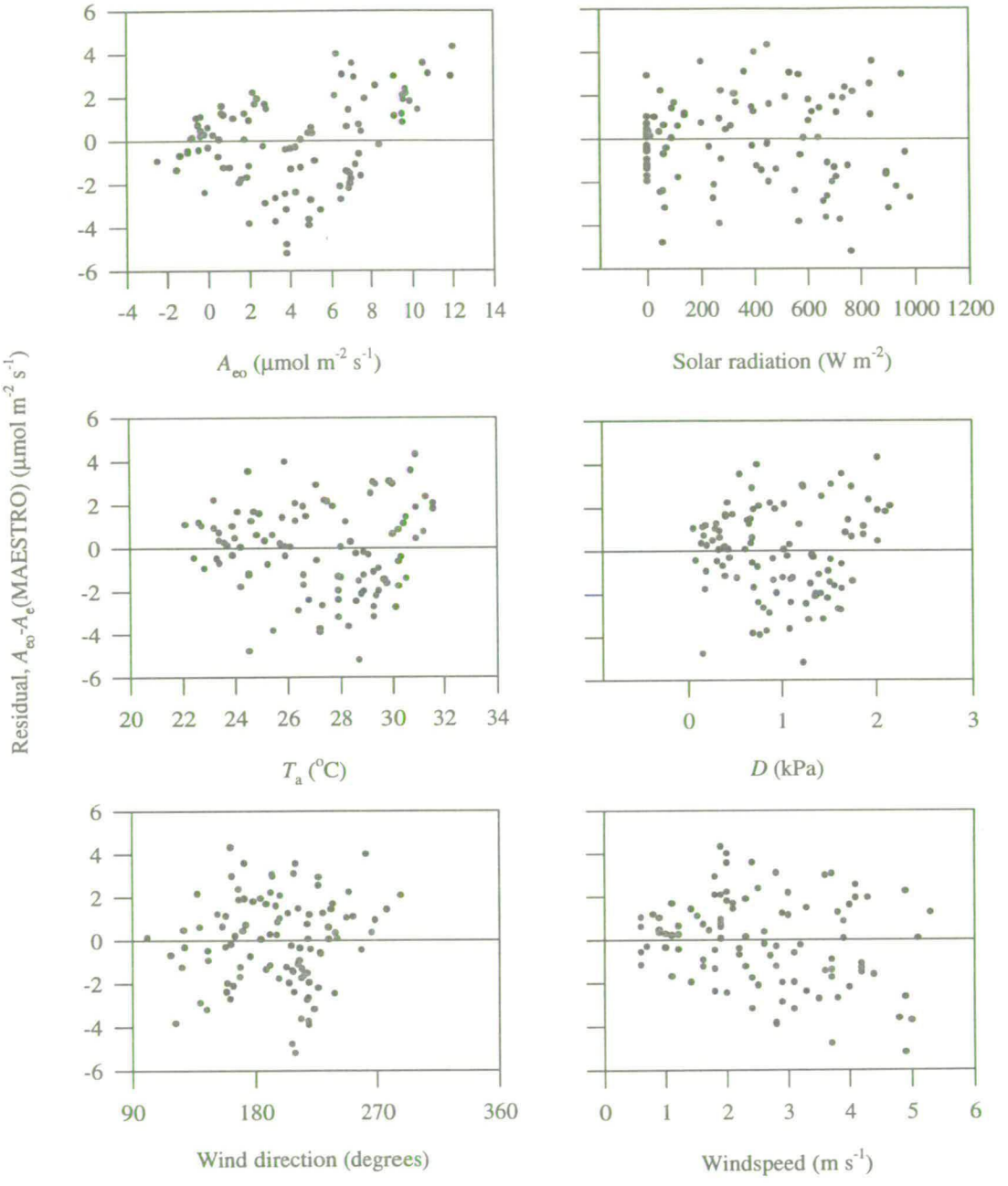

Figure 7.9b The distribution of residuals (the difference between MAESTRO predictions of daytime ecosystem CO_2 flux, A_e(MAESTRO), and values measured by eddy covariance, A_{eo}) in relation to A_{eo} and environmental variables for the fallow data set.

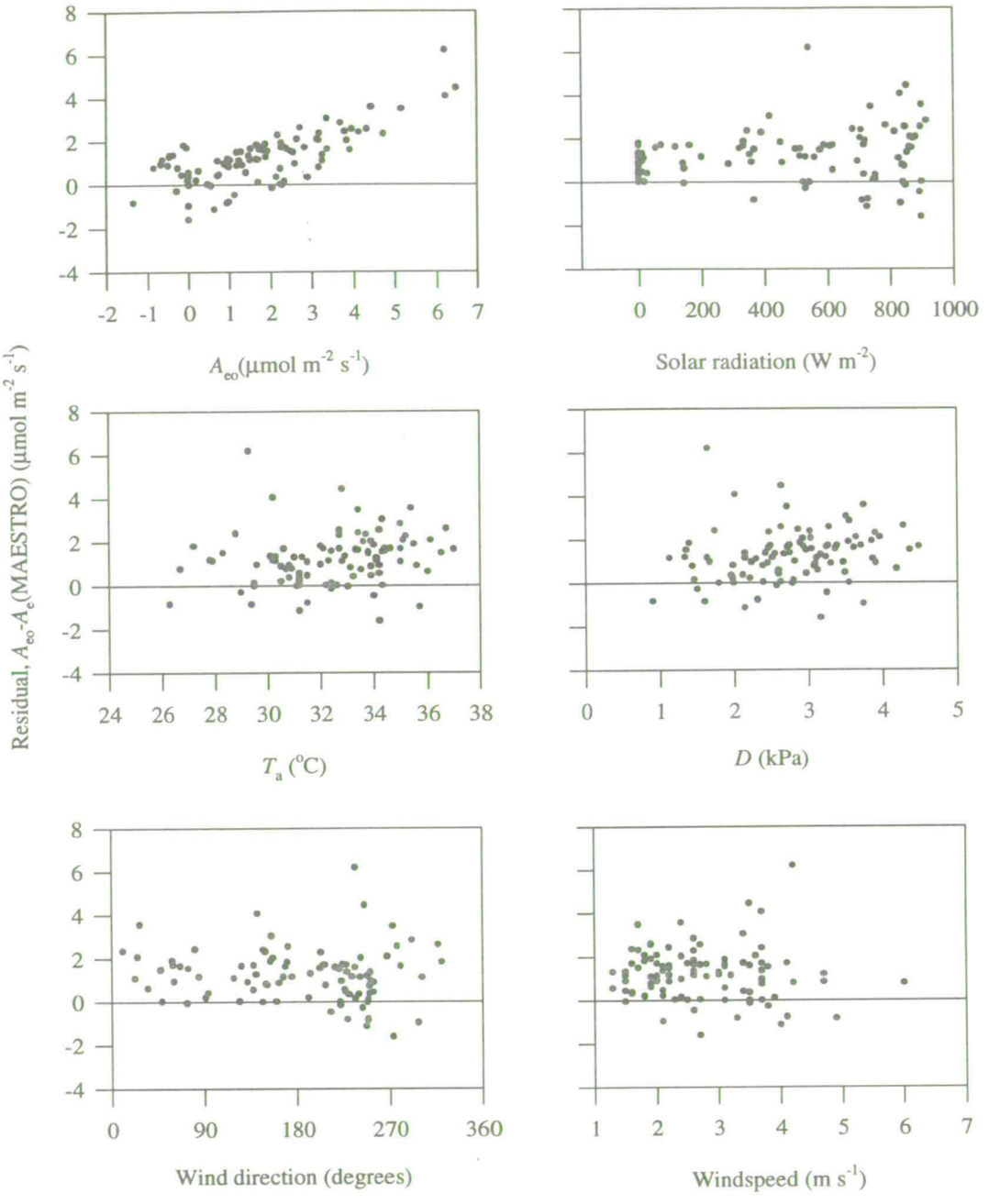

Figure 7.9c The distribution of residuals (the difference between MAESTRO predictions of daytime ecosystem CO_2 flux, A_e(MAESTRO), and values measured by eddy covariance, A_{eo}) in relation to A_{eo} and environmental variables for the tiger bush data set.

7.4.3 Discussion

Variability

The larger variability in measurements relative to model predictions at the fallow and, particularly, the tiger bush sites is presumably because the models simulate a single patch, whilst the area measured by eddy covariance changes as the "flux footprint" changes with wind speed and direction. The differences amongst the areas being sampled are largest in tiger bush, and as the footprint changes, the L_l of the area sampled may range from zero to 4 or 5 (Chapter 6). The short-term variability in A_e is much less at the millet site, as the canopy is much more homogeneous.

Night-time fluxes

Night-time data are considerably more variable than daytime data at all sites, relative to model predictions. Other workers have found similar variability in night-time fluxes (eg. Hollinger *et al.*, 1994; Amthor *et al.*, 1994; Grace *et al.*, 1995), which in forests has been attributed to storage within the canopy air space. When there is little turbulent mixing because of low horizontal windspeed and/or atmospheric stability, CO_2 may build up in the air space below the sensor, and this CO_2 is only sporadically flushed out by large, infrequent eddies (Fitzjarrald and Moore, 1990). However, accounting for storage often does not remove this variability, and there is as yet no consensus on how such phenomena affect the measurement and interpretation of night-time fluxes.

The consistent underestimation of the night-time millet fluxes may be because the respiration of above-ground parts is based on the measurements made on leaves and extrapolated to include culm area. However, there may be a substantial mass of living cells within the volume of the culm, and so the respiration rate of the culm may be higher when expressed on a surface area basis.

Accuracy of predictions

The models predict the magnitude of fluxes at the millet site more accurately than at the fallow or tiger bush sites, irrespective of the difference in variability in the measurements. This is likely to be for two reasons. Firstly, the A_l-Q response is close to linearity, as discussed in Sections 3.4. Secondly, the measurement of canopy properties was considerably easier at the millet site than at the other sites. The millet canopy was relatively uniform at a scale of tens of metres and has a regular structure, allowing the biomass, leaf area and its spatial distribution to be measured accurately. The measurement of the amount and distribution of leaf area in the irregular canopies found in natural ecosystems is one of the most difficult tasks involved in this approach.

A tendency for models to overestimate fluxes in the afternoon has been observed in some studies (eg. Amthor *et al.*, 1994) and has been attributed to various phenomena, such as stomatal closure because of entrained rhythms or feedback inhibition of photosynthesis caused by carbohydrate accumulation in

the afternoon. However, the fluxes measured in the afternoon were not lower than model predictions, and in the case of the tiger bush, MAESTRO tends to underestimate more in the afternoon than in the morning.

Comparison of MAESTRO and big leaf model

Figures 7.5 and 7.8(a) show that MAESTRO and the big leaf model give almost identical values for CO_2 fluxes at the millet site. Clearly, canopy photosynthesis calculated using the range of Q absorbed by leaves in the 60 subvolumes simulated by MAESTRO is the same as canopy photosynthesis based on the total absorbed Q. This result is very similar to the result obtained by Sinclair, Murphy and Knoerr (1976), in which a big leaf model predicted photosynthesic rates in a maize crop to within 5 % of a sophisticated 2-D multi-layer model. Close agreement was also found between MAESTRO and the model BIOMASS, which is similar in principles to the big leaf model described here, except that it has a daily time step (Wang, McMurtrie and Landsberg, 1992; Wang and McMurtrie, 1993). Over a range of values of L_l between 1 and 9, little difference was found between daily canopy photosynthesis predicted by the two models on clear days, and differences were not more than about 10 % on cloudy days. Kruijt *et al.* (1995) compared predictions from MAESTRO and a big leaf model, and found good agreement at an L_l of 7, but the big leaf model increasingly overestimated absorbed Q as the leaf area distribution became more heterogeneous, and as L_l decreased.

The similarity in results from MAESTRO and the big leaf model for millet has two implications:

(1) The Beer's Law equation in the big leaf model adequately predicts the amount of radiation absorbed by the canopy, and so the implicit assumption of spatial homogeneity is reasonable. This is perhaps not surprising as the effects of clumping and leaf angle distribution should be accounted for by using the empirically derived value of K, which is based on measurements of how much Q is actually transmitted through a section of canopy with known L_l.

(2) The photosynthetic response of leaves in the canopy to Q can be approximated as linear. Figure 3.3 shows that the response is indeed close to linear, especially if $g_s > 200$ mmol m^{-2} s^{-1} and is $Q < 1500$ μmol m^{-2} s^{-1}, as it would be in most of the simulated canopy subvolumes.

Figures 7.6 and 7.8(b) show that MAESTRO and big leaf model predictions of fluxes at the falllow site do not differ systematically, except that the big leaf model tends to predict higher peak fluxes. This suggests that the assumptions of the big leaf model hold reasonably well in the fallow vegetation as well as in millet. Presumably, this is because the ground flora component, which dominates the flux, forms a relatively homogeneous layer and the fitted A_l-Q response is close to linear in *E. tremula*. Differences between predictions from the two models are larger than at the millet site, but these differences are not systematic, and the complexity of MAESTRO does not produce a more accurate prediction.

The big leaf model predicts higher fluxes than MAESTRO at the tiger bush site. The difference may arise from the assumption made about the distribution of Q in the big leaf model. All three species represented at this site are C3, and have distinctly non-linear photosynthesis A_1-Q response curves, saturating at around 500 μmol m^{-2} s^{-1} (Figures 3.5 to 3.7). Using a single value for absorbed Q rather than the 60 values calculated by MAESTRO as the input to the photosynthesis model will tend to give an overestimate of the ecosystem flux. Also, because of the spatial heterogeneity, there may be considerable sampling error in the estimate of K. If the estimate were too high, the predicted Q absorbed by the canopy would be higher and so the predicted ecosystem photosynthetic rate would be higher. However, this seems unlikely, as the transects did not pass through the densest patches of vegetation, as they were effectively impenetrable, and so there was a bias in the measurements which would tend to reduced the estimate of K.

To test this, a sensitivity analysis was carried out on the big leaf model. Each parameter was varied over the likely range of possible values, with the other two parameters held constant at the values listed in Table 7.1. The results shown in Figure 7.10 show that the big leaf model predictions are not very sensitive to either K or ρ over the likely range of variation. The relatively large uncertainty in L_1 has a greater effect on model predictions, but this was the same in both models.

MAESTRO would be expected to be more accurate than the big leaf model at the tiger bush site as the assumption of canopy homogeneity is obviously not met. However, the big leaf model predictions are closer to the measurements, whilst MAESTRO underestimates the CO_2 flux. It may be that the better fit of the big leaf model is merely fortuitous, and the underestimation by MAESTRO is caused by error in the L_1 estimate and canopy structure parameters. Most errors in the hemispherical photograph method for determining L_1 are caused by clumping of canopy elements and lead to underestimation of L_1 (Chapter 6). Also, the description of canopy structure was based on a very small number of measurements (Chapter 5), and is not expected to be very accurate. However, with a canopy as heterogeneous as that of the tiger bush, there is a very real problem in finding representative parameter values by any direct means.

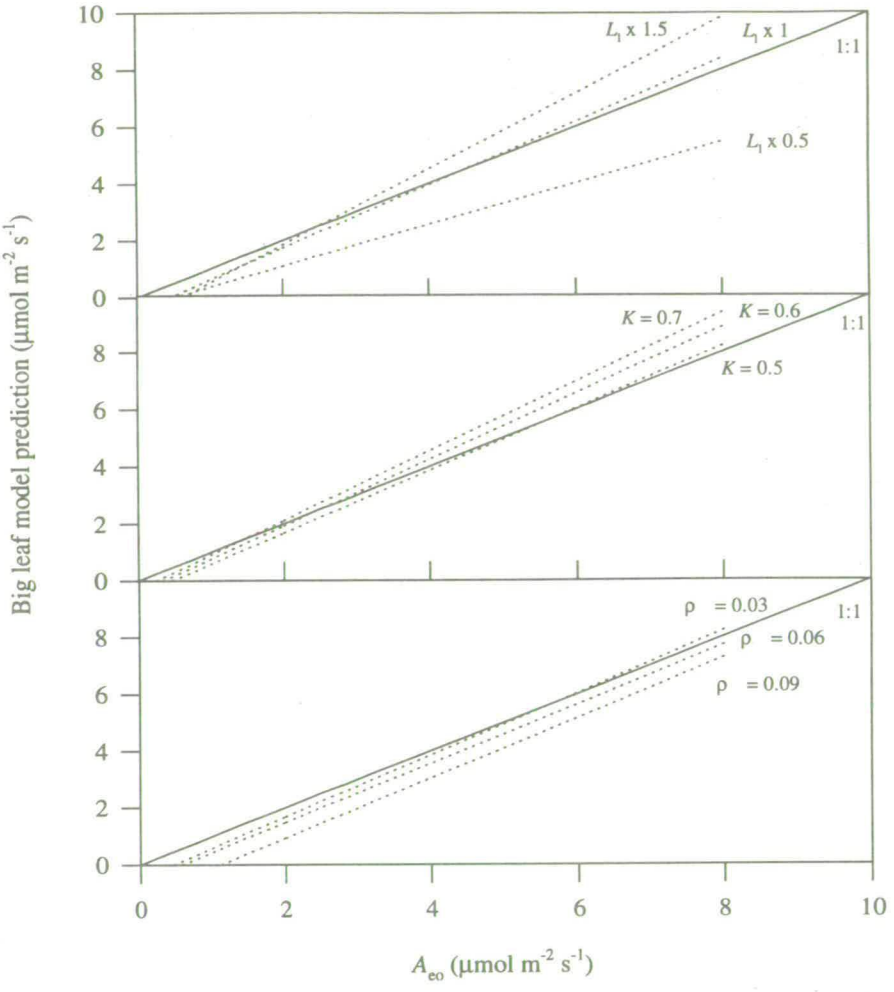

Figure 7.10 Sensitivity analysis of the big leaf model predictions of ecosystem CO_2 flux at the tiger bush site. Except where shown, parameter values were as listed in Table 7.1. Predictions were regressed against observed values from eddy covariance measurements, A_{eo}, to produce the summary lines shown. The model is relatively insensitive to the K and ρ parameters. Model predictions are influenced more by the relatively large uncertainty in L_1.

7.4.4 General points and conclusions

Comparison with model predictions is potentially a useful tool for analysing ecosystem measurements, in that the model represents what should be happening according to our current understanding. The comparison represents a test of this understanding. For example, the discrepancy between the very constant night-time fluxes in the model and the very variable fluxes measured highlights a phenomenon which requires explanation. Unfortunately, the models could only be tested under a rather limited range of conditions, as the course of environmental variables was rather similar on all days during the period of eddy covariance measurements. The models could be tested more rigorously

if ecosystem flux data were obtained over a greater portion of the growing season and preferably part of the dry season.

Although the models appear to simulate ecosystem fluxes with reasonable accuracy, they do have weaknesses concerning processes which are known to occur but difficult to quantify given the logistical constraints. These may become more significant when extrapolating to more stressful environmental conditions (particularly in the early and late stages of the growing season). No below-ground interactions are simulated. On time scales of hours to a few days, there is likely to be a response of stomatal conductance to water availability, most noticeably after rain events. Although rain events will be reflected to some extent in changes in D, the time scales are quite different and the associated stomatal changes will not be captured in the model. Whether this response is generally mediated by leaf water potential or by root-shoot signals (which may generate more complicated feedforward responses) is still the subject of research (eg. Davies and Zhang, 1991; Schurr, Gollan and Schulze, 1992).

Other than the simulation of the Q distribution and wind profile within the canopy, no microclimatic variation is represented. The model was originally developed primarily for use in temperate forest canopies, which are aerodynamically rough surfaces and so tend to be well coupled with the atmosphere (Jarvis and McNaughton, 1986). In these conditions, profiles of air temperature, CO_2 and water vapour concentrations within the canopy can be assumed to be neutral, and leaf temperature can be assumed to be the same as air temperature. However, in the tropical crop and shrub canopies studied here, the errors introduced by making these assumptions may be substantial. However, respiration is the only process represented which has a temperature sensitivity, as effects of temperature on photosynthesis and stomatal conductance were not detected, partly because of the strong correlation with humidity. The modelling work of Sinclair *et al.* (1976) showed that simulating the CO_2 and water vapour concentration gradients that occur within a maize canopy only changed results by 5 %.

Very few such comparisons between measurements of CO_2 flux and models have been made, largely because the eddy covariance technique only became practicable in the 1980s with the advent of fast-response IRGAs. Few have tackled the problem of canopy heterogeneity, or compared ecosystem fluxes with models parameterised using leaf fluxes measured in the same canopy. However, in the comparisons which have been made, using parameters obtained from the literature, reasonable agreement has generally been obtained. Baldocchi, Verma and Anderson (1987) and Baldocchi (1993) compared ecosystem fluxes measured over soybean and temperate deciduous forest with a model similar in many respects to those used here, except that radiative transfer was simulated very simply using a negative binomial expansion to take account of foliage clumping. The big leaf

approach was used by Amthor *et al.* (1994) in temperate oak-maple forest, and the fit between predictions and observations was similar to that obtained here. The canopy was described as heterogeneous, but as it was a closed canopy with an L_t of 3.5, it may have met the assumptions of the big leaf model rather better than the sparse canopies studied here. Their result, that the big leaf model accounted for the non-linearity of the A_t-Q response, was ascribed to acclimation, although there were no measurements to confirm this. Very good agreement between a big leaf model and ecosystem measurements was obtained by Kim and Verma (1991) in temperate grassland in the FIFE experiment. This canopy was similar to those at the millet and fallow sites described here, as it was relatively homogeneous and dominated by C4 grasses (82 %), although L_t was higher, peaking at 3. These factors, and the use of leaf fluxes measured within the same canopy to parameterise the model, may explain the close fit with measurements.

Conclusions

In the case of MAESTRO, the model simulates the magnitude and features of the diurnal curve at the millet and fallow sites very accurately. At the tiger bush site, MAESTRO underestimates by an average of around 1 μmol m^{-2} s^{-1}. This is a small absolute error but large in comparison with the magnitude of the measured ecosystem fluxes. However, as the model simulates the shape of diurnal curve reasonably well, it seems likely that the discrepancy is related to the considerable uncertainty in the L_t parameter. We conclude that, on the whole, our understanding of leaf-scale CO_2 flux in terms of Q, temperature and conductance and the within-canopy distribution of these respresented in MAESTRO is satisfactory.

In the case of the big leaf model, the agreement at the millet and fallow sites is again excellent. The better agreement at the tiger bush site, relative to MAESTRO, is unexpected. However, the related problems of variability in the ecosystem flux data and uncertainty in L_t estimates caused by canopy heterogeneity mean that the testing of the models here is much less rigorous. This is paradoxical, as these are precisely the conditions under which the models most require validation. We conclude that the big leaf model is likely to be adequate in C4 canopies where appropriate values of K can be obtained. However, judgement is reserved on whether the model will generally simulate heterogeneous C3 canopies well, particularly at low values of L_t.

The two models performed similarily at two out of the three sites, and it is hard to interpret the result at the third site. An important failing of the big leaf model is that the values of the K parameter are purely empirical, and may change as canopy structure changes with time. As MAESTRO has a more sound theoretical basis, it was considered more appropriate for extrapolating fluxes to larger space and time scales.

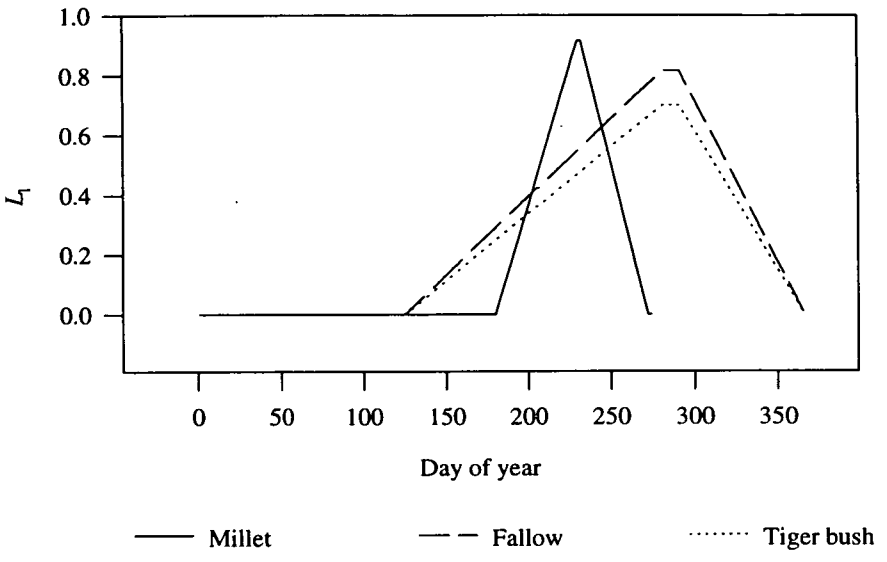

Figure 7.11 Simulated seasonal course of L_l used in MAESTRO based on the measurements described in Chapters 5 and 6.

7.5 Scaling up in time

7.5.1 Method

The validated parameterisations of MAESTRO for the three sites were used to predict fluxes for the wet season of 1992. Hourly meteorological data recorded at ISC were used for the periods when weather stations were not running at the sites (courtesy of M.V.K. Sivakumar, ICRISAT). The leaf phenology parameters were derived from the measurements described in Chapters 5 and 6, producing the simulated course of L_l shown in Figure 7.11. These were used to update the leaf area parameters in the model on a daily time step. Growth respiration parameters were changed according to the season using the data in Table 4.2.

At the millet and fallow sites, comparison can be made with the biomass production measurements described in Chapter 5 and those of Brouwer *et al.* (in prep.), by assuming that the biomass consisted of 47 % carbon (Penning de Vries *et al.*, 1989). The value of millet root biomass was obtained by assuming that the root:shoot ratio measured by Brouwer *et al.* (in prep.) in September is applicable to the August above-ground biomass measurements.

7.5.2 Results

The predicted daily net fluxes shown in Figure 7.12 closely follow the course of L_l over the growing season. At the millet site, the fluxes are concentrated within the short growing season of the crop but are approximately two and three times higher than at the fallow and tiger bush sites, respectively. The

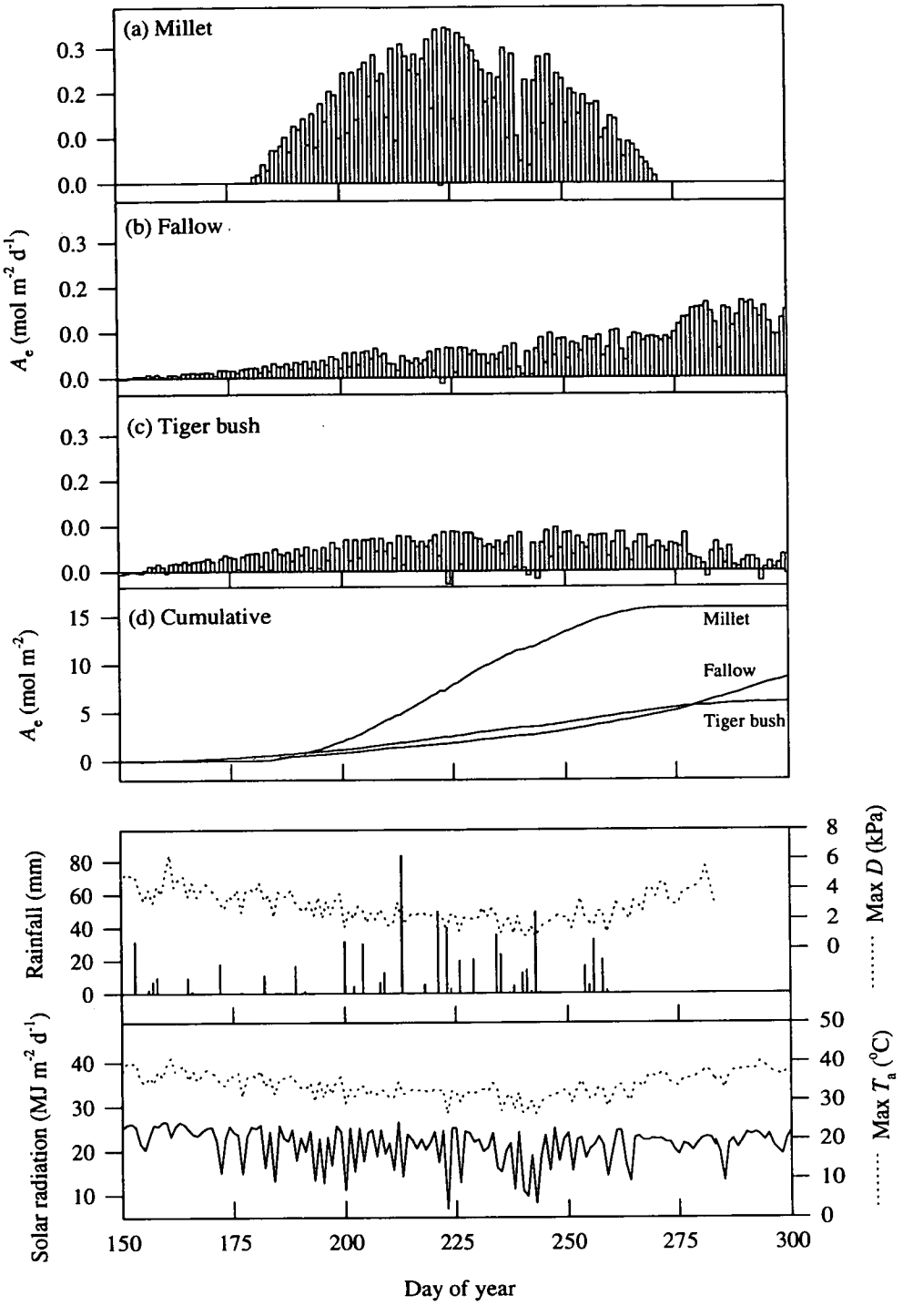

Figure 12 MAESTRO predictions of daily and cumulative net ecosystem CO_2 flux, A_e, at the three sites over the 1992 wet season, together with key weather variables.

accumulated sums of these daily fluxes are shown in Table 7.2 and Figure 7.12(d). The predictions of wet season net fluxes are in similar proportions to the daily fluxes, with the millet fixing twice as much carbon as the fallow vegetation, and fives times as much as the tiger bush. The large flux predicted at the millet site is to be expected, given that it is a fast growing C4 crop.

Table 7.2 Cumulative net CO_2 fluxes over the wet season (DOY 150-300) predicted by MAESTRO.

Site	Millet	Fallow	Tiger bush
CO_2 assimilated (mol m^{-2})	15.78	8.56	6.03

Table 7.3 Comparison of harvest measurements of biomass production over the 1992 wet season with MAESTRO predictions. In millet, comparisons are made with two sets of measurements: (1) those made in mid-August, described in Chapter 5 and (2) those of Brouwer *et al.* (in prep.), made in mid-September in the 1 ha millet growth plot (Figure 2.4). *Assumes that dry foliage consists of 47 % carbon by weight.

Site	Millet[1]	Millet[2]	Fallow
Time period (DOY)	150-232	150-261	170 - 286
Harvest measurements			
Above-ground biomass production (g m^{-2})	258	273	77
Below-ground biomass production (g m^{-2})	50	65	?
Total biomass production (g m^{-2}) (+/- 95 % confidence interval)	308 +/- 65	338 +/- 19	77+?
MAESTRO predictions of biomass production (g m^{-2})*	250	403	166

In millet, the model predictions differ from the two biomass production measurements by -19 % and +19 %, respectively. However, the model prediction is within the confidence limits of the first biomass estimate. The model overestimates biomass production later in the season, and this may be related to loss of plant parts during senescence, which are not included in harvest measurements, and the change in the balance between respiration and photosynthesis which is known to occur in the late stages of crop development. In general, the level of agreement is reasonable given these factors and the accumulation of errors that occurs when going from leaf measurements made over periods of seconds to the ecosystem on a seasonal time scale.

At the fallow site, biomass values from harvest measurements show only 46 % of the increase in biomass predicted by MAESTRO. However, the comparison is not really valid as only the growth of foliage was quantified, yet a substantial portion of the assimilate pool would be partitioned into the woody stem and roots. No measurements of root biomass were made, and changes in stem mass were not detected because the measurement technique was not sensitive enough (Chapter 5). As so few biomass measurements were made at the tiger bush site, the comparison was not made here.

7.5.3 Discussion

The agreement between harvest measurements of biomass production and MAESTRO predictions found at the millet site (Table 7.3) suggests that the model works well, at least where the parameters can be measured accurately, and a degree of confidence can be placed in the predictions of the wet season net fluxes. However, these cannot be directly related to the annual net CO_2 flux. In the case of millet, most of the carbon sequestered will be returned to the atmosphere via animal (including human) respiration and decomposition whilst some is temporarily stored as grain, products made with the straw and as soil organic matter. If considered on a long enough time scale, the net carbon balance will be zero. The prediction in Figure 7.12(d) therefore represents only the temporary sequestration of carbon that occurs over the months of the growing season.

The situation is somewhat similar at the fallow site, although it would be expected that there would be a net increase in the amount of carbon stored in the fallow vegetation, as it is an early successsional stage and the bushes are growing. However, a lot of the carbon sequestered in the annual ground flora and the *G. senegalensis* foliage would be released by decomposition in the early dry season. Again, the prediction in Figure 7.12(d) represents only the sequestration of carbon that occurs over the months of the growing season. In any case, as the fallow land will be put back into millet cultivation after five to ten years, the net carbon balance for the above-ground component is zero when considered over this period, although the amount of carbon stored below-ground may increase.

The situation is potentially different in tiger bush vegetation, as it is dominated by perennial plants and sequestered carbon may be stored there as biomass *ad infinitum*. However, it is to be expected that the net annual flux would be around zero, as the vegetation is mature and would have reached a more or less steady state, wherein photosynthesis is balanced by respiratory losses. As in the fallow vegetation, the predicted positive CO_2 flux only represents the temporary sequestration of carbon during the growing season. This may be completely counterbalanced by the decomposition flux following leaf fall in the early dry season. Furthermore, larger scale processes in which CO_2 is released will be operating, such as the removal of wood for fuel and grazing by livestock, which are not simulated or measured by eddy covariance. Offsetting this, it is possible that the vegetation could be responding to the rising concentration of CO_2 by photosynthesising more and be shifting towards a new equilibrium state (Gifford, 1994). There is more uncertainty associated with the predictions at the fallow and tiger bush sites because of the difficulties of L_1 and biomass measurements and the extrapolation of leaf phenology outwith the period of measurements. These problems are more severe at the tiger bush site and the predictions are accordingly less accurate.

Ideally, the model should also be tested against CO_2 flux measurements made over the same time period, as there is a degree of uncertainty in the comparison with biomass estimates because the

carbon content of the vegetation was not measured. However, because of the logistical problems associated with micrometeorological measurements, this was not possible. Only a very few data sets extend over more than a few weeks (eg. Biscoe, Scott and Monteith, 1975), but with the current interest in the global carbon balance, more studies are being directed towards the longer term (eg. Wofsy *et al.*, 1993).

7.6 Scaling up in space

7.6.1 Methods and Results

There are several possible ways in which the measurements and model predictions of ecosystem-scale CO_2 flux can be extrapolated to the larger spatial scales covered in the HAPEX experiment, some of which are considered below.

(1) Surface type classification

Table 7.4 lists the percentages of land cover types for the area around the southern supersite (a square area of 38.5 x 38.5 km^2 centred on ISC) were derived from a maximum likelihood classification of a Landsat TM scene.

Table 7.4 Percentage of land cover types for the southern supersite (a square area of 38.5 x 38.5 km^2 centred on ISC) (courtesy of J. Finch, IH).

Land surface type	Area (% of image)
Millet	29
Fallow	4
Degraded Tiger Bush	28
Tiger Bush	16
Degraded Forest	21
Water (the river Niger)	2

The land cover classes are essentially those used on the local 1:50 000 maps. The tiger bush site is in what is defined as degraded tiger bush. Tiger bush is a denser vegetation on a laterite soil, whilst degraded forest is a very dense collection of bushes on laterite. However, as no distinctions could be made between these sub-categories of tiger bush in terms of model inputs, they were lumped together. The area of millet is effectively the areas of sandy soil not covered by fallow. The Landsat data are available for the whole HAPEX 1° square but a similar classification analysis has not been performed.

These data were used to scale up in a very simple way by applying the proportion of each land surface type as a weighting factor to the calculated daily flux for that surface type, to give an estimate of the flux for the whole of the southern supersite. The daily and cumulative fluxes calculated in this way are

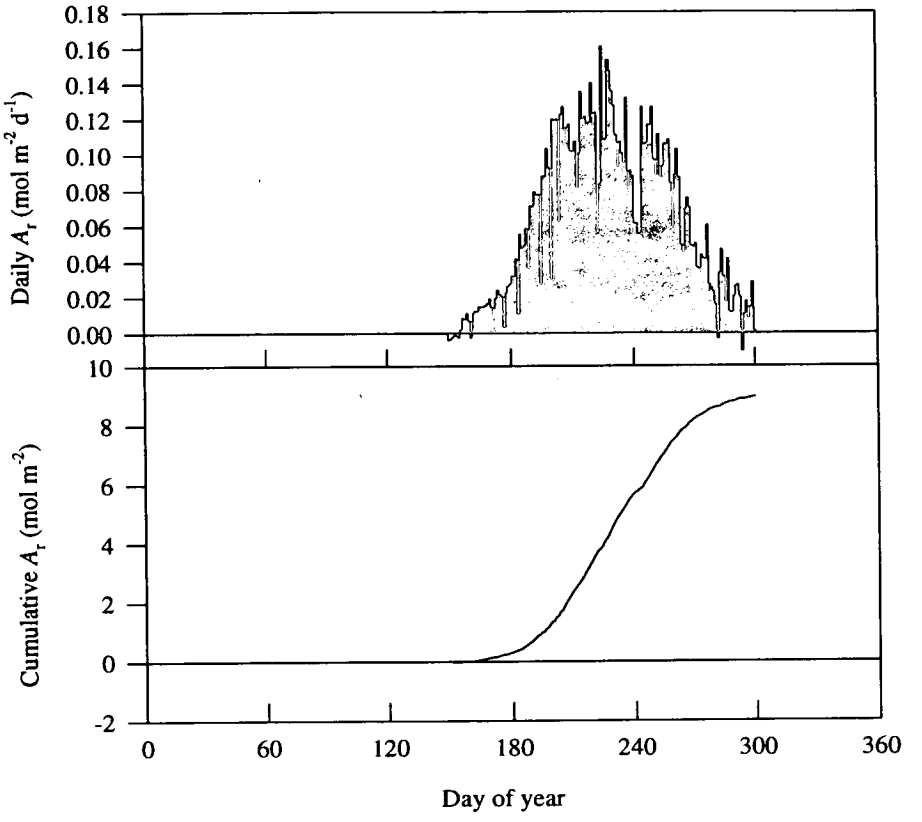

Figure 7.13 MAESTRO predictions of daily and cumulative regional CO_2 fluxes, A_r, at the southern super-site (38.5 x 38.5 km^2), calculated using the percentage of land covered by each vegetation type to weight the predicted site fluxes (Section 7.6.1).

shown in Figure 7.13. The sum of these fluxes over the 1992 wet season (DOY 150-300) gives a value of 8.96 mol m^{-2}. The impicit assumption of this approach is that the vegetation forms discrete types rather than varying continuously in space (with variables such as L_l). It is also assumed that weather was the same all over the area, which is reasonable for solar radiation and air temperature, but was not the case for rainfall (Chapter 2).

(2) Satellite NDVI data

Normalised Difference Vegetaion Index (NDVI) data are available for the whole of the 1° square from the Advanced Very High Resolution Radiometer (AVHRR) on the NOAA-11 and -12 satellites. Daily values are available for most of 1992, covering the whole square at a spatial resolution of about 200 m. A more sophisticated way of scaling up would be to use these NDVI data as a substitute for the transmission and reflection term in Equation 7.1 in the calculation of absorbed Q on an array of points covering the whole square.

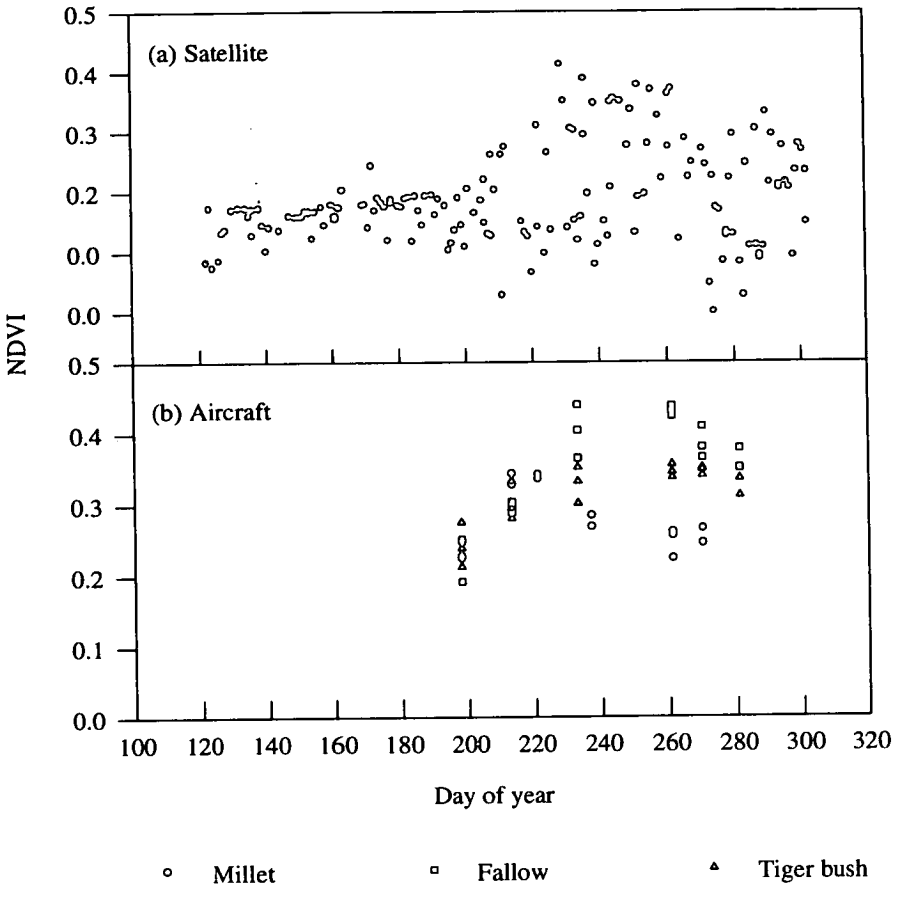

Figure 7.14 NDVI data collected by (a) AVHRR on the NOAA satellites at the millet site and (b) aircraft measurements from the Piper Saratoge (courtesy of N.P. Hanan, University of Maryland).

However, there are several problems with this approach. Firstly, the assumption that the weather is similar over the whole region no longer holds when considering the 100 x 100 km scale. Weather data with the relevant variables are only available for a few points within the three supersites and some means of interpolating between these points would need to be employed. Secondly, the satellite NDVI data are very noisy (Figure 7.14(a)). Comparison of these with aircraft NDVI measurements (Figure 7.14(b)) suggest that the upper boundary of the scatter of points delimits the true value, whilst the lower values may be distorted by view angle effects. An algorithm removing such effects would need to be applied to the data before it could be used as model input. Thirdly, some classification analysis similar to that used in (1) above would have to be applied to identify the surface type for each pixel so that the correct physiology parameters were used. It is clear from Figure 7.12 that the different vegetation types have different properties, and NDVI alone would not predict fluxes very accurately. Although this more sophisticated approach could give an estimate of the flux for a much larger area

than (1) (10 000 cf. 1485 km^2), overcoming these problems is time consuming and has not been pursued further.

7.6.2 Validation

Introduction

Model extrapolations from the leaf scale were tested at ecosystem scale by eddy covariance measurements (Section 7.6) and at the seasonal scale by biomass measurements (Section 7.7). In the same way, it would be useful to compare the extrapolation of ecosystem-scale fluxes to regional scale described above with measurements at this scale. Although larger scale eddy covariance measurements can be made from aircraft, no measurements of CO_2 fluxes were made in this way in HAPEX-Sahel. An alternative approach to estimating regional-scale fluxes was suggested by McNaughton (1989) and developed by Raupach, Denmead and Dunin (1992), Raupach (1993) and Raupach *et al.* (unpubl.) and is based on analysis of the mass balance of the convective boundary layer (CBL). A marked diurnal pattern in CO_2 concentration was observed throughout this experiment, which closely followed the CO_2 flux (Figure 7.15). If consideration is made of the volume within which this concentration change occurs, it may be used to infer the regional surface flux.

Under commonly encountered daytime weather conditions, a CBL is present over the surface of the earth (Garratt, 1992). At the top of this layer is a temperature inversion, which effectively separates the air which has been influenced by the surface from the overlying air of the free atmosphere. Over the course of a day, the CBL grows from tens of meters in the early morning to a height of 1 to 2 km in the late afternoon, entraining air from the free atmosphere as it rises. The growth of the CBL, measured by radiosondes released from the fallow site on 9 October 1992, is shown in Figure 7.16. In principle, the CBL can be treated as a huge cuvette, in which the surface fluxes can be inferred from measured changes in scalar concentration and boundary layer height over time. The temporal resolution is limited by the frequency of CBL height measurements (typically a few hours). For simplicity, only daily values were considered here. The inferred flux should be representive of the area traversed by a column of air in the course of a day, and so may extend a few hundred km upwind and cover an area of 1000 to 10 000 km^2 (Raupach *et al.*, unpubl.). The relevant variables are the maximum height of CBL attained in the late afternoon (h) and the change in CO_2 concentration between dawn and this time (ΔC_a). The flux over this period (A_r) can then be written as

$$A_r = h\,\Delta C_a \quad \frac{1}{V_m} \qquad [7.2]$$

where V_m is the volume occupied by one mole of air (22.4 x 10^{-3} m^3 at STP). The height of concentration measurements was at most 17 m, which is likely to be within the surface layer of the

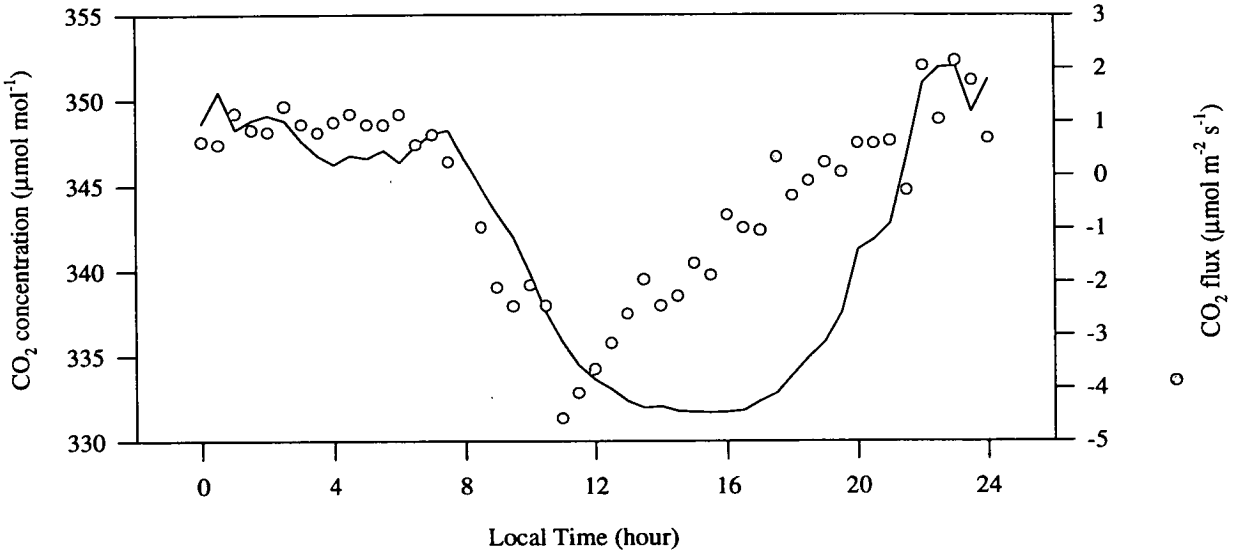

Figure 7.15 Diurnal change in CO_2 concentration measured at 17 m on 9 October 1992 at the tiger bush site. The CO_2 flux is plotted using the micrometeorolgical convention where fluxes to the surface are negative.

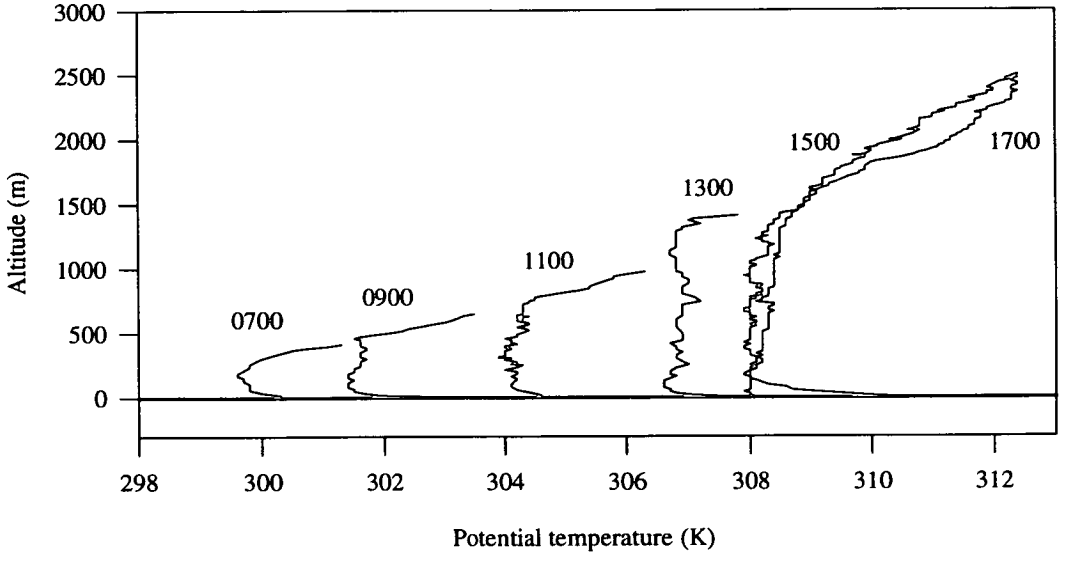

Figure 7.16 Growth of the convective boundary layer over the course of 9 October 1992. Measurements were made at the fallow site using free-flight radiosondes (data courtesy of A. Culf, IH).

CBL, where vertical gradients extending down to the surface are present. The measured amplitude of the diurnal wave will then be exaggerated relative to that in the well-mixed layer, which may start at around 50 m (see Figure 7.16). A correction to account for this can be made using surface aerodynamic resistance values (r_a) whereby

$$A_r = \frac{h\,\Delta C_a}{1 + h\,r_a / t}\,\frac{1}{V_m} \qquad [7.3]$$

where t is the time over which the flux is integrated (Raupach *et al.*, unpubl.). Surface aerodynamic resistance data are not currently available but values can be estimated from the literature. For a first approximation, a value of 50 s m^{-1} was used, representing the high end of the range of r_a values for crops, grassland, heathland and tropical tree plantation given by Grace (1983). Additional terms included by Raupach *et al.* (unpubl.) accounting for other effects, such as subsidence of the atmosphere above the CBL, can be neglected in a first approximation.

The equations of Raupach *et al.* (unpubl.) assume that the CO_2 concentration is constant throughout the CBL, and thereby do not take into account the decline in temperature and pressure with altitude. Whilst the mole fraction remains the same, the CO_2 concentration expressed as mass per unit volume changes with air density, which decreases with height because pressure falls more rapidly than temperature. As the height of the CBL rises, fewer moles of air are entrained with each increment in h, and the average pressure within the CBL falls. This effect can be accounted for by introducing the mean air density within the CBL, ρ_a, into the equation:

$$A_r = \frac{\rho_a\,h\,\Delta C_a}{1 + h\,r_a / t} \qquad [7.4]$$

$$\rho_a = \frac{P}{RT} \qquad [7.5]$$

where P and T are the mean pressure and temperature within the CBL and R is the molar gas constant (8.314 J mol^{-1} K^{-1}). The vertical profiles of P and T were linear throughout the CBL (Figure 7.17), so the mean values could be calculated as:

$$P = P_h + 0.5(P_o - P_h) \qquad [7.6]$$

and

$$T = T_h + 0.5(T_o - T_h) \qquad [7.7]$$

where the subscripts o and h denote the values at the surface and top of the CBL, respectively.

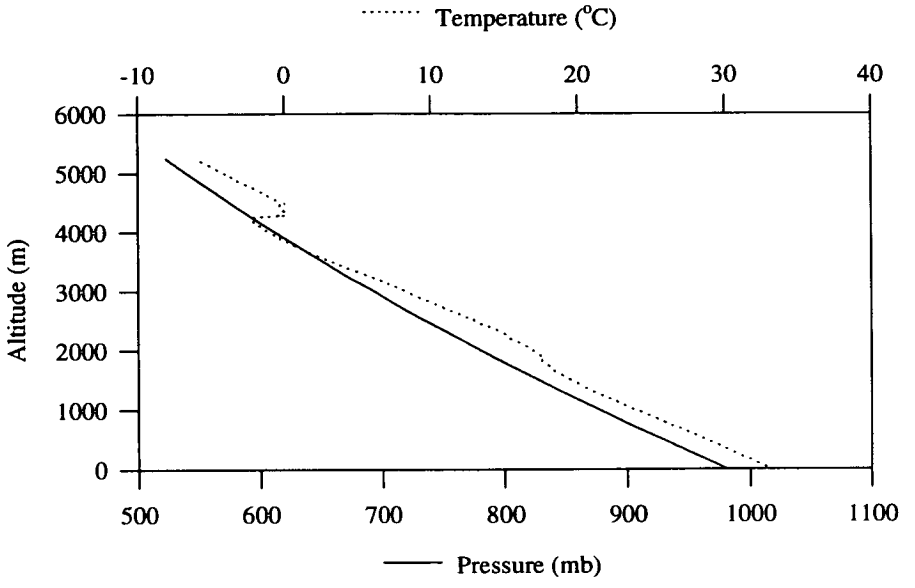

Figure 7.17 Vertical profiles of temperature and pressure measured at the fallow site on 9 October 1992 using a free-flight radiosonde (data courtesy of A. Culf, IH).

Method

The variable h was obtained for several days during the IOP from radiosonde measurements made by IH (data courtesy of A. Culf), and was fairly constant over this period, at around 1.5 km. This value of h was used in all subsequent calculations. C_a was measured during eddy covariance measurements at the top of the micrometeorological masts. ΔC_a was initially calculated as the difference between the daily CO_2 maxima and minima. However, because CO_2 produced by ecosystem respiration can build up in the nocturnal boundary layer, the daily maximum C_a may be inappropriate for estimating the daytime drawdown of CO_2, and an estimate of the value in the free atmosphere (C_+) was used instead (ie. $\Delta C_a = C_+ - C_{min}$, where C_{min} is the daily minimum value of C_a). A value for C_+ of 348 ppm was obtained from the "Trends 91" data set (Boden, Sepanski and Stoss, 1991), using the September figure for Izana, Canary Islands (28 ° 18' N, 16 ° 29' W), the nearest maritime station.

Results

Fluxes calculated by this method were compared with MAESTRO predictions of daytime regional CO_2 flux, which were obtained by scaling up ecosystem fluxes to the southern supersite using the surface type classification described in Section 7.6.1. The CBL budget method overestimated by a factor of about 15 when the simple formula given in Equation 7.2 was used. When the correction for the concentration gradient in the surface layer was included (Equation 7.3), the agreement was much better (Figure 7.18(a)). Although the choice of a representative aerodynamic surface conductance

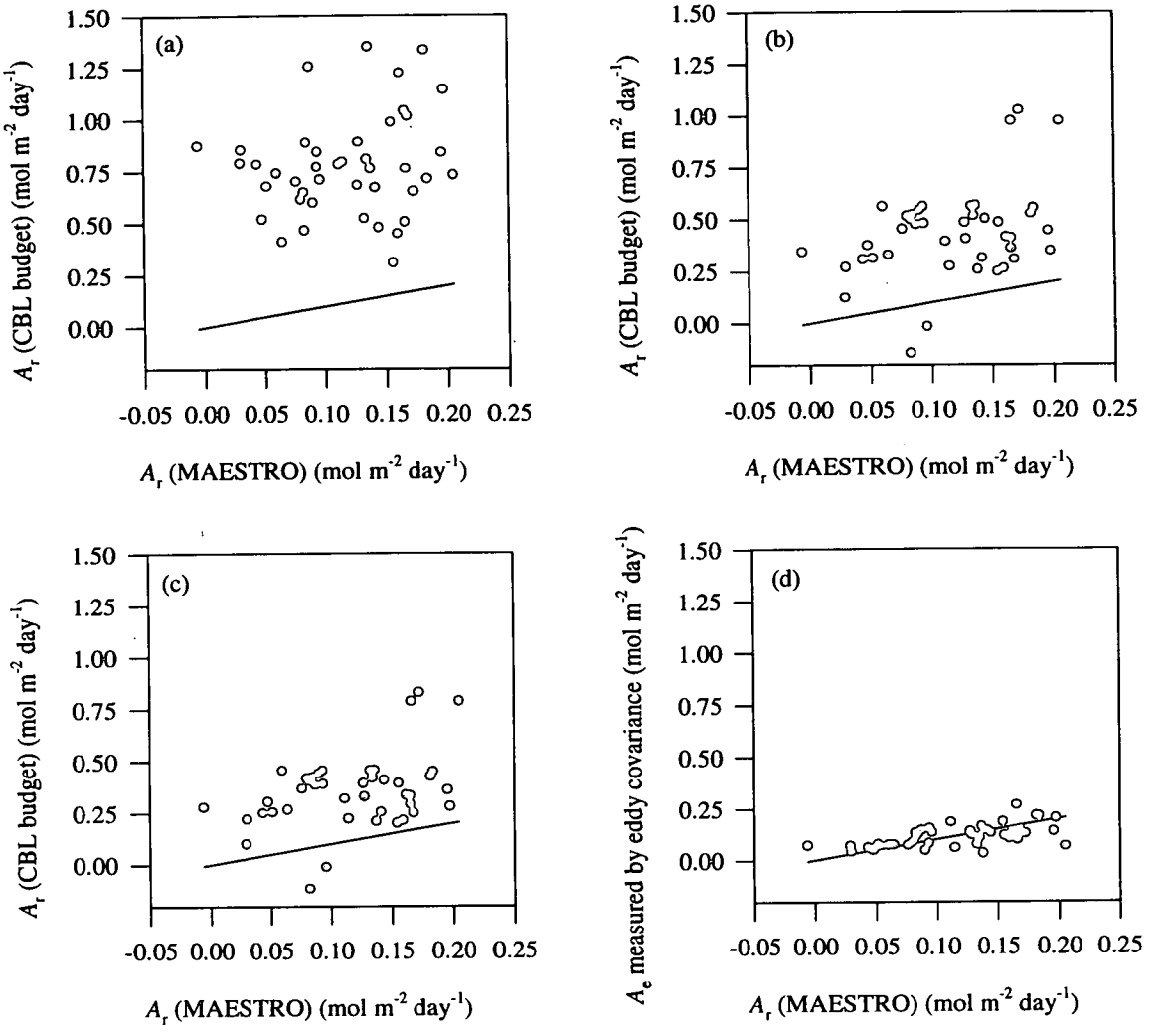

Figure 7.18 Comparison of regional-scale daytime CO_2 flux, A_r, estimated by the CBL budget method and predicted by MAESTRO for the southern super-site using the surface type classification (Section 7.6.1) during the IOP. (a) shows results from the CBL budget method when the correction is made for the concentration gradient in the surface layer (Equation 7.3), assuming a r_a value of 50 s m^{-1}. (b) shows results from the CBL budget method when correction is also made for the CO_2 concentration of the free atmosphere, assuming a value of C_+ of 348 μmol mol^{-1}. (c) shows results from the CBL budget when corrections are also applied for the vertical gradients of pressure and temperature (Equation 7.4). (d) MAESTRO predictions of A_r are plotted against eddy covariance measurements of A_e made at the sub-sites over the same period. This relationship is not expected to be very close, as predictions do not refer to the same area as measurements, but shows that the MAESTRO predictions of A_r are in the same same range as independent measurements of A_e. 1:1 lines are shown in all plots. Raw data are listed in Appendix A.5.

value was rather arbitrary, CBL budget calculations of A_r were decreased by a factor of 3.3 with respect to Equation 7.2, when using a r_a value of 50 s m^{-1}. Some of the remaining discrepancy was attributable to the overestimation of ΔC_a values when the daily maxima of C_a were used, as Figure 7.18(b) shows that closer agreement was achieved when the correction using C_+ was made. The agreement was improved by a further 19 % when the corrections were made for temperature and pressure (Figure 7.18(c)). However, even when all these corrections were made, the discrepancy between estimates still appears large, a factor of around 1.5-5. Figure 7.18(d) indicates that it is the CBL budget method that is likely to be in error, as the MAESTRO predictions of A_r are in the same range as the independent measurements of A_e made by eddy covariance.

Discussion

The discrepancy between the CBL budget method and MAESTRO predictions of A_r is not easily explicable. Error caused by the entrainment flux through the capping inversion, whereby air of higher C_a passes into the CBL, would cause the method to underestimate A_r. The method also assumes that dC_+/dz above the CBL is small, but measurements suggest this is reasonable (Pearman and Garratt, 1973; Garratt and Pearman, 1973; Tanaka, Nakazawa and Aoki, 1983; Wofsy *et al.*, 1988). Day-to-day variation in h was not large, and although the upper limit of the CBL was not very clearly defined in the late afternoon on some days, it was never less than 1500 m, and so cannot explain the observed overestimation of A_r. It is possible that the three sites were not suitably representative of whole region. However, casual observation suggested that the sites were, if anything, more productive than was typical for these vegetation types. There may also be errors in the classification of surface types based on the Landsat TM image, but differences in A_e between sites were not large enough for this to cause a serious discrepancy.

The assumption that C_+ will be equal to 348 μmol mol^{-1} may be unsound, as the air mass will have undergone a long overland trajectory of several thousand kilometres. Photosynthesis by terrestrial vegetation is likely to lower this value, and so ΔC_a may have been overestimated here, and might conceivably account for some of the observed discrepancy. Also, C_+ will be lower if the residual layer is not well mixed with the free atmosphere at night, which could be a significant effect as the drawdown during the day within the CBL is relatively large.

Day-to-day variation in C_+ is also possible, which would produce noise in the data. Depending on the synoptic weather situation, it is possible that large-scale advection of CO_2 plays a role, as lateral inputs and outputs of CO_2 may contribute to the budget. In order to quantify this, the horizontal gradient in C_a in the CBL would need to be measured at two or more locations in the area of interest. However, measurements of C_a were only made at a single site on each day (except with the open-path IRGA, which was unreliable). In any case, it seems unlikely that advection would cause a systematic error in

the CBL budget method. Without measurements of C_a in the mixed layer, and preferably at more than one location and in the free atmosphere above the CBL also, it is not possible to identify the cause of the apparent discrepancy more definitely.

Only one other attempt has been made to compare this method with ground-based flux measurements (Raupach *et al.*, unpubl.). Better agreement was found than here, and values of A_r from the CBL budget method were between 50 and 125 % of ground-based estimates, although there was a strong tendency to underestimate, in contrast to the overestimation found here.

7.7 Conclusions

Scaling from leaf to ecosystem

In the case of MAESTRO, predictions were accurate at the millet and fallow sites, but rather poor at the tiger bush site. The much simpler big leaf model worked well in millet and fallow, and apparently also in tiger bush, but results from this site are harder to interpret. The difference between predictions from the two models at the tiger bush site suggests that canopy spatial heterogeneity poses serious problems for model parameterisation. Although eddy covariance can measure the fluxes successfully, and MAESTRO can potentially represent the complex form of the tiger bush, the largest uncertainty in the comparison is in the model leaf area and canopy structure parameters.

Scaling from minutes to months

MAESTRO predicts the ecosystem CO_2 flux at the millet site over the growing season reasonably well, given the uncertainty introduced by the comparison with biomass production rather than measured CO_2 fluxes. The good agreement suggests that the theory on which the model is based is sound, as it apparently copes well with the range of L_l and environmental variables encountered over the season, and a degree of confidence can be placed in the extrapolation of fluxes at the other sites to seasonal scale.

Scaling from leaf to region

A simple procedure was used for scaling leaf fluxes to the regional scale, using the MAESTRO predictions of A_e for each site, weighted by the proportion of the region covered by the different vegetation types. An attempt was made to validate this by comparison with regional fluxes calculated from the mass budget of the CBL. Values of A_r from the CBL budget method were ~1.5-5 times higher than MAESTRO predictions. It is likely that the CBL budget method is in error, as the MAESTRO predictions of A_r are in the same range as the independent measurements of A_e made by eddy covariance. Neither entrainment nor error in the estimate of h can explain this difference. It is possible that C_+ (and therefore ΔC_a) was overestimated, as the air mass will have undergone a long

overland trajectory of several thousand kilometres, and this could account for some of the observed discrepancy. Day-to-day variation in C_+ is also possible, which would produce noise in the data. Large-scale advection of CO_2 may play a role, although it seems unlikely that advection would cause a systematic error in the CBL budget method.

Long term regional-scale carbon balance

It is not possible to infer anything about the long term regional carbon balance from this work, as it depends largely on man's activities, which are not amenable to the kind of modelling described here. The region as a whole is likely to be acting as a source of CO_2. With the increasing human population, the area in millet culivation has been increased over recent years by shortening the fallow rotation period. This will reduce the area of fallow land, and result in a reduction in the amount of carbon stored by the vegetation over the region. It is unlikely that this could be offset by increased photosynthesis in response to elevated CO_2, as the human population increase also gives rise to greater livestock numbers and greater demand for fuelwood, and has resulted in the tiger bush being degraded.

Information on the long term regional carbon balance can be obtained from modelling studies, such as those of Fung *et al.* (1983), Box (1988), Tans, Fung and Takahashi (1990), Enting and Mansbridge (1991) and Stocker, Broecker and Wright (1994). It is possible to predict the latitudinal distribution of annual CO_2 fluxes by inverting a two or three-dimensional atmospheric transport model, using the annual variation in CO_2 concentrations from the global flask network as the input. The results typically predict a small net sink in these latitudes. However, the resolution is extremely coarse and the earth is largely covered by ocean at this latitude, so it is difficult to infer anything about the terrestrial vegetation from these results.

Suggestions for further work

The use of satellite remote sensing indices such as NDVI appears to have potential as a means of scaling up in space. However, as well as the problems outlined in Section 7.6.1, the number of computations involved requires a simple model akin to the big leaf model. A valid role of highly complex models such as MAESTRO is to examine the limitations of these simple models, for example, by quantifying the error resulting from the assumption of canopy homogeneity. The output of the complex model could be used to modify big leaf type models (eg. to calculate a simple correction factor for different canopy structures) or alternatively, as the basis for a simpler model. The complex model could be run for several combinations of parameters (different L_l, canopy structures etc.) and a simple empirical model derived by fitting curves to the resulting n-dimensional response surfaces.

Longer term eddy covariance measurements would provide better validation data for model extrapolations in time, although the biomass comparison gives information about partitioning. However, in order to model the longer term mechanistically, it becomes necessary to simulate growth dynamically, rather than prescribe it with constant parameters. This requires a knowldedge of assimilate partitioning, which may be determined by plant nutrient status and so would need some simulation of nutrient cycling. A more complete soil model is also desirable, as the functions used here are based solely upon temperature, whilst the R_0 parameter would probably change with the amount of soil organic carbon.

The regional-scale flux technique described in Section 7.6.2 provides a way of measuring the actual large scale flux of interest, as it encompasses a large enough area to take in both physiological and anthropogenic fluxes without the need for subsequent modelling. Although the agreement with other measurements here was poor, better agreement was obtained by Raupach *et al.* (unpubl.), and the technique merits further research as its potential is great. An obvious improvement would be to measure directly the concentration in the well-mixed layer, rather than inferring it from surface layer measurements. Taller masts or tethered weather balloons, such as those currently used to measure temperature and humidity profiles in boundary layer studies offer two possibilities. Measurements are simple and cheap enough to be made over long time periods and to be replicated in several places, so as to give useful information on the long term regional-scale carbon balance.

Adams, R. M., Rosenzweig, C., Peart, R.M., Ritchie, J.T., McCarl, B.A., Glyer, J.D., Curry, R.B., Jones, J.W., Boote, K.J. and Allen, L.H. (1990) Global climate change and US agriculture. Nature, 345, 219-224.

ADC (1990) *Instruction Manual for LCA3: Leaf Chamber Analysis System.* ADC Ltd, Hoddeson.

Allen, L. H., Yocum, C. S. and Lemon, E. R. (1964) Photosynthesis under field conditions: VII. Radiant energy exchange. Agronomy Journal, 56, 253-259.

Allen, S. J. and Grime, V. L. (in press) Measurements of transpiration from savannah shrubs using sap flow gauges. Agric. Forest Met.

Allen, S. J., Wallace, J. S., Gash, J. H. C. and Sivakumar, M. V. K. (1994) Measurements of albedo variation over natural vegetation in the Sahel. International Journal of Climatology, 14, 625-636.

Ambouta, K. (1984) *Contribution a l'edaphologie de la brousse tigree de l'ouest nigerien.* University of Nancy. Unpublished PhD thesis.

Amthor, J. S. (1989) *Respiration and Crop Productivity.* Springer-Verlag, New York.

Amthor, J. S., Goulden, M. L., Munger, J. W. and Wofsy, S. C. (1994) Testing a mechanistic model of forest-canopy mass and energy exchange using eddy correlation: carbon dioxide and ozone uptake by a mixed oak-maple stand. Aust. J. Plant Physiol., 21, 623-51.

Andersen, P. C., Brodbeck, B. V. and Mizell, R. F. (1993) Diurnal variations of amino acids and organic acids in xylem fluid from Lagerstroemia indica: an endogenous circadian rhythm. Physiologia Plantarum, 89, 783-790.

Anderson, D. E. and Verma, S. B. (1986) Carbon dioxide, water vapour and sensible heat exchanges of a grain sorghum canopy. Boundary Layer Meteorology, 34, 317-331.

Anderson, M. C. (1966) Stand structure and light penetration. II. A theoretical analysis. Journal of Applied Ecology, 3(41-54)

Andre, J.-C., Goutorbe, J.-P. and Perrier, A. et al. (1988) Evaporation over land surfaces: First results from HAPEX-MOBILHY special observing period. Annales Geophysicae, 6, 477-492.

Andre, J.-C., Goutorbe, J.-P. and Perrier, A. (1986) A hydrologic atmospheric experiment for the study of water budget and evaporation flux at the climatic scale. Bull. Am. Met. Soc., 67, 134-144.

Azcon-Bieto, J., Lambers, H. and Day, D. A. (1983) Effect of photosynthesis and carbohydrate status on respiratory rates and the involvement of the alternative pathway of leaf respiration. Plant Physiology, 72, 598-603.

Azcon-Bieto, J. and Osmond, C. B. (1983) Relationship between photosynthesis and respiration. Plant Physiology, 71, 574-581.

Baker, J. M. and van Bavel, C. H. M. (1987) Measurements of mass flow of water in the stems of herbaceous plants. Plant, Cell and Environment, 10, 777-782.

Baldocchi, D. D. (1993) Scaling water vapor and carbon dioxide exchange from leaves to a canopy: rules and tools in *Scaling Physiological Processes: Leaf to Globe* by J.R. Ehleringer and C.B. Field. Academic Press, San Diego. pp. 77-114.

Baldocchi, D. D., Hicks, B. B. and Meyers, P. P. (1988) Measuring biosphere-atmosphere exchanges of biologically related gases with micrometeorological methods. Ecology, 69(5), 1331-40.

Baldocchi, D. D., Verma, S. B. and Anderson, D. E. (1987) Canopy photosynthesis and water-use efficiency in a deciduous forest. J. Appl. Ecol., 24, 241-260.

Barry, R. G. and Chorley, R. J. (1992) *Atmosphere, Weather and Climate*. 6th Edn. Methuen, London.

Biscoe, P. V., Scott, R. K. and Monteith, J. L. (1975) Barley and its environment. III. Carbon budget of the stand. Journal of Applied Ecology, 12, 269-293.

Blyth, E. M. (1995) Two-source SVAT modelling in semi-arid terrain. Annales Geophysicae, 13(Supplement II), 293.

Boden, T. A., Sepanski, R. J. and Stoss, F. W. (1991) *Trends '91: a compendium of data on global change*. Oak Ridge National Laboratory, Oak Ridge, Tennesse.

Bolle, H. J., Andre, J.-C. and Arrue, J. L. et al. (1993) European field experiment in a desertification threatened area. Annales Geophysicae, 11, 43-64.

Bolstad, P. V. and Gower, S. T. (1990) Estimations of leaf area index in 14 southern Wisconsin forest stands using a portable radiometer. Tree Phys., 7, 115-124.

Bossard, C. C. and Rejmanek, M. (1992) Why have green stems? Functional Ecology, 6(2), 197-205.

Box, E. O. (1988) Estimating the seasonal carbon source-sink geography of a natural, steady-state biosphere. J. Appl. Meteorol., 27, 1109-1124.

Brouwer, J., Buerkert, A. C., Levy, P. E. and Simmonds, L. P. (unpubl.) Spatial variability and upscaling of millet root, shoot and leaf growth at the HAPEX-Sahel southern supersite. Submitted to J. Hydrology,

Bunce, J. A. (1990) Short- and long-term inhibition of respiratory carbon dioxide efflux by elevated carbon dioxide. Annals of Botany, 65, 637-642.

Butler, D. R. and Landsberg, J. J. (1981) Respiration rates of apple trees, estimated by CO_2 efflux measurements. Plant, Cell and Environment, 4, 153-159.

Campbell, G. S. (1986) Extinction coefficients for radiation in plant canopies calculated using an ellipsoidal inclination angle distribution. Agric. Forest Meteorol., 36, 317-321.

Campbell, G. S. and Norman, J. M. (1989) The description and measurement of plant canopy structure in *Plant Canopies: their growth, form and function* by G. Russell, B. Marshall and P. G. Jarvis. Cambridge University Press, Cambridge.

Carter, M. C. and Larsen, H. S. (1965) Soil nutrients and loblolly pine xylem sap composition. Forest Science, 11, 216-220.

Charney (1975) Dynamics of deserts and droughts in the Sahel. Quart. J. Royal. Met. Soc., 101, 193-202.

Charney, J., Stone, P. H. and Quirk, W. J. (1975) Drought in the Sahara: A biogeophysical feedback mechanism. Science, 187, 434-435.

Chase, W. W. (1934) The composition, quantity and physiological significance of gases in tree stems. Minnesota Agr. Expt. Sta. Tech. Bull., 99

Chen, J. M., Black, T. A. and Adams, R. S. (1991) Evaluation of hemispherical photography for determining plant area index and geometry of a forest stand. Agricultural and Forest Meteorology, 56, 129-143.

Clos Ardec, M. (1956) Etude sur photographies aeriennes d'une formation vegetale sahelienne: la brousse tigree. Bull. de l'IFAN, XVII(A)(3), 677-684.

Cloudsley-Thompson, J. L. (1974) The expanding Sahara. Environmental Conservation, 1(1), 5-13.

Cornic, G. and Jarvis, P. G. (1972) Effects of oxygen on CO_2 exchange and stomatal resistance in Sitka spruce and maize at low irradiance. Photosynthetica, 6, 225-239.

Cunnington, W. M. and Rowntree, P. R. (1986) Simulations of the Saharan atmosphere-dependence on moisture and albedo. Quarterly Journal of the Royal Meteorological Society, 112, 971-999.

Daudet, F. A. and Tchamitchian, M. (1993) Radiative exchange and photosynthesis in Crop Structure and Light Microclimate by C. Varlet-Grancher, R. Bonhomme and H. Sinoquet. INRA, Paris. pp. 401-418.

Davies, D. D., Goivanelli, J. and Ap Rees, T. (1964) Plant Biochemistry. Blackwell, Oxford.

Dickinson, R. (1984) Modelling evapotranspiration for three dimensional global climate models. in Climate Processes and Climate Sensitivity Elsevier, Amsterdam.

Eamus, D. and Jarvis, P. G. (1989) The direct effects of increase in the global atmospheric CO_2 concentration on natural and commercial trees and forests. Advances in Ecological Research, 19, 1-55.

Edwards, G. and Walker, D. A. (1983) *C3,C4: mechanisms, and cellular and environmental regulation, of photosynthesis*. Blackwell, Oxford.

Ehleringer, J. R. and Field, C. B. (1993) *Scaling Physiological Processes: Leaf to Globe*. Academic Press, San Diego.

Ehleringer, J. R. and Pearcy, R. W. (1983) Variation in quantum yield for CO_2 uptake among C3 and C4 plants. Plant Physiology, 73, 555-559.

Enting, I. G. and Mansbridge, J. V. (1991) Latitudinal distribution of sources and sinks of CO_2: Results of an inversion study. Tellus, 43B, 156-170.

Enting, I. G. and Mansbridge, J. V. (1989) Seasonal sources of and sinks of atmospheric CO_2: Direct inversion of filtered data. Tellus, 41B, 111-126.

Farquhar, G. D. and von Caemmerer, S. (1982) Modelling of photosynthetic response to environmental conditions in *Water Relations and Carbon Assimilation. Encyclopaedia of Plant Physiology 12(B)* by O.L. Lange, P.S. Nobel, C.B. Osmond and H. Ziegler. Springer-Verlag, pp. 550-587.

Fang, C.-M. and Moncrieff, J.B. (in press) An improved dynamic chamber technique for measuring CO_2 efflux from the soil. Functional Ecology.

Field, C.B., Ball, J.T. and Berry, J.A. (1989) Photosynthesis: principles and field techniques in *Plant Physiological Ecology: field methods and instrumentation* by R. W. Pearcy, J. Ehleringer, H.A. Mooney and P.W. Rundel (eds). Chapman and Hall, London. pp. 209-253.

Fitzgarrald, D. R. and Moore, K. E. (1990) Mechanisms of nocturnal exchange between the Amazon forest and the atmosphere. J. Geophys. Res., 95(16839-16850)

Folland, C. K., Palmer, T. N. and Parker, D. E. (1986) Sahel rainfall and worldwide sea surface temperatures 1901-85. Nature, 320, 602-607.

France, J. and Thornley, J. H. M. (1984) *Mathematical Models in Agriculture*. Butterworths, London.

Friedli, H., Loetscher, H., Oeschger, H., Siegenthaler, U. and Stauffer, B. (1986) Ice core record of the 13C/12C record of atmospheric CO_2 in the past two centuries. Nature, 324, 237-238.

Fung, I., Prentice, K., Mathews, E., Lerner, J. and Russell, G. (1983) Three-dimensional tracer model study of atmospheric CO_2: response to seasonal exchanges with the terrestrial biosphere. J. Geophys. Res., 88, 1281-1294.

Garratt, J. R. (1992) *The Atmospheric Boundary Layer*. Cambridge University Press, Cambridge.

Garratt, J. R. and Pearman, G. I. (1973) CO_2 concentration in the atmospheric boundary layer over south-east Australia. Atmos. Environ., 7, 1257-1266.

Gazarini, L. C., Araujo, M. C. C., Borralho, N. and Pereira, J. S. (1990) Plant area index in Eucalyptus globulus plantations determined indirectly by a light interception method. Tree Physiology, 7, 107-114.

Gedney, N. and Valdes, P. J. (1994) Sensitivity of a GCM surface parameterisation to HAPEX-Sahel data. Annales Geophysicae, 12(Supplement II), 343.

Gedney, N. and Valdes, P. J. (1995) The surface response to the temporal variability of convective rainfall. Annales Geophysicae, 13(Supplement II), 296.

Gifford, R. M. (1994) The global carbon cycle: a viewpoint on the missing sink. Aust. J. Plant Physiol., 21, 1-15.

Gillet, H. (1986) Desert and Sahel in *Plant Ecology in West Africa: systems and processes* by G. W. Lawson. John Wiley, London.

Gollan, T., Schurr, U. and Schulze, E.-D. (1992) Stomatal response to drying soil in relation to changes in the xylem sap composition of Helianthus annuus. I. The concentration of cations, anions, amino acids in, and pH of, the xylem sap. Plant, Cell and Environment, 15(5), 551-560.

Goutorbe, J. P. and Lebel, T. Tinga, A., Dolman, H., Engman, E.T., Gash, J.H.C., Kabat, P., Kerr, Y., Monteny, B., Prince, S., Sellers, P., Wallace, J., Hoepffner, M. (1992) *Experimental Plan for HAPEX-Sahel*. Third Draft (August 1992).

Goutorbe, J. P., Lebel, T. and Tinga, A. et al. (1994) HAPEX-Sahel: a large-scale study of land-atmosphere interactions in the semi-arid tropics. Annales Geophysicae, 12, 53-64.

Grace, J. (1983) *Plant-Atmosphere Relationships*. Chapman and Hall, London.

Grace, J. C., Jarvis, P. G. and Norman, J. M. (1987) Description, sensitivity and field test of a radiative transfer model for widely spaced stands. N. Z. J. Forest Sci., 17, 193-209.

Grace, J., Okali, D. U. U. and Fasehun, F. E. (1982) Stomatal conductance of two tropical trees during the wet season in Nigeria. J. Appl. Ecol., 19, 659-670.

Hagihara, A. and Hozumi, K. (1981) Respiration consumption by woody organs in a Chamaecyparis obtusa plantation. J. Jpn. For. Soc., 63(156)

Hansen, G. K. (1977) Adaptation to photosynthesis and diurnal oscillation of root respiration rates for Lolium multiflorum. Physiologia Plantarum, 39, 275-279.

Hare, F. K. (1977) Connections between climate and desertification. Environmental Conservation, 4(2), 81-90.

Hari, P. Nygren, P. and Korpilahti, E. (1991) Internal circulation of carbon within a tree. Can. J. For. Res., 21, 514-515.

Harley, P. C., Thomas, R. B., Reynolds, J. F. and Strain, B. R. (1992) Modelling photosynthesis of cotton grown in elevated CO_2. Plant, Cell and Environment, 15(3), 271-282.

Havranek, W. M. (1981) Stem respiration, radial growth and photosynthesis of a cembran pine tree (Pinus cembra L.) at the timberline in *Radial Growth in Trees* by W. Tranquillini. Mittleil der Forstl Bundesversuchsanstalt, pp. 443.

Hayward, D. F. and Oguntoyinbo, J.S. (1987) *The Climatology of West Africa*. Hutchinson, London.

Henderson-Sellers, A. (1987) Effects of change in land use on climate in the humid tropics in *The Geophysiology of Amazonia* by R. E. Dickinson (ed). John Wiley,

Hoepffner, M. and Goutorbe, J-P (1989) HAPEX-II-Sahel: A water and energy balance modelling project in dry tropical climate. Introduction and call for an international collaboration. ORSTOM,

Hollinger, D. Y., Kelliher, F. M., Byers, J. N., Hunt, J. E., McSeveny, T. M. and Weir, P. L. (1994) Carbon dioxide exchange between an undisturbed old-growth temperate forest and the atmosphere. Ecology, 75(1), 134-150.

Huntley, B. J. and Walker, B. H. (1982) *Ecology of Tropical Savannas*. Ecological Studies 42. Springer-Verlag,

Huston, M. A. (1991) Use of individual-based forest succession models to link physiological whole-tree methods to landscape-scale ecosystem models. Tree Physiology, 9, 293-306.

IGBP (1990) *The International Geosphere-Biosphere Programme: A Study of Global Change. The Initial Core Projects*. IBGP Report 12 (June 1990). IGBP/ICSU, Stockholm.

IPCC (1990) *Climate Change: The IPCC Scientific Assessment*. Cambridge University Press, Cambridge.

IPCC (1992) *Climate Change: The supplementary report to the IPCC scientific assessment*. Cambridge University Press, Cambridge.

IPCC (1994) *Climate Change: The supplementary report to the IPCC scientific assessment.* Cambridge University Press, Cambridge.

Jackson, W. A. and Volk, R. J. (1970) Photorespiration. Annual Review of Plant Physiology, 21, 385-432.

Jarvis, P. G. (1976) The interpretation of the variations in in leaf water potential and stomatal conductance found in canopies in the field. Phil. Trans. Roy. Soc. London (B), 273, 593-610.

Jarvis, P. G. and Dewar, R. C. (1993) Forests in the global carbon balance: from stand to region in *Scaling Physiological Processes: Leaf to Globe* by J.R. Ehleringer and C.B. Field. Academic Press, San Diego. pp. 191-221.

Jarvis, P. G. and Leverenz, J. W. (1983) Productivity of temperate deciduous and evergreen forests in *Encyclopaedia of Plant Physiology, Vol. 12(D)* by O.L. Lange, P.S. Nobel, C.B. Osmond and H. Ziegler. Springer-Verlag, pp. 233-280.

Jarvis, P. G. and McNaughton, K. G. (1986) Stomatal control of transpiration: scaling up from leaf to region. Advances in Ecological Research, 15, 1-49.

Jarvis, P. G., Miranda, H. S. and Muetzelfeldt, R. M. (1985) Modelling canopy exchanges of water vapour and carbon dioxide in coniferous forest plantations in The Forest-Atmosphere Interaction by B.A. Hutchison and B.B. Hicks. Reidel, Dordrecht, The Netherlands. pp. 521-542.

Jones, H. G. (1992) *Plants and Microclimate.* 2nd Edn. Cambridge University Press, Cambridge.

Jong, E. de, Redmann, R. E. and Ripley, E. A. (1979) A comparison of methods to measure soil respiration. Soil Science, 127, 300-306.

Kanemasu, E. T., Powers, W. L. and Sij, J. W. (1974) Field chamber measurements of CO_2 flux from soil surface. Soil Science, 118, 233-237.

Kellog, W. W. (1983) Feedback mechanisms in the climate system affecting future levels of carbon dioxide. J. Geophys. Res., 88(C2), 1263-1269.

Kim, J. and Verma, S. B. (1990) Carbon dioxide exchange in a temperate grassland ecosystem. Boundary Layer Meteorology, 53, 135-149.

Kim, J. and Verma, S. B. (1991) Modelling canopy photosynthesis: scaling up from a leaf to canopy in a temperate grassland ecosystem. Agric. Forest Meteorol., 57, 187-208.

Kramer, P. J. and Kozlowski, T. T. (1960) *Physiology of Trees.* McGraw-Hill, New York.

Kruijt, B., Ongeri, S. and Jarvis, P. G. (in prep.) Scaling up from leaf to canopy in *Scaling Up.* SEB Seminar series by P. Van Gardingen, G. Foody and P. Curran. Cambridge University Press, Cambridge.

Kucera, C. L. and Kirkham, D. R. (1971) Soil respiration studies in tallgrass prairie in Missouri. Ecology, 52, 912-915.

Landsberg, J. J. (1986) *Physiological Ecology of Forest Production.* Academic Press, London.

Landsberg, J. J., Jarvis, P. G. and Slater, M. B. (1973) The radiation regime of a spruce forest in Plant Response to Climatic Factors Unesco, Proc. Uppsala Symp. pp. 411-418.

Lang, A. R. G. (1986) Leaf area and average leaf angle from transmission of direct sunlight. Australian Journal of Botany, 34, 349-355.

Lang, A. R. G. (1987) Simplified estimates of leaf area index from transmittance of the sun's beam. Agricultural and Forest Meteorology, 41, 179-186.

Lang, A. R. G., Yuequin, X. and Norman, J. M. (1985) Crop structure and the penetration of direct sunlight. Agricultural and Forest Meteorology, 35, 83-101.

Lang, A. R. G. and Yuequin, X. (1986) Estimation of leaf area index from transmission of direct sunlight in discontinuous canopies. Agric. For. Meteorol., 37, 229-243.

Larcher, W. (1980) *Physiological Plant Ecology*. Springer-Verlag, Berlin.

Laval, K. and Picon, L. (1986) Effect of a change of surface albedo of the sahel on climate. J. Atmos. Sci., 43, 2418-2429.

Lawson, G. W. (1986) *Plant Ecology in West Africa*. John Wiley, London.

Le Houerou, H. N. (1989) *The Grazing Land Ecosystems of the African Sahel*. Ecological Studies 75. Springer-Verlag, Berlin.

Leuning, R. (1995) A critical appraisal of a combined stomatal-photosynthesis model for C3 plants. Plant, Cell and Environment, 18(4), 339-356.

Leuning, R. and Moncrieff, J. B. (1990) Eddy covariance CO_2 flux measurements using open- and closed-path CO_2 analysers: corrections for analyser water vapour sensitivity and damping of fluctuations in air sampling tubes. Boundary Layer Meteorology, 53, 63-76.

Leverenz, J. W. (1981) Photosynthesis and transpiration inlarge forest-grown Douglas fir: diurnal variation. Can. J. Bot., 59(3), 349-356.

Leverenz, J., Deans, J. D., Ford, E. D., Jarvis, P. G., Milne, R. and Whitehead, D. (1982) Systematic spatial variation of stomatal conductance in a Sitka spruce plantation. J. Appl. Ecol., 19, 835-851.

Linder, S. and Troeng, E. (1981) The seasonal variation in stem and coarse root respiration of a 20-year-old Scots pine (Pinus sylvestris L.) in *Radial Growth in Trees* by W. Tranquillini. Mitt. Forstl. Bundes-Versuchant., Wien. pp. 125-139.

Lloyd, J., Grace, J., Miranda, A. C., Meir, P., Wong, S. C., Miranda, H. S., Wright, I. R., Gash, J. H. C. and McIntyre, J. (1995) A simple calibrated (SiC) model of Amazon rainforest productivity based on leaf biochemical properties. Plant, Cell and Environment, in press.

Lohammer, T., Larson, S., Linder, S. and Falk, F.O. (1980) FAST - a simulation model of gaseous exchange in Scots pine. Ecological Bulletin, 32, 505-523.

Ludlow, M. M. and Jarvis, P. G. (1971) Photosynthesis in Sitka spruce (Picea sitchensis (Bong.) Carr.). I. General characteristics. J. Appl. Ecol., 8, 925-953.

Luxmoore, R. J., King, A. W. and Tharp, M. L. (1991) Approaches to scaling up physiologically based soil-plant models in space and time. Tree Physiology, 9, 281-292.

Marshall, J. D. and Ehleringer, J. R. (1990) Are xylem-tapping mistletoes partially heterotrophic? Oecologia, 84, 244-248.

Marshall, J. D., Ehleringer, J. R., Schulze, E.-D. and Farquhar, G. D. (1994) Carbon isotope composition, gas exchange and heterotrophy in Australian mistletoes. Functional Ecology, 8(2), 237-241.

Martin, T. A., Teskey, R. O. and Dougherty, P. M. (1994) Movement of respiratory CO_2 in stems of loblolly pine (Pinus taeda L.) seedlings. Tree Physiology, 14, 481-495.

McGinn, S. M. and King, K. M. (1990) Simultaneous measurements of heat, water and CO_2 fluxes above alfalfa and maize. Agricultural and Forest Meteorology, 49(4), 331-350.

McMurtrie, R. E. and Wang, Y.-P. (1993) Mathematical models of the photosynthetic response of tree stands to rising CO_2 concentrations and temperatures. Plant, Cell and Environment, 16(1), 1-14.

McNaughton, K. G. (1989) Regional interactions between canopies and the atmosphere in *Plant Canopies: their Growth, Form and Function* by G. Russell, B. Marshall and P.G. Jarvis. Cambridge University Press, Cambridge. pp. 63-81.

McNaughton, K. G. and Jarvis, P. G. (1991) Effects of spatial scale on stomatal control of transpiration. Agric. Forest Meteorol., 54, 279-301.

Meir, P. Grace, J., Lloyd, J. and Miranda, A.C. (1996) Soil respiration in a rain forest in Amazonia, and in cerrado in Central Brazil in *Amazonian Deforestation and Climate* by J. H. C. Gash, C. A. Nobre, J. M. Roberts and R. L. Victoria. John Wiley and Sons, UK.

Moncrieff, J.B., Verma, S.B. and Cook, D.R. (1992) Intercomparison of eddy correlation carbon dioxide sensors during FIFE 1989. J. Geophys. Res., 97, 18725-18730.

Moncrieff, J. B., Monteny, B. and Verhoef, A. *et al.* (1996, in press) Spatial and temporal variations in net carbon flux during HAPEX-Sahel. J. Hydrology.

Moncrieff, J. B., Monteny, B. and Verhoef, A. *et al.* (1996, in press) A system to measure surface fluxes of carbon dioxide, water vapour and sensible heat. J. Hydrology.

Monod, T. (1954) Modes contractes et diffus de la vegetation saharienne in *Biology of Deserts* by J.L. Cloudsley-Thompson. Institute of Biology, London. pp. 35-44.

Monod, T. (1986) The Sahel zone north of the equator in *Ecosystems of the World vol 12B: Hot Deserts and Arid Shrublands* by M. Evenari, I. Noy-Meir and D. W. (eds) Goodall.

Monsi, M. and Saeki, T. (1953) Uben den Lichtfaktor in den Pflanzengesellschaften und seine Bedeutung fur die Stoff produktion. Jap. J. Bot., 14(1), 22-52.

Monteith, J. L. (1965) Light distribution and photosynthesis in field crops. Annals of Botany, 29, 17-37.

Monteith, J. L. (1969) Light interception and radiative exchange in crop stands in Physiological Aspects of Crop Yield by J.D.Eastin, F.A. Haskins, C.Y. Sullivan and C.H.M. van Bavel. American Society of Agronomy, Madison, USA. pp. 89-110.

Monteith, J. L. (1962) Measurement and interpretation of carbon dioxide fluxes in the field. Netherlands Journal of Agricultural Science, 10, 334-346.

Monteith, J. L. (1995) A reinterpretation of stomatal responses to humidity. Plant, Cell and Environment, 18(4), 357-364.

Monteith, J. L. and Unsworth, M. H. (1990) *Principles of Environmental Physics*. Edward Arnold, London.

Mooney, H. A., Drake, B. J. and Luxmoore, R. J. (1991) Predicting ecosystem responses to elevated CO_2 concentrations. Bioscience, 41(2), 96-104.

Mooney, H. A., Vitousek, P. M. and Matson, P. A. (1987) Exchanges of materials between terrestrial ecosystems and the atmosphere. Science, 238, 926-932.

Moore, C.J. (1986) Frequency corrections for eddy correlation systems. Boundary Layer Meteorology, 37: 17-35.

Morales, C. (1977) Rainfall variability - a natural phenomenon. Ambio, 6(1), 30-33.

Neftel, A., Moor, E., Oeschger, H. and Stauffer, B. (1985) Evidence from polar ice cores for the increase in atmospheric CO_2 in the past two centuries. Nature, 315, 45-47.

Negisi, K. (1979) Bark respiration rate in stem segments detached from young Pinus densiflora trees in relation to velocity of artificial sap flow. J. Jpn. For. Soc., 61(3), 88-93.

Negisi, K. (1981) Diurnal and seasonal fluctuations in the stem bark respiration of a standing Quercus myrsinaefolia tree. J. Jpn. For. Soc., 63, 235-241.

Nicholson, S. E. (1989) Long term changes in African rainfall. Weather, 44, 46-64.

Norman, J. M. and Campbell, G. S. (1989) Canopy structure in *Plant Physiological Ecology: field methods and instrumentation* by R. W. Pearcy, J. Ehleringer, H.A. Mooney and P.W. Rundel (eds). Chapman and Hall, London. pp. 301-326.

Norman, J. M. and Jarvis, P. G. (1974) Photosynthesis in Sitka spruce (Picea sitchensis (Bong.) Carr.). III. Measurement of canopy structure and interception of radiation. J. Appl. Ecol., 11, 375-398.

Norman, J. M. and Welles, J. M. (1983) Radiative transfer in an array of canopies. Agronomy Journal, 75, 481-488.

Norman, J.M., Garcia, R. and Verma, S.B. (1992) Soil surface CO_2 fluxes and the carbon budget of grassland. J. Geophys. Res., 97, 18845-18543.

Parkinson, K. J. (1983) Porometry in *Instrumentation for Environmental Physiology* by F. I. Woodward (ed.). CUP, Cambridge.

Pearman, G. I. and Garratt, J. R. (1973) Space and time variations of tropospheric carbon dioxide in the southern hemisphere. Tellus, 25, 309-311.

Penning de Vries, F. W. T. (1975) The cost of maintenance processes in plant cells. Annals of Botany, 39, 77-92.

Penning de Vries, F. W. T., Jansen, D. M., ten Berge, H. F. M. and Bakema, A. (1989) Simulation of ecophysiological processes of growth in several annual crops. Pudoc, Wageningen.

Perry, T. O. (1971) Winter-season photosynthesis and respiration by twigs and seedlings of deciduous and evergreen trees. Forest Science, 17(1), 41-43.

Pierce, L. L. and Running, S. W. (1988) Rapid estimation of LAI using a portable integrating radiometer. Ecology, 69, 1762-7.

Potter, G. L., Ellsaesser, H. W., MacCracken, M. C. and Luther, F. M. (1975) Possible climatic impact of tropical deforestation. Nature, 258, 697-698.

Prince, S. D., Kerr, Y. H., Goutorbe, J. P., Lebel, T., Bessemoulin, P., Brouwer, J., Dolman, A. J., Engman, E. T., Gash, J. H. C., Hoepffner, M., Kabat, P., Monteny, B., Said, F., Sellers, P. and Wallace, J. (in press) Geographical, biological and remotesensing aspects of the Hydrological Atmospheric Pilot Experiment in the Sahel (HAPEX-Sahel). J. Hydrol.,

Raupach, M. R., Denmead, O. T. and Dunin, F. X. (1992) Challenges in linking atmospheric CO_2 concentrations to fluxes at local and regional scales. Aust. J. Bot., 40, 697-716.

Raupach, M. R., Denmead, O. T., Dunin, F. X. and McNaughton, K. G. (unpubl.) Inferring regionally averaged surface fluxes of conserved scalars from convective boundary layer budgets. Submitted to J. Geophysical Research,

Raven, J. A. and Farquhar, G. D. (1989) Leaf apoplast pH estimation in Phaseolus vulgaris in Plant Membrane Transport: The Current Position by J. Dainty, M.I. De Michels, E. Marre and F. Rasi-Caldogno. Elsevier, Amsterdam. pp. 607-610.

Redmann, R. E. (1970) Seasonal dynamics of CO_2 exchange in a mixed grassland ecosystem. Canadian Journal of Botany, 56(3), 1999-2005.

Reed, K. L., Hamerly, E. R., Dinger, B. E. and Jarvis, P. G. (1976) An analytical model for field measurements of photosynthesis. Journal of Applied Ecology, 13, 925-932.

Reynolds, J. F., Chen, J., Harley, P. C., Hilbert, D. W., Dougherty, R. L. and Tenhunen, J. D. (1992) Modelling the effects of elevated CO_2 on plants: extrapolating leaf response to a canopy. Agric. Forest. Meteorol., 61, 69-84.

Ripley, E. A. (1976) Drought in the Sahara: insufficient biogeophysical feedback? Science, 191(1), 100.

Ross, J. (1981) The Radiation Regime and Architecture of Plant Stands. Junk, The Hague.

Le Roux, X. and Mordelet, P. (in press) Leaf and canopy CO_2 assimilation in a West African humid savanna during the early growing season. J. Trop. Ecol.

Rowntree, P. R. and Bolton, J. A. (1983) Simulation of the atmospheric response to soil moisture anomalies over Europe. Quarterly Journal of the Royal Meteorological Society, 109, 501-526.

Ruimy, A., Jarvis, P. G., Baldocchi, D. D. and Saugier, B. (1995) CO_2 fluxes over plant canopies and solar radiation: a review. Submitted to Advances in Ecological Research,

Ryan, M. G. (1990) Growth and maintenance respiration in stems of Pinus contorta and Picea engelmannii. Can. J. For. Res., 20, 48-57.

Ryan, M. G., Hubbard, R. M., Clark, D. L. and Sanford, R. L. (1994) Woody tissue respiration for Simarouba amara and Minquartia guianensis, two tropical wet forest trees with different growth habits. Oecologia, 100(3), 213-220.

Ryan, M. G., Gower, S. T., Hubbard, R. M., Waring, R. H., Gholz, H. L., Cropper, W. P. and Running, S. W. (in press) Stem maintenance respiration of four conifers in contrasting climates. Oecologia.

Schuepp, P.H., Leclerc, M.Y., Macpherson, J.I. and Desjardins, R.I. (1990) Footprint prediction of scalar fluxes from analytical solutions of the diffusion equation. Boundary Layer Meteorology, 9: 355-373.

Schulze, E.-D. (1993) Soil water deficits and atmospheric humidity as enironmental signals in *Water Deficits: Plant responses from cell to community* by J.A.C. Smith and H. Griffiths. BIOS, Oxford, UK. pp. 129-146.

Schurr, U., Gollan, T. and Schulze, E.-D. (1992) Stomatal response to drying soil in relation to changes in the xylem sap composition of Helianthus annuus. II. Stomatal sensitivity to abscisic acid imported from the xylem sap. Plant, Cell and Environment, 15(5), 561-568.

Schurr, U. and Schulze, E.-D. (1995) The concentration of xylem sap constituents in root exudate, and in sap from intact, transpiring castor bean plants. Plant, Cell and Environment, 18(4), 409-420.

Sellers. P.J., Hall, F. G., Asrar, G., Strebel, D. E. and Murphy, R. E. (1988) The First ISLSCP Field Experiment (FIFE). Bull. Am. Meteorol. Soc., 69, 22-27.

Sellers, P. J. (1987) Modelling effects of vegetation on climate in *The Geophysiology of Amazonia* by R. E. (ed) Dickinson. John Wiley,

Sellers, P. J., Berry, J. A., Collatz, G. J., Field, C. B. and Hall, F. G. (1992) Canopy reflectance, photosynthesis and transpiration. III. A reanalysis using improved leaf models and a new canopy integration scheme. Remote Sens. Environ., 42, 187-216.

Sellers, P. J., Hall, F. G., Asrar, G., Strebel, D. E. and Murphy, R. E. (1992) An overview of the First International Satellite Land Surface Climatology Project (ISLSCP) Field Experiment (FIFE). J. Geophys. Res., 97(D17), 18345-18373.

Sellers, P. J., Heiser, M. D. and Hall, F. G. (1992) Relations between surface conductance and spectral vegetation indices at intermediate (100 m2 to 15 km2) length scales. J. Geophys. Res., 97(D17), 19033-19059.

Sellers, P. J., Mintz, Y., Sud, Y. C. and Dalcher, A. (1986) A simple biosphere model (SiB) for use within General Circulation Models. Journal of Atmospheric Science, 43, 505-531.

Sinclair, T. R., Murphy, C. E. Jr. and Knoerr, K. R. (1976) Development and evaluation of simplified models for simulating canopy photosyynthesis and transpiration. J. Appl. Ecol., 13, 813-829.

Sivakumar, M. V. K. (1987) *Climate of Niamey*. Progree Report 1. ICRISAT, Niamey, Niger.

Smith, T. M. and Shugart, H. (1993) The transient response of terrestrial carbon storage to a perturbed climate. Nature, 361, 523-526.

Soil Survey Staff (1975) Soil taxonomy: a basic system for making and interpreting soil surveys. USDA, US Government Printing Office, Washington, D.C.

Sprugel, D. G. and Benecke, U. (1991) Measuring woody-tissue respiration and photosynthesis in Techniques and Approaches in Forest Tree Ecophysiology by J.P. Lassoie and T.M. Hinckley. CRC Press, Berlin. pp. 329-355.

Sprugel, D. G., Ryan, M. G., Brooks, J. R., Vogt, K. A. and Martin, T. A. (1993) Respiration from the organ level to the stand in *Physiological Ecology of Coniferous Forests* by W.K. Smith and T.M. Hinckley.

Stocker, T. F., Broecker, W. S. and Wright, D. G. (1994) Carbon uptake experiments with a zonally-averaged global ocean circulation model. Tellus, 46(B), 103-122.

Stumm, W. and Morgan, J. J. (1981) *Aquatic Chemistry*. John Wiley and Sons, New York.

Sud, Y. C., Sellers, P. J., Mintz, Y., Chou, M. D., Walker, G. K. and Smith, W. E. (1990) Influence of the biosphere on the global circulation and hydrologic cycle - a GCM simulation experiment. Agricultural and Forest Meteorolology, 52(1-2), 133-180.

Tanaka, M., Nakazawa, T. and Aoki, S. (1983) Concentration of atmospheric carbon dioxide over Japan. J. Geophys. Res., 88(C2), 1339-1344.

Tans, P. P., Fung, I. Y. and Takahashi, T. (1990) Observational constraints on the global atmospheric CO_2 budget. Science, 247, 1431-1438.

Thornley, J. H. M. (1976) *Mathematical Models in Plant Physiology*. Academic Press, London.

Vandenbeldt, R. J. and Williams, J. H. (1992) The effect of soil surface temperature on the growth of millet in relation to the effect of Faidherbia albida trees. Agric. Forest Meteorol., 60, 93-100.

Vapaavuori, E. M. and Pelkonen, P. (1985) HCO3- uptake through the roots and its effect on the productivity of willow cuttings. Plant, Cell and Environment, 8, 531-534.

Verma, S.B., Baldocchi, D.D., Anderson, D.E. et al. (1986) Eddy fluxes of CO_2, water vapour and sensible heat over deciduous forest. Boundary layer Meteorology, 36, 71-91.

Verma, S.B., Kim, J. and Clement, R.J. (1989) CO_2, H_2O and sensible heat fluxes over a tallgrass prairie. Boundary Layer Meteorology, 46, 53-67.

Von Caemmerer and Farquhar, G. D. (1981) Some relationships between the biochemistry of photosynthesis and the gas exchange of leaves. Planta, 153, 376-387.

Von Maydell, H. J. (1990) *Trees and Shrubs of the Sahel: their characteristics and uses*. GTZ, Eschborn.

Vose, J. M. and Swank, W. T. (1990) Assessing seasonal LAI dynamics and vertical leaf area distribution in eastern white pine with a portable light meter. Tree Physiology, 7, 125-134.

Vuorinen, A. H., Vapaavuori, E. M. and Lapinjoki, S. (1989) Time course of uptake of dissolved inorganic carbon through willow roots in light and in darkness. Physiologia Plantarum, 77, 33-38.

Wallace, J., Brouwer, J. and Allen, S. J. et al. (1994) *HAPEX-Sahel Southern Super-Site Report: An overview of the site and the experimental programme during the intensive observation period in 1992*. Institute of Hydrology, Wallingford.

Wallace, J. S., Roberts, J. M. and Sivakumar, M. V. K. (1990) The estimation of transpiration from sparse dryland millet using stomatal conductance and vegetation area indices. Agric. Forest Meteorol., 51, 35-49.

Wang, Y. P. and Jarvis, P. G. (1990) Description and validation of an array model - MAESTRO. Agric. Forest Meteorol., 51, 251-280.

Wang, Y. P., Massheder, J. M., Barton, C. V. M. and Jarvis, P. G. (1992) *Documentation for the model MAESTRO*. University of Edinburgh, Edinburgh.

Wang, Y.-P., McMurtrie, R. E. and Landsberg, J. J. (1992) Modelling canopy photosynthetic productivity in *Crop Photosynthesis: Spatial and Temporal Determinants* by N.R. Baker and H. Thomas. Elsevier, Amsterdam. pp. 43-67.

Wang, Y. S. and Miller, D. R. (1987) Calibration of the hemispherical photographic technique to measure LAI distributions in hardwood forests. Forest Science, 33, 210-216.

Watson, R. L., Landsberg, J. J. and Thorpe, M. R. (1978) Photosynthetic characteristics of the leaves of 'Golden Delicious' apple trees. Plant, Cell and Environment, 1, 51-58.

Waygood, E. R. (1961) Respiration in *Encyclopaedia of the Biological Sciences* by P. Gray (ed.). Reinhold, New York. pp. 879-883.

Webb, E. K., Pearman, G. I. and Leuning, R. (1980) Correction of flux measurements for density effects due to heat and water vapour transfer. Quart. J. Roy. Meteorol. Soc., 106, 85-100.

West, L. T., Wilding, L. P., Landeck, J. K. and Calhoun, F. G. (1984) Soil survey of the ICRISAT Sahelian Centre, Niger, West Africa. Texas A&M University, College Station, Texas.,

White, F. (1983) *The Vegetation of Africa*. UNESCO.

White, L. P. (1970) Brousse Tigree patterns in southern Niger. Journal of Ecology, 58, 549-553.

White, L. P. (1969) Vegetation arcs in Jordan. Journal of Ecology, 57, 461-464.

White, L. P. (1971) Vegetation stripes on sheet wash surfaces. Journal of Ecology, 59, 615-622.

Whitehead, D., Okali, D. U. U. and Fasehun, F. E. (1981) Stomatal response to environmental variables in two tropical forest species during the dry season in Nigeria. J. Appl. Ecol., 18, 571-587.

Wickens, G. E. and Collier, F. W. (1971) Some vegetation patterns in the Republic of Sudan. Geoderma, 6, 43-59.

Wofsy, S. C., Goulden, M. L., Munger, J. W., Fan, S. M., Bakwin, P. S., Daube, B. C., Bassow, S. L. and Bazzaz, F. A. (1993) Net exchange of CO_2 in a mid-latitude forest. Science, 260, 1314-1317.

Wong, S. C. and Dunin, F. X. (1987) Photosynthesis and transpiration of trees in a Eucalyptus forest stand: CO_2, light and humidity responses. Aust. J. Plant Phys., 14, 619-632.

Wood, E. F. (1991) *Land Surface-Atmosphere Interactions for Climate Modelling: Observations, Models and Analysis*. Kluwer Academic, Dordrecht.

Woodrow, I. E. et al. (1990) Control of photosynthesis by gs, gb and RUBISCO. Plant, Cell and Environment, 13(4), 339-349.

Worral, G. A. (1959) The Butana grass patterns. Journal of Soil Science, 10, 34-53.

Worral, G. A. (1960) Patchiness in vegetation in the northern Sudan. Journal of Ecology, 48, 107-115.

Worral, G. A. (1960) Tree patterns in the Sudan. Journal of Soil Science, 11, 63-67.

Xue, Y., Liou, K-N and Kashara, A. (1990) Investigations of biogeophysical feedback on the African climate using a 2-D model. Journal of Climatology, 3, 337-352.

Xue, Y. and Shukla, J. (1993) The influence of land surface properties on Sahel climate. Part 1: Desertification. J. Climate, 6, 2232-2245.

Yeh, T. C., Wetherald, R. T. and Manabe, S. (1984) The effect of soil moisture on the short term climate and hydrology change. A numerical experiment. Monthly Weather Review, 112, 474-490.

A.1 LCA3 photosynthesis system

A.1.1 Description

Measurements of leaf CO_2 flux and stomatal conductance were made using a portable leaf gas exchange system (Leaf chamber analysis system (LCA3) and Parkinson leaf chambers (PLC3(C) and PLC3(N), ADC, Hoddeson, Herts, UK). This operates as an open system, drawing ambient air into the leaf chamber via a 2.75 m mast through a 1 dm^3 buffering volume and through soda lime, desiccant and humidifier if required. A sample of this air is passed to the infra-red gas analyser (IRGA) to determine its CO_2 concentration. After passing through the leaf chamber, a sample of the air is returned to the IRGA and its CO_2 concentration measured once more. The IRGA works as a semi-differential analyser, although there is only a single sample cell, because the different air streams are passed through it sequentially. The air passing through the IRGA sample cell is controlled by two solenoid valves which operate a ten second cycle (2.5 seconds each on reference air (ie. air entering the leaf chamber), CO_2-free air (to set the zero), analysis air (ie. air leaving the leaf chamber) and CO_2-free air again). The absorption of the sample gas in the 4.26 μm band, emitted by a source bulb, is measured by a pyroelectric detector. The absolute sensitivity to water vapour in this band is very small. Corrections are made for dilution of CO_2 by water vapour and broadening of the CO_2 absorption band by water vapour.

Humidity of the air entering and leaving the chamber is measured by Coreci humidity sensors mounted in the PLC inlet and outlet. These consist of a thin film of a hygroscopic polymer separating two metal electrodes. The capacitance of the polymer changes with humidity, as water molecules move in or out of the pores. One of the electrodes is very thinly plated on (approx. 0.02 um) so that water can diffuse through it rapidly, producing a relatively fast response time of less than a second, although the response is slower above 75-80 % RH. Furthermore, the sensors exhibit hysteresis above this point as the polymer film swells and absorbs additional water vapour which is only slowly lost when returned to low humidity. Air temperature is measured by a "Betatherm" precision thermistor mounted in the chamber head. Leaf temperature can be measured by a thermistor which plugs into a socket on the outside of the PLC. Alternatively, leaf temperature can be calculated from the energy balance (Parkinson, 1983). Photosynthetic photon flux density (Q) is measured by a filtered selenium photocell mounted on top of the chamber.

A.1.2 Calibration

IRGA

The IRGA is easily calibrated via the LCA3 software when supplying air of known CO_2 concentration. This was obtained in Edinburgh using Wosthoff pumps or cylinders of compressed air which had been measured by an analyser with a recent calibration. The latter were shipped from Edinburgh to Niger

as no other facilities were available there. The calibration was made at a concentration close to ambient, so as to be within the normal operating range.

Humidity sensors

The PLC3 humidity sensors are calibrated by adjusting potentiometers inside the PLC handle whilst supplying air of known relative humidity to the chamber. In Edinburgh, this was obtained using a water bath system. Air was drawn from the laboratory by a pump and bubbled through water so as to saturate it with water vapour. The air was then pumped through a long coil of thin copper tubing immersed in a water bath held at a constant temperature below that of room temperature. Excess water vapour condenses out and the vapour pressure of the air is then equal to the saturation vapour pressure (SVP) at water bath temperature. This air was then passed to the PLC where the relative humidity, H, is given by:

$$H = e_{sw} / e_{sc}$$

where e_{sw} is SVP at water bath temperature and e_{sc} is SVP at leaf chamber temperature as measured by the temperature sensor in the PLC.

A water bath was not available in Niger, so an alternative method was used, utilising a water vapour generator (WG-600, ADC, Hoddeson, Herts, UK). This works by mixing dry air with air saturated with water vapour from ferrous sulphate crystals held at a known, constant temperature in an aluminium block. The two air streams are mixed together to give a range of humidities by switching them through a set of five precisely calibrated critical flow orifices. This seemed to work satisfactorily in Niger although the system may be susceptible to errors caused by contamination of the orifices by dirt or ferrous sulphate particles. Much more drift was observed in the calibration of the outlet humidity sensor, presumably as this was exposed to higher humidities. On a short term basis, the outlet sensor could be recalibrated to give the same value as the inlet sensor when running with the chamber empty. The sensors seem to be sensitive to pressure, as the reading from a given sensor will change depending on whether air is passed in through the chamber inlet or outlet. They were therefore calibrated with the air being passed through the inlet (not as recommended in the manual).

Temperature sensors

The leaf temperature thermistor circuit was calibrated using standard resistors of 2 kohm (equivalent to 25 °C) and 1.15 kohm (equivalent to 40 oC) soldered on to jack plugs and inserted into the thermistor socket. Potentiometers inside the PLC handle could then be adjusted. The air temperature thermistor could not be calibrated.

Mass flowmeters

The mass flowmeters were checked in winter 1991 using the soap bubble technique, in which the air stream is passed through a large burette with soap solution at the bottom. Bubbles are formed which move up the cylinder and can be timed as they pass marks on the glass which mark a known volume (1 dm^3 in this case). No recalibration was needed as results were satisfactory, typically within 2 cm^3 min^{-1} at 500 cm^3 min^{-1}.

A.1.3 Boundary layer resistance measurement

The boundary layer resistance of a leaf or shoot in the chamber needs to be known so that the stomatal resistance can be inferred from evaporation measurements. For the PLC(N), designed for single leaves of broadleaved species, wet filter paper was suspended inside the chamber to simulate a leaf with no stomatal resistance. A 2 x 1 cm hole was cut in a plastic bag and the wet filter placed inside. This was held in the chamber as a leaf would be. The boundary layer resistance is then calculated from the equilibrium relative humidity reached in the chamber when supplying dry air (Parkinson, 1984; ADC, 1990). For the PLC(C), designed for conifer shoots and used for measurements on *G. senegalensis* which has very small leaves (typically 2 x 1 cm), a similar procedure was used. A *G. senegalensis* shoot thoroughly wetted in water with a few drops of detergent added was used in place of the bag containing wet filter paper. This was repeated several times using shoots of different sizes and shapes. Variability was relatively small for a range of *G. senegalensis* shoots (boundary layer resistances of 0.75-0.92 m^2 s mol^{-1}). Average boundary layer resistance values of 0.21 and 0.84 m^2 s mol^{-1} were obtained for the PLC(N) and PLC(C), respectively.

A.1.4 System response time

It is necessary to know the length of time needed for the system to reach equilibrium after placing a leaf in the chamber for measurement. This depends on the chamber volume and flow rate used. For the PLC(N), with a volume of 12 cm3, equilibrium is reached within 30 seconds using a flow rate of 300 cm^3 min^{-1}. For the PLC(C), with a volume of 137 cm^3, this takes about 1.5 minutes using a flow rate of 500 cm^3 min^{-1}: thus, higher flow rates were generally used with this chamber.

A.1.5 Problems

The LCA3 exhibited several minor problems, most apparently the result of bugs in the software on the PROM chip. After pressing the display change key, leaf temperature (whether calculated or measured) takes the value 0 oC. Leaf temperature cannot therefore be monitored whilst making measurements, which would be useful as the measurements cause an increase in the temperature of the leaf. Similarily, erratic CO_2 readings (usually about zero or several thousand ppm) would occur occasionally when recording measurements. When altering flow rate whilst in record mode, the main

pump would sometimes stop. Unless the change in tone is audible, this is only noticed as a build up of humidity in the chamber when making a measurement.

Overheating of the LCA3 did occur if left in the sun for a number of hours but was not a serious problem. Overheating always led to the liquid crystal display failing first, before any other potentially more serious problems occurred. The display was restored if left in the shade for 5-15 minutes. The PLC inevitably became hot during measurement periods because of exposure to solar radiation. This did not cause any operational problems with the equipment but altered the environment to which the leaf was exposed whilst being measured. Except at the tiger bush site, shading between measurements was impractical because of the lack of shade, and the relatively large thermal mass of the chamber (the chamber would take several minutes to cool down significantly).

A.2 Weather station

A weather station was erected at each site and left in place over the growing seasons in 1991 and 1992. All instruments were initially mounted on 2 m masts with a cross arm at 1.5 m, although some were mounted on the micrometeorological towers in 1992. A solid state data logger (21X and CR10, Campbell Scientific Ltd, Loughborough, UK) was used to record output every 10 seconds and average over 5 or 10 minutes. On some occassions during the IOP in 1992 instruments failed and data from the IH weather station were used. This was made up of similar instruments on an adjacent micrometeorological tower.

Net radiation

Three single dome hemispherical net radiometers (Q5.5, REBS, Seattle, Washington, USA) were used. These had been converted from the double dome Q4 design and had been calibrated by the manufacturer in 1991. These, and all other radiation sensors, were checked at the beginning of the field season in 1991 and 1992 by running all instruments together in an open space at the ISC.

Photosynthetic photon flux density

Around 30 Macam and home-made quantum sensors were used for incident and transmitted Q measurements. These were calibrated on the Darwin building roof in Edinburgh over several days against a quantum sensor (LI-140, Li-Cor Inc., Lincoln, Nebraska, USA) kept in the laboratory for this purpose .

Total solar radiation

Three solarimeters (CM3, Kipp-Zonen, Delft, Netherlands) were used. These were calibrated against a fourth "Kipp" solarimeter with a recent calibration on the Darwin building roof in 1991.

Wind speed

Two cup anemometers (A100, Vector Instruments, Rhyl, UK) were used to measure horizontal wind speed at 1.5 m. The manufacturers calibration was used and close agreement was found when checked against other Vector and Met One anemometers at ISC.

Wind direction

A potentiometric wind vane (W200P, Vector Instruments, Rhyl, UK) was used to measure wind direction.

Air temperature and humidity

Ten psychrometers were constructed to the design of Allen, Brenner and Grace (1994). These consist of a section of white plastic piping containing wet and dry "bulb" themometers and a fan to aspirate them. The wet bulb consists of a length of tubular cotton wick (actually a shoe lace, softened and degreased by boiling in dilute NaOH), stretched over a plastic tube and supplied with water from a resevoir, which is allowed to freely evaporate. The dry bulb temperature is measured by a thermistor. A Cu-Con thermocouple with a junction in both wet and dry bulbs measures the temperature difference between the two. Water is initially forced from the resevoir (a water bottle mounted on the plastic pipe) to the bulb by blowing into the bottle until the bulb drips so as to ensure a continuous column of water is present. The height of the resevoir can then be adjusted so that water is not dripping from the bulb.

Table A.3.1 Parameters values fitted to the Jarvis *et al.* (1985) model (Equations 3.2-3.12) when Γ was not fixed. All data collected in 1992 were used in the analysis. Although physiologically realistic values of Γ were not obtained, these parameters gave a better fit to the data than when Γ was fixed (Table 3.5) and were used in MAESTRO. The units of α are mol of CO_2 per mol of quanta.
* indicates fixed parameters; † indicates parameters which reached their constraint.

Species	α	θ	g_m (mol m^{-2} s^{-1})	Γ (μmol mol^{-1})	R_o (μmol m^{-2} s^{-1})	k ($°C^{-1}$)	r^2	n
Millet	0.031	0	13.967	177.0	0.697	0.0469	0.92	216
E. tremula	0.024	0.997	4.257	128.58	1.179	0.010†	0.91	97
G. senegalensis	0.025	0.442	0.139	211.87	1.479	0.010†	0.87	271
C. micranthum	0.024	0.846	0.170	188.4	0.868	0.024	0.87	367
C. nigricans	0.025	0	0.182	207.4	0.413*	0.054*	0.76	304
A. ataxacantha	0.029	0.694	0.587	247.2	1.213	0.004	0.92	16

Table A.3.2 Asymptotic standard errors in parameters values in Table A.3.1.

Species	α	θ	g_m (mol m^{-2} s^{-1})	Γ (μmol mol^{-1})	R_o (μmol m^{-2} s^{-1})	k ($°C^{-1}$)
Millet	0.0029	0.455	3.044	3.7	1.057	0.0427
E. tremula	0.0009	0.061	4.329	5.2	1.940	0.0476
G. senegalensis	0.0047	0.349	0.023	10.7	1.262	0.0267
C. micranthum	0.0022	0.114	0.033	5.4	0.461	0.0141
C. nigricans	0.0054	0.988	0.068	13.5	0.307	0.0195
A. ataxacantha	0.070	1.699	1.177	35.1	175.8	3.7876

Table A.3.3 Parameters values fitted to the Jarvis *et al.* (1985) model (Equations 3.2-3.12) for a variety of different data sets. * indicates fixed parameters; † indicates parameters which reached their constraint.

Species	Data set	α	θ	g_m (mol m^{-2} s^{-1})	Γ (μmol mol^{-1})	R_o (μmol m^{-2} s^{-1})	k ($°C^{-1}$)	r^2	n
Millet	Green leaves, July+Aug 92	0.041	0	0.743	39.7	0.885*	0.048*	0.97	139
	"	0.036	0.603	0.568	52.0	0.85	0.0417	0.97	139
	"	0.037	0.272	0.886	-	1.07	0.0353	0.97	139
	All data 92	0.031	0	13.967	177.0	0.70	0.0469	0.92	216
	All data 91 + 92	0.037	0	1.710	163.5	0.88*	0.048*	0.88	407
E.tremula	All data 92	0.038	0	2.663	129.5	0.88*	0.048*	0.85	98
	All data 92	0.0269	0	11.410	130.7	1.48	0.010†	0.92	97
	All data 92	0.028	0.99	1.010	130.3	1.58	0.010†	0.88	98
	All data 92	0.024	0.99	4.257	128.58	1.18	0.010†	0.91	97
G. senegalensis	All data 92	0.025	0.44	0.139	211.87	1.48	0.010†	0.87	271
A. ataxacantha	All data 91	0.029	0.69	0.587	247.2	1.21	0.004	0.92	16
C. micranthum	Shoot 15, Sept 92	0.030	0	0.483	206.7	0.41*	0.054*	0.93	116
	"	0.034	0	0.436	206.4	2.02	0.010†	0.94	116
	All data 92	0.032	0.49	0.203	186.8	0.41*	0.054*	0.86	367
	"	0.024	0.85	0.170	188.4	0.87	0.024	0.87	367
C. nigricans	All data Sept 92	0.022	0.95	0.045	74.2	0.41*	0.054*	0.79	69
	All data 92	0.025	0	0.182	207.4	0.41*	0.054*	0.76	304
	All data 92	0.026	0	0.194	213.3	1.20	0.023	0.76	304

Table A.3.4 Parameters fitted to the stomatal conductance model (Equations 3.13-3.15) based on that of Jarvis (1976). Although the parameter values obtained appear less physiologically realistic, these parameters gave a slightly better fit to the data than those in Table 3.7, and were used in MAESTRO. The units of g_{slope} are mmol of H_2O per mol of quanta. † indicates parameters which reached their constraint.

Species	g_{smax} (mol m^{-2} s^{-1})	g_{slope}	g_{sdark} (mol m^{-2} s^{-1})	D_o	r^2	n
Millet	0.767	0.907	0.178	11.59	0.24	140
G. senegalensis	0.280	16.3	0.0†	8.24	0.32	344
C. micranthum	0.213	2.63	0.0†	2.87	0.30	297
C. nigricans	5.132	0.017	0.328	10.42	0.46	158

Table A.3.5 Asymptotic standard errors in parameters values in Table A.3.4.

Species	g_{smax} (mol m^{-2} s^{-1})	g_{slope}	g_{sdark} (mol m^{-2} s^{-1})	D_o
Millet	0.344	0.608	0.127	8.72
G. senegalensis	0.023	0.584	0.064	0.99
C. micranthum	0.038	2.224	0.180	0.40
C. nigricans	6272	2.858	25.56	1.42

Table A.3.6 Parameters fitted to the stomatal conductance model (Equations 3.13-3.15) based on that of Jarvis (1976) for individual shoots of *G. senegalensis* measured on 12/9/92. The units of g_{slope} are mmol of H_2O per mol of quanta. The data show that, for the each of these shoots, the model could be fitted extremely closely. When the model was fitted separately to data from each of 14 different shoots from four stems measured on several occasions on the same day, the mean r^2 was 0.87. However, when data from these shoots were pooled together, the r^2 was reduced to 0.59, and when data for all the shoots measured over the year were pooled together, the r^2 was reduced to 0.28.

Stem, Shoot number	g_{smax} (mol m^{-2} s^{-1})	g_{slope}	g_{sdark} (mol m^{-2} s^{-1})	D_o	r^2	n
1,1	396.2	0.536	0.0131	3.52	0.88	9
1,2	181.4	0.182	0.0388	3.76	0.90	9
1,3	1.229	0.189	0.0528	2.23	0.96	9
2,1	0.237	0.839	0.0203	3.04	0.66	9
2,2	0.293	0.788	0.0†	8.52	0.92	9
2,3	0.636	0.474	0.0189	4.35	0.89	10
2,4	0.313	0.575	0.0226	3.50	0.87	9
3,1	0.240	1.461	0.0†	36.31	0.82	10
3,2	201.1	0.130	0.0704	351.76	0.95	9
3,3	441.1	0.152	0.0660	441.05	0.86	9
3,4	0.252	1.37	0.0†	5.84	0.87	7
4,1	21.53	0.151	0.1145	3.98	0.94	7
4,2	0.377	0.725	0.1187	26.39	0.90	8
4,3	156.4	0.164	0.0884	7.68	0.77	8
All 12/9/92	0.304	0.755	0.017	10.51	0.59	122
All data 1992	0.280	16.3	0.0†	8.24	0.28	344

Table A.4.1 Parameters for the MAESTRO site file (referred to as the "structure file" by Wang *et al.* (1992)). "v" denotes parameters which took a range of values.

Parameter	Units	Millet	Fallow	Tiger bush	Description / Comment
Start date	day, month, year	-	-	-	no longer used -read directly from met file
End date	day, month, yearr	-	-	-	"
Xmax	m	14.4	67.5	20	plot dimensions
Ymax	m	14.4	100	40	plot dimensions
Xslope	degrees	0	0	0	slope in x direction
Yslope	degrees	0	0	0	slope in y direction
Bear	degrees	-90	-90	-90	bearing of x-axis from south
Prop(1)	-	1	1	1	proportion of leaves in age classes 1
Prop(2)	-	0	0	0	proportion of leaves in age classes 2
Prop(3)	-	0	0	0	proportion of leaves in age classes 3
NPHN	switch	v	v	v	0=leaf area constant with time 1=use phenology routine
Mbeta	switch	0	0	0	1=use beta interpolation routine 0=don't
IGMSWH	switch	0	0	0	0=max mesophyll constant 1=vary seasonally
Parameters for beta function	-	-	-	-	parameters describing leaf area density as f(height, radial distance from stem), used if Jleaf=1. Not used
Transmittance in PAR waveband	-	0.02	0.02	0.02	see Figure 7.3
Transmittance in NIR waveband	-	0.32	0.32	0.32	see Figure 7.3
Transmittance in thermal waveband	-	0.01	0.01	0.01	Estimated (Monteith and Unsworth, 1990)
Reflectance in PAR waveband	-	0.05	0.05	0.05	see Figure 7.3
Reflectance in NIR waveband	-	0.45	0.45	0.45	see Figure 7.3
Reflectance in thermal waveband	-	0.05	0.05	0.05	Estimated (Monteith and Unsworth, 1990)
Soil reflectance in PAR waveband	-	0.1	0.1	0.1	Estimated (Monteith and Unsworth, 1990)
Soil reflectance in NIR waveband	-	0.3	0.3	0.3	Estimated (Monteith and Unsworth, 1990)
Soil reflectance in thermal waveband	-	0.05	0.05	0.05	Estimated (Monteith and Unsworth, 1990)
Shape	-	CONE	ELIP	ELIP	crown shape (conical or hemi-ellipsoidal)
NT	-	100	100	100	no. of nearest plants to be included in radiation calculations
NTREE	-	v	v	v	number of target tree
Nalpha	-	5	5	5	number of leaf angle classes

Table A.4.1 (cont.)

Parameter	Units	Millet	Fallow	Tiger bush	Description / Comment
Random	-	1	1	1	Foliage clumping: 1=random, <1=clumped, >1=regular
Elp	-	0.71	1	1	Leaf angle distribution, ratio of horizontal to vertical projections
Jleaf	switch	0	0	0	0=leaf area density constant within crown, 1=leaf area density is f(height), 2=f(height,radial distance from stem)
SLAswt	switch	1	1	1	0=average PAR over all leaf area in subvolume, 1=use sunlit and shaded fractions
MGD	switch	0	0	0	0=grid points in target tree, 1=grid point co-ordinates read from file
NumPnt	-	60	60	60	No. of grid points
Nzen	-	5	5	5	No. of zenith angle classes for calculation diffuse transmittances
Naz	-	11	11	11	No. of azimuth angle classes for calculation diffuse transmittances
NPHO	switch	0	0	0	1=calculate radiation only, 0=simulate physiology as well
Lat	deg, min, s	13 14 38	13 14 38	13 14 38	latitude of site
Long	deg, min, s	02 14 43	02 14 43	02 14 43	longitude of site
LongTM	deg, min, s	02 00 00	02 00 00	02 00 00	longitude of time zone
Pf	-	0.8	0.8	0.8	proportion ppt as free throughfall
Ps	-	0.32	0.32	0.32	prop of ppt reaching plant that goes to the stem
Sc	Mmol m-2 leaf	9.4e-6	9.4e-6	9.4e-6	canopy ppt storage capacity
CcLim	Mmol m-2 leaf	0	0	0	threshold storage at which evaporation begins
Ds	-	-	-	-	Not used
b	-	-	-	-	Not used
Ss	Mmol stand-1	9.1e-3	9.1e-3	9.1e-3	stem ppt storage capacity
e	-	0.04	0.04	0.04	potential evaporation rate of the stem relative to that of the canopy
NSoilLyrs	-	3	3	3	no. of soil layers
Csoil	mm/mm	0.06	0.06	0.06	Initial soil water content
Ssoil	mm/mm	0.12	0.12	0.12	soil water capacity
DepthSoil	m	0.5	0.5	0.5	depth of soil layer
P	kPa	101.3	101.3	101.3	atmospheric pressure

Table A.4.2 Canopy structure parameters in the "tree file", containing co-ordinates, dimensions and leaf area of all plants in the plot. "v" denotes parameters which took a range of values.

Parameter	Units	Millet	Fallow	Tiger bush	Description / Comment
Xpos	m	v	see Fig. 5.13 and Table 5.2	v	x co-ordinate
Ypos	m	v		v	y co-ordinate
Xrad	m	0.5		v	crown radius in x direction
Yrad	m	0.5		v	crown radius in y direction
Z	m	2.55		v	plant height
Trunk	m	0		v	length of bare stem
Leafarea	m2	v		v	leaf area

Table A.4.3 Parameters for the stomatal conductance, leaf photosynthesis and phenology sub-models in MAESTRO contained in the "Physiology" file.

Parameter name in MAESTRO	Symbol in text	Units	Millet	Fallow	Tiger bush	Description / Comment
Co2min	-	µmol mol^{-1}	300	300	300	Min daily atmospheric CO2 conc
Co2max	C_{min}	µmol mol^{-1}	360	360	360	Max daily atmospheric CO2 conc
Rcoet	k	$°C^{-1}$	see Table A.3.1			temperature coefficient for leaf respiration
Rcoeq	-	-	Not used			light coefficient for leaf respiration
Ro	R_o	µmol m^{-2} s^{-1}	see Table A.3.1			leaf respiration rate at 0 oC
AHT	-	m	3.5	9	6	anemometer height
Tmmax	T_{max}	°C	Not used			maximum temp for mesophyll conductance func
Tmopt	T_{opt}	°C				optimum temp for mesophyll conductance func
Tmmin	T_{min}	°C				minimum temp for mesophyll conductance func
Tsmax	-	°C				maximum temp for stomatal conductance func
Tsopt	-	°C				optimum temp for stomatal conductance func
Tsmin	-	°C				minimum temp for stomatal conductance func
gslpl	g_{slope}	mmol mol^{-1}	see Table A.3.3			initial slope of stomatal light response curve
gdark	g_{dark}	mol m^{-2} s^{-1}				stomatal conductance in the dark
VPDthresh	-	kPa	Not used			VPD at which stomata first begin to close
Do	D_o	kPa	see Table A.3.3			VPD at which stomata are closed completely
PXPzro	-	-MPa	Not used			g_s leaf water potential parameter

Table A.4.3 (cont.)

Parameter name in MAESTRO	Symbol in text	Units	Millet	Fallow	Tiger bush	Description / Comment
MaxGm	g_m	mol m^{-2} s^{-1}	see Table A.3.1			max mesophyll conductance
MaxGs	g_{smax}	mol m^{-2} s^{-1}	see Table A.3.3			max stomatal conductance
QFE	α	mol mol^{-1}	see Table A.3.1			photosynthetic quantum efficiency
Vex	θ	-				convexity of light response curve
Gmm	-	-	Not used			relative change in max mesophyll conductance if varying seasonally
Gsm	-	-				relative change in max stomatal conductance if varying seasonally
Area	-	m^2	0.006	0.0006	0.0006	area of a single leaf
Dens	L_s		0	0.117	0.453	stem area index
dbh	-		0.23	0	0	root area index
Splfar	-	cm^2 g^{-1}	-	-	-	specific leaf area (not used)
Proot	-	-	Not used			prop of biomass in root
Prootf	-	-				prop of fine root in root mass
kw	k	$°C^{-1}$	see Table 4.2			temp coefficient for wood respiration
Row	R_o	µmol mol^{-1}				wood respiration rate at 0 oC
ks	k	$°C^{-1}$	see Section 4.8			temp coefficient for soil respiration
Ros	R_o	µmol mol^{-1}				soil respiration rate at 0 oC
Theta	-	-	Not used			Parameters for Farquhar model
MaxN	-	g m^{-2}				"
RelN	-	-				"
AccJmax	-	-				"
AccVcmax	-	-				"
SF	-	DOY	180	125	125	phenology dates: start of flush
EF	-	DOY	230	280	280	end of flush
SS	-	DOY	232	290	290	start of senescence
ES	-	DOY	272	365	365	end of senescence
AR	-	-	1	1	1	proportion of leaf area at EF remaining at SS
ANNUAL	-	switch	1	0/1	0	1=annual, 0=perennial (for respiration purposes only)

A.5 Data used in CBL budget method comparison

Shown in Figure 7.17.

DoY	CO_2 max	CO_2 min	A_e (eddy covariance)	A_r (MAESTRO)
Fallow			mol m^{-2} d^{-1}	
232	329.6	297.4	0.129	0.173
234	337.5	300.0	0.098	0.167
237	335.9	300.0	0.067	0.205
240	372.9	335.2	0.033	0.137
241	380.8	341.8	0.070	0.029
242	383.7	348.7	0.134	0.096
243	387.0	355.0	0.132	0.082
244	386.4	324.5	0.145	0.087
245	387.1	330.9	0.203	0.197
246	384.3	335.8	0.185	0.154
247	379.0	327.7	0.266	0.166
248	387.7	322.0	0.213	0.182
Millet				
249	339.2	324.0	0.119	0.156
250	355.7	320.6	0.213	0.184
251	365.6	332.5	0.143	0.141
252	371.9	327.9	0.122	0.127
253	387.8	327.5	0.132	0.162
254	357.7	324.0	0.139	0.126
255	386.6	320.0	0.163	0.136
Tiger bush				
259	357.2	335.0	0.104	0.160
260	367.2	328.6	0.184	0.111
261	382.8	332.8	0.148	0.168
262	367.5	326.1	0.139	0.196
263	355.1	330.2	0.130	0.166
264	365.8	324.2	0.154	0.094
265	366.0	322.2	0.126	0.084
266	346.0	320.2	0.076	0.132
267	346.8	323.1	0.132	0.144
268	362.2	322.4	0.107	0.134
269	358.2	320.2	0.080	0.093
270	350.7	321.1	0.048	0.090
273	356.7	320.2	0.074	0.060
274	346.3	323.3	0.113	0.083
275	352.8	322.5	0.089	0.080
276	360.0	325.5	0.074	0.076
277	373.6	334.4	0.060	0.115
278	365.9	332.5	0.077	0.052
279	355.0	329.4	0.050	0.048
280	371.4	332.7	0.062	0.044
281	376.7	334.6	0.043	0.030
282	374.1	331.0	0.071	-0.006
283	352.0	331.7	0.075	0.064